The Geology of the High Zagros (Iran) : tectonic and thermal evolution during the Paleozoic.

Saeid Tavakolishirazi

ÉCOLE DOCTORALE SCIENCE ET INGÉNIERIE
de l'Université de Cergy-Pontoise

THÈSE

Présentée pour obtenir le grade de docteur d'Université
Spécialité: Géologie (Tectonique)

The Geology of the High Zagros (Iran)

Tectonic and Thermal Evolution during the Paleozoic

La Géologie du Haut Zagros (Iran)
Évolution Tectonique et Thermique au Paléozoïque

Par

Saeid TAVAKOLI SHIRAZI

Département Géosciences et Environnement

Soutenu le 19 Décembre 2012 devant le jury composé de :

Pr. Dominique FRIZON de LAMOTTE, Univ. Cergy-Pontoise	Directeur de thèse
Dr. Jean-Claude RINGENBACH, TOTAL	Co-directeur de thèse
Pr. Jaume VERGES, Inst. Of Earth Sciences, Barcelona	Rapporteur
Pr. François ROURE, Institute France du pétrole	Rapporteur
Dr. Shahram SHERKATI, National Iranian Oil Company	Examinateur
Dr. Jocelyn BARBARAND, Université Paris XI, Orsay	Examinateur
Pr. Jean-Paul CALLOT, Dept. des Sciences de la Terre, Pau	Examinateur

TABLE OF CONTENTS

ACKNOWLEDGMENTS IX

ABSTRACT XI

RÉSUMÉ XIII

INTRODUCTION **1**

1. General context of the thesis 3

2.Contents of the thesis 6

CHAPTER I: THE STRUCTURE AND KINEMATICS OF THE HIGH ZAGROS BELT (IRAN) **9**

I.1) Introduction **11**

I.2) Structural style and kinematic evolution of the High Zagros Belt (Iran), (Paper N° 1) **13**

I.2.1. Abstract 13

I.2.2. Introduction 14

I.2.3. General geological setting and Methods 16

I.2.3.1. Tectono-stratigraphy of the Western and Eastern High Zagros 18

I.2.3.2. Materials and Methods 23

I.2.4. Geometry and Kinematics of the Western High Zagros 26

I.2.4.1. The Lajin cross-section (transect C) 28

I.2.4.2. Cross-sections A, B and D in the Western High Zagros 32

I.2.5. Geometry and Kinematics of the Eastern High Zagros 40

I.2.5.1. The Faraghan cross-section 41

I.2.5.2. Gahkum and Kuh-e-Khush cross-sections: Comparison with the Faraghan transect 46

I.2.6. Discussion 50

I.2.6.1. The geometry of the High Zagros Belt 50

I.2.6.2. Shortening values in the Western High Zagros 50

I.2.6.3. Discrepancies between cover and basement shortening 51

I.2.6.4. The role of Palaeozoic décollement levels: existence of duplex structures at depth 52

I.2.6.5. Timing of deformation 53

I.2.7. Conclusion 53
I.3) Additional Data and Remarks 56
I.3.1. Back-thrust in the Baznavid area 58
I.3.2. Frontal auxiliary folds 59
I.3.3. Normal faulting in Kuh-e-Khush 61
I.3.4. Assymetric drag folds of the carbonate beds in the EHZ 62
I.3.5. Deep seismic lines in the ZFTB 63
I.3.5.1. High Zagros Seismic lines 64
I.3.5.2. Seismic profile crosses the Arabian basement lineaments 65
I.3.5.3. Décollement within the Lower Paleozoic evidenced by seismic data ... 67

CHAPTER II: PRE-PERMIAN UPLIFT AND EXTENSIONAL DEFORMATION IN THE HIGH ZAGROS 69

II.1) Introduction 71

II.2) Paper N° 2: Pre-Permian uplift and diffuse extensional deformation in the High Zagros Belt (Iran): integration in the geodynamic evolution of the Arabian plate 72

II.3) Further comments and illustrations 87

II.3.1. Pre-Permian paleosol in the Western High Zagros 88
II.3.2. Additional evidence for extensional deformations in Western High Zagros 89
II.3.3. Remarks from seismic data 92
II.3.3.1. Offshore seismic studies 92
II.3.3.2. Onshore seismic study 95

CHAPTER III: TOWARD UNDERSTANDING OF THE HIGH ZAGROS BELT THERMAL HISTORY 97
III.1) Introduction 99
III.2) An outline of High Zagros Belt thermal history 101
III.2.1. Construction of two synthetic boreholes 101
III.2.2. Thermal history modeling 106
III.2.2.1. Input data 106
III.2.2.2. Tested scenarios 109
III.2.3. Conclusion 112

III.3) (U-Th)/He thermochronology, a tool for quantifying of Paleozoic uplift 113

III.3.1. Analytical method 113

III.3.2. Presentation of the laboratory results 113

III.3.3. Discussion 118

III.4) Conclusion **121**

III.5) Appendixes to chapter III **122**

APPENDIX 1: List, location maps and Photos of the samples 123

APPENDIX 2: Principles of source rock maturity analysis 132

APPENDIX 3: Results of measurements on potential source rocks 137

APPENDIX 4: Principles of (U-Th)/He thermochronology on zircon 141

APPENDIX 5: Thermochronology results (U-Th)/He ages on Zircon 145

GENERAL CONCLUSIONS **147**

ANNEX 1: A short memo on the Surmeh structure in the Fars Arc 153

ANNEX 2: Evidence for Late Devonian vertical movements and extensional deformation in Northern Africa and Arabia, Integration in the geodynamics of the Devonian world (Paper in press) 163

ANNEX 3: Location map of figures of the sections I.3 and II.3 207

ANNEX 4: Geological map and structural cross-sections of Baznavid and Zardkuh areas (Western High Zagros) 209

ANNEX 5: Geological map and structural cross-sections of Lajin and Dena areas (Western High Zagros) 211

ANNEX 6-1 & 6-2: Geological map and structural cross-sections of Gahkum, Faraghan and Kuh-e-Khush anticlines (Eastern High Zagros) 213, 215

REFERENCES 217

TABLE OF FIGURES

CHAPTER I:

Figure I.1. Structural divisions of the Zagros fold-and-thrust belt with the locations of the Western and Eastern High Zagros 15

Figure I.2. Tectonostratigraphic columns for (a) Western and (b) Eastern High Zagros Belt. 19-20

Figure I.3. Geological map of the West High Zagros plotted over SRTM data. Lines A, B, C and D are the location of the structural transects 25

Figure I.4. Detailed geological map of the Lajin and Dena regions plotted over SRTM data. Sections C and D correspond to Lajin and Dena 27

Figure I.5. Structural cross-section of the Lajin and Bazman anticlines 28

Figure I.6. (a) Aerial view of the Lajin anticline and adjacent areas (b) Line drawing of figure I.6.a. The NE dipping High Zagros Fault at the base of the cliff has juxtaposed Cambrian siliciclastics against Upper Cretaceous carbonates. The southern flank of the Lajin structure has been removed after erosion which formed a deep gorge. 29

Figure I.7. Incremental three-step (two-phase) forward model of the Lajin cross-section. Restoration of the cross-section yields 14.7 km of shortening in the cover versus 3.25 km in the basement 31

Figure I.8. Detailed geological map of the Baznavid and Zardkuh regions plotted over SRTM data. Sections A and B are Baznavid and Zardkuh, respectively 34

Figure I.9. Structural transect of the Baznavid area 36

Figure I.10. Structural transect of the Zardkuh area 37

Figure I.11. (a) Field photograph of the Cretaceous Garau Fm in the NW of the West High Zagros (b) Line drawing of figure I.11.a. The Garau Formation was not folded isopach and steep thrust fault flattened within this Formation. It acted as a detachment level in this area..... 38

Figure I.12. Structural transect of Dena anticline. The depth-to-detachment of the minor anticline within the broad syncline is not clear 39

Figure I.13. Deformed carbonate rocks in the footwall of the High Zagros Fault at Dena Mountain. Slickensides with a dip-slip component are present on the polished surfaces of the fault plane 40

Figure I.14. Geological map of the East High Zagros overlain on SRTM data. Lines E, F and G are the locations of the structural transects 41

Figure I.15. Structural section across the Faraghan anticline 43

Figure I.16. Field view of the south-dipping back-thrust which places the Ordovician Syahoo Fm over the Triassic Khanekat Fm in the core of the Faraghan anticline. The north-dipping fore-thrust is an out-of-sequence basement thrust, which cuts out all the other structure 43

Figure I.17. Two-phase (thin- and thick-skinned) kinematic scenario of the Faraghan anticline.This scenario consists of a four-stage kinematic model for structural development of the anticline. 45

Figure I.18. Frontal view of the Gahkum anticline. Sedimentary rocks (Lower Palaeozoic to Upper Cretaceous) on the hanging wall of the High Zagros Fault are thrust over the Quaternary alluvium which covers the underlying Upper Miocene Aghajari Formation 47

Figure I.19. Gahkum structural cross-section 48

Figure I.20. Structural transect of Kuh-e-Khush anticline. The buried Hormuz salt has probably been disconnected from its feeder source layer. 49

Figure I.21. Field photo of the emergent Hormuz salt in the incised valley of Kuh-e-Khush. Detail of reverse motion on the fault plane can be seen in the inset 50

Figure I.22. (a) Back-thrust carried out the Ordovician rocks over Upper Cretaceous (b) The structural cross-section of the Baznavid area depicts the location of figure I.22.a 58-59

Figure I.23. (a) Cross-section along the frontal zone of Fraghan Ant. The red square marks the area within the Fig. 1.23.b. (b) Side view of foot-wall syncline and secondary thrust branches from the basement fault of the Faraghan anticline (c) Detail of the superficial fold on the frontal zone of Faraghan structure. This fold detaches either in Razak or in Gurpi-Pabdeh Formations. 60-61

Figure I.24. (a) Aerial view of the normal fault in the carbonate Asmari of the Kuh-e-Khush Structure (b) Cross-section illustrating the normal fault in the back-limb of Kuh-e-Khush. The black square displays the picture in Fig.I.24.a. 62

Figure I.25. Drag folding in the carbonate layers of the eastern zone. Small thrust faults were generated by simple shearing and cut the steep flank of the asymmetric drag antiform. 63

Figure I.26. (a) Non-interpreted (b) interpreted seismic profile in the Dena Area (Western High Zagros) The yellow short line depicts rotated pre-Permian block sealed by the unconformity 65

Figure I.27. (a) Non-interpreted (b) interpreted seismic image in the NW of the Persian Gulf clearly show the impact of the North-South HBF (Fig. I.1) on the pre-Permian thickness variations. Evident thinning of Paleozoic succession toward the

"Hendijan-Bahregansar" high can be observed. The lowermost interpreted reflector indicated a tentative horizon within the Lower Paleozoic 66

Figure I.28. a) Non-interpreted and b) interpreted seismic profiles in the East Fars. Divergence within the deep reflectors and significant increasing of the Lower Paleozoic thickness indicate the activation of incompetent zone (décollement level 68

CHAPTER II:

Figure II.1. Stratigraphic log on the High Zagros Belt. Modified after Tavakoli-Shirazi et al.(2012) 88

Figure II.2.Paleosol consisting of bauxite and laterite in Dena section. This layer on top of the Cambrian marks the hiatus corresponding to the pre-Permian uplift. 89

Figure II.3. Presence of "Paleosol" which is covered by Permian sediments indicating a long-lived continental evolution 89

Figure II.4. Extensional deformation of the Ordovician rocks in Baznavid area (Western High Zagros) indicated by normal movements along the fault which is sealed by pre-Permian unconformity 90

Figure II.5 (a),(b). Dislocation of Mila "B" limestone because of meso-scale normal faults in Kuh-e-Lajin..... 90

Figure II.6. Field picture of Dena Mountain (Putak valley) illustrating the tilted normal faults within the Cambrian carbonate of Mila Fm. Angular unconformity at the base of Faraghan Fm caps the faults..... 91

Figure II.7. Interpretative sketches of successive deformation observed in Dena Mountain (a) Tilted block and normal fault in pre-Permian uplifted sediments which is topped by erosion surface(b) Onset of deposition in carbonate platform from Permian to Cretaceous starting with basal siliciclasticts just above the unconformity (c) Rotation of preceding structures due to the late Alpine compression in Zagros. 92

Figure II.8. (a) Non-interpreted and (b) interpreted seismic strike line in the Persian Gulf Illustrates the uplifted region (Paleo-High) which is bounded to extensional faults. Note to the decreasing of pre-Faraghan thickness above this Paleo-high. ... 93

Figure II.9. (a) Non-interpreted and (b) interpreted seismic profile in the Persian Gulf illustrates the lateral thickness variation of Early Permian Faraghan formation.. 94

Figure II.10. (a) Non-interpreted and (b) interpreted sections of the Persian Gulf seismic study (PC 2000). The flattening on top of the Kangan Fm revealed tilted pre-Permian deposits beneath the unconformity. The rotation of pre-Permian rocks is likely attributed to the extensional deformations and uplift (See Tavakoli-Shirazi, 2012) 95

Figure II.11 (a) Non-interpreted and (b) interpreted seismic profile in the west of Fars Arc 96

CHAPTER III:

Figure III.1. Schematic configuration of the sedimentary deposits in the Arabian Plate [from Frizon de Lamotte et al. 2012 (in press), see annex 2] 99

Figure III.2. (a) Synthetic borehole assumed to be typical of the Western High Zagros (b) Synthetic borehole assumed to be typical of the Eestern High Zagros. 103-104

Figure III.3. Schematic reconstruction of the Zagros before the onset of propagation of the deformation within the Arabian Plate (from Wrobel Daveau, 2011).This drawing illustrates the extra-load over the Asmari-Qom Fm. It could be either the Razak Fm or a thrust sheet issued from the Sanandaj-Sirjan Zone 106

Figure III.4. Estimated present-day heat flow in the Zagros (TOTAL database) ... 108

Figure III.5. Heat-flow values for sedimentary basins in different geodynamic contexts (Allen & Allen, 1990) 108

Figure III.6. Scenario 1: thermal 1D modeling with a constant and low heat flow value at the bottom of the crust..... 110

Figure III.7. Scenario 2: thermal 1D modeling with variable heat flow value at the bottom of the crust 111

Figure III.8. Scenario 3: thermal 1D modeling with a quite constant and high heat flow value at the bottom of the crust during the Paleozoic 112

Figure III.9. Radius length versus ZHe ages of the samples collected from the HZB 115

Figure III.10. Ages of Fish Canyon Zircons from Orsay (this study) compared to Fish Canyon Zircons of Tagami et al. (2003) 115

Figure III.11. Histogram of ZHe ages on zircons for Orsay samples 116

Figure III.12. eU (ppm) versus ZHe ages (Ma) for all data including this study and bibliography (Gavillot et al., 2010), eU is calculated after the equation eU=U+0.24xTh 117

Figure III.13. Alpha dose versus Zircon (U-Th)/He ages (Ma) for all available data 118

Figure III.14. Relative age probability diagrams displaying the U-Pb detrital zircon age distribution for Cambrian, Devonian and Permian sandstone samples from the High Zagros (after Horton et al., 2005). The samples were collected from: (a) Cambrian Lalun Fm. (b) Devonian Zakeen Fm (c) Permian Faraghan Fm 119

Figure III.15. Closure temperatures versus Cooling rate for apatite He and zircon He. (after Reiners et al. 2004). AFT and ZFT closure temperatures are always higher than those for the (U-Th)/He system on the same minerals.. 120

Figure III.16. Location of Eastern High Zagros samples on the Geological map over the SRTM background 124

Figure III.17. Location of Wrobel-Daveau's samples on the geological map of the Lurestan area 125

Figure III.18. Location of Western High Zagros samples on the SRTM data overlain by Geological map 126

Figure III.19. Location of the Surmeh anticline samples on the Geological map ... 127

Figure III.20. Location of samples on the synthetics boreholes 128

Figure III.21. Samples for Organic matter tests from Western High Zagros 129

Figure III.22. Samples for Organic matter experiments from Surmeh and Fahraghan anticlines 129

Figure III.23. Samples for thermochronology (U-Th)/He from Eastern High Zagros 129

Figure III.24. Samples for thermochronology (U-Th)/He from Western High Zagros 130

Figure III.25. Microscopic photos of hand-picked Zircons from High Zagros samples 130

Figure III.26. Mineral separation and (U-Th)/He measurements 131

Figure III.27. Carbonaceous materials in sample LU 09-30 138

Figure III.28. Organic matter sample (Fa-STS-4) collected from Faraghan anticline 140

ACKNOWLEDGMENTS

This dissertation is the result of a program agreement between the Université de Cergy Pontoise (UCP), the National Iranian Oil Company (NIOC) and TOTAL .It would not have been possible without the guidance and the help of several individuals who in one way or another contributed and shared their valuable assistance in the preparation and completion of this study. First and foremost, I offer my sincerest gratitude to my supervisor, Pr. Dominique FRIZON de LAMOTTE, who has supported me continuously throughout my thesis in the field and in the lab with his patience and the best knowledge. I would like to express my cordial appreciation to the management of NIOC, Exploration Directorate for encouragement and providing data and logistics during field trips. I acknowledge also my colleagues of NIOC who participated in regional studies and field campaigns as well as geophysics department to help me for seismic lines.

I am very grateful to Dr. Jean-Claude RINGENBACH from Total for unfailing support of this thesis. I am especially thankful to the Jury members, François ROURE, Jaume VERGES, Shahram SHERKATI, Jocelyn BARBARAND and Jean-Paul CALLOT who accepted to be as the referees of this thesis. My appreciation also goes to the members of department of “science de la Terre” of UCP for a friendly and collaborative atmosphere, particularly Danielle Lacoeuilhe secretary of the geosciences lab for her administrative aid, Pascale Leturmy for technical discussions, Christian David (director of the department) and Jean-Christian Colombier for preliminary preparation of Thermochrono samples. I am indebted to Mélanie Denecker, Jean-Baptiste Regnet, Camille Raulin, Fabian Humbert, and Nicolas Mouchot, the present and former PhD students of UCP geosciences department for pleasure dialogues and my French language queries and especially Baptiste Mary who shared the office with me for three years. I would like to thank Camille de le Taille for cooperation to build a database for Genex modeling and (U-Th)/He measurements and Jean-Christophe Wrobel-Daveau for helpful advices about drawings and scientific discussions. Many thanks go to the structural group of Total (Pau), mainly Jean-François Ballard who introduced me with Geosec 2D software.

Last but not the least; my family deserves special gratitude who maintained this period calm for me towards the conclusion of my research.

ABSTRACT:

This Thesis presents the results of a study of the “High Zagros”, the most internal part of the Zagros-Fold-Thrust-Belt (ZFTB). On map view, the High Zagros is exposed in two separated domains (Western and Eastern High Zagros respectively) and partly hidden as an under-plated region beneath the Sanandaj-Sirjan Domain. The High Zagros is the only place in the ZFTB where the Paleozoic rocks are widely exposed.

A primary objective was to reevaluate the structural style and kinematic evolution of the High Zagros. It is shown that the most significant geological elements within this area are large scale faulted detachment folds, associated with a complex system of thrust faults segmented by strike-slip faults. This work suggests that the existence of active Ordovician and/or Silurian décollements led to the development of duplex structures which are confined in the core of the anticlines. A two-step kinematic scenario, similar to the one already proposed elsewhere in the belt, is proposed for the High Zagros. Firstly, a thin-skinned phase led to establish detachment folding over the basal Hormuz salt. Then, a thick-skinned phase resulted in the basement thrusting and allowed the exhumation of Lower Paleozoic succession.

After this presentation of the tectonic context of the High Zagros, the thesis focuses on the tectonic significance of the pre-Permian unconformity, which was known through a major hiatus between Cambro-Ordovicien to Early Permian and between Devonian to Permian rocks in the western and eastern High Zagros respectively. It is shown that (1) the High Zagros presents below the unconformity a large “Arch-and-Basin” geometry; and that (2) only extensional features such as normal faults and rotated blocks, without evidence of contractional deformation, can be observed below the unconformity. Thermal uplift of possible Late Devonian is proposed as a probable mechanism explaining both the uplift and the diffuse extensional deformation. This proposal strongly modifies the “classical” interpretation of the pre-Permian hiatus as a far effect of the Variscan Orogeny.

Thermal modeling based on maturity data from potential source rocks cropping out in the High Zagros has been performed. The most probable modeled scenario suggests an important heat flow during the Devonian and the erosion of ~3900m of the sedimentary pile prior to the deposition of Permian sequence. This outcome reinforces our interpretation of a thermal uplift scenario responsible for pre-Permian vertical movements. On the other hand, a set of new (U-Th)/He ages obtained from the Lower Paleozoic, Devonian and early Permian clastic rocks show a partial reset of zircon grains. These two results are fairly consistent with the published data describing a major thermo-tectonic event during Late Devonian-Early Carboniferous in the Levant Arch (Israel, Jordan) and suggest a common mechanism at the scale of the Arabian Plate.
Key Words: High Zagros (Iran), Kinematic evolution, Paleozoic History, Thermal modeling, Thermochronologic data.

RÉSUMÉ :

Cette thèse présente les résultats d'une étude du Haut Zagros, la partie la plus interne du Zagros plissé. Sur les cartes, le Haut Zagros est présent dans deux régions séparées l'une de l'autre, le Haut Zagros Occidental et Oriental respectivement, et partiellement masqué comme un domaine sous-plaqué sous la Zone de Sanandaj-Sirjan. Le Haut Zagros est l'unique endroit du Zagros où les roches paléozoïques affleurent largement.

Un premier objectif était de réévaluer le style tectonique et l'évolution cinématique du Haut Zagros. Il est montré que la caractéristique structurale principale de cette zone est l'existence de plis de décollement faillés, associés à un réseau complexe de chevauchements et de failles décrochantes. Ce travail suggère que l'existence de niveaux de décollement au sein des couches ordoviciennes et/ou silurienne a permis le développement de duplex aux cœurs des anticlinaux. Un scénario tectonique en deux étapes, identique à celui proposé ailleurs dans la chaîne, est mis en avant. Une première phase en tectonique de couverture a permis la formation d'un train de plis de décollement au dessus du sel précambrien d'Hormuz. Le socle est impliqué dans la déformation dans un second tempspermettant l'exhumation des roches du Paléozoïque Inférieur.

Après cette présentation du contexte tectonique du Haut Zagros, la thèse se concentre sur la signification tectonique de la discordance pré-permienne dont la manifestation la plus évidente est l'existence d'un très important hiatus sédimentaire allant du Cambro-Ordovicien au Permien dans le Zagros Occidental et du Dévonien terminal au Permien dans le Zagros Oriental. Il est montré que : (1) le Haut Zagros présente sous la discordance une géométrie générale en Arche et Bassin et que (2) seules des structures extensives comme des failles normales et des blocs basculés sont présentes sous la discordance, sans aucune trace de structures compressives. Un soulèvement thermique d'âge possible fini-dévonien est proposé comme mécanisme expliquant à la fois le mouvement vertical et l'extension diffuse. Cette hypothèse modifie considérablement l'interprétation classique associant le hiatus pré-permien à un effet lointain de l'orogenèse varisque.

Des modélisations thermiques basées sur des données de maturité de la matière organique provenant des roches-mères potentielles du Haut Zagros ont été réalisé. Le modèle le plus probable suggère un flux de chaleur important pendant le Dévonien et l'érosion de ~3900m de sédiments avant le dépôt du Permien. Ce résultat est en accord avec l'hypothèse d'un soulèvement thermique évoqué plus haut. Par ailleurs, des mesures d'âges (U-Th)/He sur zircon montrent une remise à zéro partielle. Ces deux gammes de résultats sont en accord avec les données publiées suggérant l'existence d'un événement thermo-mécanique majeur au cours du Dévonien terminal et du Carbonifère Inférieur dans l'Arche du Levant (Israël, Jordanie). Un mécanisme commun est suggéré à l'échelle de la Plaque Arabe.
Mots-Clés : Haut Zagros (Iran), évolution cinématique, Histoire Paléozoïque, Modélisation thermique, Données thermochronologiques.

INTRODUCTION

1. General context of the thesis

My PhD thesis can be considered as dual-purpose dissertation dealing with some issues of the structural geology of the Zagros Fold-Thrust Belt (ZFTB). The first aspect is related to the research and education in University where students are taught to challenge and answer the questions by scientific methods. In this regard, my project was conducted in the "Earth and Environmental Sciences" Department of Cergy-Pontoise University (UCP), France. I also benefitted from willing cooperation with Paris-Sud (Orsay) University for thermochronology measurements and also with the Technical and Scientific center of TOTAL in Pau for sections balancing and lab analysis of organic matters.

Another perspective is to suggest new ideas and techniques to overcome the problems occurring in up-stream energy industry especially the hydrocarbon exploration. In the present case, National Iranian Oil Company (NIOC), where I originally come from, would like to study the Paleozoic structural style and basin evolution in the ZFTB. Total, as a big partner for petroleum industry around the world, has the same interest and helps the oil-rich countries to develop their projects.

My PhD thesis is integrated into a scientific project focusing on the geodynamic evolution of the Zagros orogeny (Fig. I.1).This project led to the defense of several theses, which have been achieved at the University of Cergy-Pontoise during the last decade. They have been supported by different technical cooperation including: (1) the MEBE (Middle East Basin Evolution) project sponsored by a consortium of petroleum companies; (2) a research study between Institute Français du Pétrole (IFP), NIOC (National Iranian Oil Company) and the Université de Cergy-Pontoise and finally (3) a scientific agreement between TOTAL, NIOC and the Université de Cergy-Pontoise.

In this general frame, the University of Cergy-Pontoise has been the host of some recent structural studies concerning the ZFTB:

-Matteo Molinaro (2004) studied the southeastern part of the Fars Arc and the transition from the Zagros to the Makran accretionary prism. He presented a structural balanced section and the first kinematic modeling for the Eastern Zagros.

Based on the interpretation of geophysical data, he proposed a model associating lithospheric thinning with a slab break-off beneath the Zagros collisional region.

-Shahram Sherkati (2004) focused on the style of folding and impact of the basement faults on the thickness and facies changes in the Izeh zone, Dezful embayment and Western Fars. He drew five balanced cross-sections using field data and seismic lines. He performed sand box modeling at IFP (now IFPen) to illustrate the role of basal and intermediate décollement horizons during folding of the sedimentary cover.

-Salman Jahani (2008) mainly worked on the halokinesis in the eastern Fars Arc and adjacent area. He studied the activation of late pre-Cambrian to early Cambrian Hormuz salt formation during and before Zagros Orogeny and showed pre-existing diapirs controlled the localization of Late Cenozoic folding. He made four Structural balanced transects from inner zone to the Persian Gulf foreland basin using field and seismic data.

- Finally, Jean-Christophe Wrobel-Daveau (2011) proposed the occurrence of mantle exhumation along detachment faults in crush zone of northwest Zagros (Kermanshah area). His main job deals with constraining vertical movements and propagation of deformation along various segments of the ZFTB using combination of section balancing and low temperature thermochronology (Apatite (U-Th)/He and Apatite Fission Track Analysis).

In the same way, my PhD program was defined as a collaborative project between UCP, NIOC and Total. More explanations for these two facets of my work are given below:

a. Academic point of view:

Apart from the western border of the Arabian Plate, Internal zone of the Zagros fold belt is a unique area containing outcrops of Lower Paleozoic rocks in the core of several thrust anticlines. This area is simply defined as the High Zagros. Elsewhere, except some small and scattered Paleozoic rocks exhumed with the Hormuz salt plugs in the Fars Arc (Eastern Zagros), they are only known by sub-surface data (e.g. some seismic acquisitions frequently poor for pre-Permian level

and/or scarce boreholes). The High Zagros maintains these outcrops and associated structures accessible for academic studies and training purposes. On the other hand, the High Zagros is an imbricated zone locating just south of the Neo-Tethys. Thick Paleozoic sedimentary sequence recorded all stages of geodynamic evolution of the Zagros basin in this area from Late Proterozoic-Early Cambrian epicontinental shelf to the Neo-Tethys rifting period and subsequent passive margin evolution. These events can only be examined through field observations of the sedimentary and tectonic evolution within the High Zagros.

Then, the main purpose of my thesis was to revisit the High Zagros with two main objectives:

- To address the Paleozoic tectonic evolution of this area which was known mainly through stratigraphic and palynological studies (Setudehnia, 1972; Ghavidel-Syooki, 2003; Ghavidel-Syooki et al., 2011), and to integrate it in the more general frame of the Arabian Plate.

- To show how the lithology contrast within the Paleozoic sedimentary pile could explain some aspects of the structural development during the Cenozoic Zagros Orogeny.

b. Industrial point of view:

The ZFTB is one of the most prolific oil and gas fields in the world. Exploration and exploitation of hydrocarbon reservoirs (e.g. Permo-Triassic, Jurassic, Cretaceous and Oligo-Miocene horizons) in the Zagros foreland basin were underway since one century ago. Decreasing of production rate of current fields and excessive energy world demand require to find additional and/or substitution resources. Last two decades successful explorations of economic hydrocarbon reserves in the pre-Permian rocks of central and eastern part of the Arabian plate (e.g. Saudi Arabia and Oman) encourage the efforts to investigate the equivalent series in the ZFTB. Therefore NIOC plans to discover new oil and gas potentials within deep targets. My thesis aims to help this mission with a best structural analysis of the High Zagros where most Paleozoic sequences are accessible.

2. Contents of the thesis

My PhD dissertation is arranged in three chapters and completed by several annexes.

The **chapter one** is dedicated to the" Structural Style and Kinematic Evolution of the High Zagros Belt (Iran)". It is presented under the form of a scientific paper currently submitted for publication in the "Journal of Petroleum Geology". This paper presents the geometrical configuration of the High Zagros district in the rear of the Zagros mountain chains. It is accompanied by complementary remarks illustrating more structural features by field photos, sections and sketches. Further arguments would be presented by fairly seismic profiles selected from dataset supplied by exploration directorate of NIOC. For the purpose of the thesis, this paper presents the general structural frame in which the Paleozoic rocks are exposed. The main results of this study were given as an oral presentation in the General Assembly (2012) of European Geosciences Union (EGU) in Austria.

The **second chapter** is baptized "Pre-Permian uplift and diffuse extensional deformation in the High Zagros Belt (Iran): Integration in the geodynamic evolution of the Arabian Plate". It includes a scientific paper already published in the "Arabian Journal of Geosciences" and some additional explanations. It discusses the evidence of extensional deformation expressed by normal faults which are sealed by pre-Permian unconformity and accompanied by a significant thermal uplift consequently. The concept of "Hercynian Unconformity", extensively used in the Arabian Plate, is strongly modified by this paper. The complements to this chapter bring fresh arguments for existence of pre-Permian hiatus in the High Zagros and observed structural configurations. This article was presented as a poster in the General Assembly (2011) of European Geosciences Union (EGU) in Vienna (Austria).

The **chapter three** reports the efforts to understand the thermal history of the High Zagros Belt during Phanerozoic time. In this chapter, I combine modeling of organic matter maturities coming from Paleozoic and Mesozoic potential source rocks with high temperature thermochronology [(U-Th)/He on zircon from Lower Paleozoic and Permian rocks] in order to constrain the vertical movements (uplift vs.

subsidence) and erosion value through time. The results would be contributed in the paper explaining the “Origin and timing of uplift in the upper Paleozoic of the ZFTB”.

Finally I provide some conclusions and perspectives. I also include some recommendations for further detailed field reconnaissance and geophysical studies in order to deeper understanding of the High Zagros. The generalization of my results at the scale of the Arabian Plate and the North African domain is given in the Annex 2 in the frame of a paper which is presently in press.

CHAPTER I

THE STRUCTURE AND KINEMATICS OF THE HIGH ZAGROS BELT

I.1) Introduction

The purpose of this chapter is to present the geometry of the High Zagros in which the Paleozoic rocks studied in the following sections are cropping out. I mainly focused on the geometry and geological setting of the High Zagros domain, its frontiers and general structural characteristics gained during two field reconnaissances. The field observations also allowed me to analyze and present the deformation style and kinematic evolution of the High Zagros. The core of these investigations was summarized in the frame of an article which has been submitted to the "journal of petroleum geology" in September 2012. The title of this article is "Structural Style and Kinematic Evolution of the High Zagros Belt, Iran". The aim of this work is essentially to set up a new geological definition of the High Zagros belt. In this frame, I drew 4 and 3 balanced cross-sections within the Western High Zagros and Eastern High Zagros respectively to constrain the structural specifications of the folds and faults in these domains.

Shortening values for the sedimentary cover and rigid basement were subsequently calculated for 3 of those in the Western zone in order to compare with the shortenings obtained by previous authors (e.g. Sherkati et al. 2006). Diverse shortening amounts which accommodated in the cover and basement and total decoupling along the basal Hormuz detachment in the High Zagros were also discussed in detail. The detachment folding is the dominant structural mechanism to form the initial fold architecture in the High Zagros Belt. However, multiple décollement horizons influence the style of the structures during deformation accommodation. In this regard, presence of duplex structures at the level of Lower Paleozoic rocks in this zone is proposed.

The manuscript was principally prepared using collected field data alone. Neither elaborative seismic lines nor well data were available to control the formation or structural styles at depths. Further field work and deep seismic information in the High Zagros are absolutely required for better interpretations, timing of the structures and more precise explanation of this domain. Finally, I have attached some complements to the paper No.1 in the current chapter focusing on the technical aspects and outstanding geological exposures for further explanations.

Paper N°1

Structural style and kinematic evolution of the High Zagros Belt

Submitted to: Journal of Petroleum Geology

(September 2012)

I.2) STRUCTURAL STYLE AND KINEMATIC EVOLUTION OF THE HIGH ZAGROS, IRAN

S. Tavakoli-Shirazi[1'2], D. Frizon de lamotte[2'3], P. Leturmy[2], J.-C. Ringenbach[4], and J.-F. Ballard[4]

[1] NIOC, Exploration Directorate, Geology Dept., Seoul Ave., P.O. Box 19395-6669, Tehran, Iran.

[2] Univ. Cergy-Pontoise, Dept.Géoscience and Environnement, F95000 Cergy-Pontoise, France.

[3] TOTAL, Projets Nouveaux, TBF, Place Jean Millier, F92 400 Paris-La Défense, France.

[4] TOTAL, Département d'interprétation structurale et sédimentaire, CSTJF, Av. Larribeau, F64 000 Pau, France.

I.2.1. Abstract

The High Zagros is the most internal portion of the Zagros fold-and-thrust belt. It is bounded to the south by the High Zagros Fault and to the north either by the Main Zagros Thrust or by the frontal zones of the discontinuous Cretaceous nappes which include elements derived from the former Neo-Tethys margin. The High Zagros is only present in two areas referred to here as the Western and Eastern High Zagros, respectively; these areas are mountainous and elevations reach 4400 m. In this paper we present new maps of these regions together with seven new balanced cross-sections and two new kinematic models. Contrasting with previous models, the presence of an intermediate décollement located within the Ordovician-Silurian shale succession is proposed. From a geometric point of view, deformation on this detachment, together with deformation on the décollement within the Infracambrian Hormuz salt, has resulted in the development of duplexes which are confined within the cores of anticlines. From a kinematic point of view, a two-phase scenario of structural evolution is suggested. During the first (thin-skinned) phase, large detachment folds developed over the Hormuz salt, and different intermediate décollements were activated together with fore- and back-thrusts. This was followed

by a thick-skinned phase marked by the activation of major out-of-sequence basement thrusts, which were responsible for the exhumation of the Lower Palaeozoic succession. This new model is integrated into a general tectonic scenario for the Zagros fold-and-thrust belt.

Key words: High Zagros, Iran, thrust belt, duplex structure, kinematic model, crustal shortening, décollement, Hormuz salt.

I.2.2. Introduction

The 1800 km long Zagros Fold-and-Thrust Belt (ZFTB), at the boundary between the Arabian Platform and the Central Iran Block (Fig. I.1), extends from the Bitlis suture zone in the NW to the boundary with the Makran accretionary wedge to the SE. It varies in width with two main salients (Lurestan and Fars Arcs) and two main embayments (Kirkuk and Dezful). The belt is also divided into several structural zones from NE to SW. In the latter category, the “High Zagros Belt” in the most internal part of the Zagros orogen, is an imbricated zone with relatively little seismicity.

The ZFTB has been extensively studied in recent years (e.g. Berberian, 1995; Hessami et al., 2001; Blanc et al., 2003; Homke et al., 2004; Agard et al., 2005, Sherkati et al., 2006; Jahani et al. 2009; Emami et al. 2010; Leturmy et al., 2010; Vergés et al. 2011; Mouthereau et al., 2011) as it is the location of one of the oldest and richest oil and gas provinces in the world (Versfelt, 2001). Exploration and development of hydrocarbon accumulations in Permo-Triassic, Jurassic, Cretaceous and Oligo-Miocene reservoirs in the Zagros area began more than 100 years ago.

However, with the exception of studies by Bosold (2005), Gavillot (2010) and some local mapping, relatively little attention has been devoted to the High Zagros compared to the rest of the Zagros fold belt. This may be because the main reservoir intervals are exposed at the surface in the High Zagros, so the area has not been considered economically attractive. Structural complexity and lack of accessibility are other reasons why the area has received relatively little attention.

This study aims to investigate the detailed structure of the High Zagros. The Lower Palaeozoic succession, Devonian and Upper Carboniferous - Lower Permian sequences which, in countries to the south (Saudi Arabia, Oman) are known to host large volumes of hydrocarbons are exposed at the surface here, although they have not been studied in detail. Therefore, a second objective of this article is to investigate the structural style and kinematic evolution of the High Zagros, which may help the evaluation of the area's hydrocarbon prospectivity. Emphasis is placed on the geometrical configuration and role of detachment levels within the Lower Palaeozoic succession in the structural development of the High Zagros; the presence of duplex structures in the cores of large-scale anticlines in this area is proposed for the first time.

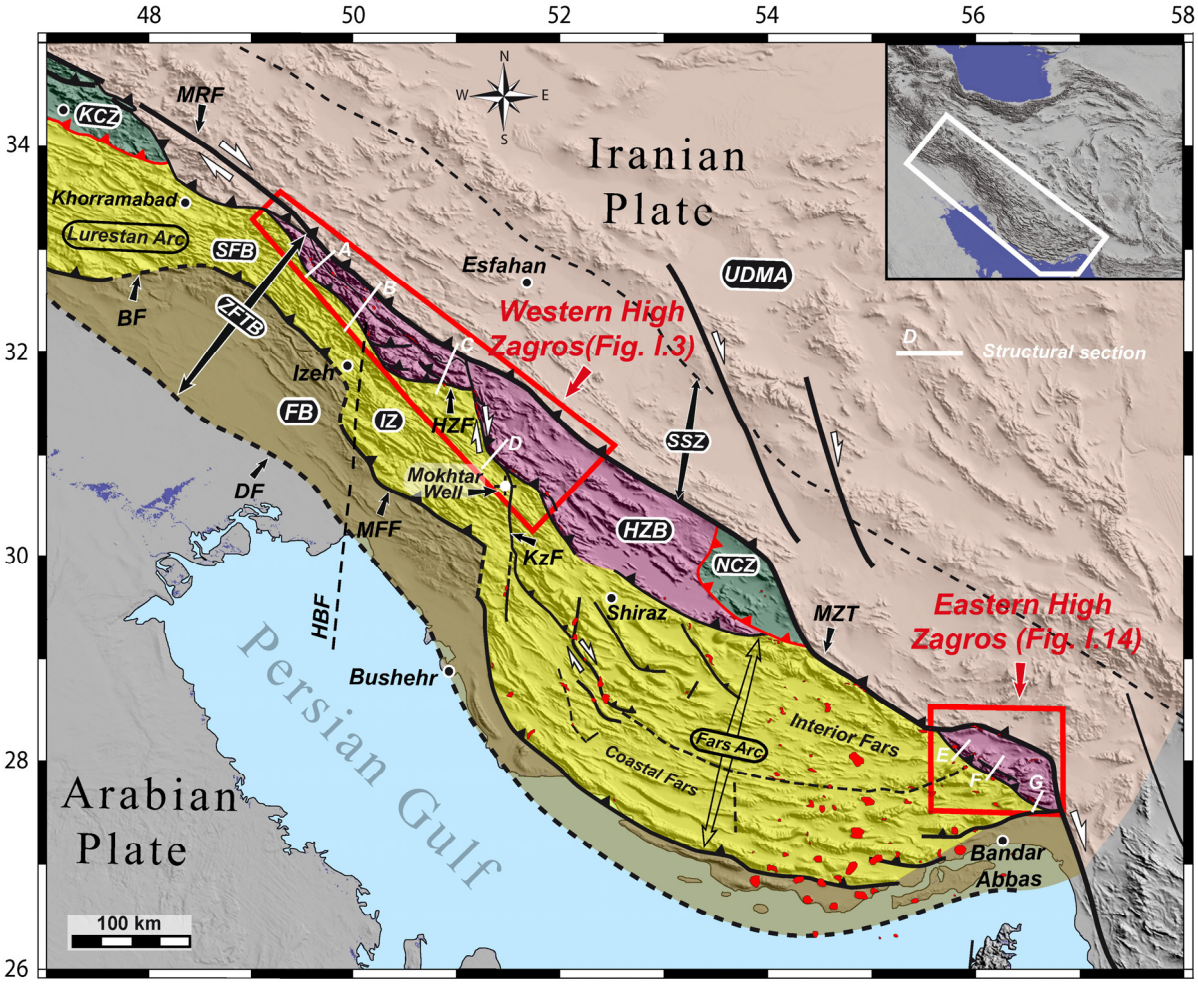

Fig. I.1. Structural divisions of the Zagros fold-and-thrust belt with the locations of the Western High Zagros (WHZ) and Eastern High Zagros (EHZ). BF Balarud Fault, DF Deformation Front, FB Foreland Basin, HBF Hendijan-Bahregansar Fault, HZB High Zagros Belt, HZF High Zagros Fault, IZ Izeh zone, KCZ Kermanshah Crush Zone, KzF Kazerun

Fault, MFF Mountain Front Fault, MRF Main Recent Fault, MZT Main Zagros Thrust, NCZ Neyriz Crush Zone, SFB Simply Folded Belt, SSZ Sanandaj-Sirjan Zone, UDMA Urumiyeh Dokhtar Magmatic Arc, ZFTB Zagros Fold Thrust Belt.

I.2.3. General geological setting and Methods

The ZFTB is a part of the Alpine-Himalayan orogenic system resulting from the Cenozoic closure of the Neo-Tethys (Haynes and McQuillan, 1974; Ricou et al., 1977; Alavi, 1994; Agard et al., 2011; Frizon de Lamotte et al., 2011; Mouthereau et al., 2012). Two main stages in the geodynamic development of the belt are distinguished: (i) emplacement ("obduction") of Cretaceous nappes comprising mantle rocks and deep-marine sediments onto the Arabian Platform margin during the Late Cretaceous (Santonian to Campanian), (Ricou et al. 1977); and (ii) continent -- continent collision between Arabia and Eurasia at the end of the Eocene (Jolivet and Faccenna, 2000; Kazmin, 2002; Frizon de Lammote et al., 2011).

The Zagros belt is flanked to the SW by the Arabian Platform and Persian Gulf, representing a Mesopotamian Basin in front of the orogen and to the NE by a 150 to 250 km wide belt of highly deformed sedimentary-metamorphic rocks known as the Sanandaj-Sirjan Zone (Fig. I.1), (Stocklin, 1968; Ricou et al., 1977). The Sanandaj-Sirjan Zone is interpreted to be a Cimmerian block which separated from the northern margin of Gondwana at the end of the Permian and then became attached to Eurasia during the Late Triassic Cimmerian orogeny, following the closure of the Palaeo-Tethys (Zanchi et al., 2009).

The Deformation Front, a major flexure, separates the Zagros fold-and-thrust belt from the Mesopotamian foreland basin to the SW (Berberian, 1995). To the NE, the Main Zagros Thrust (Ricou et al., 1977; Berberian, 1995; Agard et al., 2005; Paul et al., 2006) is a major reverse fault which accommodates underthrusting of the Zagros foldbelt beneath the Sanandaj-Sirjan Zone. The Urumieh-Dokhtar Magmatic Arc, adjacent and parallel to the latter zone, is an Andean-type volcanic-magmatic arc (Alavi, 1994; Agard et al., 2011) formed during Jurassic to Eocene subduction of the Neo-Tethys below the Iranian continental plate.

The Zagros fold-and-thrust belt is made up of four main structural zones (Fig. I.1), which are as follows from NE to SW.

1. The **Cretaceous nappe domain,** including the Kermanshah and Neyriz Crush Zones, comprising elements derived from the former ocean floor and continental slope (Robin et al., 2010; Wrobel Daveau et al., 2010) which were thrust over the Arabian Platform during the Late Cretaceous (Ricou, 1971). The Cretaceous nappes are located between the Sanandaj-Sirjan Zone and the Simply Folded Belt or High Zagros Belt in the Lurestan and Fars Arcs, respectively. To the north, these areas are bounded by the Zagros suture which runs along the Main Zagros Thrust.

2. The **High Zagros** which corresponds topographically to the NW-SE striking, highest mountain ranges, reaching elevations of more than 4400 m, and is bounded by the Main Zagros Thrust to the north and High Zagros Fault to the south. This belt includes exposures of Lower Palaeozoic rocks thrust south-westward over Mesozoic and Tertiary sedimentary rocks along the High Zagros Fault (Tavakoli-Shirazi et al., 2012). The High Zagros does not extend continuously along the Zagros orogen but is restricted to two distinct locations: the Western and Eastern High Zagros respectively (Fig. I.1).

3. The **Simply Folded Belt** is located NE of the Mountain Front Fault and SW of the High Zagros Fault (Berberian, 1995). Its width varies along strike (Fig. I.1) due to the variable nature of the basal décollement in the Hormuz salt (e.g. lateral facies and/or thickness change). This area includes numerous “whale-back” anticlines and box-folds which deform the sedimentary cover of the Arabian platform.

4. The **Foreland Basin** is bounded to the NE by the Mountain Front Fault and to the SW by the Deformation Front, and was formed as a consequence of the Miocene propagation of deformation toward the foreland and coeval subsidence (Mouthereau et al. 2007, 2011). In this zone there are widespread outcrops of the Miocene Fars Group. The Oligo-Miocene Asmari Formation, which forms an

excellent carbonate reservoir, is buried in this area except at the Kuh-e-Asmari anticline in the Dezful Embayment.

I.2.3.1. Tectono-stratigraphy of the Western and Eastern High Zagros

In the Zagros orogen, the Phanerozoic succession comprises 7-12 km of sediments overlying Precambrian crystalline basement (Alavi, 2004) (Figs. I.2.a and I.2.b). Basement consists of the NNE-ward extension of the Arabian Shield (Late Proterozoic, Pan-African) (Motiei, 1993), and equivalent basement rocks are exposed in western Saudi Arabia but do not crop out within the Zagros. Top-basement shallows approaching the Main Zagros Thrust and is exposed at the surface in Central Iran, on the northern side of the Neo-Tethys suture, consisting here of magmatic and metamorphic rocks similar to those observed at the western margin of the Arabian Plate (Alavi, 1991).

The basement has been studied by means of aero-magnetic data and from exotic blocks brought to the surface in diapirs of Hormuz salt (Haynes and McQuillan, 1974; Kent, 1979). The top-basement surface is irregular and is cut by major north-south trending (“Arabian”) faults and by NW-SE trending faults (parallel to the Zagros suture) which have produced a step-wise geometry (Berberian, 1995). Vertical movements and periodic reactivation along basement faults have strongly affected the architecture of the Zagros basin and may explain lateral facies and thickness variations (Koop and Stoneley, 1982; Sherkati and Letouzey, 2004).

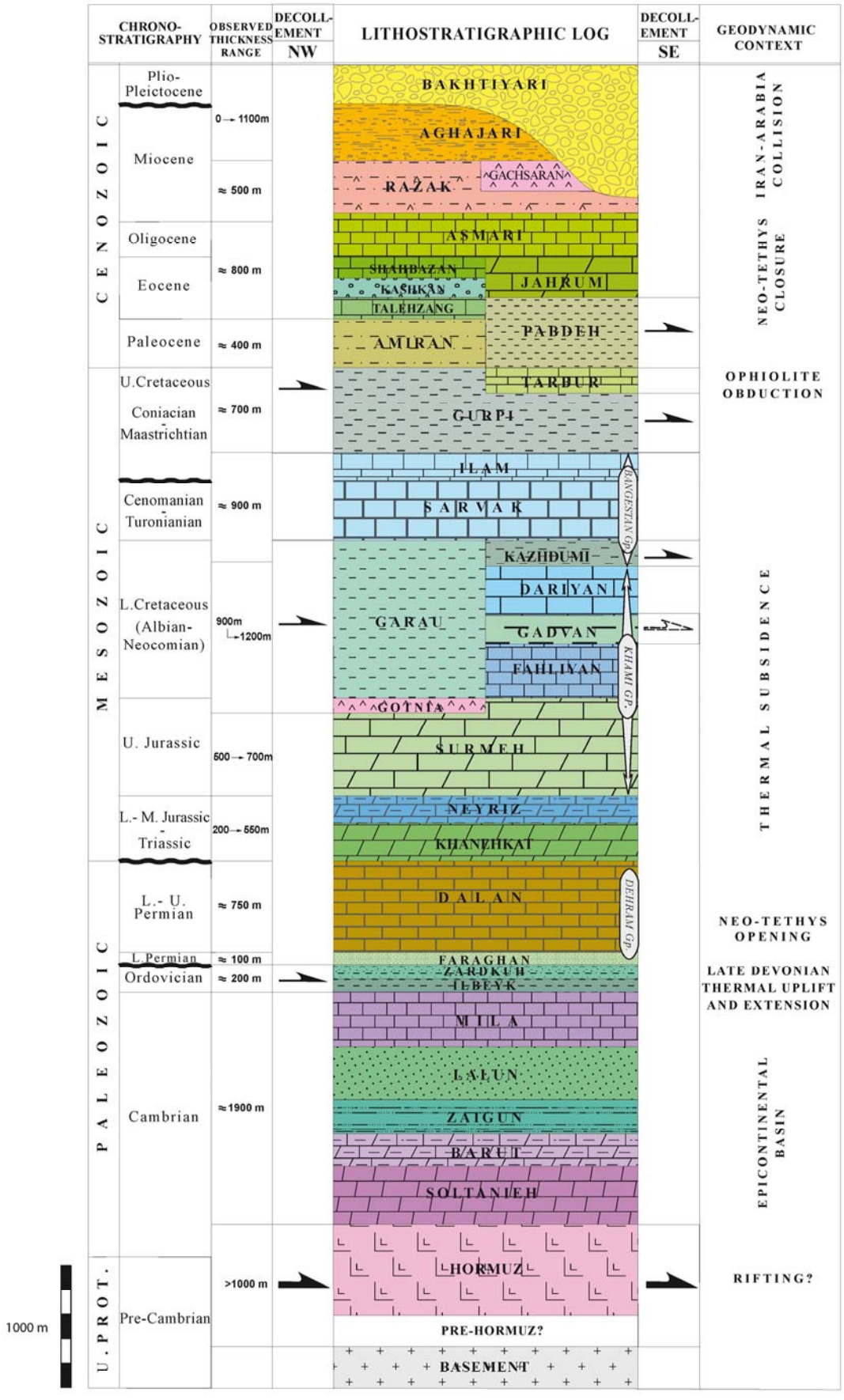
CHRONO-STRATIGRAPHY
OBSERVED THICKNESS RANGE
DECOLL-EMENT NW
LITHOSTRATIGRAPHIC LOG
DECOLL-EMENT SE
GEODYNAMIC CONTEXT
CENOZOIC
MESOZOIC
PALEOZOIC
U. PROT.
Plio-Pleictocene
Miocene
Oligocene
Eocene
Paleocene
U.Cretaceous
Coniacian
Maastrichtian
Cenomanian
Turonianian
L.Cretaceous (Albian-Neocomian)
U. Jurassic
L.- M. Jurassic - Triassic
L.- U. Permian
L. Permian
Ordovician
Cambrian
Pre-Cambrian
0 → 1100m
≈ 500 m
≈ 800 m
≈ 400 m
≈ 700 m
≈ 900 m
900m → 1200m
500 → 700m
200 → 550m
≈ 750 m
≈ 100 m
≈ 200 m
≈1900 m
>1000 m
1000 m
BAKHTIYARI
AGHAJARI
GACHSARAN
RAZAK
ASMARI
SHAHBAZAN
KASHKAN
JAHRUM
TALEHZANG
PABDEH
AMIRAN
TARBUR
GURPI
ILAM
SARVAK
BANGESTAN Gp.
KAZHDUMI
DARIYAN
GARAU
GADVAN
FAHLIYAN
KHAMI Gp.
GOTNIA
SURMEH
NEYRIZ
KHANEHKAT
DALAN
DEHRAM Gp.
FARAGHAN
ZARDKUH
ILBEYK
MILA
LALUN
ZAIGUN
BARUT
SOLTANIEH
HORMUZ
PRE-HORMUZ?
BASEMENT
IRAN-ARABIA COLLISION
NEO-TETHYS CLOSURE
OPHIOLITE OBDUCTION
THERMAL SUBSIDENCE
NEO-TETHYS OPENING
LATE DEVONIAN THERMAL UPLIFT AND EXTENSION
EPICONTINENTAL BASIN
RIFTING?

ⓐ

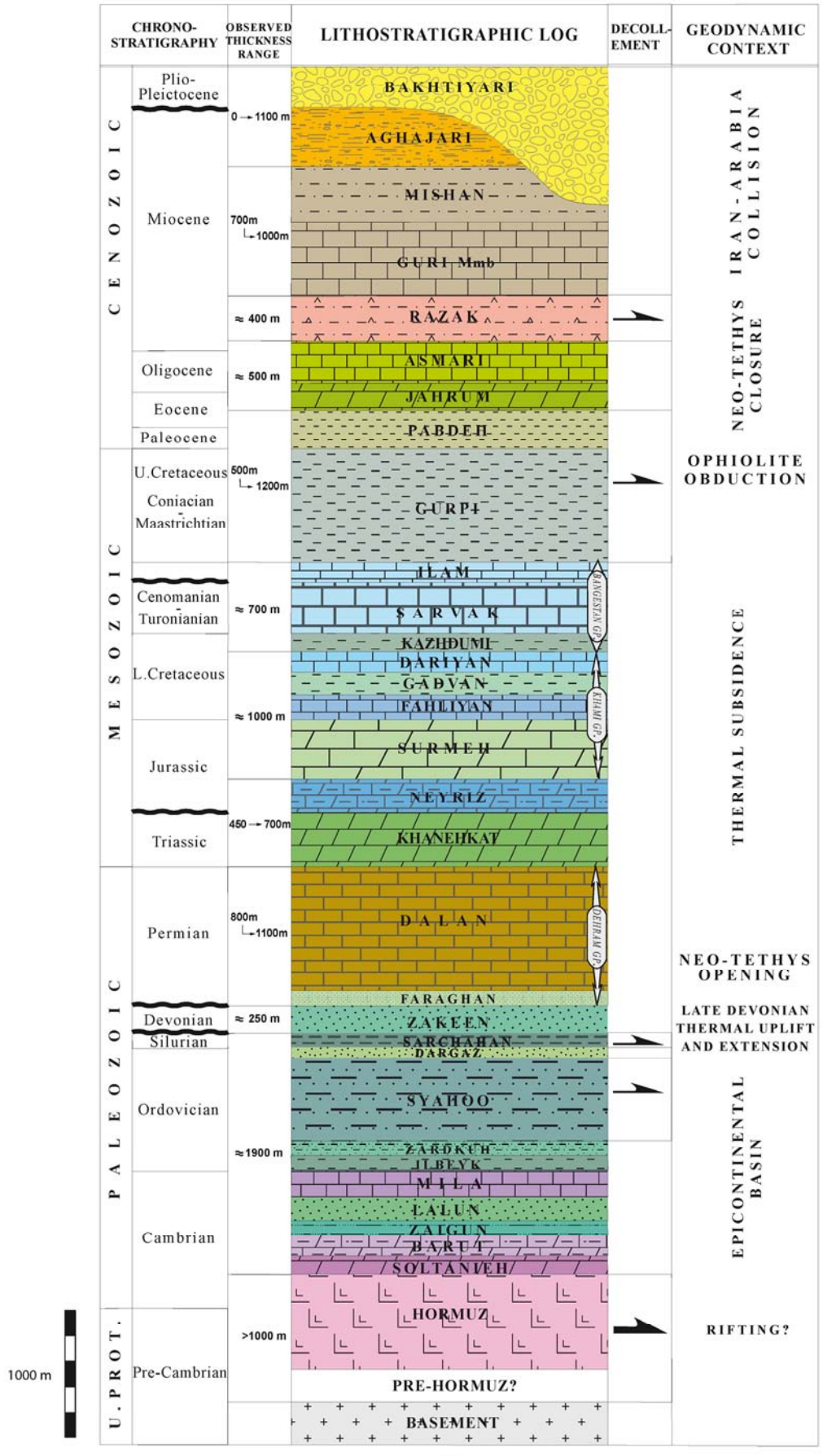
CHRONO-STRATIGRAPHY
OBSERVED THICKNESS RANGE
LITHOSTRATIGRAPHIC LOG
DECOLL-EMENT
GEODYNAMIC CONTEXT
CENOZOIC
MESOZOIC
PALEOZOIC
U.PROT.
Plio-Pleictocene
Miocene
Oligocene
Eocene
Paleocene
U.Cretaceous
Coniacian
Maastrichtian
Cenomanian
Turonianian
L.Cretaceous
Jurassic
Triassic
Permian
Devonian
Silurian
Ordovician
Cambrian
Pre-Cambrian
0 → 1100 m
700m → 1000m
≈ 400 m
≈ 500 m
500m → 1200m
≈ 700 m
≈ 1000 m
450 → 700m
800m → 1100m
≈ 250 m
≈1900 m
>1000 m
1000 m
BAKHTIYARI
AGHAJARI
MISHAN
GURI Mmb
RAZAK
ASMARI
JAHRUM
PABDEH
GURPI
ILAM
SARVAK
KAZHDUMI
DARIYAN
GADVAN
FAHLIYAN
SURMEH
NEYRIZ
KHANEHKAT
DALAN
FARAGHAN
ZAKEEN
SARCHAHAN
DARGAZ
SYAHOO
ZARDKUH
JLBEYK
MILA
LALUN
ZAIGUN
BARUT
SOLTANIEH
HORMUZ
PRE-HORMUZ?
BASEMENT
GANGESTAN GP.
KHAMI GP.
OEHRAM GP.
IRAN-ARABIA COLLISION
NEO-TETHYS CLOSURE
OPHIOLITE OBDUCTION
THERMAL SUBSIDENCE
NEO-TETHYS OPENING
LATE DEVONIAN THERMAL UPLIFT AND EXTENSION
EPICONTINENTAL BASIN
RIFTING?

b

Fig. I.2. *Tectonostratigraphic column for High Zagros Belt. The arrows identify décollement levels. a) Western High Zagros.. Note to the lateral variations of the mechanical behaviours along the belt. b) Eastern High Zagros.*

At the base of the sedimentary cover, the Infracambrian Hormuz salt (1000 to 1500 m thick) rests on basement and forms a major décollement (Fig. 1.2.a), decoupling the overlying sedimentary sequence from the rigid basement and sub-salt sediments (Jahani et al., 2009). The thickness of the salt interval may change significantly from the base of synclines to the crests of adjacent anticlines (Molinaro, 2005).

Late Precambrian - Early Palaeozoic rifting led to the development of an evaporitic basin to the east of the Qatar-Fars Arch, and the Hormuz Salt may be interpreted as a syn- to post-rift deposit (Jahani et al., 2009). A narrow branch of this evaporite basin extended towards the High Zagros Belt parallel to the Main Zagros Thrust (Sherkati et al., 2006; Jahani et al., 2009).

Thick pre-Permian siliciclastics were deposited in intra-cratonic basins throughout northern Gondwana (Ghienne et al., 2010). Cambro-Ordovician siliciclastics and minor carbonates (Figs. I.2.a and I.2.b) are recorded in numerous places at the base of the High Zagros Thrust, and at a single exposure within the Zagros Simply Folded Belt in the core of the Kuh-e-Surmeh anticline (Setudehnia, 1972; Gavillot et al., 2010; Tavakoli-Shirazi et al., 2012). A sea level rise due to the melting of Late Ordovician polar ice (e.g. Al Husseini, 1990) led to a rapid transgression and the deposition of organic–rich black shales during the Early Silurian. These black shales form major source rocks throughout north Africa and the Arabian Plate (Abu-Ali et al., 1991; Mahmoud et al., 1992; Bordenave, 2008; Bordenave and Hegre, 2010).

Palynological studies (Ghavidel Syooki, 2003) have led to the identification of Devonian sedimentary rocks in outcrops in the Eastern High Zagros and in wells in the Fars Arc. These consist mainly of sandstones with inter-bedded shales and subordinate dolomitic limestones at Kuh-e-Faraghan. These strata include abundant palynomorphs dated as Early Devonian -- Frasnian (Ghavidel Syooki, 2003).

A major pre-Permian unconformity exists everywhere in the ZFTB and is well exposed in the High Zagros (Tavakoli-Shirazi, et al., 2012). In the Eastern High Zagros, the Devonian is overlain unconformably by the Early Formation (Ghavidel-Syooki, 2003). This erosional unconformity in the Western High Zagros occurs at the top of the Cambian and/or Ordovician which suggests along-strike development of the hiatus from SE to NW of High Zagros Belt .At large scale, this unconformity seals a succession of “Arch” (uplift) and “Basin” (Low) geometry that likely originated from Late Devonian thermal uplift. Permian siliciclastics and carbonates were deposited in a sag basin resulting from the thermal subsidence followed the uplift. (Tavakoli-Shirazi et al., 2012).

By the Late Permian, the Neo-Tethys opened between the Arabian Plate and Iran (Berberian and King, 1981; Koop and Stoneley, 1982; Stampfli et al., 1991, 2001). During the Late Triassic to Early Cretaceous, the Arabian platform was a stable, shallow shelf dominated by carbonates with some evaporitic and detrital deposits. Numerous transgressions and regressions during the Mesozoic caused lateral facies changes of carbonates from the SE Zagros to Lurestan Province (Setudehnia, 1978; Van Buchem et al., 2003). Patterns of sedimentation on the Arabian and Zagros platform during the Mesozoic (particularly in the Cretaceous) were strongly influenced by the presence of deep-seated basement faults (Sherkati and Letouzey, 2004).

“Obduction” (i.e. emplacement of the Cretaceous nappe complex) occurred during the Coniacian – Santonian, and changed the configuration of the NE margin of the Arabian plate by forming a flexural basin characterised by accumulation of Campanian flysch (Homke et al., 2009). Nappe emplacement was followed by uplift, which resulted in Palaeocene erosion in the High Zagros (Sherkati et al. 2006). This was followed by a relatively quiescent period from the Late Eocene (deposition of the Jahrum carbonate) to the Early Miocene (Asmari Limestone. Progressive closure of the Neo-Tethys led to development of regressive evaporitic and siliciclastic sequences (Fars Group) during the Mio-Pliocene (Figs. I.2.a and I.2.b); these are unconformably overlain by synorogenic conglomerates of the Bakhtiyari Formation (Berberian, 1995; Fakhari et al., 2008). The Bakhtiyari Formation has been dated as

Pliocene (James and Wynd, 1965; Stocklin, 1968; Setudehnia, 1972; Berberian and King, 1981), but its age in the Western High Zagros was recently revised by Fakhari et al. (2008) to Late Oligocene (?) -- Early Miocene. This is consistent with an outward propagation of folding during the Zagros orogeny.

I.2.3.2. Materials and Methods

The study area consists of two separated domains located south of the Main Zagros Thrust fault (Fig. I.1). These areas are already covered by some published general geological maps and associated sections. Our close field examination revealed necessity of some revisions especially in the western zone.

In the Western High Zagros, field investigations were carried out between Sisakht in the SE and an area beyond Baznavid and Ghalikuh to the NW. The outcropping Palaeozoic succession was studied and four SE-NW oriented, regional-scale transects (Fig. I.3) were constructed. Two major structures, the Lajin and Bazman anticlines, were mapped in detail to investigate the angular unconformity between the Lower Permian and Cambro-Ordovician succession. These field studies resulted in the preparation of a geological map of the Western High Zagros combined with a Digital Elevation Model (DEM) (Fig. I.3).

In the Eastern High Zagros, three large-scale anticlines (Gahkum, Faraghan and Kuh-e–Khush) were investigated. These anticlines are located in SE margin of the orogen, north of Bandar-Abbas city. An integrated geological map and DEM was prepared to illustrate the major tectonic features and rock units in this area, and three structural cross-sections were constructed. Also benefitted from numerous field photos, taken during previous geological reconnaissance. In order to produce the finished drawings, existing 1:100,000 and 1:250,000 scale geological maps were modified and complemented by Shuttle Radar Topography Mission (SRTM) elevation data, satellite Landsat™ Images, and geological information based upon new fieldwork.

Geosec® software, licensed to TOTAL CSTJF, was used to validate and balance the structural cross-sections. This is a multi-faceted geology tool that provides valuable insights about the basin geometry and structural history. It supports multiple modules to assist in the analysis of tectonic processes. For each section, a “pin line” was first defined to limit the deformation, and crustal components which were assumed to have been transferred by similar kinematic mechanisms were then identified. “Flexural Slip” and “Vertical/Oblique Slip” were two restoration techniques utilized in the modelling. The “Transfer Flexural Slip” tool was used to restore the cross-sections to a pre-deformation state. The tool performs slip movements along fault planes and parallel bedding planes using geometrical rules, and respecting the preservation of bed lengths and thicknesses for stiff units (c.f. Dahlstrom, 1969; Woodward et al., 1985).

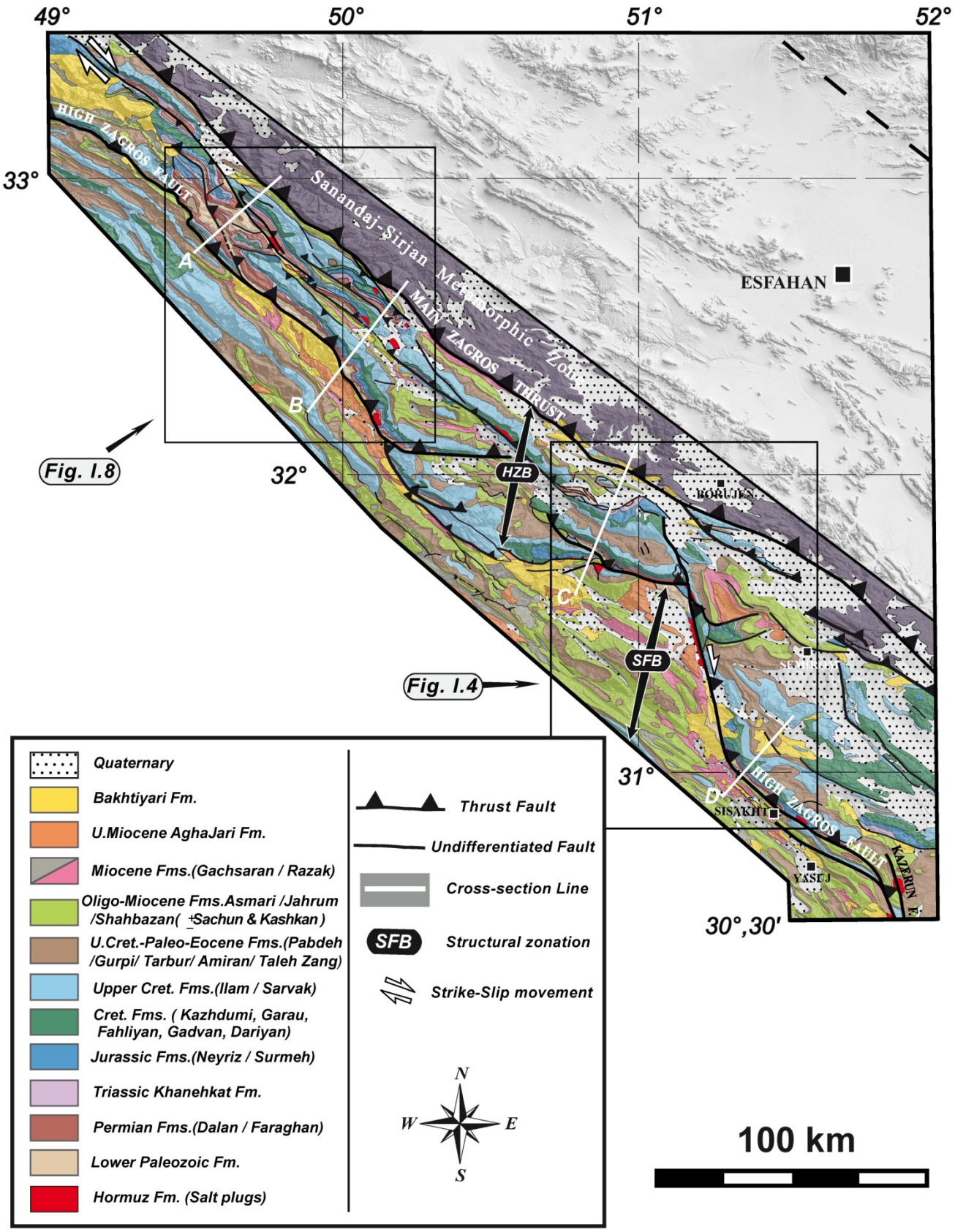

Fig. I.3. Geological map of the West High Zagros plotted over SRTM data. Lines A, B, C and D are the location of the structural transects and refer to Figs. I.5, I.9, I.10 and I.12, respectively.

I.2.4. Geometry and Kinematics of the Western High Zagros

This area is located between approximately lat. 30°00' - 33°30' N and long. 49°00' - 53°00' E (Figs. I.1 and I.3). It is about 450 km long and 40 to 80 km wide, the width increasing to the SE. On detailed geological maps (Figs. I.4 and I.8), NW-trending imbricated folds and thrust-faults associated with strike-slip movements can be observed. In general, this region is the oldest part of the Zagros fold-and-thrust belt. Increasing and progressive regional compression led to a high amount of shortening in this zone, and the propagation of the deformation front toward the SW.

The four balanced cross-sections extend from the Main Zagros Thrust fault in the north to the High Zagros Fault in the south, and are labelled A, B, C and D from NW to SE (Figs. I.1 and I.3). All the sections are oriented NE-SW, i.e. parallel to the inferred tectonic transport direction and perpendicular to the trends of folds and thrusts. The sections are based on field investigations and on data in surface stratigraphic logs, as well as information in maps provided by the National Iranian Oil Company (NIOC) and Geological Survey of Iran (GSI). No seismic lines were available to calibrate the tops of subsurface formations, or the style and geometry of structures at depth.

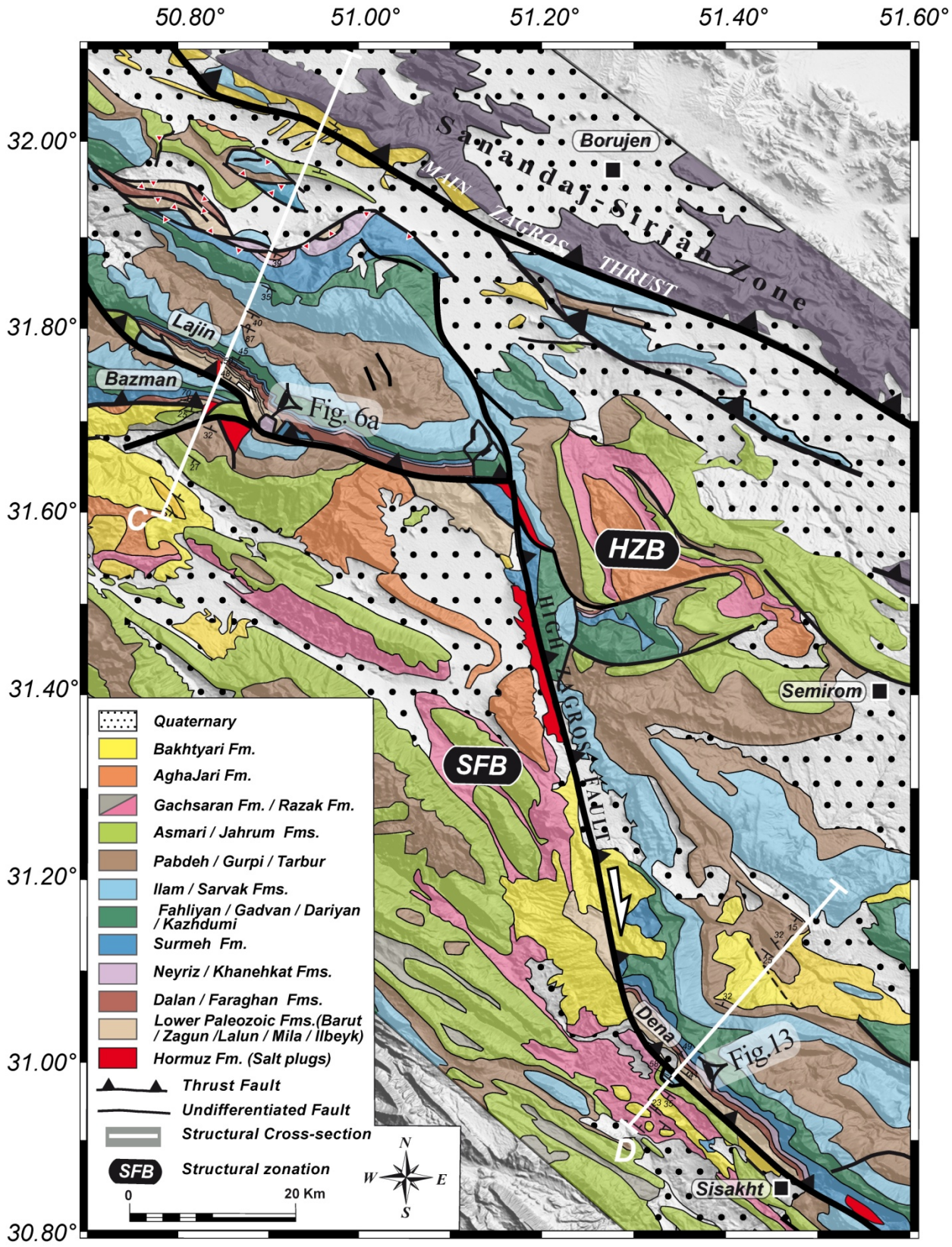

Fig. I.4. Detailed geological map of the Lajin and Dena regions plotted over SRTM data. Sections C and D correspond to Lajin and Dena.

I.2.4.1. The Lajin cross-section (transect C)

Gavillot et al. (2010) used thermo-chronometric data to study the Lajin and adjacent structures in order to constrain the timing of thrust activity in this part of the High Zagros. They drew a cross-section profiling shallow crustal structures, which was used to investigate thrust sheet exhumation in the context of cooling ages given by the (U-Th)/He method. The new, 60-km long cross-section is shown in figure. I.5. Shortening of the sedimentary cover for this section was calculated to be 14.7 km (24%). The section exhibits a succession of folds cut by mostly south-verging thrust faults. Kuh-e-Lajin, one of the highest mountains in this area, is located on the hanging wall of the High Zagros Fault. Figures. I.6.a and I.6.b illustrate Cambrian siliciclastics at the base of Lajin Mountain which are thrust onto Cretaceous limestone and were exhumed along this fault. Kuh-e-Bazman is an adjacent structure to the south where a diapir of Hormuz salt has penetrated up through the equivalent thrust plane to the surface, emerging as the Bazman diapir. This thrust fault, and the Lajin fault, may be interpreted as splays of the High Zagros basement Fault, and are out-of-sequence thrusts which cut through the entire sedimentary succession.

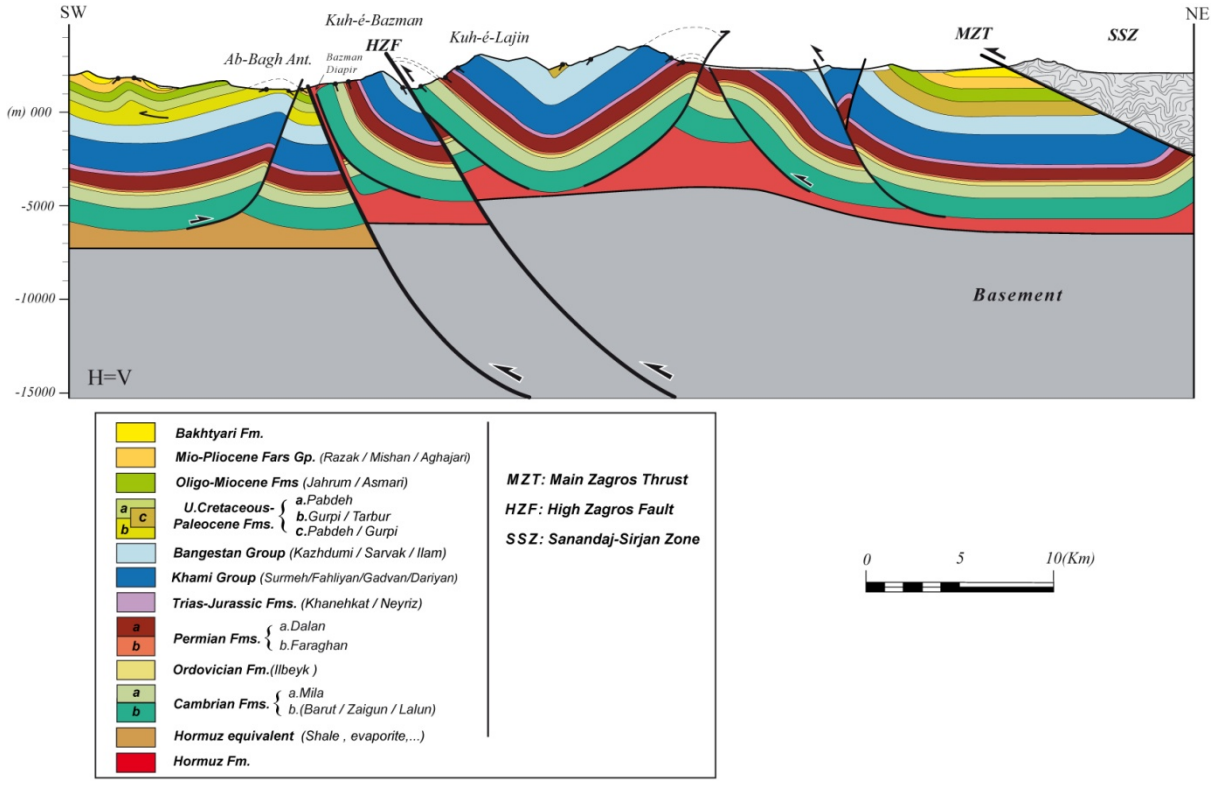

Fig. I.5. Structural cross-section of the Lajin and Bazman anticlines (see location on Fig. I.4)

The cross-section illustrates the activation of back thrusts rooting in the Hormuz salt. These structures can be traced in the northern flanks of Kuh-e-Lajin and the northern limb of the asymmetric Ab-Bagh anticline (Fig. I.5). In the absence of multiple intermediate décollements in this section (except the probable Late Cretaceous - Early Eocene Gurpi-Pabdeh Formations in the south of the section), the structural configuration is mainly characterized by the development of large-scale detachment folds over the ductile Hormuz salt, which have been cut subsequently by deep-rooted fore- and back thrusts. Progressive growth and uplift of this fold-thrust system was followed by intense erosion and the removal of the frontal limbs of the anticlines (in most cases the southern ones), causing them to resemble a series of monoclines.

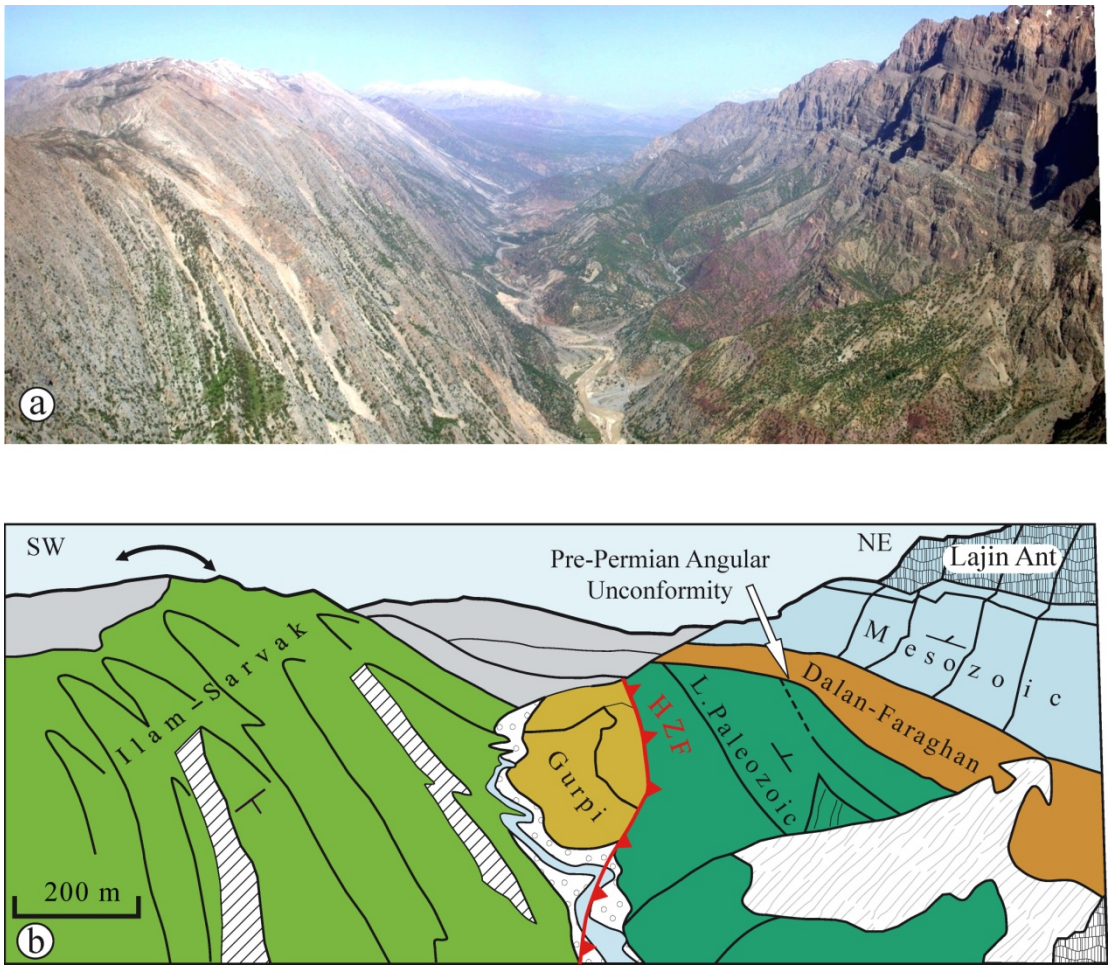

Fig. I.6. *a) Aerial view of the Lajin anticline and adjacent areas (see location on Fig. I.4).*
b) Line drawing of Fig. I.6.a. The NE dipping High Zagros Fault at the base of the cliff has juxtaposed Cambrian siliciclastics against Upper Cretaceous carbonates. The southern flank of the Lajin structure has been removed after erosion which formed a deep gorge.

A mature salt-cored structure can be observed between the Main Zagros Thrust and Kuh-e-Lajin (Fig. I.5). This structure consists of two faulted detachment anticlines with two high-angle fore- and back-thrusts in the southern and northern flanks respectively, which are separated by an intervening shallow syncline. Thickening of Hormuz salt in the central part of this area is inferred due to compression associated with cover shortening. The Hormuz salt responded in a ductile manner to fold growth, leading to the migration of material towards the cores of anticlines from adjacent synclines. Depletion of the salt from synclines led to "downwarping" and possible welding of the basal salt onto the basement (e.g., Sherkati et al. 2006; Callot et al. 2007). During advanced stages of deformation, the lack of supplementary salt prevented further amplification of salt-cored anticlines, resulting in steepening and subsequent failure of the limbs.

Kinematics of the Lajin cross-section

Structural analysis of cross-section "C" allows the main stages in the history of folding and thrusting in this area to be studied. A three-stage kinematic restoration for section C is proposed (Fig. I.7).

During stage (1), buckling of sedimentary strata above the Hormuz basal décollement was responsible for the initiation of salt-cored anticlinal folds which grew as relatively symmetrical structures. This mechanism has been discussed by Davis and Engelder (1985), Davis and Lille (1994) and Sherkati et al. (2005), and has been presented by scaled analogue modelling (e.g. Letouzey et al., 1995; Cotton and Koyi, 2000; Sherkati et al., 2006). The Hormuz salt totally decouples the structures of the sedimentary cover from the underlying crystalline basement.The wavelength of the cover structures was controlled by the thickness of competent units in the overlying succession.

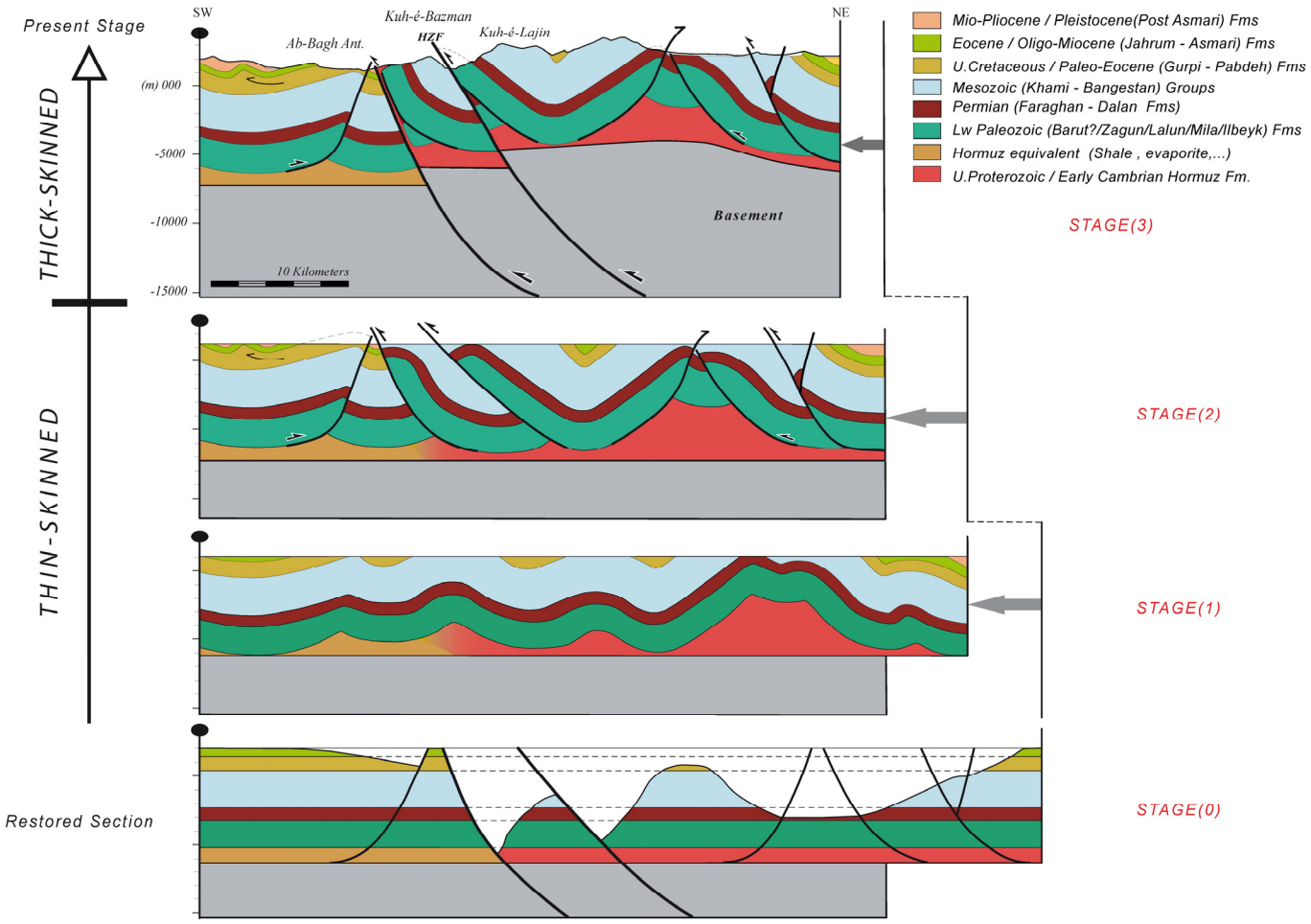

Fig. I.7. *Incremental three-step (two-phase) forward model of the Lajin cross-section (Fig. I.5). Restoration of the cross-section yields 14.7 km of shortening in the cover versus 3.25 km in the basement.*

Stage (2) was characterized by the progressive development of the earlier-formed structures and by a transition from concentric folding to fault-detachment folding. During this stage, the growth of anticlines due to the amplification and tightening resulted in the initiation of shearing in the over-steepened flanks. Progressive deformation led to failure of high-strain zones in the fold with the development of major thrust fault. The vergence of these faults was mainly to the south, and they transferred the displacement from the floor to shallower crustal levels. Lower flats originated as sole thrusts (McClay, 2000) in the low friction basal Hormuz décollement and ramped-up to cut the folds. The upper flats are inferred to have terminated at an intermediate-level detachment (e.g. the Pabdeh-Gurpi Formation shales) or at a contemporaneous erosion surface. The generation of

footwall synclines, high-angle faults and hanging wall monoclines are other significant structural features of stage (2).

Stage (3) was characterized by the activation of basement faults during the final stages of orogenesis, and by the development of a crustal-scale out-of-sequence thrust. This stage corresponds to the initiation of two master basement faults interpreted as segments of the High Zagros Fault at the base of the Lajin and Bazman structures, respectively (Fig. I.7). Due to sense of reverse displacements on these thrusts, the basement and associated sedimentary succession have been significantly uplifted. Such huge vertical offset indicates the location of a major step in the basement. Differences in the level of cover rocks exposed on either side of these faults can be explained by this feature. The involvement of the basement is also indicated by analysis of seismic activity (Berberian, 1995; Molinaro et al., 2005) showing that earthquake hypocentres are located in the basement.

The geometry and timing of basement deformation is difficult to evaluate in most of the Zagros fold-and-thrust belt as faults are commonly blind and strike parallel to the major surface structures (Sherkati et al., 2005). In the Eastern High Zagros, by contrast, basement faults cut obliquely across earlier detachment folds (Molinaro et al., 2005; Leturmy et al., 2010) and result in significant interference structures (see below).

I.2.4.2. Cross-sections A, B and D in the Western High Zagros

In order to investigate lateral variations in structural characteristics and shortening ratios, cross-sections A, B and D were constructed (Fig. I.3) approximately parallel to the Lajin cross-section.

Transect “A” (Figs. I.8 and I.9), the most NW section through the Western High Zagros, is located near the village of Baznavid and is about 43 km long. Cover shortening in this section is estimated at 20 km (33.5%). As in section C, fault-detachment folding in the cover, subsequently cut by later basement thrusting, is a prominent feature of the section. In addition, the section is characterised by a central uplifted zone [(“pop-up” structure, (McClay, 2000)] involving both basement and

cover (Fig. I.9). This structure formed as a result of movement along a major deep-rooted back-thrust associated with the displacement on the High Zagros Fault. Lower Palaeozoic (Cambrian and Ordovician) rocks have been exhumed either in the unroofed cores of asymmetric anticlines in this area or due to displacement on fore- and back- thrusts.

Sherkati and Letouzey (2004) proposed that back thrusts in the Dezful embayment formed due to deposition of the Fars Group which acted as a resistant buttress preventing the forward propagation of deformation and causing the tightening of folds and the piling-up of structures in the hinterland (e.g. Izeh zone and Western High Zagros). A significant feature in the Baznavid area is the presence of emergent Hormuz salt diapirs which coincide with the surface expression of deep-seated fault systems.

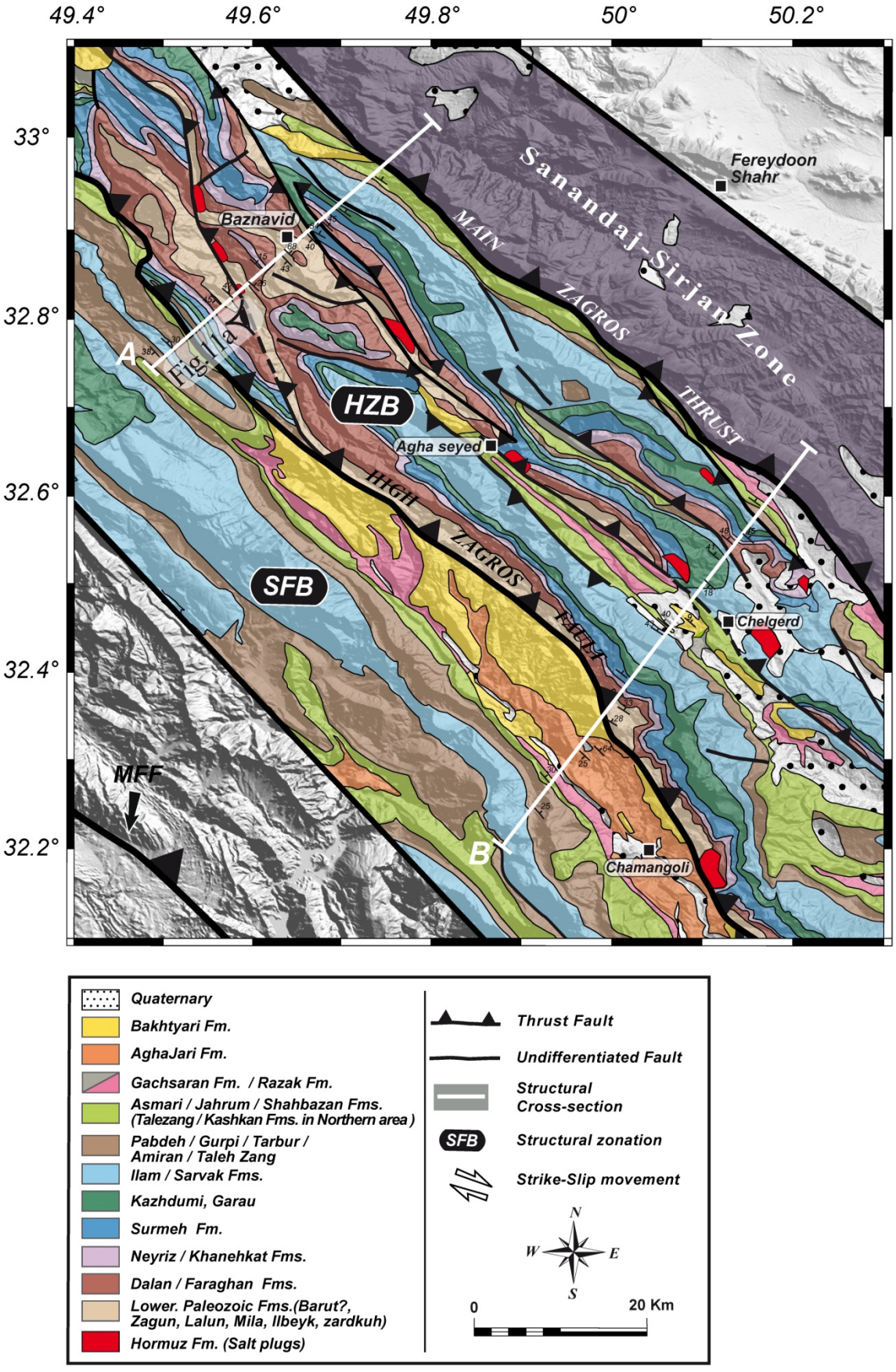

Fig. I.8. Detailed geological map of the Baznavid and Zardkuh regions plotted over SRTM data.Sections A and B are Baznavid and Zardkuh, respectively.

The northern part of the Baznavid transect is affected by a major contrast in mechanical behaviour of formations within the Palaeozoic succession. Sherkati and Letouzey (2004) presented evidence for the reactivation of N-S basement faults (e.g. the Hendijan-Bahregansar Fault: figure I.1) on basin architecture and on lateral changes of facies and formation thickness in the Izeh zone and Dezful Embayment. Consistent with this, the present study indicates the influence of the Hendijan-Bahregansar fault on the geometry of the basin.

A possible northward extension of this fault (Fig. I.1) may cross the High Zagros Belt and divide it into two parts. Activation of this sub-vertical or vertical structure during the Ordovician may have controlled the depth, and accordingly the thickness and facies, of deposits. The deeper-water depositional environment to the NW of the Western High Zagros may have been suitable for the deposition of thick Ordovician shales (e.g. the Ilbeyk Formation; figure. I.2.a) which probably do not exist to the east. Therefore, this difference makes variations in mechanical stratigraphy from one side to the other side of the Hendijan-Bahregansar fault. Due to the presence of the incompetent Ilbeyk and Zardkuh Formations in the NW of the Baznavid cross-section, near the Main Zagros Thrust, the presence of disharmonic folding within the Palaeozoic succession can be inferred. These intervals may have acted as a deep-intermediate décollement and together with that in the Hormuz salt, resulted in the development of duplex structures within the cores of Lower Palaeozoic anticlines (Fig. I.9).

Moreover, figure. I.8 suggests that the oldest outcrops to the north of the back thrust are of Permian age and this can be linked to the activation of an underlying intermediate-level detachment and consequently to the presence of duplex structures within the Lower Palaeozoic.

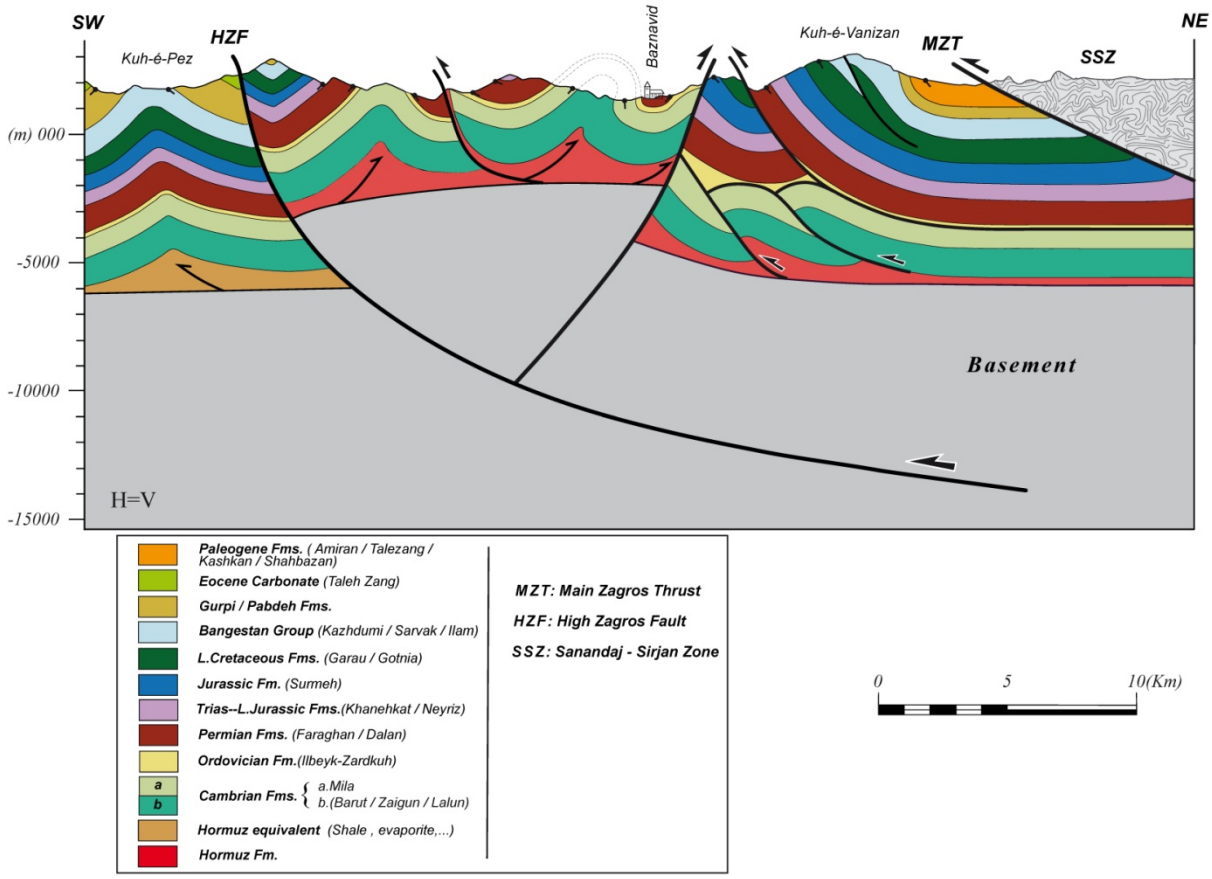

Fig. I.9. *Structural transect of the Baznavid area (see Fig. I.8 for section line).*

Transect B (Fig. I.8), also referred to as the Zardkuh cross-section (Fig. I.10), is located further to the east and is about 57 km long. After restoration, the shortening in the cover was estimated at 22.3 km (~ 28%). The section is characterized by a sequence of south-vergent anticlines and footwall synclines separated by successive thrusts. The tectonic style of this transect (Fig. I.10) is similar to that in cross-sections A and C, and comprises large-scale detachment folds decoupled from the basement along the Hormuz salt. These folds have been cut by later reverse and thrust faults.

The Zardkuh section is located to the west of the Hendijan-Bahregansar fault, allowing the construction of a duplex model for the Lower Palaeozoic succession. Similarly, NW-ward facies variations in the Cretaceous succession may indicate the presence of other décollements at upper-intermediate levels in this area, probably comprising the shales and marls of the Cretaceous Garau and Gurpi Formations

(Fig. I.2.a).These units were able to localize deformation in the form of superficial and short-wavelength folds (Figs. I.11.a and I.11.b).

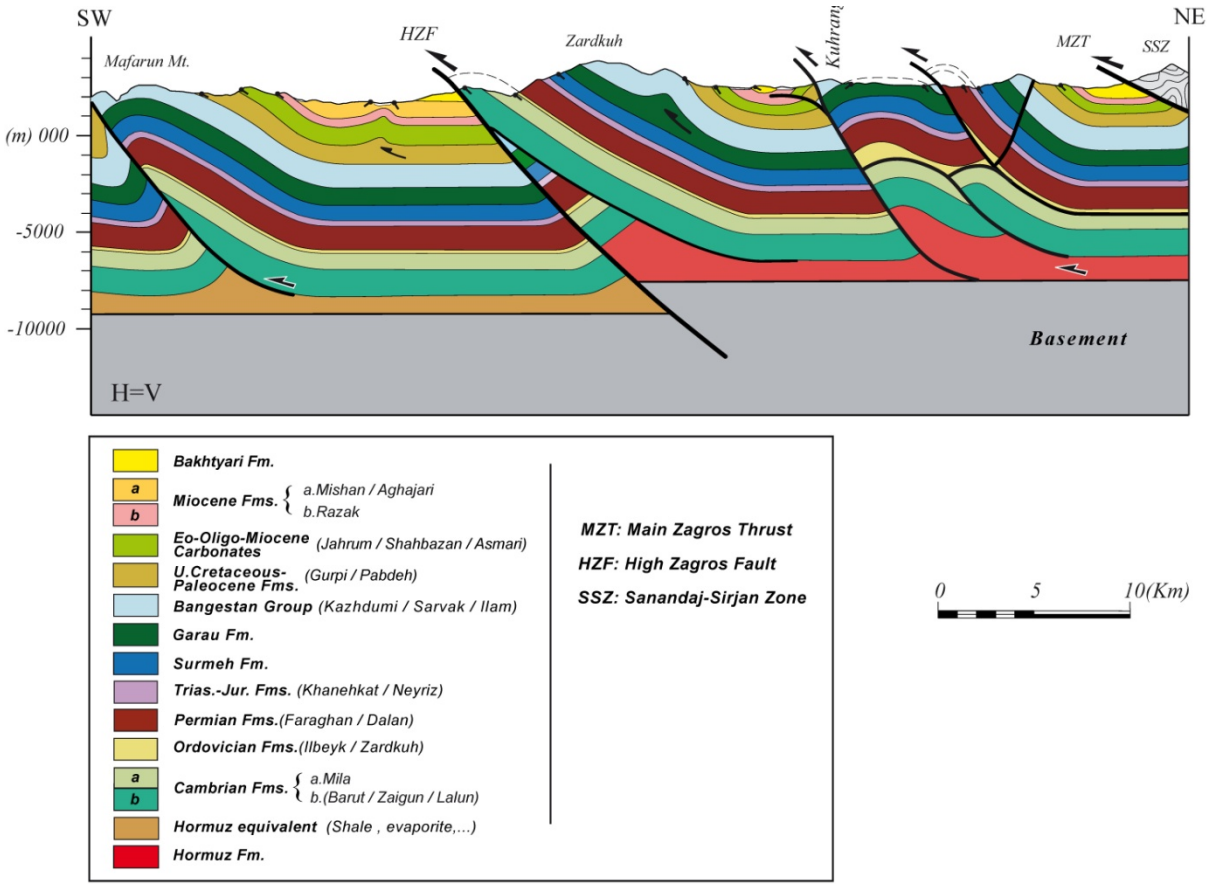

Fig. I.10. *Structural transect of the Zardkuh area (see section line on Fig. I.8).*

The latest stage of structural evolution in this area corresponds to vertical offset along the High Zagros Fault. On the south of this fault, the Bakhtiyari Formation conglomerates rest on the upper Miocene Aghajari Formation with no visible unconformity. Lower Palaeozoic rocks have been thrust over the Bakhtiyari Formation along the High Zagros Fault. This observation suggests that the most recent activation of the High Zagros basement fault occurred after the Middle Miocene, which is the revised age of this latter unit (Fakhari et al., 2008).

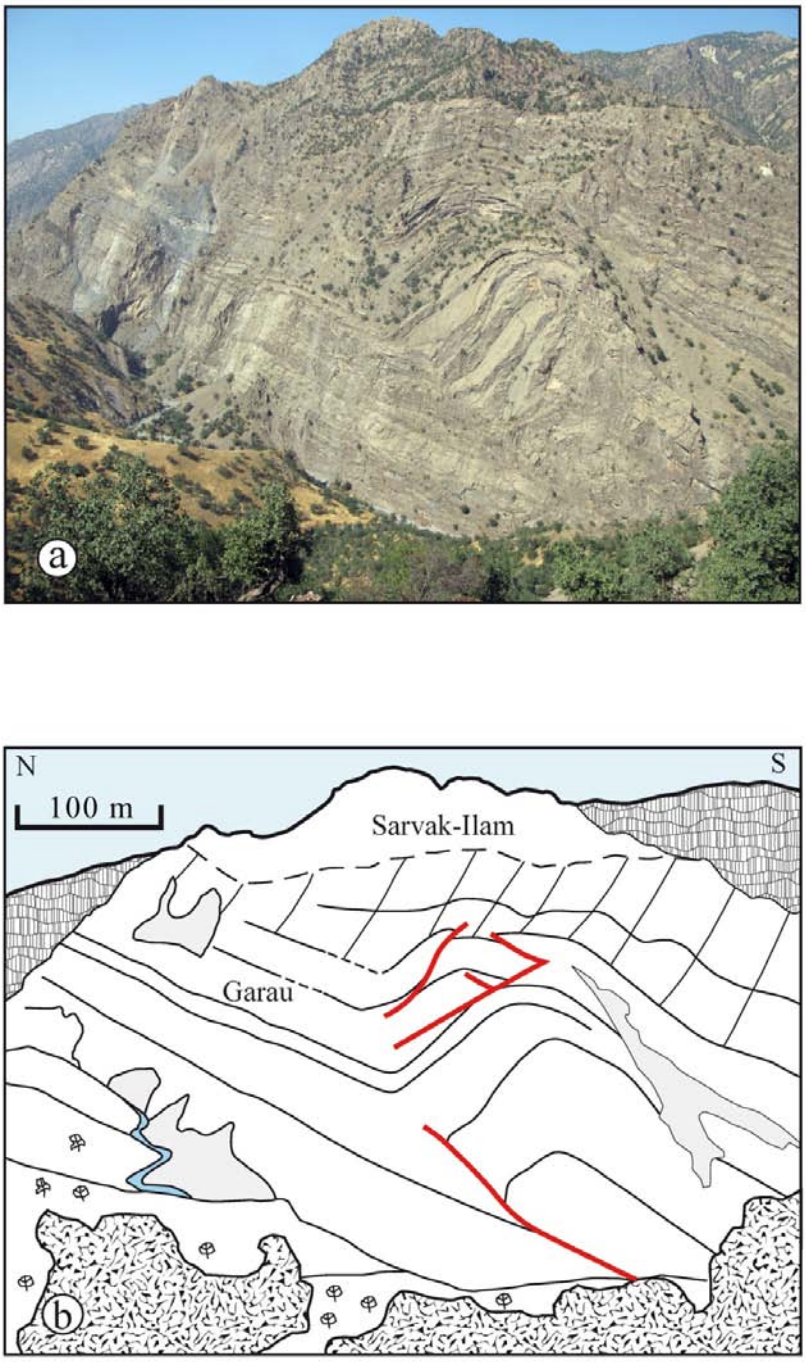

Fig. I.11 a) *Field photograph of the Cretaceous Garau Formation in the NW of the West High Zagros (see Fig. I.8).* ***b****) Line drawing of Fig. I.11.a. The Garau Formation was not folded isopach and steep thrust fault flattened within this Formation. It acted as a detachment level in this area.*

Transect D (Fig. I.12) illustrates the architecture of the major Dena anticline and the surrounding areas. Dena Mountain (about 4400 m) has the highest topography of the entire Zagros. Detachment folding and late-stage out-of-sequence

thrusting has controlled the deformation style in this section, as elsewhere in the Western High Zagros. Basal part of the high-amplitude Dena monocline on the hanging-wall of the High Zagros Fault consists of a Cambrian succession (Zaigun, Lalun and Mila Formations) which has been transported to the surface and juxtaposed against Mesozoic carbonates. Well-preserved slickensides (Fig. I.13) on fault planes at the base of Dena Mountain show that offset along this fault is reverse.

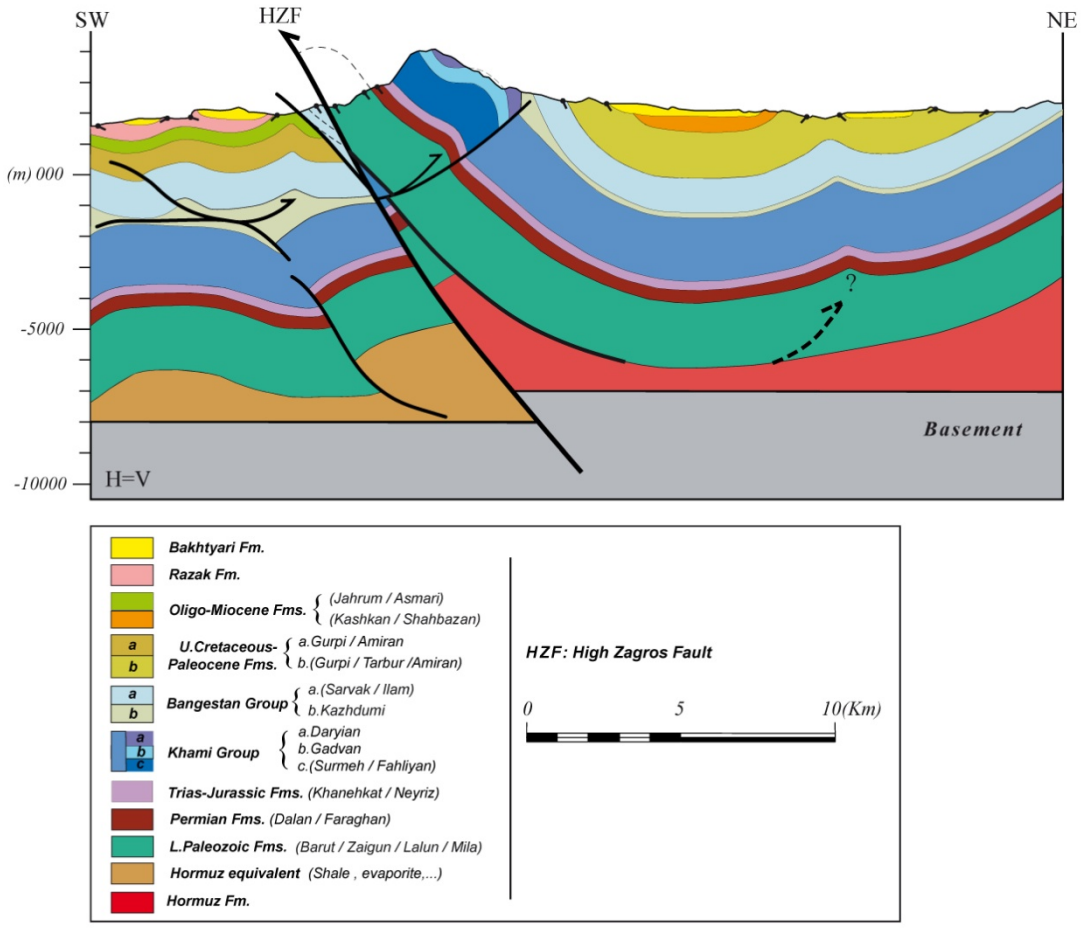

Fig. I.12. *Structural transect of the Dena anticline. The depth-to-detachment of the minor anticline within the broad syncline is not clear.*

In view of the major increase in thickness of the Albian shales (Kazhdumi Formation) from 350 m to 1100 m in the *Mokhtar-1* borehole (Fig. I.1) and the studies by Sherkati and Letouzey (2004) in this region, the presence of disharmonic folding in the Dena transect can be inferred. The Albian shales may be interpreted as a mid-intermediate detachment level (Fig. I.2.a), which masks underlying structures by the development of minor surface folds. There is subsidiary folding on the back-

limb of the Dena anticline, which may be interpreted as the product of a back thrust verging towards the hinterland

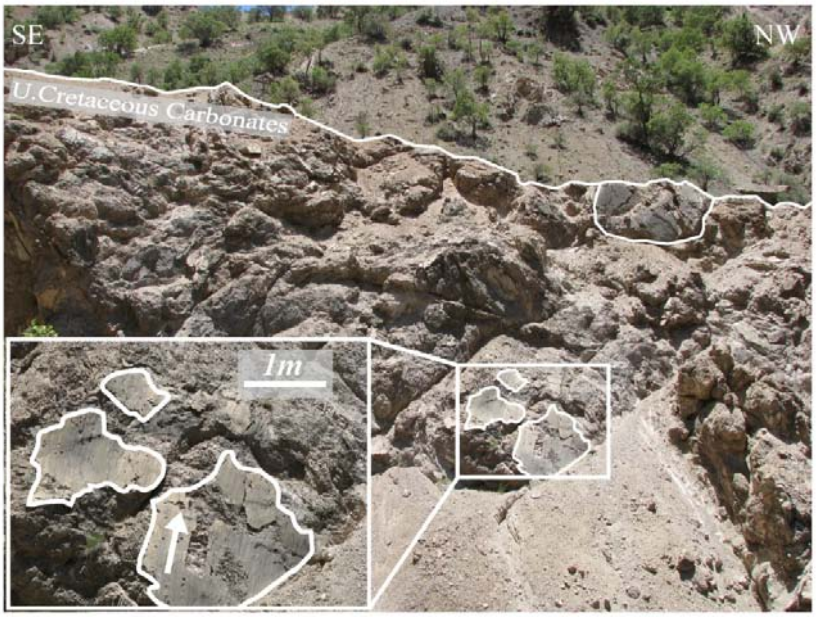

Fig. I.13. Deformed carbonate rocks in the footwall of the High Zagros Fault at Dena Mountain.Slickensides with a dip-slip component are present on the polished surfaces of the fault plane (see Fig. I.4 for layout).

I.2.5. Geometry and Kinematics of the Eastern High Zagros

This area is located in the eastern part of the Fars Arc, between lat. 27°30'-28°30' N and long. 55°30' – 57°00' E (Fig. I.14). Three major NW-trending anticlines (Gahkum, Faraghan and Kuh-e–Khush) are located here and cross-cut older east-west structural trends in the Bandar-Abbas syntaxis. These structures represent major topographic features and reach the highest elevations in the SE Zagros, exposing rocks as old as Ordovician in their cores. The dominant trend of these structures is NW-SE, although the eastern tips trend ENE as with other folds in this area. The en echelon alignment of these three structures was noted by Ricou (1974) and coincides with the alignment of seismic events which Berberian (1995) attributed to movement on the High Zagros basement fault. Basement faults, the timing of structures and halokinesis in this area have been studied by Molinaro et al. (2005), Jahani et al. (2009) and Leturmy et al. (2010).

Three cross-sections across the above-mentioned structures in the Eastern High Zagros were constructed and are referred to as sections E (Gahkum), F (Faraghan) and G (Kuh-e-Khush) (Fig. I.14).

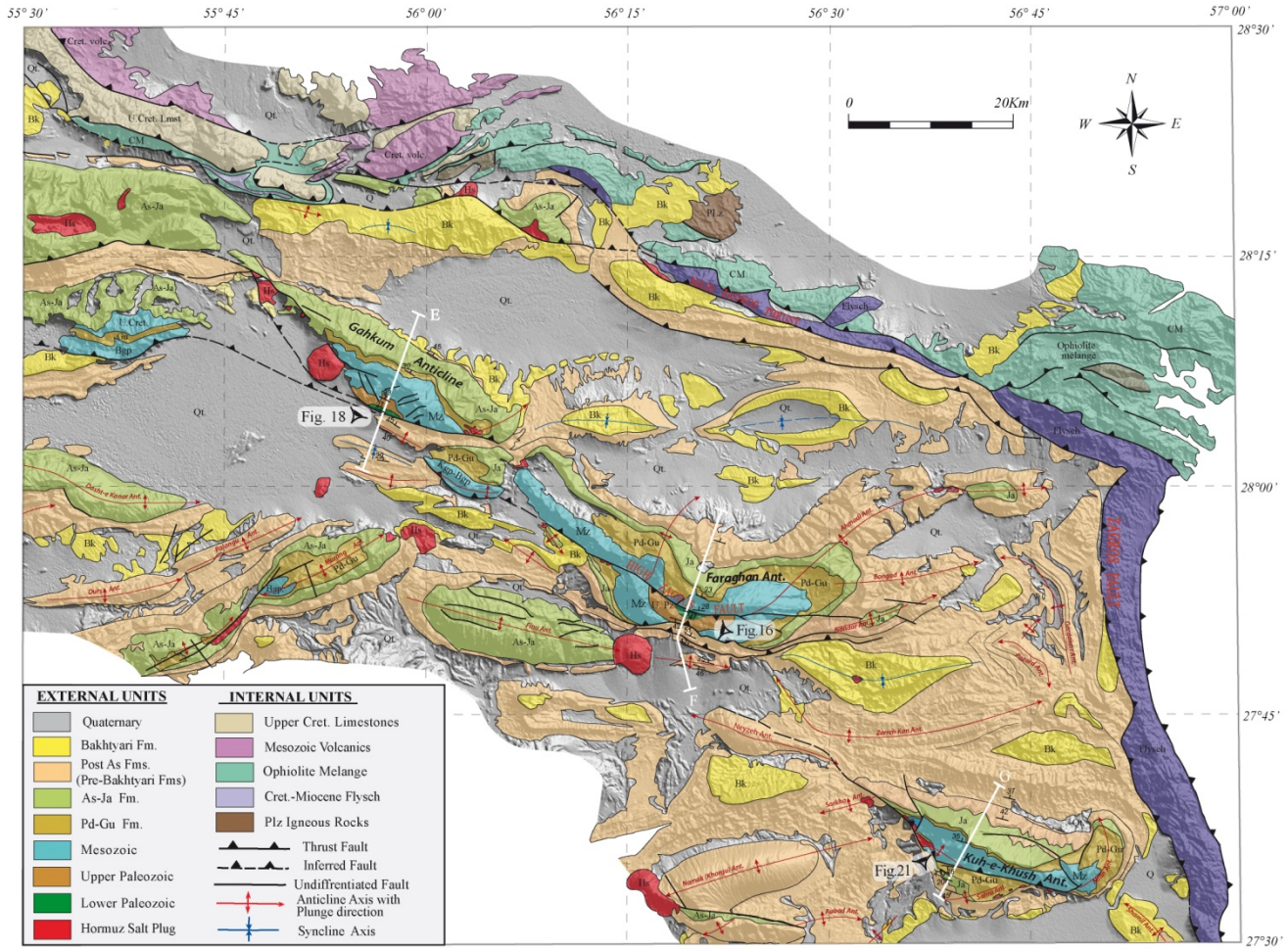

Fig. I.14. *Geological map overlain on SRTM data of the East High Zagros. Lines E, F and G are the locations of the structural transects and refer to Figs. I.15, I.19 and I.20, respectively.*

I.2.5.1. The Faraghan cross-section

Faraghan is the most prominent structure in the eastern Zagros with an elevation of about 3200 m. This anticline presents in map view a “butterfly” shape (Fig. I.14) due to superimposed folding (Molinaro et al., 2005). It was generated initially as a concentric detachment fold above the Hormuz Formation (Fig. I.2.b) with migration of the salt from the adjacent syncline into the core of the anticline Molinaro et al. (2005). In the east of the Fars Arc, pre-existing diapirs are responsible for the

initiation of structures including folds and thrusts (Letouzey and Sherkati, 2004; Callot et al., 2007; Jahani et al., 2009). Salt movement may result in thickness variations of strata along the flanks of the structures and may explain decreases in Palaeozoic (and Mesozoic?) stratal thicknesses from the bottom of synclines toward the crests of anticlines.

The exposed core of the Faraghan structure is composed of Permian Dalan Formation carbonates and Faraghan Formation sandstones, Devonian Zakeen Formation siliciclastics and Sacharan-Syahoo Formation black shales and sandstones (Silurian-Ordovician), all dipping to the south and presenting an arcuate shape (Fig. I.14). This part of the fold is bounded by tectonic contacts: to the south by a north-dipping basement fault over a footwall syncline of Mishan marls; and to the north by a south-dipping back thrust over the Mesozoic carbonates (Figs. I.15 and I.16).

The structural style in this section is also affected by interference of the intermediate décollement horizons. The geometry of the Faraghan anticline is only compatible with a deep-seated principal detachment (Hormuz salt), whereas the short wavelength of the superficial folds implies the probable activation of secondary, shallower décollements for example in the Upper Cretaceous - Palaeogene shales and marls (Gurpi - Pabdeh Formations) or Oligo-Miocene evaporates and siliciclastics (Razak-Mishan Formations) during folding (Fig. I.15). Another possible intermediate-level detachment may correspond to the shales of the Syahoo and Sarchahan Formations, which together with the Hormuz salt have isolated the more competent Cambrian rocks and accommodated deformation as a duplex structure in the core of the anticline (Fig. I.15). Deep-intermediate décollement levels were active throughout the progressive shortening of the sedimentary cover, and led to the generation of disharmonic folding, subordinate faults and duplexes.

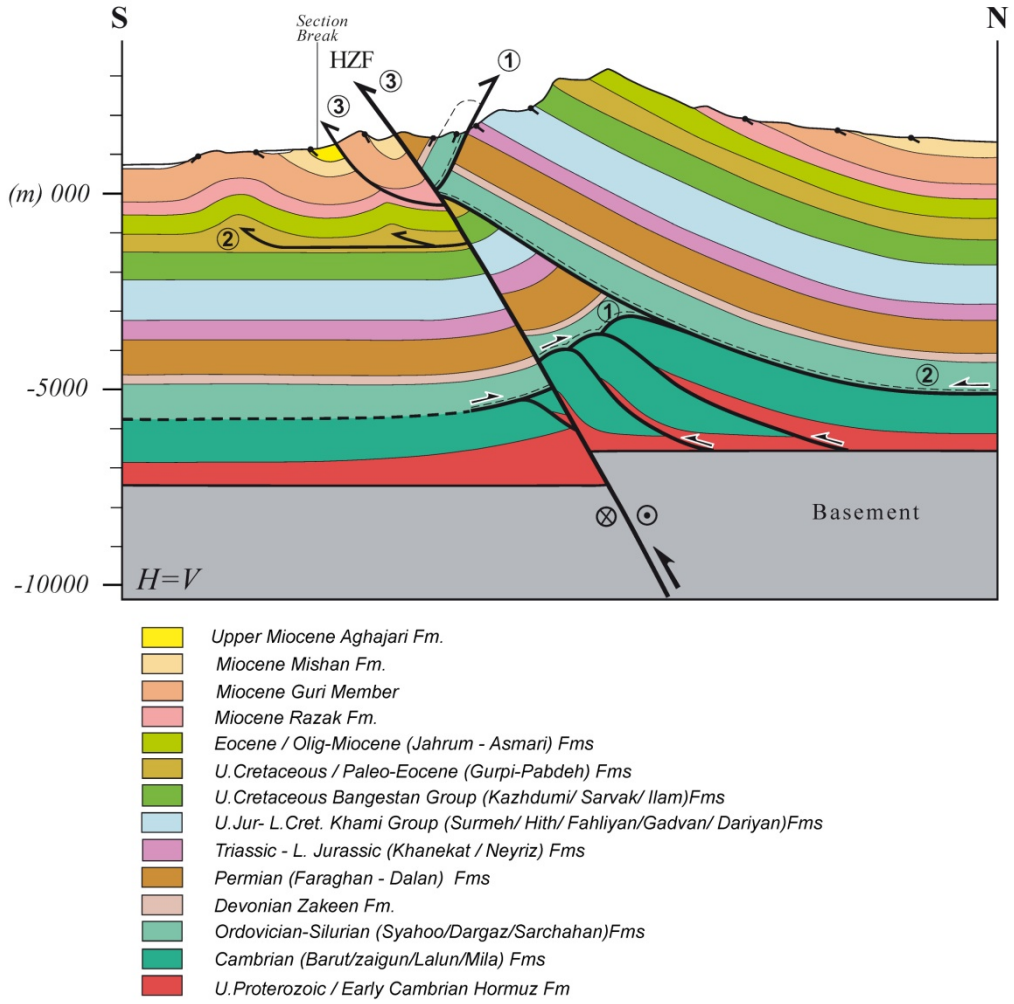

Fig. I.15. Structural section across the Faraghan anticline (see section line on Fig. I.14).

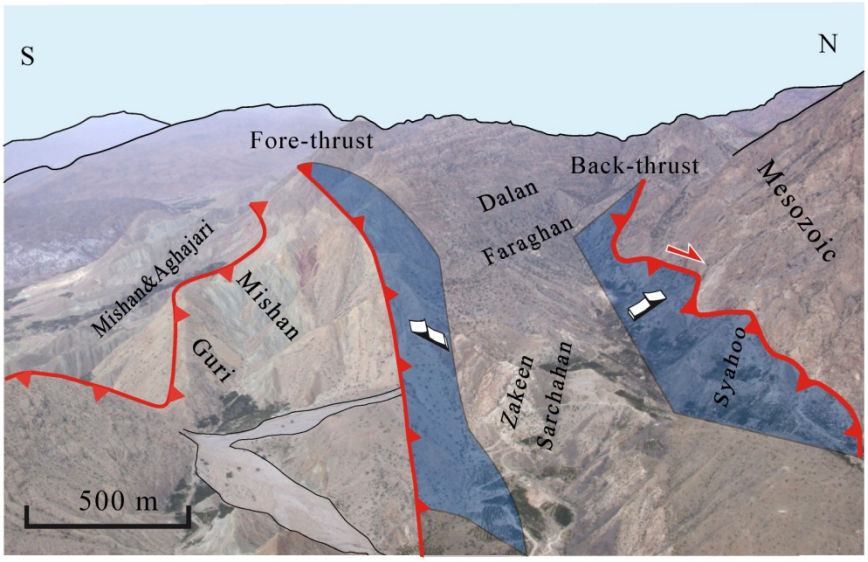

Fig. I.16. Field view of the south-dipping back-thrust which places the Ordovician Syahoo Fm over the Triassic Khanekat Fm in the core of the Faraghan anticline. The north-dipping fore thrust is an out-of-sequence basement thrust, which cuts out all the other structures (see Fig. I.14 for layout).

Kinematics of the Faraghan Anticline

The Bandar-Abbas syntaxis has been studied extensively (Molinaro et al., 2005; Sherkati et al., 2005; Jahani et al., 2009; Leturmy et al., 2010). Molinaro et al. (2005) proposed a two-phase kinematic model for this area based on careful restoration of a balanced cross-section. A thin-skinned phase created most of the fold and thrust structures in the cover. Then a Pliocene-to-Recent thick-skinned phase, suggested by out-of-sequence thrusts, linked to the basement faults and cut overlying cover structures. This general scenario matches the present interpretation of the kinematic evolution of the Faraghan anticline.

According to a restoration of the cross-section through the Faraghan structure (Fig. I.17), a four-stage deformation scenario can be recognized with the framework of a two-phase kinematic history. The first (thin-skinned) phase consists of three episodes. After deposition of the Fars Group and during the initial stages of the Zagros orogeny (most probably in the Miocene), the Faraghan anticline started to grow as a buckle fold. Subsequent deformation led to the amplification and tightening of the anticline, and simultaneously the creation of a small fore-thrust within the underlying Cambrian succession (stage 1, Fig. I.17).

The second stage corresponds to the generation of a back-thrust as part of a “fish-tail” structure (Letouzey et al., 1995) originating from the former fore-thrust (Stage 2, Fig. I.17). This back-thrust transferred deformation from depth to an upper surface using the thick Ordovician Syahoo Formation shales, which was activated as a lower-intermediate décollement (Fig. I.2.b).This level initiates a south-dipping ramp which cross-cut the sedimentary cover and exhumed the Lower Palaeozoic succession over the Mesozoic platform. Similar structures have been described by McClay (2000) as “passive roof duplexes”. A space problem may exist at depth in the anticline, and can be solved by the construction of duplex structures within the Cambrian succession.

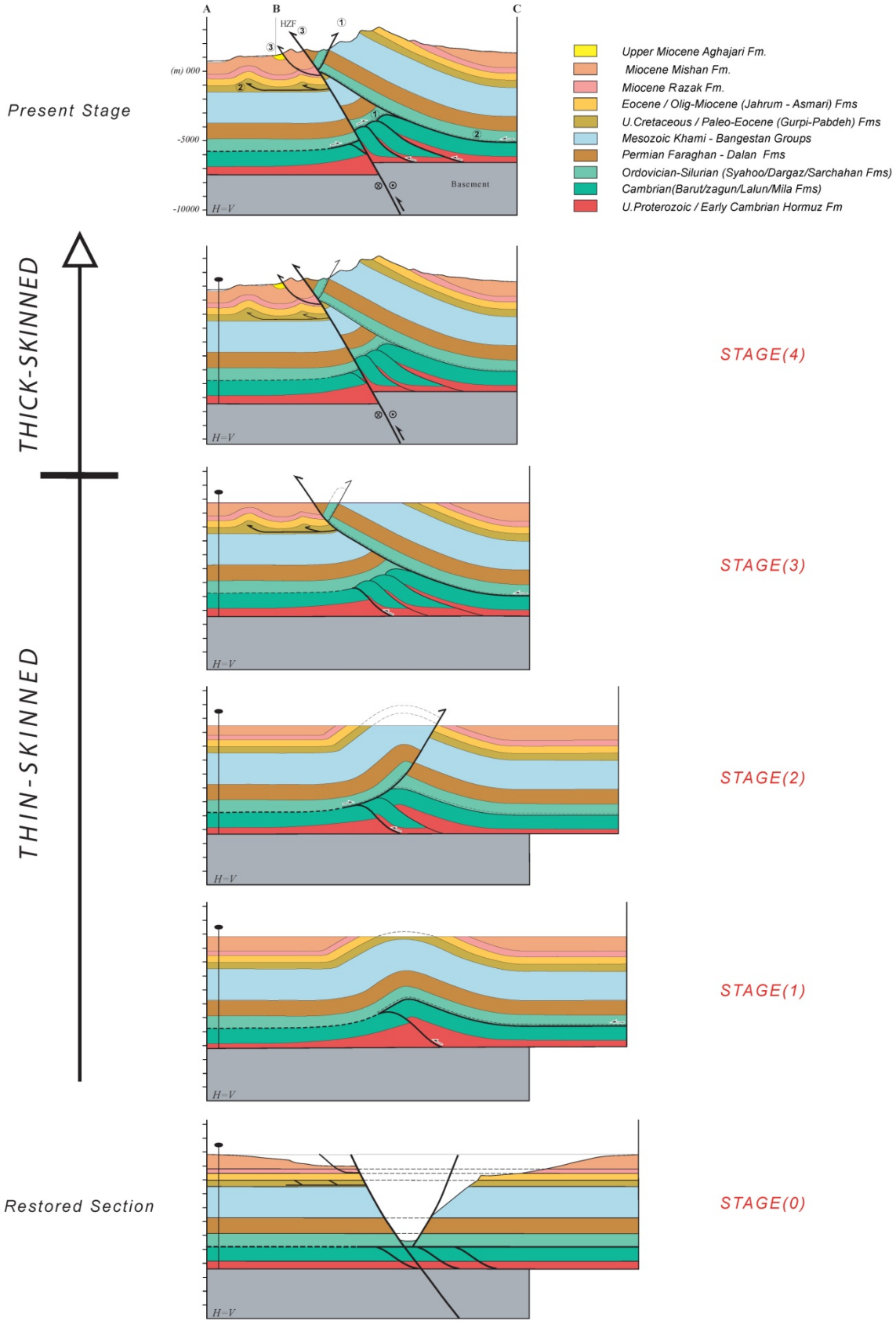

Fig. I.17. Two-phase (thin- and thick-skinned) kinematic scenario of the Faraghan anticline. This scenario consists of a four-stage kinematic model for structural development of the anticline.

During the third deformation stage (stage 3, Fig. I.17), also thin-skinned, the back thrust became inactive and a new forelimb thrust fault with considerable displacement toward the foreland developed. The thrust generated a gently-dipping south-verging ramp and terminated as a leading flat within the marls of the Gurpi-Pabdeh Formation. This unit constituted a shallow-intermediate detachment (Fig. I.2.b) and accommodated deformation in the form of folded structures within the overlying beds (Fig. I.17). The imbrication of competent Cambrian rocks between two décollements (Hormuz and Syahoo Formations) probably continued and completed during this phase.

Finally, the fourth stage (thick-skinned phase) corresponds to the reactivation of the inherited basement normal fault as a high angle thrust. This master up-dip ramp, the High Zagros Fault, which cross-cuts the entire cover succession and its associated structures, is an out-of-sequence thrust (Fig. I.17). The sequence of thrust faulting was summarized with labels (1 to 3) in the present stage of the Faraghan anticline (Figs. I.15 and I.17).

I.2.5.2. Gahkum and Kuh-e-Khush cross-sections:

Comparison with the Faraghan transect

Cross-sections and a kinematic model for the Gahkum anticline were published by Molinaro et al. (2005). Gahkum and Kuh-e-Khush were revisited in order to establish an integrated structural evolution scenario for the Eastern high Zagros. A new interpretation of the fault geometries and the role of a deep intermediate décollement in the development of these anticlines is presented below.

The Gahkum anticline is the most westerly of the three salt-cored anticlines in the Eastern High Zagros (Fig. I.14), and has a summit elevation of about 2900 m. The present-day morphology of the structure resembles a monocline due to the erosion of the forelimb (Figs. I.18 and I.19). This master fold results primarily from detachment folding over a Hormuz salt décollement (Fig. I.19), similar to the Faraghan structure. Subsequent deformation caused activation of a décollement in

the Silurian Sarchahan Formation shales. This level decouples the overlying deformations from below and makes an appropriate horizon to initiate a south-vergent thrust fault. The Sarchahan and Hormuz décollements also probably caused the intervening units to be folded as duplex structures and imbricated (Fig. I.19), similar to the Faraghan anticline. The next deformation phase was characterized by activity on deep-seated faults, and the occurrence of an emergent basement thrust caused Silurian rocks to emerge at the surface against a small footwall syncline cored by the Aghajari Formation.

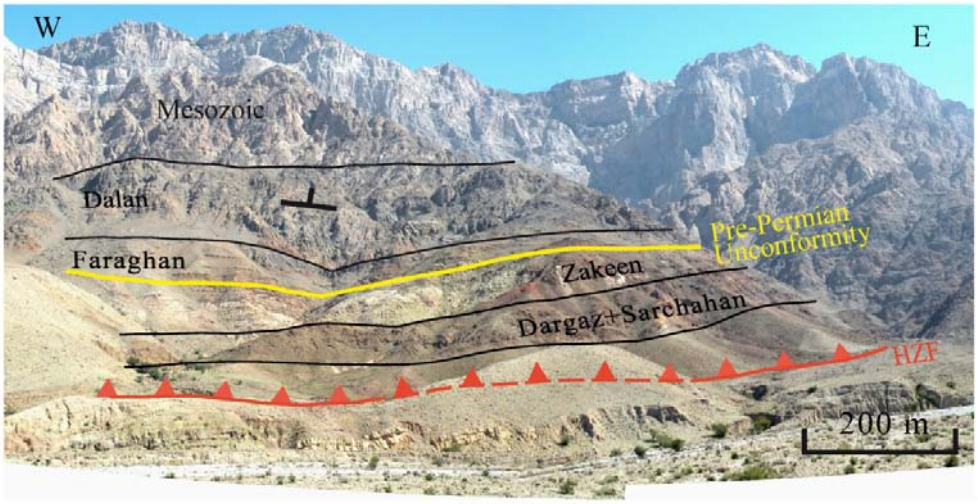

Fig. I.18. *Frontal view of the Gahkum anticline. Sedimentary rocks (Lower Palaeozoic to Upper Cretaceous) on the hanging wall of the High Zagros Fault are thrust over the Quaternary alluvium which covers the underlying Upper Miocene Aghajari Formation (for location, see Fig. I.14).*

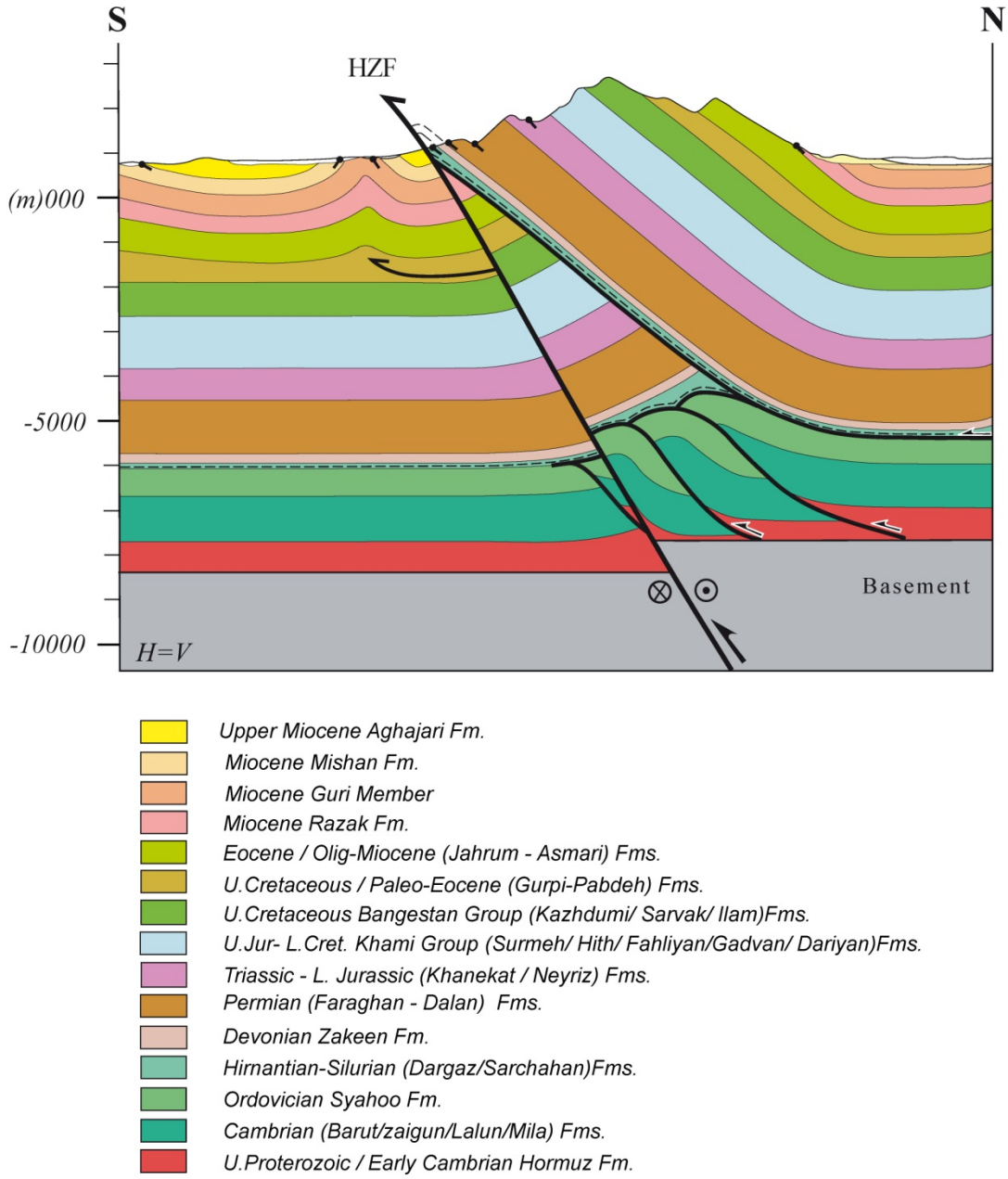

Fig. I.19. *Gahkum structural cross-section (for section location, see Fig. I.14).*

Kuh-e-Khush anticline is located in the extreme east of the Eastern High Zagros (Fig. I.14), and is presumably the youngest of the three giant structures. Figure I.20 illustrates the present-day geometry of this structure, which is similar to the Faraghan and particularly Gahkum anticlines, although with some variations. The most significant difference is associated with a distinct body of Hormuz salt in the footwall of the High Zagros Fault (Fig. I.20). This salt diapir is exposed laterally on the NW side of the section line within the core of the structure (Fig. I.14), where a deep valley is incised in the SW flank of the Kuh-e-Khush structure. The emergent

plug of Hormuz salt has risen along the High Zagros Fault, and is thrust over south-dipping carbonates of the Guri Member (Fig. I.21). In this place, the dip angle and dip direction of the High Zagros Fault are 70° and 075°, respectively. Slickensides in the Guri limestones have low angle (~ 15°) and oblique trajectories, indicating a late phase of dominantly strike-slip movements along the High Zagros Fault. In other words, the sheared thrust plane of the High Zagros Fault was reactivated as an oblique fault with minor vertical and major horizontal components of movement.

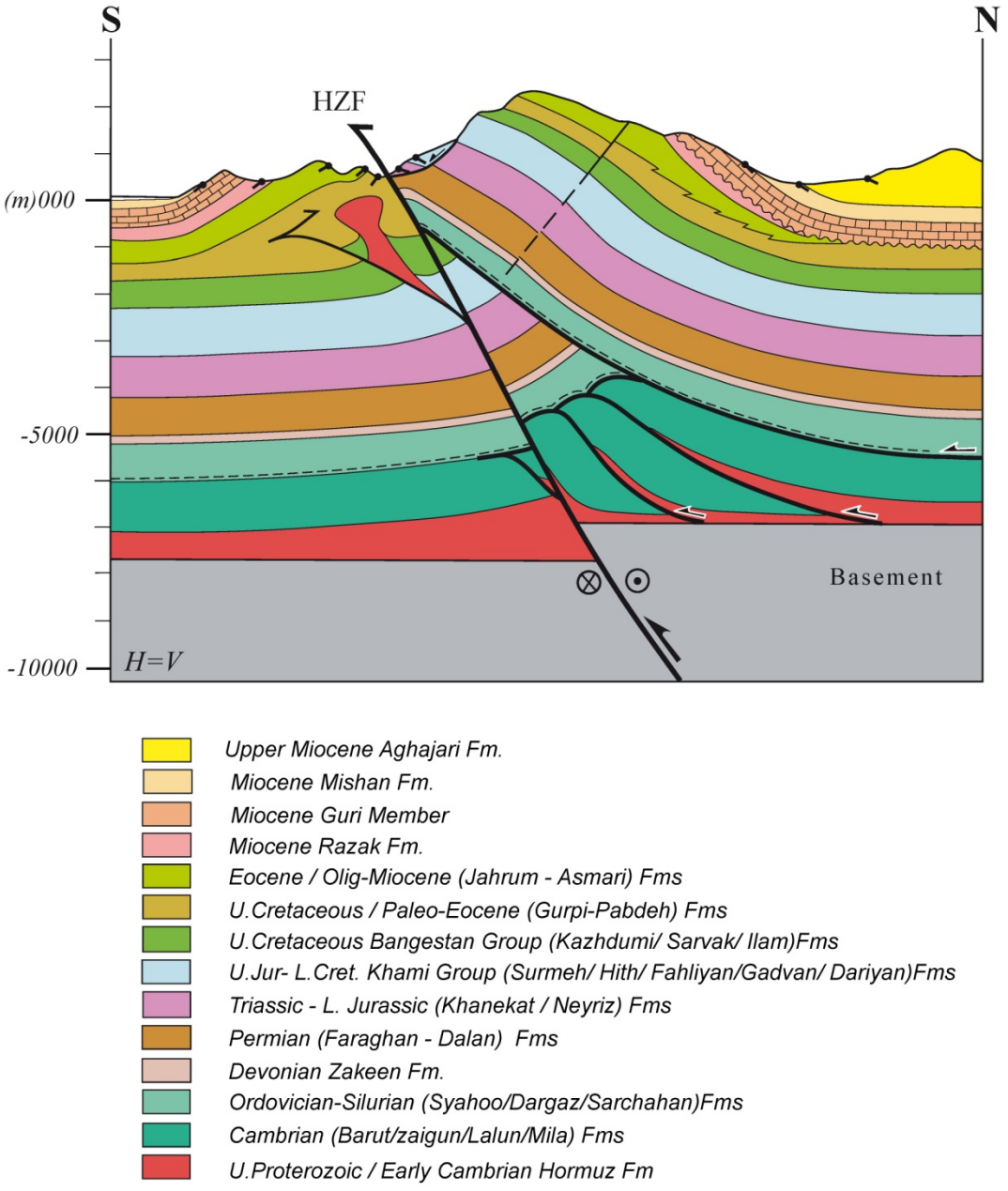

Fig. I.20. Structural transect of the Kuh-e-Khush anticline. The buried Hormuz salt has probably been disconnected from its feeder source layer.

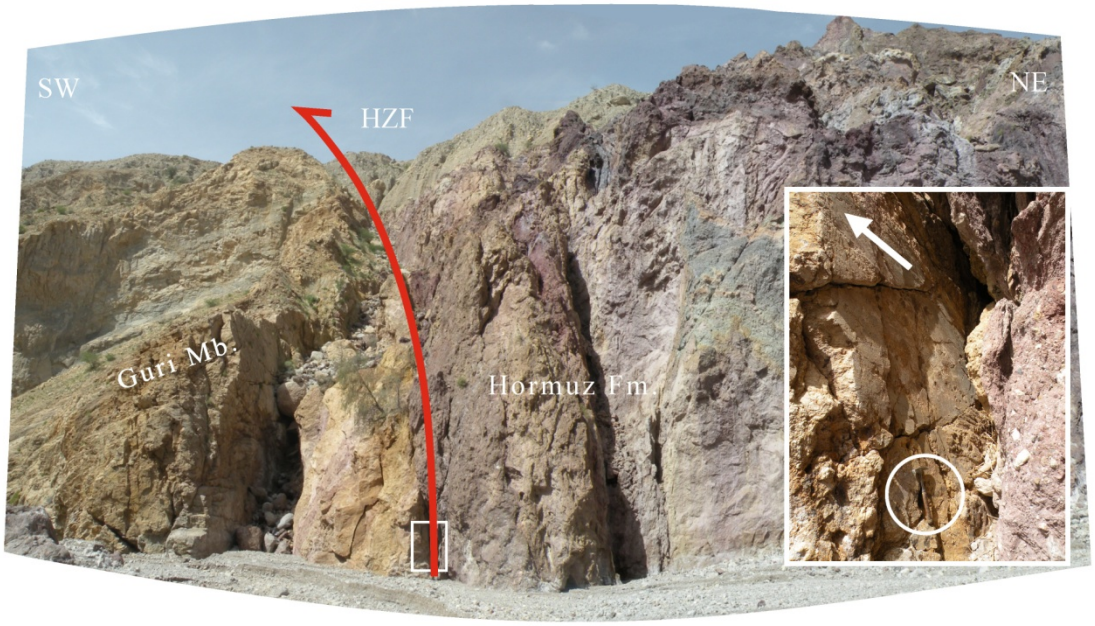

Fig. I.21. *Field photo of the emergent Hormuz salt in the incised valley of Kuh-e-Khush. Detail of reverse motion on the fault plane can be seen in the inset (for layout, see Fig.I.14).*

I.2.6. Discussion

I.2.6.1. The geometry of the High Zagros Belt

The High Zagros is discontinuous and only occurs in two locations referred to here as the Western and Eastern High Zagros, respectively. This discontinuity may have been inherited from the original geometry of the Arabian plate margin or may be a consequence of differential erosion of the Sanandaj-Sirjan Front after the Zagros orogeny. This latter hypothesis is supported by the structural map of the area (Fig. I.1), which shows that the outcrops of the High Zagros are exposed between re-entrants of the Sanandaj-Sirjan Zone. Lateral extensions of the outcrops are probably buried beneath the Sanandaj-Sirjan Zone and/or the Cretaceous Nappes.

I.2.6.2. Shortening values in the Western High Zagros

The Western High Zagros is the only region where it was possible to draw a complete cross-section using only field data. Elsewhere, in the eastern part of

Western High Zagros and the Eastern High Zagros, a substantial portion of the belt is buried below thick Quaternary deposits and it is therefore difficult to draw a section with confidence in the absence of subsurface data.

For this study, three cross-sections of the High Zagros were constructed (Lajin, Zardkuh and Baznavid, from east to west) and were restored to their pre-deformational state. Cover shortening values for these sections are 14.7 km (24%), 22.3 km (28%) and 20 km (33.5%), respectively. These sections complement the balanced cross-sections C, D and E of Sherkati et al. (2006), which cross the Dezful Embayment and the Izeh Zone. The shortening values for the cover obtained by these authors are respectively 33 km (section C ~15%), (section D ~15.5%) and (section E ~14%) for these two domains pertaining to the ZSFB (Sherkati et al., 2006). Comparison between these amounts of shortening with those determined in the present study show that compressional deformation has been mainly accommodated within the High Zagros, and the shortening values therefore decrease considerably from the hinterland toward the foreland basin. Variations in facies and thickness of the Hormuz series from the northern to the southern margins of the High Zagros Fault may explain this difference. The absence of Hormuz salt plugs or diapirs to the south of the High Zagros Fault suggests that the salt is absent or of reduced thickness here, or to a lateral facies change. This may have caused variations in the shear strength along the basal décollement (Letouzey et al., 1995; Cotton and Koyi, 2000) and resulted in an unequal strain distribution from NE toward SW. This is also suggested by the significant change in structural style (e.g. anticline wavelength, tightening) on either side of the High Zagros Fault (Fig. I.3).

I.2.6.3. Discrepancies between cover and basement shortening

The shortening values (Table I.1) obtained in the this study represent minimum values for the High Zagros, because, as mentioned above, this zone probably extends northward beneath the Iranian plate and part of the deformation is accommodated within areas which are currently underthrust below the Sanandaj-Sirjan Zone. However for all the studied sections, basement shortening is considerably less than cover shortening (Table I.1). This difference can be explained either due to the occurrence of internal deformation in the basement, [ignoring which

during the construction of balanced sections may leads an underestimate of basement shortening by at least 10% (Carminati, 2009);] or to the development of imbricated fans and/or multiple duplexes (McClay, 2000), accommodating deformation in the underplated part of the High Zagros (Mouthereau et al., 2007; Frizon de Lamotte et al., 2011; Vergès et al., 2011; Mouthereau et al., 2012). More precisely, development of imbricate horses within the basement of the Arabian Plate beneath the Sanandaj-Sirjan Zone would compensate for the lack of shortening in the deeper parts of the sections.

The apparent discrepancy in the shortening ratios requires a complete interface decoupling. From a kinematic point of view, the difference in shortening between cover and basement along the exposed sections of the High Zagros is good evidence for a two-step (thin-skinned then thick-skinned) deformation model, as previously proposed by Molinaro et al. (2005), Sherkati et al. (2006) and Vergès et al. (2011).

I.2.6.4. The role of Palaeozoic décollement levels: existence of duplex structures at depth

In previous structural studies of the Zagros foldbelt, and in all existing balanced cross-sections through it, the Palaeozoic sequence has been considered as a mechanically competent unit within the sedimentary cover (e.g. O'Brien, 1950, 1957; NIOC, 1975; Blanc et al., 2003; Sherkati et al., 2006; Emami et al., 2010; Mouthereau et al., 2011). It is usually presented as a "layer-cake" succession with no discontinuities or décollements in addition to the Hormuz salt décollement at its base. However the present study has shown that the Ordovician-Silurian interval may have acted as a secondary décollement in the study area.

In the Western High Zagros, activity on the Ordovician décollement (Ilbeyk Formation shales) in association with displacement on the Hormuz salt detachment, led to duplexing in the cores of the folds (Figs. I.9 and I.10). In the Eastern High Zagros, the Ordovician Syahoo and Silurian Sarchahan black shales were likewise activated as detachments to initiate fore- and back-thrusting during the early stages of fold development. They also formed roof thrusts during the formation of duplexes

concealed at depth in the cores of the three studied anticlines, which mark the front of the Eastern High Zagros (Figs I.15, I.19 and I.20).

I.2.6.5. Timing of deformation

It is now established that after the onset of the collision between the Arabian Plate and the Cimmerian Blocks which occurred at about 35 Ma (Frizon de Lamotte et al., 2011), deformation propagated southward in the Arabian platform. Hessami et al. (2001) proposed that the SW-ward migration of Zagros deformation was continuous in time (although not necessarily steady-state), with successive fronts between the Late Eocene to Present. However at the time of their publication, the ages of syn-orogenic deposits were poorly constrained.

In the Western High Zagros, new palaeontological dates (Fakhari et al., 2008) show that the onset of syntectonic coarse-grained deposition began at about 23 Ma (early Miocene), i.e. about 10 Ma after the closure of the Neo-Tethys. These dates are in agreement with the thermo-chronological studies of Gavillot et al. (2010), who suggested that the main period of exhumation of Lower Palaeozoic rocks in the High Zagros Belt (Lajin area) was early to Middle Miocene (~ 19-15 Ma) in the NW and Middle-Late Miocene (~ 12-8 Ma) in the SE. Wrobel-Daveau (2011) also obtained AFTA and AHe cooling ages from detrital apatites in this region, and proposed that activation of the High Zagros Fault was more or less synchronous and occurred after 16 Ma (i.e. within the estimated range given by Gavillot et al., 2010). In the two-phase kinematic model presented here, these ages refer to the first (thin-skinned) stage and not to the thick-skinned stage which occurred subsequently and which is still active at the present day.

I.2.7. Conclusion

Clarifying the previous usage, we have proposed in this paper a new definition of the High Zagros. The main point is the presence of Lower Paleozoic rocks carried out to the surface by important thrust faults, including the High Zagros Fault. On a structural map (Fig. I.1) the High Zagros appears being discontinuous, because it is partly buried below the major over-thrust sheets, which emplaced the Cretaceous

nappes and/or the Sanandaj-Sirjan domain over the Arabian Platform. The High Zagros kinematics, with its successive thin-skinned and thick-skinned phases, is similar to the general kinematics of the Zagros Fold-Thrust Belt (Molinaro et al., 2005; Sherkati et al., 2006) but with higher shortening values.

The geometry of the wide anticlines forming the High Zagros can only be explained by initial detachment folding followed by development of large duplexes at depth (Figs. I.9, I.10, I.15, I.19 and 1.20). This scenario is consistent with the existence of thick Silurian and Ordovician shale, which are not only well-known source rocks but also potential décollement levels. Such duplex structures represent possible targets for future hydrocarbon exploration. Further work, including the characterization of reservoir, petro-physical properties and modeling of the thermal evolution of source rock is required to better define the potential of this wide region.

Tables:

Table I.1:

Section Name	Basement Shortening		Cover Shortening	
	Km	%	Km	%
Lajin	3.25	6.5	14.7	24
Zardkuh	1.75	3	22.3	28
Baznavid	6.35	14	20	33.5

I.3) Additional Data and Remarks of the paper N° 1

I.3) Additional Data and Remarks

My PhD work is an “article-based” thesis which gives the results gained during this research, in the frame of several submitted and/or published manuscripts. Commonly, a manuscript must be summary and presents the core of the study. I hereby attach supplementary comments in order to explain additional geometrical and structural elements within the studied zone. These data either come from the field evidences obtained during the geological reconnaissance or the limited original seismic surveys acquired by NIOC for oil and gas explorations. The objective of the current section is to help the reader for advanced understanding of architecture and structural style provided in the paper No1.

In this framework, I will first present more illustrations and field photos of the western and eastern High Zagros and corresponding explanations. It will be followed by some of the most explicit seismic lines to elucidate the subjects discussed in above-mentioned paper.

I.3.1. Back-thrust in the Baznavid area

A dense and complicated association of NW-SE faulted structures and thrust systems are observable in the published 100 000 Geological map of “Haft Tanan” quadrangle. The existing faults are responsible for uplift and subsequent intense erosion of the folds in this area which allowed the out cropping of Lower Paleozoic rocks within the HZB. No principle north-vergent thrust (Back-thrust) involving up-dip movement of these latter exposures is visible throughout this map.

Following the field observations, I have revised this map (see Fig. I.8, paper No. 1) partly to depict the realistic view of the main structural characters and elements inside the same zone. Fig. I.22.a. depicts a field picture of the significant south-dipping back-thrust locating NE of Baznavid village (Fig. I.9, paper NO. 1).There is a number of asymmetric folds (Fig. I.22.b) on the hanging wall of this fault. The crestal area of the contiguous southern fold has been removed due to the uplift combined with erosion of the back-thrust and it’s northern limb was cut out and vertically displaced. in this scheme, the Ordovician Ilbeyk formation has thrust over upper Cretaceous Garau-Sarvak rocks. The great stratigraphic separation (~5000 m) is observable passing from hanging wall to the footwall and the high elevation of the core of the syncline would demonstrate the deep-rooted nature of this fault.

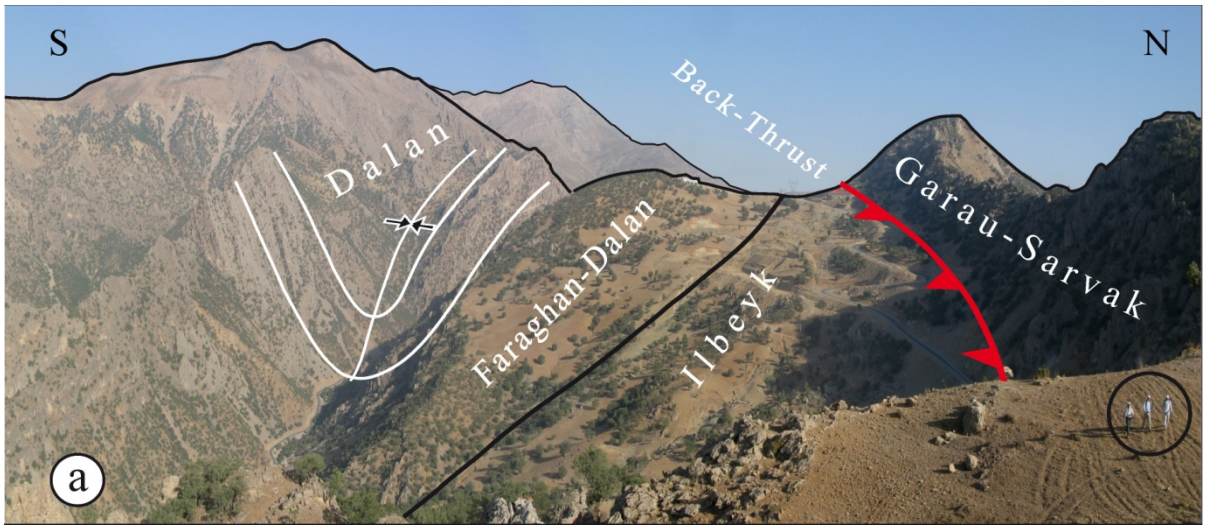

Fig. I.22.a) Back-thrust carried out the Ordovician rocks over Upper Cretaceous

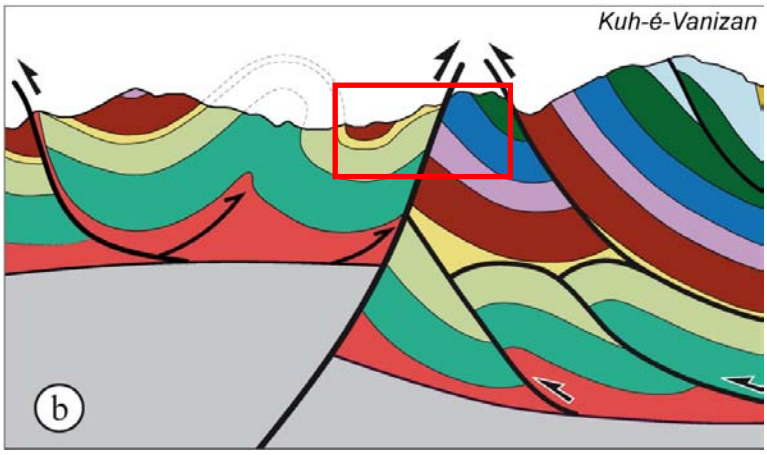

Fig. I.22.b) *Structural cross-section of the Baznavid area. The red square displays the picture in Fig. I.22.a.*

I.3.2. Frontal auxiliary folds

Several small folds with a carapace made of Guri limestone are located in front of giant Faraghan and Gahkum structures (Fig I.23.a and Figures I.15 and I.19 of the paper 1). Fig I.23.b is an oblique aerial view of Faraghan frontal structures. The exposed core of one of these frontal anticlines in the south of Kuh-e-Faraghan consists of Razak formation (equivalent of Gachsaran formation). It is an asymmetric fold with steep forelimb and gentle back-limb (Fig I.23.c) looks like a fault propagation fold. The location of this latter is outlined on the Fig I.23.b.

A small sketch (inset) of the same figure illustrates the probable existence of a fish-tail structure. This triangle zone would be feasible, assuming the upper flat of the south vergent thrust (this fault is equivalent to the fault holding label “2” in the back-limb, Fig. I.15 of paper 1) dies out within the higher level. The short wavelength of this anticline implies activation of the shallow intermediate detachments compare to deep Hormuz décollement. In other word, in addition to the Gurpi-Pabdeh formations, the Oligo-Miocene Razak deposit can be proposed as an alternative level for decoupling of this superficial fold from below. The facies (lithological composition) of Razak in the area of study contains layers of red marls and evaporates which have a strong contrast of mechanical behavior with under- and overlying carbonates. So, it is capable to be considered as a secondary detachment horizon in the Cenozoic sedimentary sequence.

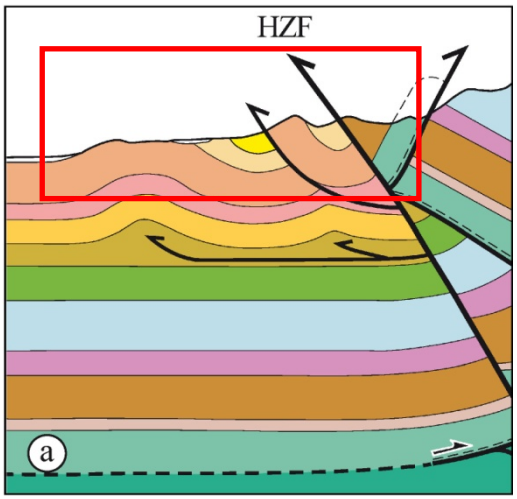

Fig. I.23.a) Cross-section along the frontal zone of Fraghan Ant.The red square marks the area within the Fig. 1.23.b.

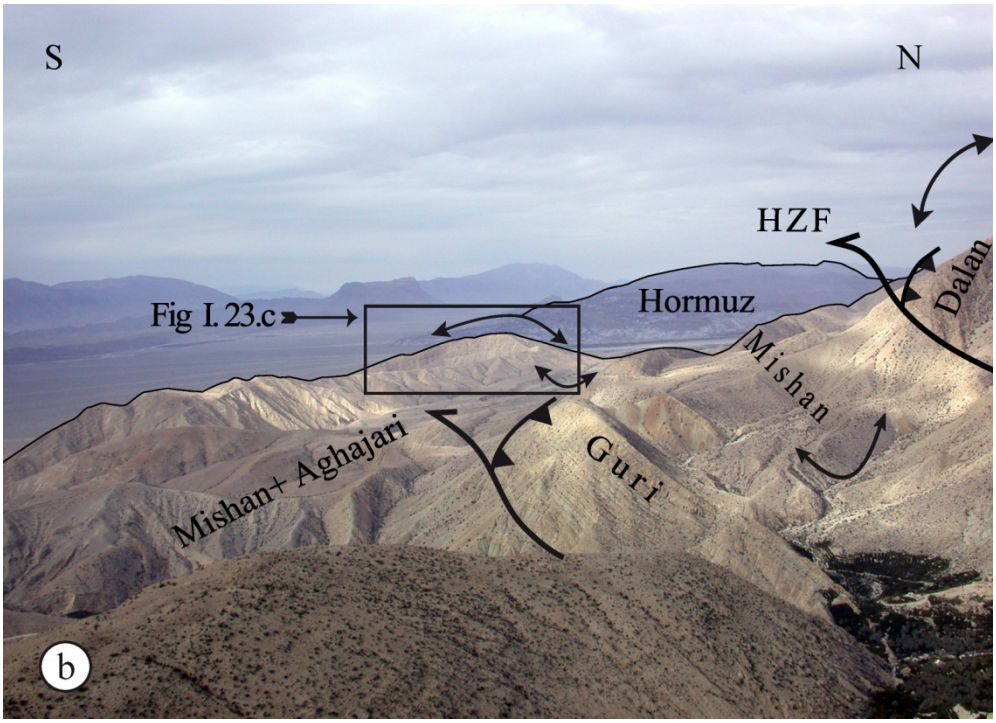

Fig. I.23.b) Side view of foot-wall syncline and secondary thrust branches from the basement fault of the Faraghan anticline.

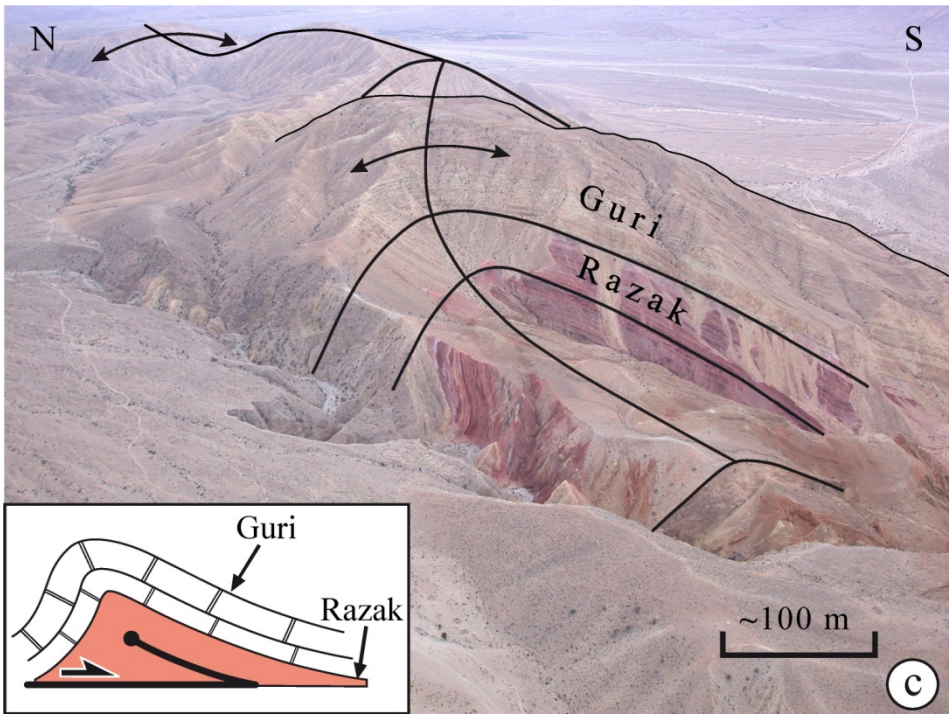

Fig.I.23.c) Detail of the superficial fold on the frontal zone of Faraghan structure. This fold detaches either in Razak or in Gurpi-Pabdeh Formations.

I.3.3. Normal faulting in Kuh-e-Khush

A normal fault, parallel to the axis (NW-SE) is visible on the back-limb of Kuh-e-Kush anticline (Fig. I.24.a). This is a high angle fault dipping toward the south. The tracing of some marker beds of thick Asmari limestones detects nearly 35 meters of vertical offset. The effective depth of this fault is ambiguous (Fig. I.24.b) however the exposed displacement along the fault plane suggests the considerable importance of this structure.

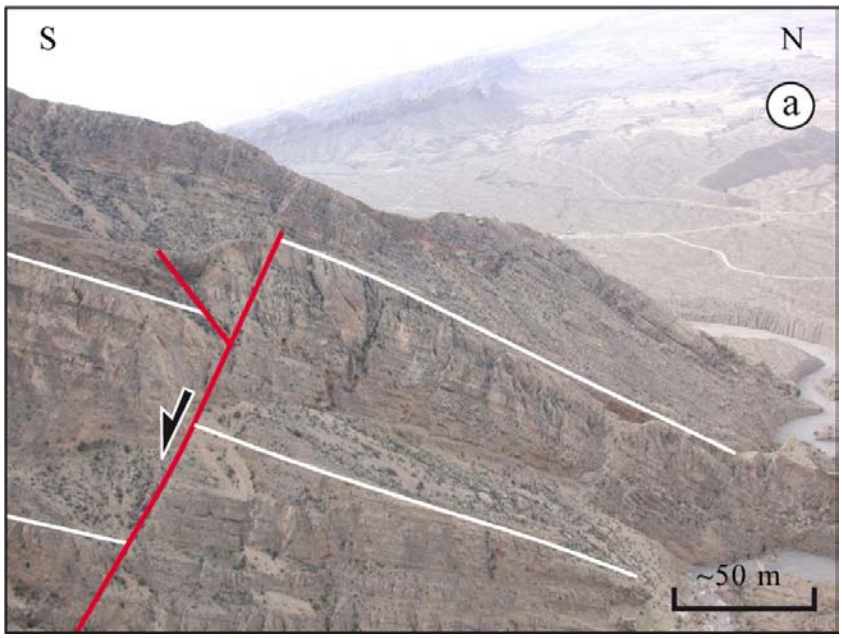

Fig. I.24.a) Aerial view of the normal fault in the Asmari carbonate of the Kuh-e-Khush structure.

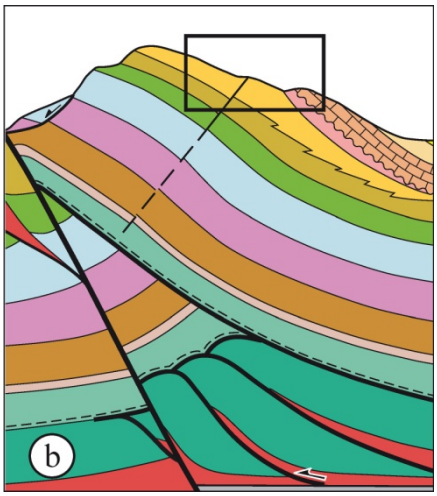

Fig.I.24.b) Cross-section illustrating the normal fault in the back-limb of Kuh-e-Khush. The black square displays the picture in Fig.I.24.a.

I.3.4. Assymetric drag folds of the carbonate beds in the EHZ

Fig.I.25 illustrates the drag folding in the thin limestone layers of Mishan formation in southern flank of Faraghan anticline. The carbonate competent strata are bounded by incompetent shaly and marly beds. The layer parallel shortening is

responsible for accommodation of deformation in the stiff layers and leads to the creation of asymmetric folding within the carbonate levels during compression. However, the competent beds control the overall geometry (amplification, wavelength, etc) of folds at the large scale. The migration of interstitial ductile materials toward the core of the small antiforms and local reverse faulting are visible.

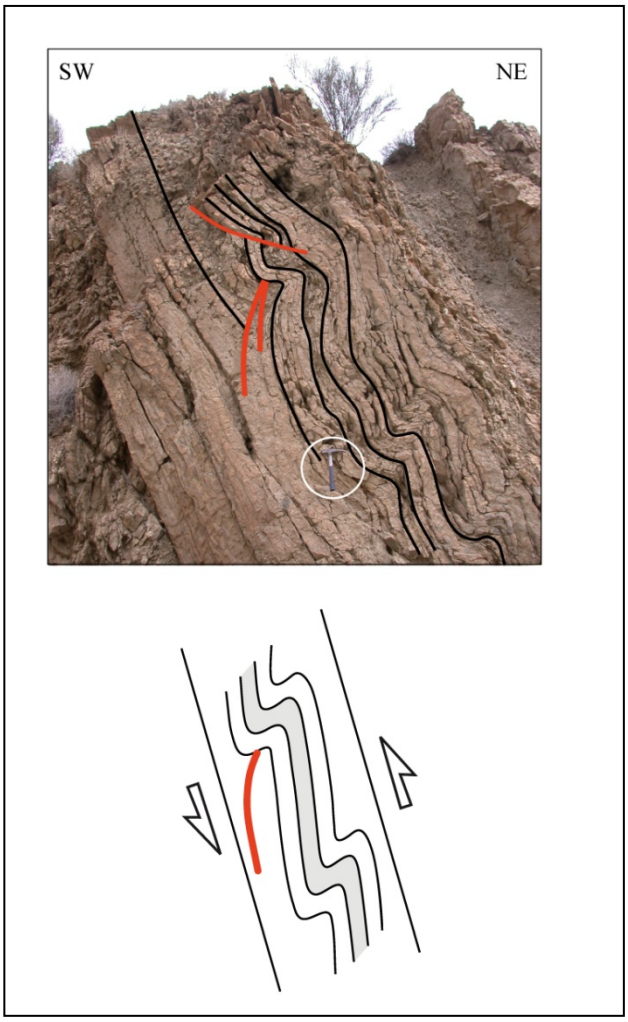

Fig.I.25. Drag folding in the carbonate layers of the eastern zone. Small thrust faults were generated by simple shearing and cut the steep flank of the asymmetric drag antiform.

I.3.5. Deep seismic lines in the ZFTB

Numerous reflection seismic studies have been acquired throughout the ZFTB for the purpose of hydrocarbon exploration and approximately all of them were designed and performed to image the Permian and post-Permian objectives. These

data usually suffers from “multiple” problems and “poor quality” for deep to very deep levels. Meanwhile, there are just a few boreholes to calibrate these limited seismic sections which can present pre-Permian reflectors. Therefore, generally speaking, the reflection seismic for the purpose of Paleozoic study cannot be robust. Among the existing huge geophysical dataset for the ZFTB, I tried to find some examples to image the structural issues explained in various parts of this thesis. I acknowledge the following cases for different aspects of the current manuscript.

I.3.5.1. High Zagros Seismic lines

Very seldom seismic study has been obtained beyond the HZF to the north. One of the best in quality point of view passes through the HZB and is given in the figure I.26. This is a dip-line with NE-SW direction and already published by Bosold et al., (2005). An alternative interpretation of this seismic profile was carried out in the current study. The main point in this figure concerns the sealing of the inclined pre-Permian horizons by overlying beds in the back limb of Kalvari anticline. The interpreted short yellow line beneath the “Near Top pre-Permian” (Fig. 1.26.b) which dips to the NE most likely marked the orientation of tilted blocks sealed by an unconformity.

Such an angular unconformity near the base of Permian can be compared with fieldwork evidences. For example, A thick pre-Permian sedimentary sequence in the southern flank of Lajin Mountain has been strongly tilted and subsequently eroded and signatures a notable pre-Permian hiatus. Permian siliciclastic rocks and carbonates overlie them with a significant angular unconformity (Tavakoli-Shirazi,et al. 2012).

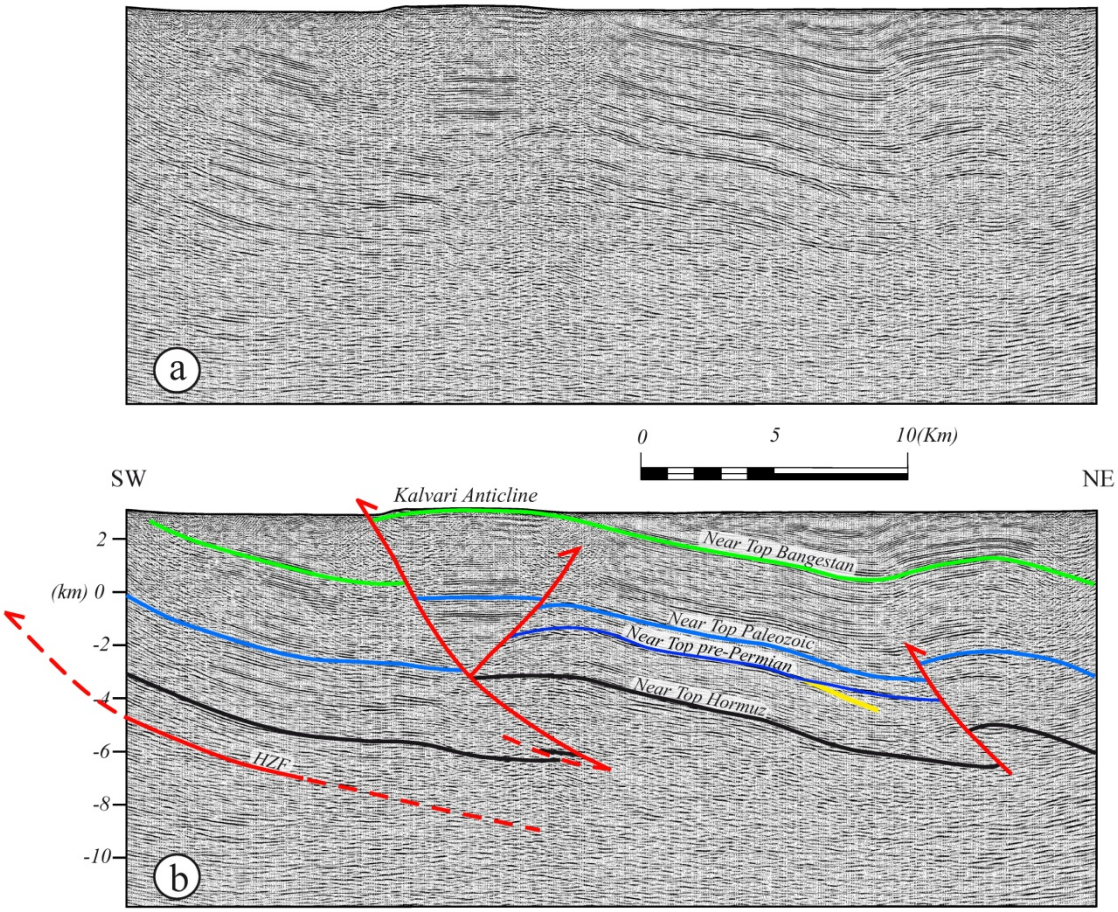

Fig.I.26. a) Non-interpreted and b) interpreted seismic profile in the Dena Area. (Western High Zagros). The yellow short line depicts rotated pre-Permian block sealed by the unconformity

I.3.5.2. Seismic profile crosses the Arabian basement lineaments

I already discussed the presence of N-S structural trends (e.g. Hendijan-Bahregansar fault) in the Arabian subcrop of the Zagros belt in the Paper 1. Fig I.27 is an offshore seismic image in the northwest of the Persian Gulf where we can see the impact of those structures on the sedimentary environment. The decreasing of the Paleozoic thickness strata to the northwest is linked to the relatively higher elevation of this domain compare to the southeast during sedimentation. The same geometry is observed in several stratigraphic levels (Kazhdumi, etc…) suggesting that the reactivation of inherited Hendijan-Bahregansar basement fault occurred throughout geological time (for onshore arguments of the same fault, see Sherkati and Letouzey, 2004).

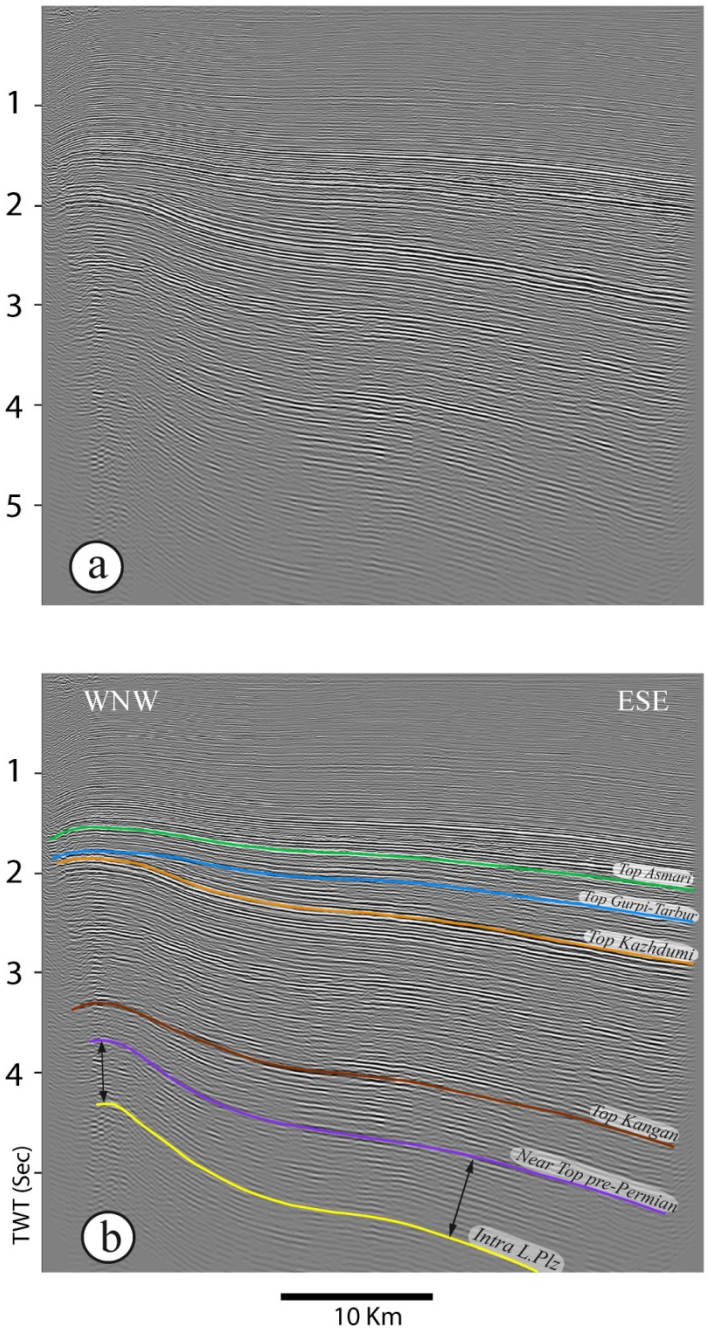

Fig.I.27. a) Non-interpreted and b) interpreted seismic image in the NW of the Persian Gulf clearly show the impact of the North-South HBF (Fig. I.1) on the pre-Permian thickness variations. Evident thinning of Paleozoic succession toward the Hendijan-Bahregansar high can be observed. The lowermost interpreted reflector indicated a tentative horizon in the Lower Paleozoic.

I.3.5.3. Décollement within the Lower Paleozoic evidenced by seismic data

For the first time, duplex structures hypothesis in the Paleozoic sequence was discussed during the structural synthesis of the HZB in this thesis (e.g. paper 1). More evidences for supporting of this idea come from some onshore seismic acquisitions done by NIOC for hydrocarbon exploration in the western sub-coastal Fars. A NE-SW seismic dip-line (Fig. I.28) crosses a couple of en-echelon anticlines in this area. Top Kangan (Triassic in age) has been regionally calibrated. The tentative reflectors which represent intra-Lower Paleozoic levels were picked based on the approximate Two-Way-Time (TWT) data. The pink horizon in the Fig. I.28 illustrates a distinct “reflector divergence” form the flank toward the crest of the anticline. The deviation of these reflectors tentatively establishes the thickness variation which could be attributed to the activity of a ductile zone. Regarding the depth of this structural feature, the activation of Ordovician-Silurian strata could set up this divergence.

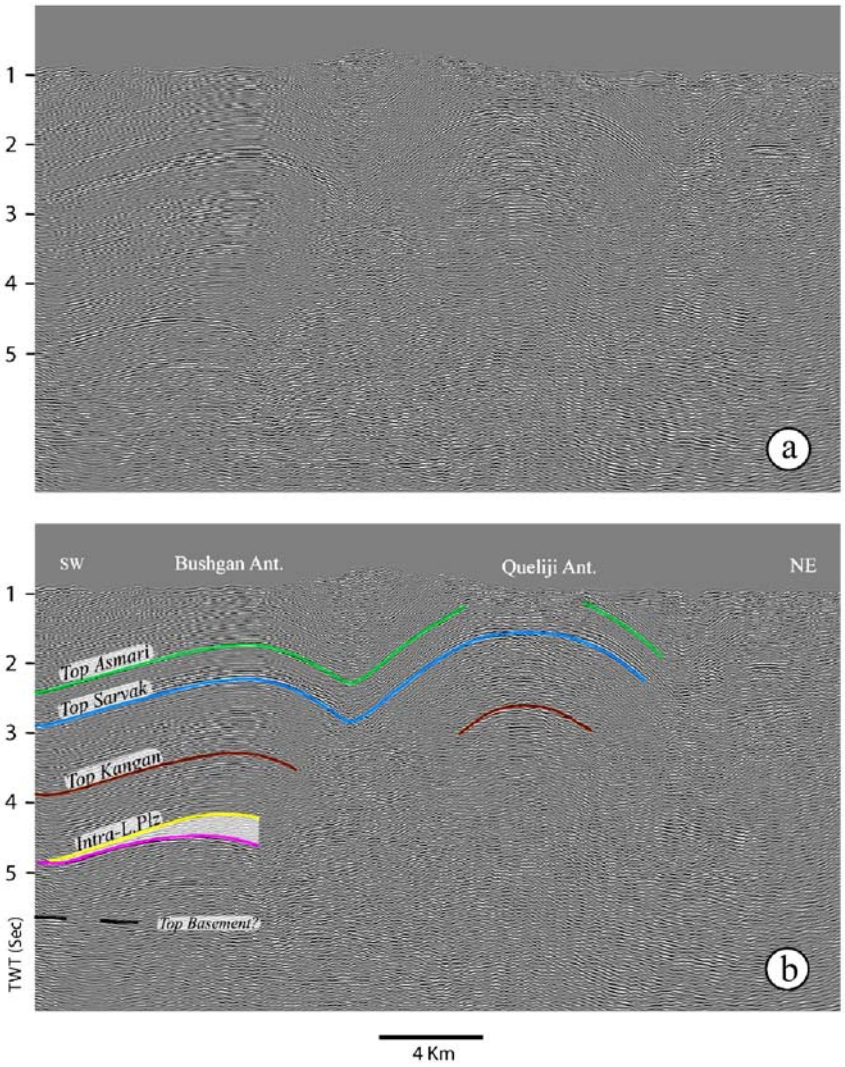

Fig. I.28. a) Non-interpreted and b) interpreted seismic profiles in the East Fars. Divergence within the deep reflectors and significant increasing of the Lower Paleozoic thickness indicate the activation of incompetent zone (décollement level).

Note1: location of all figures in the complementary note was illustrated in the Annex 3 of this thesis.

Note2: for the legend of seismic interpretations, see figure I.2.

CHAPTER II

PRE-PERMIAN UPLIFT AND EXTENSIONAL DEFORMATION IN THE HIGH ZAGROS BELT

II.1) Introduction

This chapter is organized in a similar way to the preceding one. It is mainly made up of a published paper in the Arabian Journal of Geosciences (2012) with the title of “Pre-Permian uplift and diffuse extensional deformation in the High Zagros Belt (Iran): integration in the geodynamic evolution of the Arabian plate”. This paper resulted from a couple of geological surveys focusing on the High Zagros where pre-Permian rocks are cropping out. In this domain there is a huge pre-Permian hiatus, which is known at the scale of the Arabian plate. The “Arch” and “Basin” geometry due to the activation of inherited basement north-south lineaments could explain such architecture. The observed normal faults sealed by pre-Permian sediments within the studied area evidenced the occurrence of extensional deformation instead of far influence of the so called “Hercynian” compressional tectonic phase. This paper proposes that a “thermal uplift” could be responsible for the pre-Permian geological events within the Arabian Plate. It is subsequently pursued by sedimentation of open marine carbonates accommodated by “thermal subsidence”.

Paper N° 2 is followed by related complementary remarks and further illustrations on the same topic. It is worth to note that, they do not modify the conclusions presented by the second paper.

II.2) Paper N° 2

Pre-Permian uplift and diffuse extensional deformation in the High Zagros Belt (Iran): integration in the geodynamic evolution of the Arabian plate

Published in Arabian Journal of Geosciences (2012)

Arab J Geosci
DOI 10.1007/s12517-012-0542-5

ORIGINAL PAPER

Pre-Permian uplift and diffuse extensional deformation in the High Zagros Belt (Iran): integration in the geodynamic evolution of the Arabian plate

Saeid Tavakoli-Shirazi · Dominique Frizon de Lamotte · Jean-Christophe Wrobel-Daveau · Jean-Claude Ringenbach

Received: 3 November 2011 / Accepted: 8 February 2012

Abstract The High Zagros Belt includes exposures of Lower Palaeozoic rocks in the core of several thrusted anticlines developed during the Cenozoic Zagros orogeny. The structural style and tectonic evolution of this area during the Palaeozoic remain poorly understood due to the complexity of the subsequent deformation. We present the preliminary results of a field study focusing on the structural geology of Palaeozoic rocks in this area. We confirm the existence of an angular unconformity below the Lower Permian Faraghan formation. In the geological literature, this unconformity is reported as the "Hercynian Unconformity" suggesting a relationship with the Hercynian (Variscan) orogeny, which affected Western Europe and westernmost Africa during the Carboniferous. Surprisingly the only observable structures sealed by this unconformity are N to NE trending normal faults and tilted blocks without any evidence of compressional deformation. This pre-Permian extensional deformation, which is general at the scale of the HZB, raises questions about the geodynamic significance of the "Hercynian unconformity" in the study area and, more generally, in the Arabian plate.

Keywords High Zagros Belt (Iran) · Palaeozoic · Arch · Hercynian unconformity · Normal faulting

S. Tavakoli-Shirazi · D. Frizon de Lamotte · J.-C. Wrobel-Daveau
Department of Géoscience and Environnement,
University of Cergy-Pontoise,
F95 000 Cergy-Pontoise, France

S. Tavakoli-Shirazi (✉)
Geology Department, NIOC, Exploration Directorate,
Seoul Ave, P.O. Box 19395-6669, Tehran, Iran
e-mail: saeid.tavakoli@u-cergy.fr

D. Frizon de Lamotte
TOTAL, Projets Nouveaux, TBF,
place Jean Millier,
F92 400 Paris-La Défense, France

J.-C. Wrobel-Daveau · J.-C. Ringenbach
TOTAL, Département d'interprétation structurale et sédimentaire,
CSTJF, Av. Larribeau,
F64 000 Pau, France

Introduction

Throughout the Arabian plate, a more-or-less significant sedimentary hiatus separates the continental early Permian sequence from the older sedimentary formations (e.g. Konert et al. 2001; Johnson 2008). This hiatus and related unconformity is generally referred to the "Hercynian unconformity" (see a recent synthesis by Faqira et al. 2009) suggesting a relationship with the Hercynian (Variscan) orogeny, which affected Western Europe and north-western Africa during the Carboniferous (e.g. Simancas et al. 2009; Michard et al. 2010). Our field work in the central and eastern High Zagros Belt confirms the existence of an angular unconformity below the Lower Permian Faraghan formation. Surprisingly the structures sealed by this unconformity are normal faults and tilted blocks without any evidence of compressional deformation. This observation, which is general at the scale of the High Zagros Belt, raises the question of the significance of Hercynian unconformity in the study area and, more generally, in the Arabian plate. After a short description of the geology of the High Zagros Belt, we will present field data illustrating both the attitude of the pre-Permian unconformity and the geometry of inherited normal faults and tilted blocks in both the central and eastern High Zagros Belt. We will conclude with a

Published online: 20 March 2012

discussion on the implications at the scale of the Zagros orogeny and the Arabian plate more commonly.

Geological setting: geology of the High Zagros Belt, correlation of the Palaeozoic sequences

The High Zagros Belt (HZB; Fig. 1) belongs to the Zagros Fold-and-Thrust Belt (ZFTB), which extends over about 2,000 km from south-east Turkey through southwest Iran down to the Strait of Hormuz (Fig. 1; Stocklin 1968; Falcon 1974; Berberian and King 1981; Alavi 1994; Sherkati et al. 2006). The ZFTB represents the southern palaeo-margin of the Neo-Tethys Ocean, involved in the Zagros orogeny (see a recent synthesis by Frizon de Lamotte et al. 2011). The HZB was first introduced as a continuous narrow NW-SE thrusted zone with the highest rate of topography, uplift and rainfall (Berberian 1995). The HZB is bounded to the south by the NW-SE High Zagros Fault (HZF), which we define as the southernmost principal thrust-fault carrying out Lower Palaeozoic strata (other than Hormuz salt) over Mesozoic or Cenozoic rocks, and to the north by the Main Zagros Thrust (MZT), which corresponds to the fundamental limit (Neo-Tethys suture) with the internal Sanandaj-Sirjan domain pertaining to the Eurasian plate. Following this definition the HZB does not exist everywhere along the ZFTB but correspond to elevated domains in two specific areas: the central and eastern Zagros (Fig. 1).

In the central High Zagros a complex network of branching faults combining pure reverse faults in association with right-lateral strike-slip faults allow large exposures of Palaeozoic rocks (Fig. 2). In the eastern Zagros, the HZB (Fig. 3) is made up by three giant anticlines bounded to the SW by basement faults interpreted as segments of the HZF (Molinaro et al. 2005). Lower Palaeozoic rocks are out cropping in the core of two of them, namely the Kuh-e-Faraghan and Kuh-e-Gahkum anticlines (Fig. 3). An isolated outcrop of Palaeozoic rocks also exists in the core of the Surmeh anticline, located in the external part of the Fars Arc (Fig. 1). Elsewhere in Zagros, the Palaeozoic is only known from sparse wellbore penetrations.

The litho-stratigraphy of Palaeozoic sequences has been established in the ZFTB by James and Wynd (1965) and subsequently revised by Setudehnia (1972), Koop and Stoneley (1982), Motiei (1993), Ghavidel-syooki (2003), Alavi (2004) and Ghavidel-syooki et al. (2011; Fig. 4). At the bottom of the sedimentary pile, the Hormuz salt of Late Precambrian–Early Cambrian age was deposited in an evaporitic basin located mainly on the site of the present Fars Arc (Fig. 1; Jahani et al. 2009). A branch of this basin seems to follow the trend of the central High Zagros Belt as indicated by the presence of several salt plugs underlying the main thrust faults in this domain (Fig. 2). From a structural point of view, this salt layer and its lateral equivalents form the main décollement in the area decoupling the overlying sedimentary pile from probable pre-Hormuz sediments of unknown age and from the Panafrican basement (e.g. O'Brien 1950, 1957; Berberian 1995; Alavi 2004; Sherkati et al. 2005; Mouthereau et al. 2007; Jahani et al. 2009; Vergès et al. 2011). This was followed by the development of epi-continental basins from Early Cambrian up to Late Devonian (Setudehnia 1972).

In the central High Zagros Belt, because of widespread uplift and erosion, which is generally interpreted as a far effect of the Hercynian orogeny or locally as result of Hormuz salt movement (Letouzey and Sherkati 2004; Sherkati 2004), only Cambrian and Ordovician sequences are out cropping

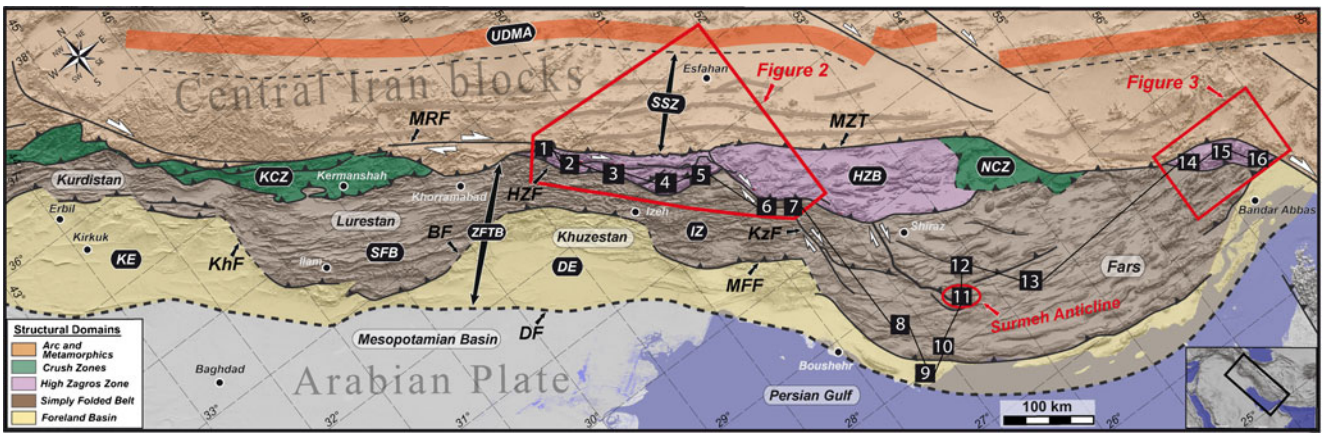

Fig. 1 Structural map of the Zagros Fold-Thrust Belt (ZFTB) emphasizing the position of the High Zagros Belt. *UDMA* Urumieh-Dokhtar Magmatic Arc, *SSZ* Sanandaj-Sirjan Zone, *KCZ* Kermanshah Crush Zone, *NCZ* Neyriz Crush Zone, *ZFTB* Zagros Fold-Thrust Belt, *HZB* High Zagros Belt, *SFB* Simply Folded Belt, *IZ* Izeh Zone, *KE* Kirkuk Embayment, *DE* Dezful Embayment, *MZT* Main Zagros Thrust, *MRF* Main Recent Fault, *HZF* High Zagros Fault, *KzF* Kazerun Fault, *MFF* main Frontal Fault, *KhF* Khanaqin Fault, *BF* Balarud Fault, *DF* Deformation Front. The *red lines* mark the areas of Figs. 2 and 3 and Surmeh anticline. Note to the location map of 16 selected Paleozoic surface and borehole logs in central High Zagros, Fars Arc and eastern High Zagros. *Connection line* shows the trace of the stratigraphic correlation diagram (Fig. 5)

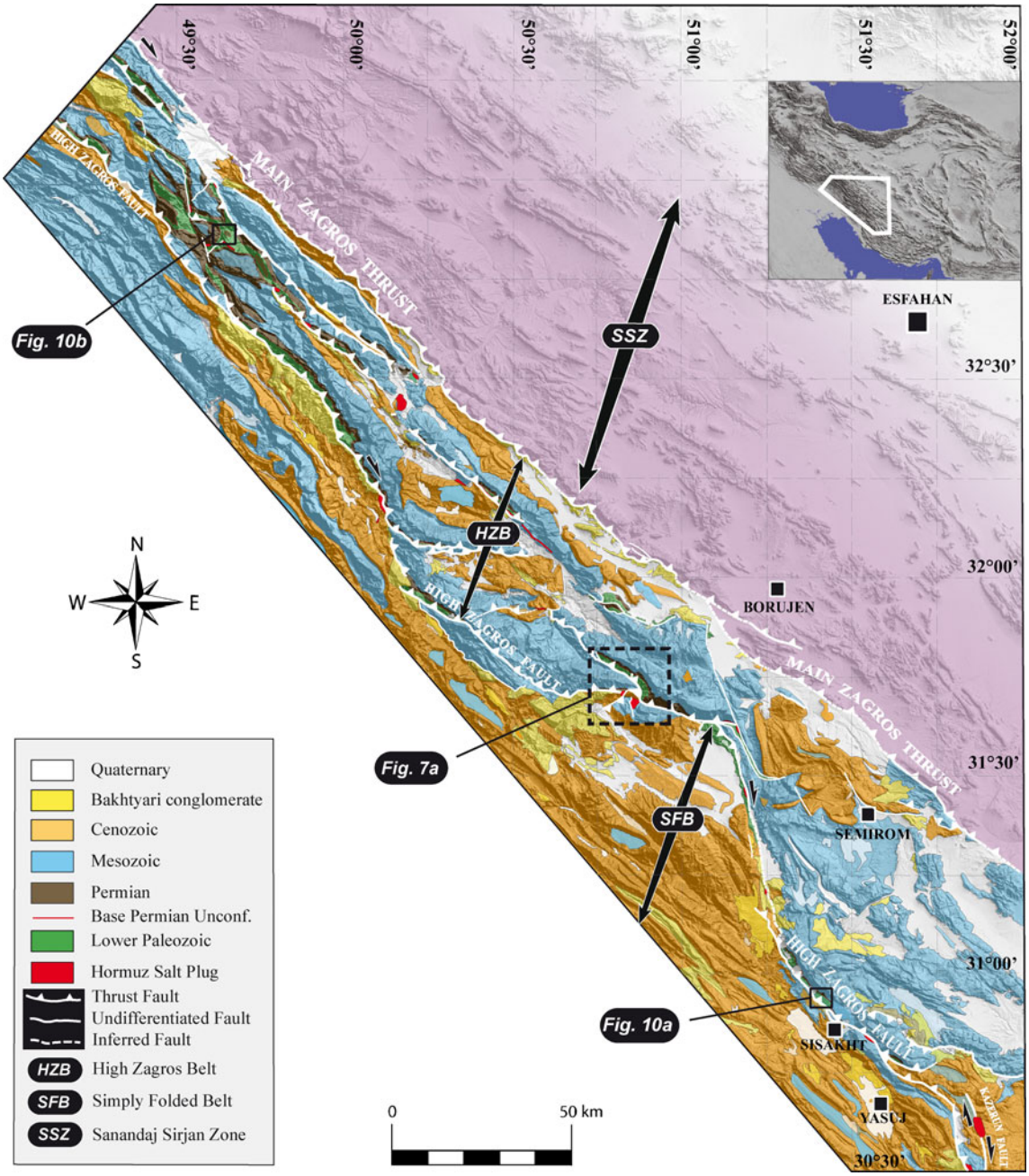

Fig. 2 Structural map of the central High Zagros Belt (HZB). This map has been compiled using SRTM, Landsat images, available geological maps published by the Geological Survey of Iran and NIOC and our field investigations. See location on Fig. 1

(Setudehnia 1972; Kheradpir and Khalili 1972). More precisely, Setudehnia (1972) recognized and dated the sandstone of the Lalun formation as well as the Mila trilogy, both of Cambrian age, in the Kuh-e-Dena and the olive shale of the Ilbek formation (Ordovician) at Zard-Kuh (Figs. 4 and 5).

Silurian and Devonian strata have not been reported and are likely absent in the central High Zagros. By contrast, they are out cropping in the eastern HZB at Kuh-e-Faraghan and Kuh-e-Gahkum anticlines (Fig. 3). These anticlines expose a quite complete lithostratigraphic succession from Lower Ordovician (Floian) to Upper Devonian (Frasnian) (see Fig. 5). More precisely, Ghavidel-syooki et al.'s (2011) study in Kuh-e Faraghan recognized the Floian to Katian Syahoo formation, Hirnantian Dargaz Sandstones and diamictites, the Silurian black shales of the Sarchahan formation and finally the clastic sequence of the Devonian Zakeen formation (Ghavidel-syooki 2003). The formations older than Middle Ordovician do not crop out in the Eastern Zagros, possibly due to a tectonic decoupling along the Syahoo formation (Fig. 5).

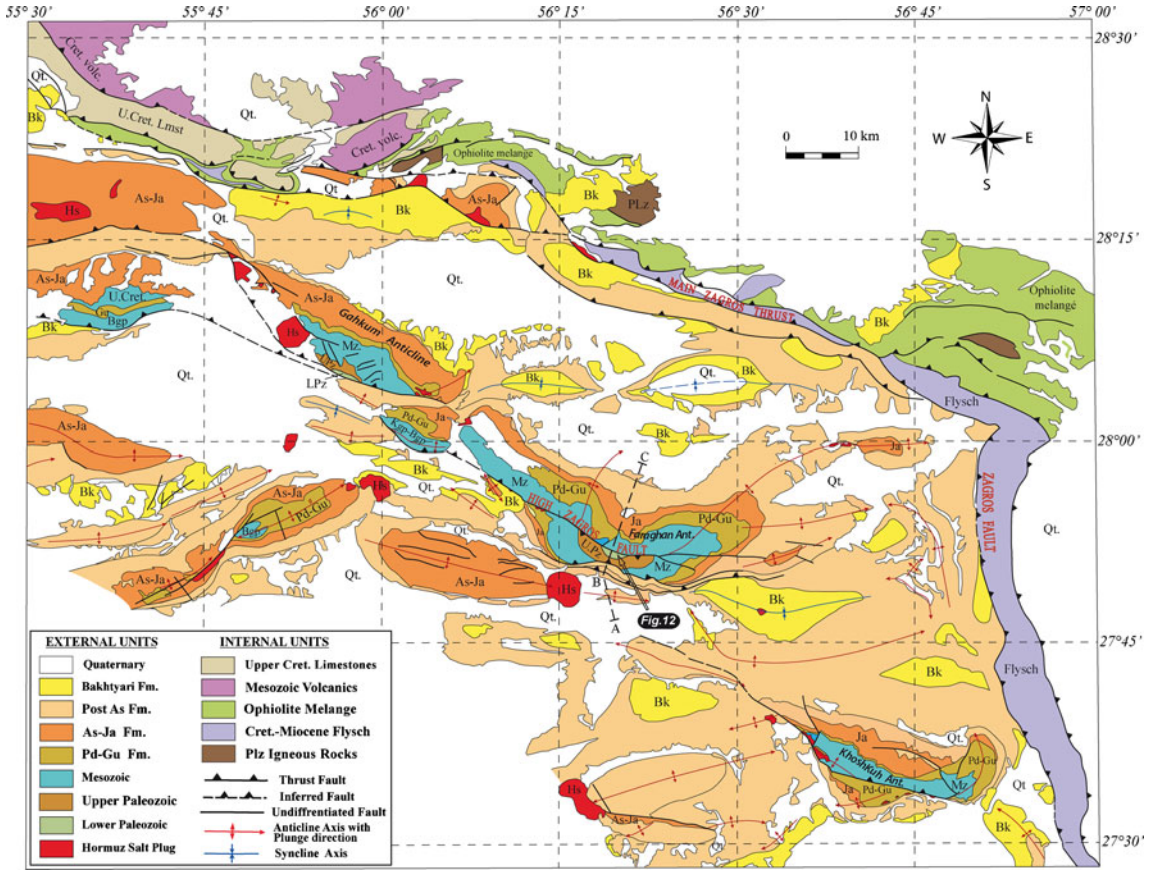

Fig. 3 Structural map of the eastern Zagros. This map has been compiled using various geological maps published by NIOC and the Geological Survey of Iran, Google Earth and Landsat imageries and our field investigations. See location on Fig. 1

Between the central and eastern High Zagros (i.e. in the Fars Arc, Figs. 1 and 6), the Palaeozoic sequences can be tentatively reconstructed using the outcrop of Surmeh anticline and a few well penetrations (Fig. 5). So, at the scale of the High Zagros Belt, we are able to rebuild long wavelength, low amplitude pre-Permian "folds" mimicking the so-called Palaeozoic "Arches" (or uplift) and intervening "Basins" well-known in Arabia (Konert et al. 2001; Faqira et al. 2009) or North Africa (Boote et al. 1998). More precisely, in the Arabian plate, Faqira et al. (2009) recognize three Arches, namely from west to east, the Levant, Al-Batin and Hadhramaut-Oman Arches and the two Basins, the Nafud-Ma'aniya and Faydah-Jafurah Basins located between the Arches (Fig. 6). Within the basins, some secondary Arches, like the Qatar Arch or the Ghawar High (Fig. 6), are present. The central HZB is located in the northeastern prolongation of the Al Batin Arch. The rest of our correlation line should be located in the Jafurah Basin and presents in its core a secondary dome (Gavbandi high), which could correspond to the northern prolongation of the Qatar Arch (Fig. 6).

Everywhere in the Zagros, Lower Permian coarse sandstone of the Faraghan formation deposited unconformably on the underlying more or less truncated beds (see below). The deposition of this formation occurred after an intense erosion leading, in the central High Zagros Belt, to the removal of post Ordovician deposits and suggesting large scale vertical movements. It is followed by a carbonate epicontinental platform covering a large time period from Permian (Dalan formation) to Cenomanian (Sarvak formation). It is worth noting that the Iranian Faraghan and Dalan formations are the strict lateral equivalent of the Saudi Unayzah and Khuff formations, respectively (Insalaco et al. 2006).The age of the Unayzah formation has been reported as Upper Carboniferous–Lower Permian in Saudi Arabia (Konert et al. 2001), but based on NIOC palynology studies, the Carboniferous has not been recognized in Zagros and the Faraghan formation is attributed to the Lower Permian (Ghavidel-syooki 2005a).

Pre-Permian unconformity and sealed tilted blocks in the central High Zagros Belt

The central High Zagros has been recently the site of extensive geological work (Ehsanbakhsh-Kermani et al. 1996; Bosold et al. 2005; Gavillot et al. 2010). These studies focus

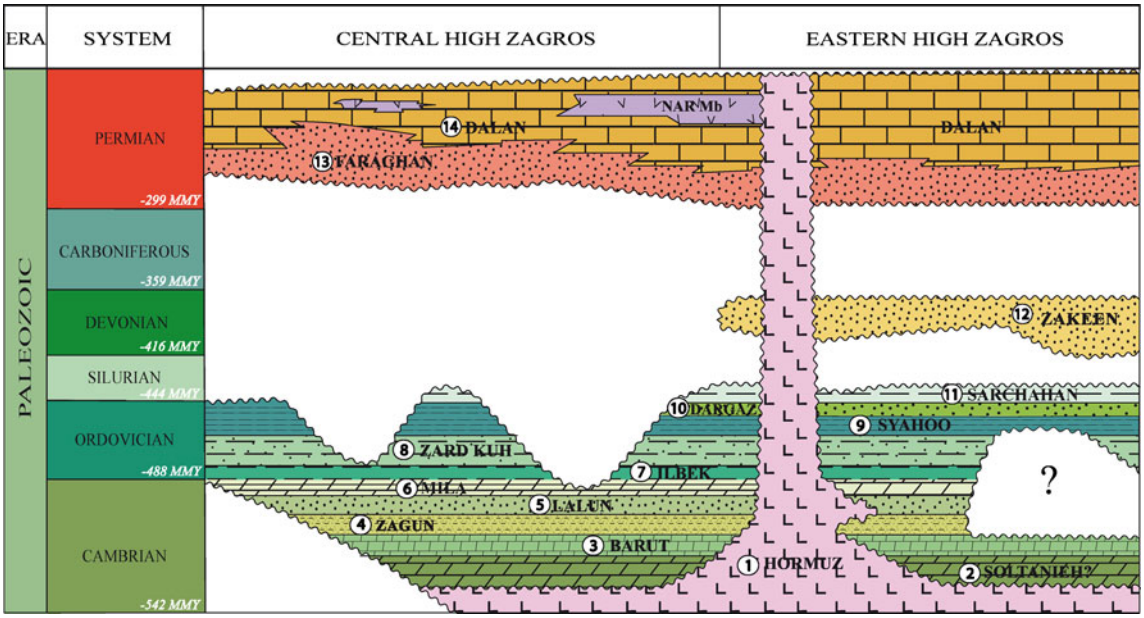

Fig. 4 General Lithostratigraphic chart for the Paleozoic sequence in the High Zagros Belt (modified after Motiei 1993). *1 Hormuz Fm* halite, anhydrite, sandstone, shale, dolomite and igneous rocks. *2 Soltanieh Fm* dolomite with shale beds. *3 Barut Fm* dolomite with interbeddings of red shales. *4 Zagun* varicoloured shale intercalated with fine sandstone on top. *5 Lalun Fm* fluviatile reddish ×-bedded sandstone and red shale on top. *6 Mila Fm* limestone, dolomite and shale. *7 Ilbek Fm* olive and black shale inter-bedded with sandstones. *8 Zardkuh Fm* predominantly shale intercalated with beds of fine grained sandstone. *9 Syahoo Fm* greenish and black shale with subordinate sandstone, siltstone, conglomerate and limestone. *10 Dargaz Fm* whitish sandstone and structureless to diffusely laminated diamictite. *11 Sarchahan Fm* black shale and a few interbeddings of conglomerate, sandstone and carbonate. *12 Zakeen Fm* sandstone with interbedded shale and subordinate dolomitic limestone. *13 Faraghan Fm* inter-beddings of shale and sandstone. *14 Dalan Fm* platform carbonate of limestone and dolomite

mainly on the geometry and kinematics of the major folds and thrust-faults, related to the Zagros orogeny, but deal only marginally with the Palaeozoic evolution. As an example, on the Ardal geological map (Ehsanbakhsh-Kermani et al. 1996) the Lower Palaeozoic strata have been drawn as a "layer cake" conformably overlain by Permian and younger rocks.

In fact and as indicated above, not only a considerable sedimentary hiatus separates the Lower Palaeozoic from the Upper Palaeozoic rocks but also the Lower Palaeozoic rocks have been tilted and truncated before the deposition of the Permian sediments. Among the different places where the pre-Permian unconformity is well exposed, the Kuh-e-Lajin is likely the most spectacular. From the revised geological map and associated cross-section (Fig. 7a, b), we can see that the Faraghan formation rests equally onto Lalun, Mila or Ilbek formations. Based on field observations, the mean dip of the Lower Palaeozoic rocks (45° ENE) is clearly higher than the dip of the Upper Palaeozoic (10° ENE; Fig. 8a, b). The unconformity is also visible in the Landsat TM satellite imagery (Fig. 8c). By contrast, it is worth noting the absence of an unconformity between the Upper Permian Dalan formation and the overlying Mesozoic rocks. Following along strike, the basal thrust of the Kuh-e-Lajin, which is a segment of the HZF, lateral missing of Ilbek formation and offset of the Lower Palaeozoic sequence are clearly observable (Fig. 7a). It is due to a west-dipping approximately N-S oriented normal fault presently hidden beneath recent formations. This early normal fault, separating two east-dipping tilted blocks, is sealed by the Faraghan formation. The whole assemblage, i. e. the Lower Palaeozoic with its embedded normal fault and their unconformable Permian to Cenozoic cover, has been uplifted and thrusted toward the WSW during the Zagros orogeny (Fig. 7a, b). A photo of the pre-Permian unconformity in Kuh-e-Lajin has been already published by Letouzey and Sherkati (2004). It was interpreted as a possible effect of a salt dome growth. In our opinion, the salt plugs existing in the footwall of the Lajin thrust (Fig. 7a, b) can explain neither the observed geometry nor the erosion preceding the deposition of the Faraghan formation.

Just south-west of the Kuh-e-Lajin is the Kuh-e-Bazman, an E-W trending faulted anticline in the core of which a small section of Lower Palaeozoic rocks is cropping out (Fig. 7a). The geology of the area is quite complex due to the vicinity of a plug of Hormuz salt. However a prominent unconformity between truncated Lower Palaeozoic formations (Lalun, Mila and Ilbek) and the Permian sequence is very well exposed in the field (Fig. 9). The eastward dip of the Lower Palaeozoic rocks suggests that, as in the Kuh-e-Lajin, this particular attitude could be controlled by a hidden west-dipping normal fault.

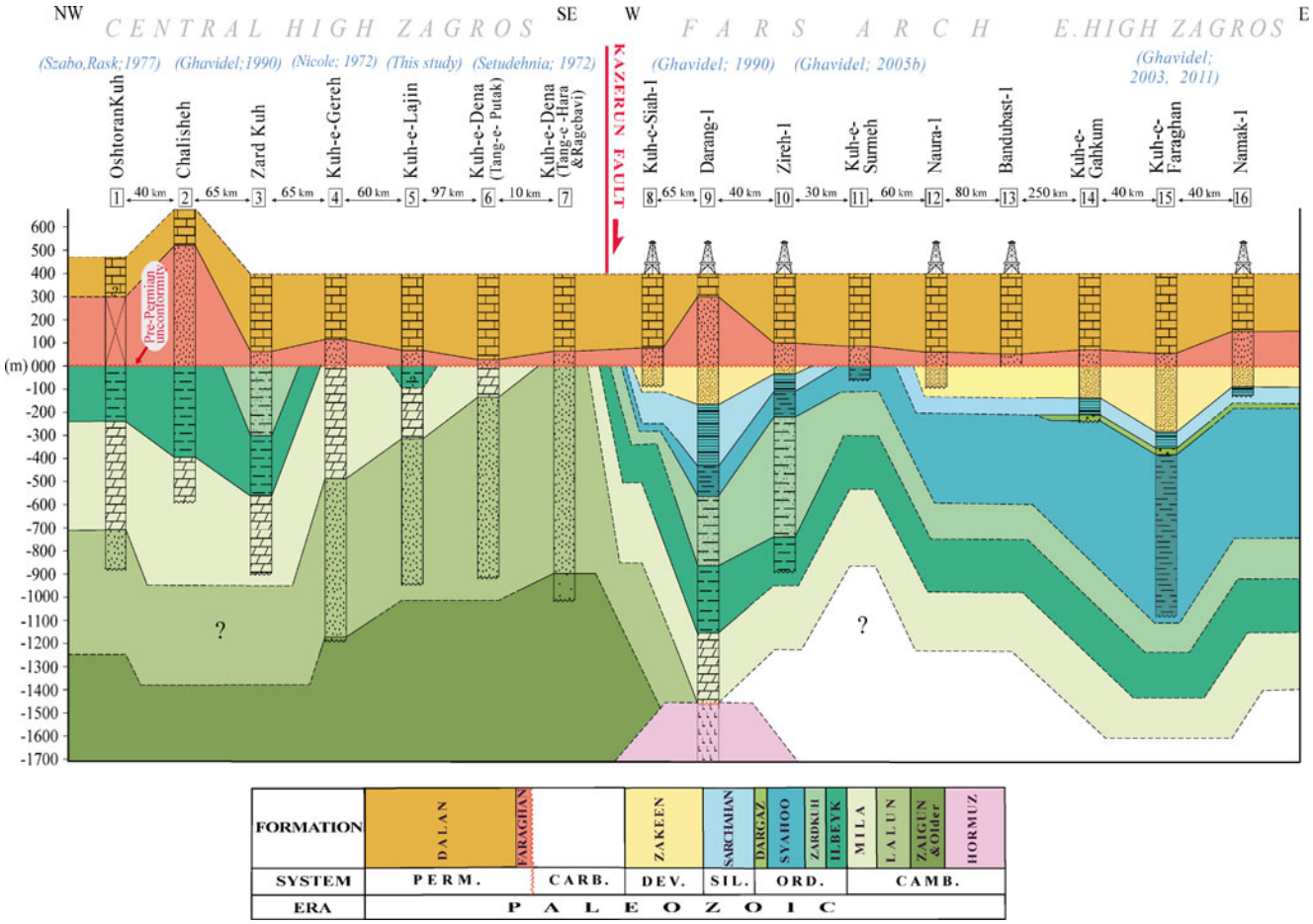

Fig. 5 Stratigraphic correlation diagram of pre-Faraghan Palaeozoic formations in High Zagros Belt. Datum: base Faraghan formation. (See Fig. 1 for location of the columns). Note to the references of the surface stratigraphic logs in blue color. Borehole data are based on the well completion reports provided by NIOC

Normal faulting restricted to Lower Palaeozoic formations has been observed in numerous other places within the central High Zagros Belt. The Fig. 10a, b present two examples, in Kuh-e-Dena and Baznavid area, respectively (see location on Fig. 2). All these normal faults are sealed by the pre-Permian unconformity.

Examination of preserved Palaeozoic stratigraphic sequence in the central HZB reveals different levels of erosion (and likely differential vertical movements) for the pre-Permian rocks (Fig. 5). In Dena mountains the basal Faraghan unconformity seals Cambrian, Lalun and Mila formations (Setudehnia 1972) whereas, towards the north-west (Zard-kuh area), the stratigraphic pile is more complete with presence of Ordovician Ilbek and Zardkuh formations (Setudehnia 1972; Fig. 5). In each place we observe the same geometrical relationships with pre-Permian rocks dipping towards the east or north-east beneath a more flat unconformable Permian cover. This configuration suggests a geometrical model of eastward tilted blocks over west-dipping normal faults. The hanging wall of each fault could preserve a more complete sedimentary sequence than the footwall, which suffered deeper erosion. Pre-Permian erosion (probably during the Carboniferous, see below) resulted in removal of huge thicknesses of Palaeozoic sequence (at least the whole Silurian and Devonian in the central HZB) before deposition of clastic Lower Permian Faraghan formation.

Pre-Permian unconformity and sealed normal faults in the eastern High Zagros Belt

In the context of the geological interpretation of the Palaeozoic rocks in Zagros, the eastern High Zagros Belt is important because it is the only place where Devonian and Silurian rocks are out cropping (Figs. 3 and 5). So, in contrast with the central HZB "Arch," the eastern HZB is located rather in a "Basin" position.

Ghavidel-syooki et al. (2011) give a new stratigaphic appraisal of the Palaeozoic sequence cropping out in both the Kuh-e-Gahkum and Kuh-e-Faraghan anticlines (Fig. 3). Following the new stratigraphic data acquired by these

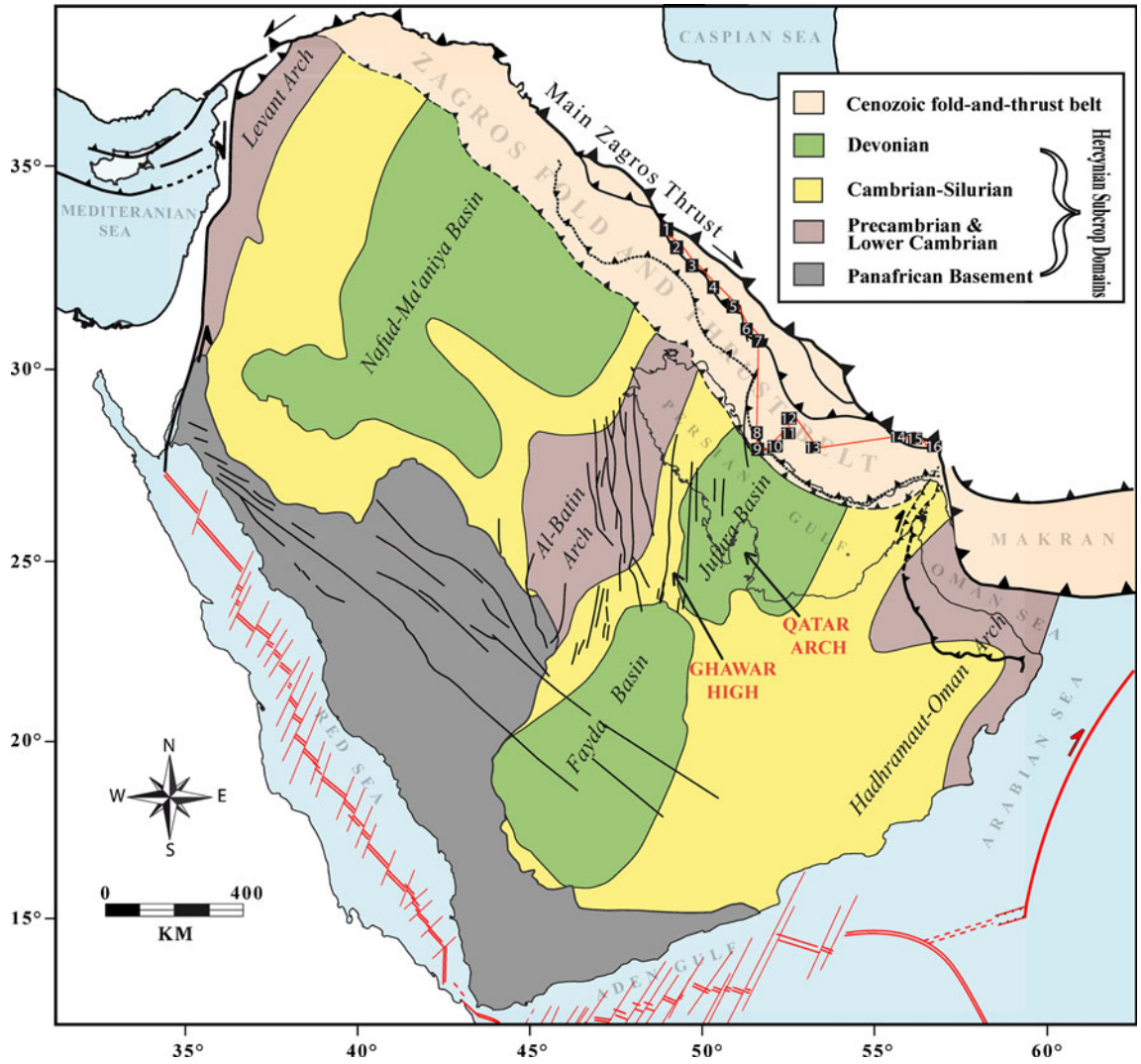

Fig. 6 Schematic structural map of the Arabian plate showing the main structural elements of the Zagros Fold-and-thrust Belt and Arabian platform. The Arabian platform is illustrated by an Hercynian subcrop map (modified from Faqira et al. 2009) in order to underline the major Paleozoic Arches and Basins

authors, the oldest rocks are Hirnantian conglomerates in Gahkum anticline suggesting a strong de-coupling within Lower Palaeozoic rocks along the Syahoo shales. This matter has not been taken into account in previous tectonic interpretations (Jahani et al. 2009; Motamedi et al. 2011).

In Kuh-e-Faraghan structural section (Fig. 11), this decoupling led to the development of a major back-thrust (thrust faults labelled 1 on the Fig. 11) putting the Palaeozoic over the Mesozoic rocks (Jahani et al. 2009). Following our interpretation, this back-thrust initiated at an early stage of the development of the structure and is due to the activation of Ordovician ductile layers. Forward progression of deformation caused the occurrence of a low angle forethrust in the core of the Faraghan anticline (thrust faults labelled 2 on the Fig. 11). The whole sequence have been subsequently cut out by a late south-west verging basement fault (thrust faults labelled 3 on the Fig. 11). Such an evolution can explain why the Cambrian and Early Ordovician rocks remain at depth and are not exposed in the field.

As in the central HZB and despite the restricted area where Palaeozoic rocks are out cropping, the Kuh-e-Faraghan presents beautiful examples of normal faults sealed by the Faraghan formation (Fig. 12a, b). This observation is of crucial importance for three main reasons: (1) it shows that normal faulting is not restricted to the Palaeozoic "Arch" as in the central HZB but developed also in the intervening "basins"; (2) it shows that the normal faults developed after the deposition of the Zakeen formation, which is dated as Early Devonian up to Frasnian (Ghavidel-syooki 2003) (Figs. 4 and 5) and (3) it shows (absence of the Carboniferous) that the pre-Permian uplift and related erosion

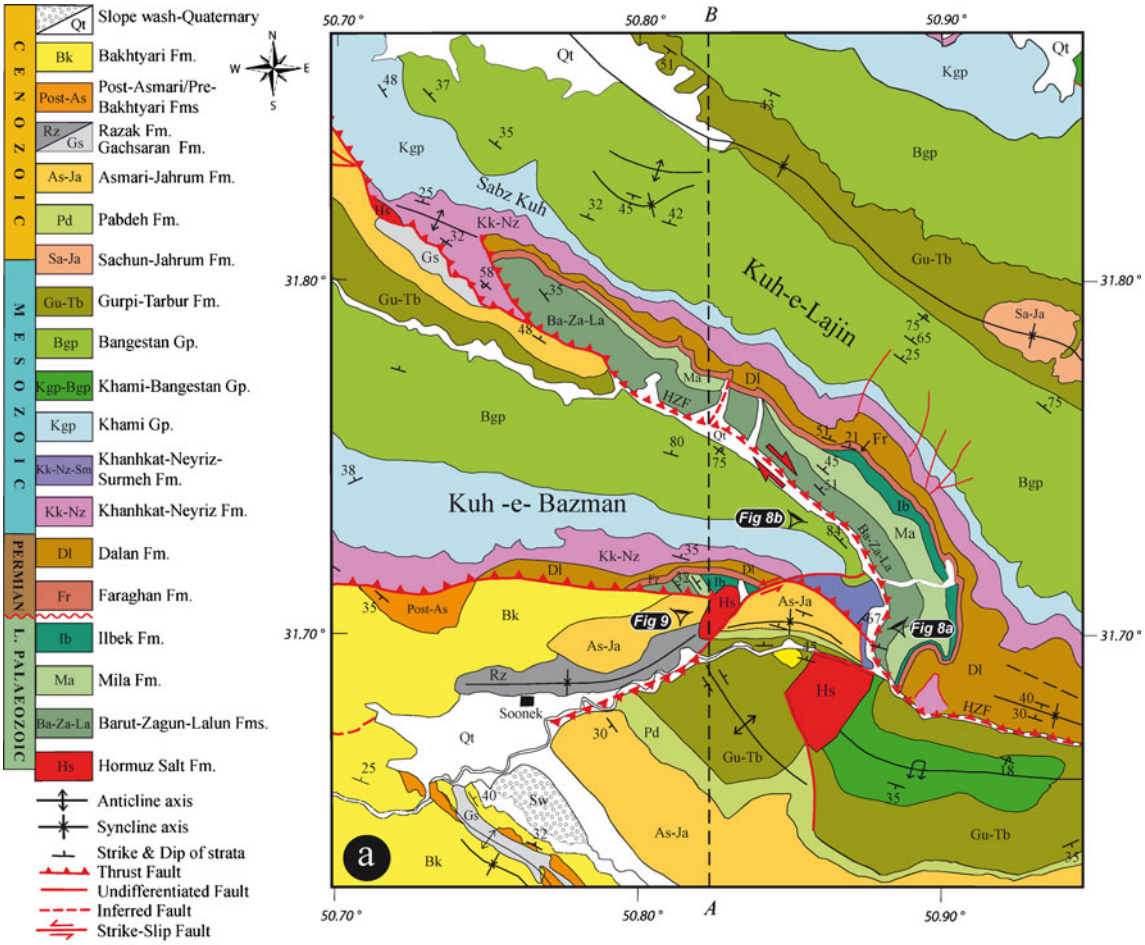

Fig. 7 **a** Geological map of the Kuh-e-Lajin, Kuh-e-Bazman and adjacent areas, modified from Ardal 1/100,000 map (Ehsanbakhsh-Kermani et al. 1996; see location on Fig. 2) with location of the section line. **b** Structural cross-section through the Kuh-e-Lajin (see location on Fig. 7a)

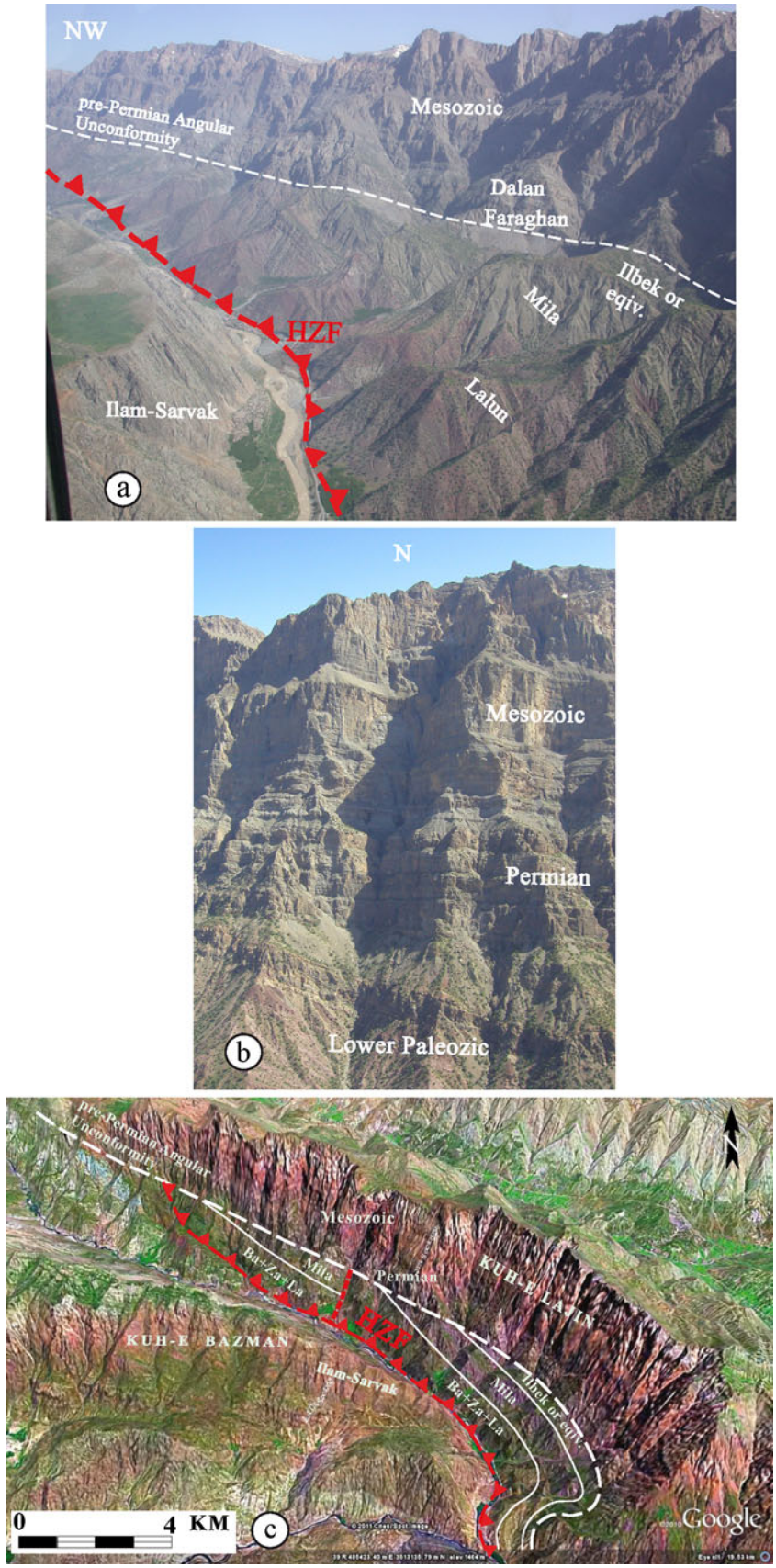

Fig. 8 **a** Helicopter view of the pre-Permian angular unconformity in Kuh-e-Lajin. **b** Detail of the unconformity in Kuh-e-Lajin. **c** Landsat image of the Kuh-e-Lajin illustrating the pre-Permian unconformity. Photos **a** and **b** are located on Fig. 7a

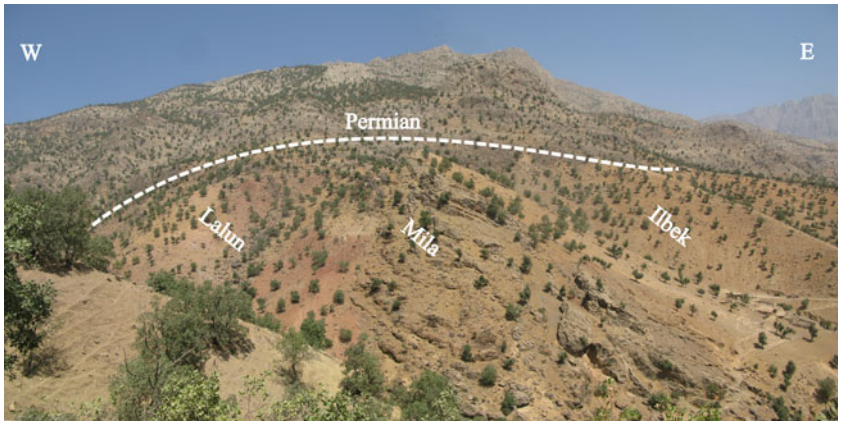

Fig. 9 The pre-Permian unconformity at Kuh-e-Bazman (see location on Fig. 7a). Note to the truncation of tilted Lower Palaeozoic formations by overlying Permian rocks

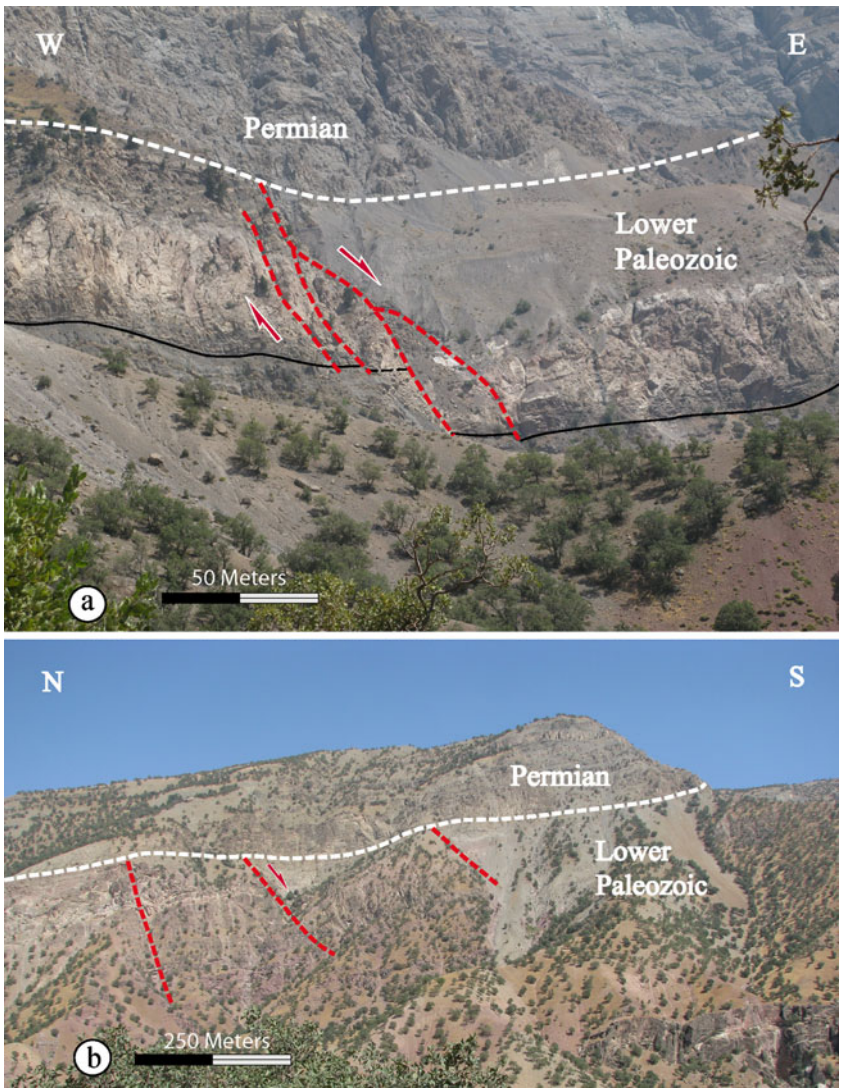

Fig. 10 Examples of pre-Permian normal faults. **a** Normal faults in Kuh-e-Dena sealed by Pre-Permian unconformity. In this case, the fault planes are dipping eastward. They are most probably antithetic faults by reference to the major normal faults. **b** Normal faults in Baznavid topped by Pre-Permian unconformity. Photos **a** and **b** are located on Fig. 2

is not restricted to the "Arch" but is general at the scale of the High Zagros Belt.

Discussion

Apart the direct border of the Arabian shield (Fig. 6), the HZB (Fig. 1) is the only place in the Arabian plate where the Lower Palaeozoic is out cropping. It is consequently of great interest for a better understanding of the Palaeozoic evolution of the whole Arabian domain.

Geometry of the Palaeozoic deposits and associated deformation

At large scale and after unfolding of the Cenozoic structures, the Palaeozoic section of the HZB presents NE trending pre-Permian long wavelength and low amplitude "folds" extending north of the Al-Batin Arch and the Jafurah Basin known in the Arabian foreland (Figs. 5 and 6; Faqira et al. 2009). These structures could be interpreted as the result of lithospheric folding. In this classical hypothesis, the normal faults observed in the central HZB should be extensional features developed in the outer stretched arc of the anticlines (Fig. 13a). However, the existence of these normal faults in the eastern HZB, which is in a "syncline" position (Fig. 5), cannot be easily integrated in such a scheme.

Our work suggests rather a gentle horst and graben geometry related to a weak extensional deformation (Fig. 13b). This deformation is accompanied by an important uplift explaining the huge erosion observed in the Arches and the hiatus of the Lower to Middle Carboniferous observed in the Basins. The origin of this general uplift remains disputable. However, the lack of important normal faults within the post-unconformity deposits strongly suggests a sag geometry for these Basins and consequently a thermal origin for the subsidence. More precisely, the post-uplift cooling of the lithosphere should be responsible for thermal subsidence by the Late Carboniferous. The same geometry can be observed in the Arabian foreland of the Zagros where the Upper Carboniferous–Lower Permian Unayzah Fm is confined in the central parts of the Palaeozoic Basins whereas the Middle-Upper Permian Khuff Fm is on-lapping the "Arches" (Faqira et al. 2009).

Faqira et al. (2009) express some doubts about the causality relationships between the Arches building and the Hercynian orogeny, which developed 5,000 km away to the west. We share these doubts and go further. The question is to know if our conclusions on the HZB (i.e. the absence of pre-Carboniferous contractional deformation) can be extended to the Arabian plate and even to other parts of the north Gondwanian domain like Pakistan (Gee 1989). As a matter of fact, this entire domain presents a unified architecture with a series of broad Basins and intervening Arches. At its present stage, our work is too local to be affirmative. However, we can emphasize several important points. Most of the faults of the Central Arabian Domain are confined in the pre-Unayzah deposits (Wender et al. 1998; Johnson 2008). Despite recent high quality data, it is difficult to understand easily their kinematics because the faults appear

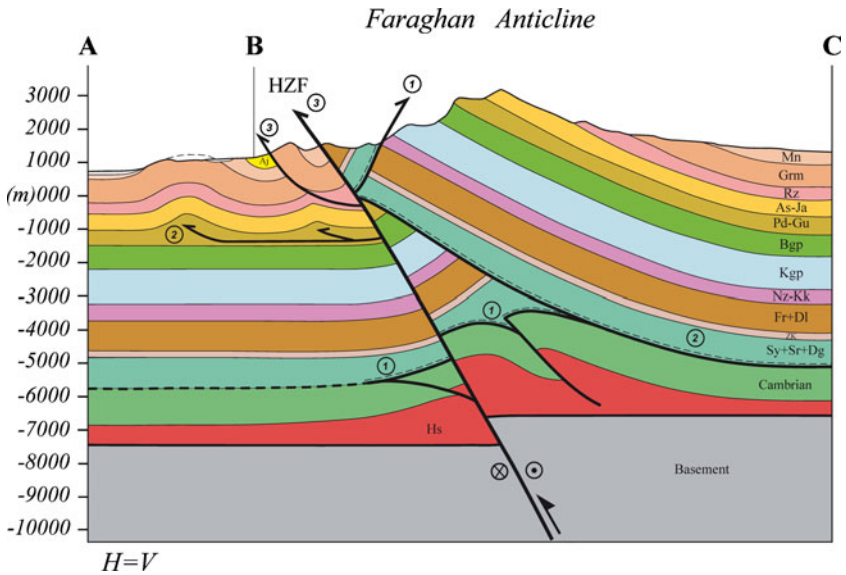

Fig. 11 Structural cross-section through Kuh-e-Faraghan (see location on Fig. 3). *Hs* Late Proterozoic to Infra-Cambrian Hormuz Salt, *Sy* Ordovician Syahoo Fm. *Dg* Hirnantian Dargaz Fm., *Sr* Silurian Sarchahan Fm., *Zk* Devonian Zakeen Fm., *Fr* Early Permian Faraghan Fm., *Dl* Permian Dalan Fm., *Kk* Triassic Khanehkat Fm., *Nz* Jurassic Neyriz Fm., *Kgp* Jurassic-L.Cretaceous khami group, *Bgp* U. Cretaceous Bangestan group, *Gu* U. Cretaceous Gurpi Fm., *Pd* Paleo-Eocene Pabdeh Fm., *Ja* Eocene Jahrum Fm., *As* Oligo-Miocene Asmari Fm., *Rz* Miocene Razak Fm., *Grm* Guri member, *Mn* Miocene Mishan Fm., *Aj* U.Miocene Aghajari Fm. *Lables* show the sequence of thrusting

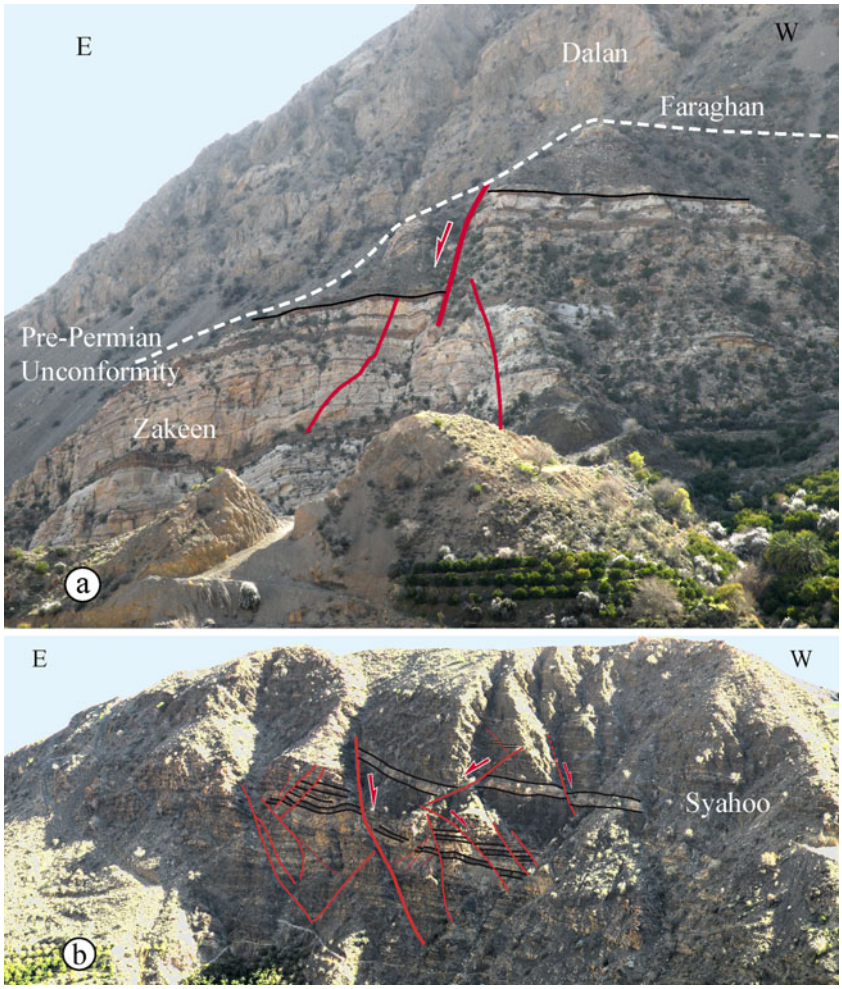

Fig. 12 **a** Tang-e-Zakeen (Kuh-e- Faraghan) illustrating normal faulting within Devonian Zakeen formation. The faults are sealed by Permian rocks (like in the Central High Zagros). **b** Conjugate sets of normal faults in Ordovician Syahoo formation exposed in the core of Faraghan anticline

in general as nearly vertical. In addition, there are strong difficulties in separating the effects of the pre-Unayzah development from the subsequent structural growth. This is particularly true for the Triassic and Upper Cretaceous periods, which are characterized by the development of normal and reverse faults, respectively (Konert et al. 2001; Faqira et al. 2009). In any case, it can be at least concluded that the so-called "Hercynian event" is quite complex and may be not expressed in the same way everywhere across the Arabian plate even if there are evident similarities between the main features of the Arabian Domain and what we have observed in the HZB. This is particularly clear for the Ghawar High (see Wender et al. 1998), which is located along the eastern flank of the Al-Batin Arch, about 800 km south of the central HZB (Fig. 6).

Timing of the processes

In the eastern HZB, the timing of the uplift and extensional deformation is quite well constrained by existing stratigraphic data as the younger formation situated below the pre-Permian unconformity has been dated as Frasnian in the Kue-e-Faraghan (Ghavidel-syooki 2003). In the central HZB, the timing is poorly constrained by stratigraphic studies

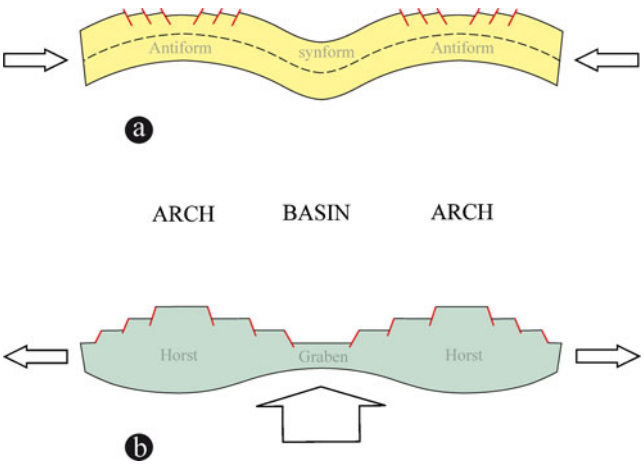

Fig. 13 Geodynamic interpretation of the Paleozoic Arches. **a** Compressive interpretation: in this classical explanation, the *Arches* represent lithosphere anticlines with possible normal faults in the extrados. **b** Extensional interpretation: in this latter (favoured in the present paper) explanation, the *Arches* are horst structures and the extension is diffused through the whole area

but the same post-Upper Devonian age is suggested by thermochronologic data. In this area, Gavillot et al. (2010) used (U-Th)/He thermochronology to date the recent thrust activity. The Palaeozoic history of the region was not the topic of their paper but they notice that a sample from the Mila formation (deposited about 500 Ma ago) was reset and then exhumed at 350 Ma (Late Devonian/Early Carboniferous).

The same exhumation age had been found by Kohn et al. (1992) in the north-western part of the Arabian plate. More precisely, the authors define a "major Late Devonian/Early Carboniferous thermotectonic event" responsible for uplift and huge erosion along a strip extending from the Gulf of Suez to north-east Syria and south-east Turkey, a zone corresponding to the Levant Arch in the terminology used by Faqira et al. (2009; Fig. 6). Using Zircon fission tracks of 17 Precambrian samples from deep boreholes and outcrops, these authors obtained 330–370 Ma ages. These ages indicate that (1) there was a total resetting of Zr fission track clocks (temperature required, 225±50°C), (2) the timing of exhumation (and related erosion) is Late Devonian/Early Carboniferous and (3) the thermal gradient was probably high (about 50°C/km) before the exhumation. It is worth noting that the same Late Devonian/Early Carboniferous age has been found by Bojar et al. (2002) in the Nubian shield of the Eastern Desert (Egypt). Again, we emphasize the convergence between ages of Arches building obtained in the HZB and elsewhere not only in the Arabian plate but also in a very large area of the northern Gondwana. In addition we note that the thermal origin for the generalized uplift of the Arabian Domain at that time has been already suggested by Fariqa et al. (2009).

Conclusion

In the central High Zagros Belt, there is no evidence of compressional deformation of Palaeozoic age. On the contrary, the only structures exposed in the field are normal faults leading to a system of tilted blocks. These field data from the central High Zagros seems consistent, at least partly, with what is shown in the Arabian domain (e.g. Wender et al. 1998; Johnson 2008; Faqira et al. 2009).

This first result raises the question about the significance of Variscan orogeny in the Arabian domain. In addition, thermochronologic data got by Kohn et al. (1992) in the north-western end of Arabia as well as the preliminary results by Gavillot et al. (2010) in the study area show that the uplift of the whole Arabia as soon as the Late Devonian is most probably of thermal and not tectonic origin. Moreover, the relief high wavelength (×1,000 km), the sag geometry of the post-unconformity deposits as well as the diffuse extensional deformation suggest a relationship with asthenosphere dynamics rather than with a far compressive field. Quantification of these processes requires more data and more modelling.

Further thermochronologic work is required to reinforce this preliminary result. However, there is an increasing body of evidence suggesting that the pre-Permian geological history results from thermal uplift accompanying normal faulting and not from a far effect of the Variscan orogeny as classically assumed. The age of the uplift is not yet well constrained but seems to occur during the Late Devonian–Early Carboniferous. The subsequent cooling of the lithosphere should be responsible for thermal subsidence and deposition of the Faraghan-Unayzah formations by the Late Carboniferous.

Acknowledgements This paper benefited from discussions with many colleagues in particular: C. Blanpied (Total), J. Letouzey (UPMC, Paris) and S. Sherkati (NIOC, Tehran). The authors would like to thank the exploration directorate of National Iranian Oil Company (NIOC) for providing data, logistics during field trip and particularly M. Mohaddes, M. Zadeh Mohammadi, D. Baghbani and M. Goodarzi for their continuous support. S. Tavakoli and J-C Wrobel-Daveau acknowledge TOTAL for Ph.D. Scholarships. This paper is a contribution of the "Groupe Recherche Industrie" "Marge Sud-Tethys", a research agreement between TOTAL on the one hand and l'Ecole Normale Supérieure (ENS), l'Université Pierre-et-Marie-Curie (UPMC) and l'Université de Cergy-Pontoise (UCP) on the other hand. The reviews by Matteo Molinaro, an anonymous reviewer and the associate editor François Roure were highly appreciated.

References

Alavi M (1994) Tectonics of the Zagros orogenic belt of Iran: new data and interpretation. Tectonophysics 229:211–238

Alavi M (2004) Regional stratigraphy of the Zagros fold-thrust belt of Iran and its proforeland evolution. American Journal of Sciences 304:1–20

Berberian M (1995) Master 'blind' thrust faults hidden under the Zagros folds: active basement tectonics and surface morphotectonics. Tectonophysics 241:193–224. doi:10.1016/0040-1951(94)00185-C

Berberian M, King GCP (1981) Towards a paleogeography and tectonic evolution of Iran. Canadian Journal of Earth Sciences 18 (2):210–265. doi:10.1139/e81-019

Bojar A, Fritz H, Kargl S, Unzog W (2002) Phanerozoic tectonothermal history of the Arabian-Nubian shield in the eastern Desert of Egypt: evidence from fission track and paleostress data. Journal of African Earth Sciences 34:191–202

Boote DRD, Clark-Lowes DD, Traut MW (1998) Paleozoic petroleum systems of North Africa. In: Macgregor DS, Moody RTJ, Clarke-Lowes DD (eds) Petroleum geology of North Africa. Geological Society, London, Special Publications 132:7–68

Bosold A, Schwarzhans W, Julapour A, Ashrafzadeh AR, Ehsani SM (2005) The structural geology of the High Central Zagros revisited (Iran). Petroleum Geoscience 11:225–238

Ehsanbakhsh-Kermani et al. (1996) Geological map of Ardal, 1:100,000. Geological Survey of Iran Ed

Falcon NL (1974) Southern Iran: Zagros Mountains. In: (eds) Mesozoic–Cenozoic orogenic belts. Geological Society, London, Special Publications 4:199–211, doi:10.1144/GSL.SP.2005

Faqira M, Rademakers M, Afifi AM (2009) New insights into the Hercynian orogeny, and their implications for the Paleozoic Hydrocarbon System in the Arabian plate. GeoArabia 14(3):199–228

Frizon de Lamotte D, Raulin C, Mouchot N, Wrobel-Daveau JC, Blanpied C, Ringenbach JC (2011) The southernmost margin of the Tethys realm during the Mesozoic and Cenozoic: initial geometry and timing of the inversion processes. Tectonics 30: TC3002. doi:10.1029/2010TC002691

Gavillot Y, Axen GJ, Stockli DF, Horton BK, Fakhari M (2010) Timing of thrust activity in the High Zagros fold-thrust belt, Iran, from (U-Th)/He thermochronometry. Tectonics 29:TC4025. doi:10.1029/2009TC002484

Gee ER (1989) Overview of the geology and structure of the Salt Range. In: Malinconico LL, Lillie RJ (eds) Tectonics of the Western Himalayas. GSA Spec. Paper, 232, 95–112

Ghavidel-syooki M (1990) The encountered achritarcs and chitinozoan from Mila, Ilebek, Zardkuh and Faraghan Formations in Tang-e-Ilebek at Zardkuh and their correlation with the Palaeozoic sequence at Chal-i-sheh area and Darang well. Symposium on diapirism with special reference to Iran 1:140–218

Ghavidel-syooki M (2003) Palynostratigraphy of Devonian sediments in the Zagros Basin, southern Iran. Review of Paleobotany and Palynology 127:241–268. doi:10.1016/S0034-6667(03)00122-2

Ghavidel-syooki M (2005a) Palynological study and age determination of Faraghan Formation in Kuh-e-Gahkum region at southeast of Iran. In: (eds) Contributions to the paleopalynology of paleozoic rock units in the Zagros, Alborz and Central Iranian Basin, published book, 15–34 in Persian

Ghavidel-syooki M (2005b) Palynological study and age determination of Ordovician sediments and Faraghan Formation in Kuh-e-Surmeh at southern Iran. In: (eds) Contributions to the paleopalynology of paleozoic rock units in the Zagros, Alborz and Central Iranian Basin, published book, 96–104 in Persian

Ghavidel-syooki M, Álvaro JJ, Popov L, Ghobadi Pour M, Ehsani MH, Suyarkova A (2011) Stratigraphic evidence for the Hirnantian (latest Ordovician) glaciation in the Zagros Mountains, Iran. Palaeogeography, Palaeoclimatology, Palaeoecology 307:1–16. doi:10.1016/j.palaeo.2011.04.011

Insalaco E, Virgone A, Courme B, Gaillot J, Kamali M, Moallemi A, Lotfpour M, Monibi S (2006) Upper Dalan Member and Kangan formations between Zagros Mountains and offshore Fars, Iran: depositional system, biostratigraphy and stratigraphic architecture. GeoArabia 11(2):75–176

Jahani S, Callot JP, Letouzey J, Frizon de Lamotte D (2009) The eastern termination of the Zagros Fold-and-Thrust Belt, Iran: structures, evolution, and relationships between salt plugs, folding, and faulting. Tectonics 28:TC6004. doi:10.1029/2008TC002418

James GA, Wynd JG (1965) Stratigraphic nomenclature of Iranian oil consortium agreement area. American Association of Petroleum Geologist Bull 49:2182–2245

Johnson CA (2008) Phanerozoic plate reconstructions of the Middle East: insights into the context of Arabian tectonics and sedimentation. SPE 118062

Kheradpir A, Khalili M (1972) Brief notes on facies and age relationships of the pre-Sarvak section in Dina/Zardkuh area. Iranian Oil Operating Companies, *Technical Memo no.* 115

Kohn BP, Eyal M, Feinstein S (1992) A major late Devonian–early Carboniferous (Hercynian) thermotectonic event at the new margin of Arabian–Nubian shield: evidence from Zircon fission track dating. Tectonics 11:1018–1027

Konert G, Afifi AM, Al-Hajri SA, Drost HJ (2001) Paleozoic stratigraphy and hydrocarbon habitat of the Arabian plate. GeoArabia 6 (3):407–442

Koop WJ, Stoneley R (1982) Subsidence history of the Middle East Zagros Basin, Permian to Recent. Philos Trans Royal Soc London Ser A 305:149–168. doi:10.1098/rsta.1982.0031

Letouzey J, Sherkati S (2004) Salt movement, tectonic events, and structural style in the Central Zagros Fold and Thrust Belt (Iran). In: Salt sediments interactions and hydrocarbon prospectivity, 24th Annual GCSSEPM Foundation, Bob F. Perkins Research Conference, Houston, Texas

Michard A, Soulaimani A, Hoepffner C, Ouanaimi H, Baidder L, Rjimati EC, Saddiqi O (2010) The South-Western branch of the Variscan Belt: evidence from Morocco. Tectonophysics 492:1–24

Molinaro M, Leturmy P, Guezou J-C, Frizon de Lamotte D, Eshraghi SA (2005) The structure and kinematics of the southeastern Zagros fold-thrust belt, Iran: from thin-skinned to thick-skinned tectonics. Tectonics 24:TC3007. doi:10.1029/2004TC001633

Motamedi H, Sepehr M, Sherkati S, Pourkermani M (2011) Multiphase hormuz salt diapirism in the Southern Zagros, SW Iran. Journal of Petroleum Geology 34:29–44

Motiei H (1993) Stratigraphy of Zagros (in Persian). Geological Survey of Iran, Tehran, 536 pp

Mouthereau F, Lacombe O, Tensi J, Bellahsen N, Kargar S, Amrouch K (2007) Mechanical constraints on the development of The Zagros Folded Belt (Fars). In: Lacombe O et al (eds) Thrust belts and foreland basins: from fold kinematics to hydrocarbon systems. Springer, New York, pp 245–264

Nicole GL, Kheradpir A (1972) Stratigraphic column, # 20509-95, Kuh-e Gereh. Oil Service Company of Iran

O'Brien CAE (1950) Tectonic problems of the oilfield belt of southwest Iran. 18th International Geological Congress, Proceeding, Great Britain

O'Brien CAE (1957) Salt diapirism in south Persia. Geologie en Mijnbouw 19:357–376

Rask DH (1977) Permo-Triassic field survey-Oshtoran Kuh, Qal'eh kuh(Chal-i-sheh) and Zard-Kuh areas. Oil Service Company, Technical note # 162

Setudehnia A (1972) The Paleozoic sequence at Zardkuh and Keh-e-Dinar. Iranian Oil Operating Companies, Report # 1196

Sherkati S, Molinaro M, Frizon de Lamotte D, Letouzey J (2005) Detachment folding in the Central and Eastern Zagros fold-belt (Iran): salt mobility, multiple detachments and late basement control. Journal of Structural Geology 27:1680–1696. doi:10.1016/j.jsg.2005.05.010

Sherkati S, Letouzey J, Frizon de Lamotte D (2006) Central Zagros fold-thrust belt (Iran): new insights from seismic data, field observation, and sandbox modeling. Tectonics 25:TC4007. doi:10.1029/2004TC001766

Simancas JF, Azor A, Martinez-Poyatos D, Tahiri A, El Hadi H, Gonzalez-Lodeiro F, Perez-Estaun A, Carbonell R (2009) Tectonic relationship of Southwest Iberia with the allochthonous of Northwest Iberia and the Morroccan Variscides. CR Geosciences 341:103–113

Stocklin J (1968) Structural history and tectonics of Iran: a review. American Association of Petroleum Geologist Bull 52:1229–1258

Szabo F (1977) Permian and Triassic stratigraphy Zagros basin, South-West Iran. Oil Service Company, Report # 1261

Vergès J, Saura E, Casciello E, Fernandez M, Villasenor A, Jimenez-Hunt I, Garcia-casellanos D (2011) Crustal-scale cross-section across the NW Zagros Belt: implications for the Arabian margin reconstruction. Geological Magazine. doi:10.1017/S00167568111000331

Wender LE, Bryant JW, Dickens M, Neville AS, Al-Moqbel AM (1998) Paleozoic (Pre-Khuff) hydrocarbon geology of the Ghawar Area, Eastern Saudi Arabia. GeoArabia 3(2):273–302

II.3) Further comments and illustrations of the paper N° 2

II.3) Further comments and illustrations

We present just below additional data supporting the main propositions of our paper, i.e. the existence of extensional deformation sealed by the pre-Permian unconformity. First of all, we will show more field data documenting existence of pre-Permian uplift and the profusion of normal faulting in the High Zagros Belt. Then, we will display some offshore seismic (reflection seismic lines from the Persian Gulf) illustrating the style of deformation beneath the unconformity at large scale.

II.3.1. Pre-Permian Paleosol in the Western High Zagros

The presence of a sedimentary hiatus, as the one observed in the High Zagros (Fig. II.1), asks a challenging question: “is the hiatus as the result of no-deposition or of erosion”? To demonstrate erosion and related continental evolution, the existence of markers is required. Among these markers, the presence of “paleosol” is indicative of development of flat surfaces during a long continental evolution. This is particularly the case for laterite, which can develop only if the weather is dry during an extended period.

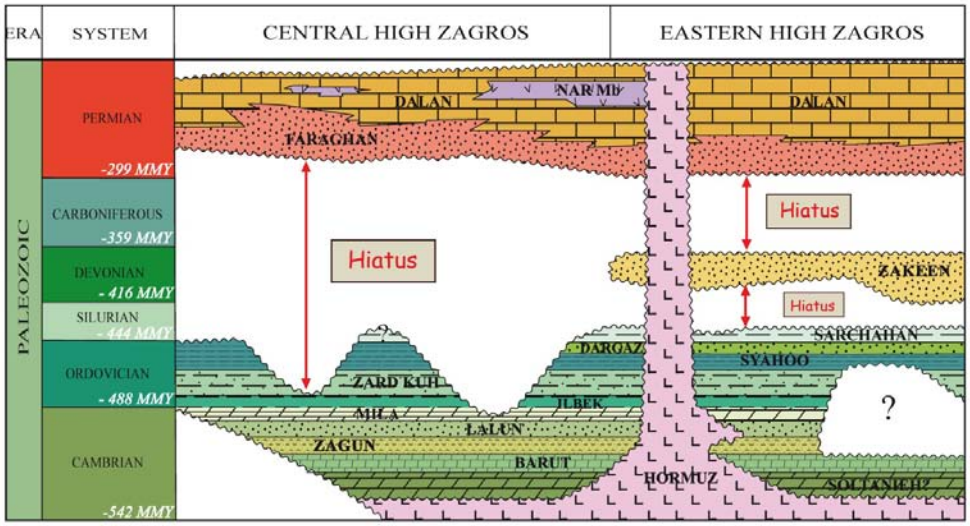

Fig. II.1. Stratigraphic log on the High Zagros Belt. Modified after Tavakoli-Shirazi et al. (2012)

Paleosols looking like laterite are exposed in two places in the High Zagros. In the area of Dena Mountain a vari-colored paleosol zone where about 1.5-2 m of bauxite and laterite preserved below the Permian rocks can be observed (Fig.II.2). A similar deposit has been observed in the Kuh-e-Lajin (Fig.II.3). These observations are important because they demonstrate that the pre-Permian hiatus observed in the

High Zagros resulted from erosion followed by a long continental evolution and not only from absence of deposition.

Fig. II.2. Paleosol consisting of bauxite and laterite in Dena section. This layer on top of the Cambrian marks the hiatus corresponding to the pre-Permian uplift.

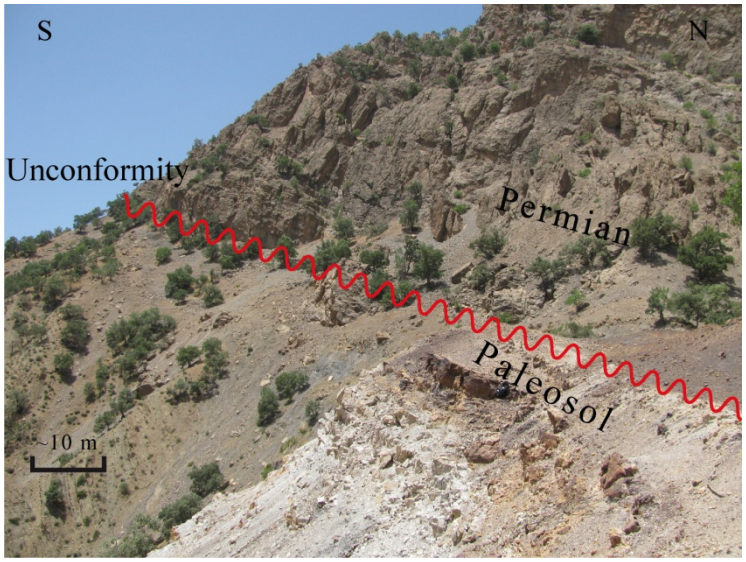

Fig. II.3. Presence of "Paleosol" which is covered by Permian sediments indicating a long-lived continental evolution.

II.3.2.Additional evidence for extensional deformations in Western High Zagros

Some indications for pre-Permian normal faulting in the High Zagros Belt were given in the paper n° 2 (Figures 10 a, b and 12 a, b). In many places of the Western High Zagros other clues of pre-Permian extensional deformation exist. The figure II.4

presents vertical displacement along a steep normal fault locating north of Baznavid village (see location in the Annex 3). This photo illustrates a conclusive downward movement of the hanging-wall block including Ordovician Ilbeyk shales interbedded with sandstone layers which are topped by pre-Permian unconformity. Sealing of the normal fault by Farghan Fm reveals that the extension occurred prior to Permian.

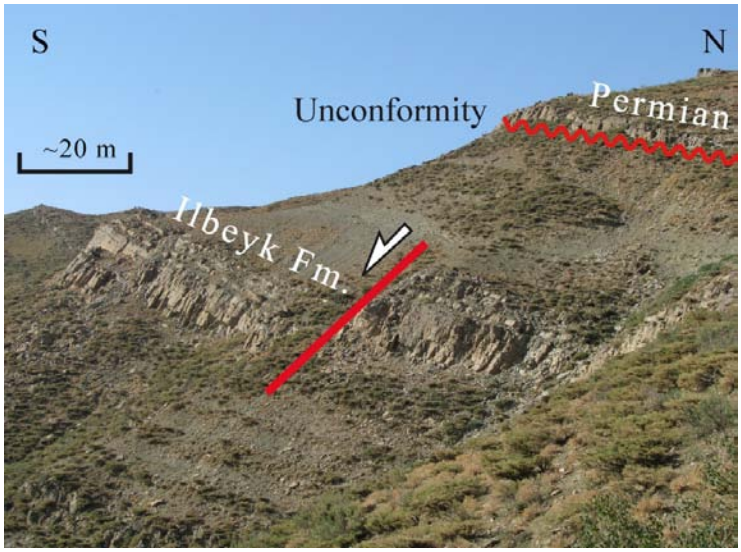

Fig. II.4. *Extensional deformation of the Ordovician rocks in Baznavid area (Western High Zagros) indicated by normal movements along the fault which is sealed by pre-Permian unconformity.*

Identical normal faulting can also be observed in the middle portion of the Western High Zagros in the northern flank of the Lajin anticline where well stratified limestones of Cambrian Mila, member “B”, have been displaced by a south-dipping meo-scale normal(Fig.II.5.a and b).

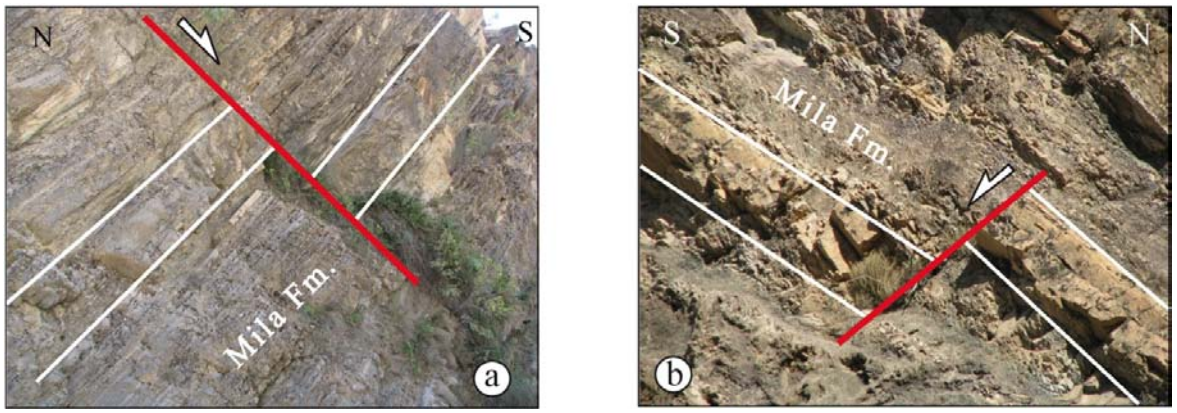

Fig.II.5. a, b) *Dislocation of Mila “B” limestone because of meso-scale normal faults in Kuh-e-Lajin*

Another example of normal displacements limited to the carbonate rocks of Cambrian Mila formation was pictured in the Fig. II.6.The site of this photo is in the Putak Valley of Dena Mountain, east of the WHZ region. The subsequent compressional deformations during Zagros orogeny were responsible for the rotation of previous structures in this area and led to the complication of geological features.

A conceptual sketch (Fig.II.7) displays the main stages of deformation in Dena area. This scenario summarizes a three-step kinematics for pre-Permian structural evolution in this region.

These observed diffuse extensional structures beneath the early Permian sediments in the HZB reinforce our interpretation: the occurrence of extensional deformations is related to a thermal uplift instead of the far effect of Hercynian tectonic phase.

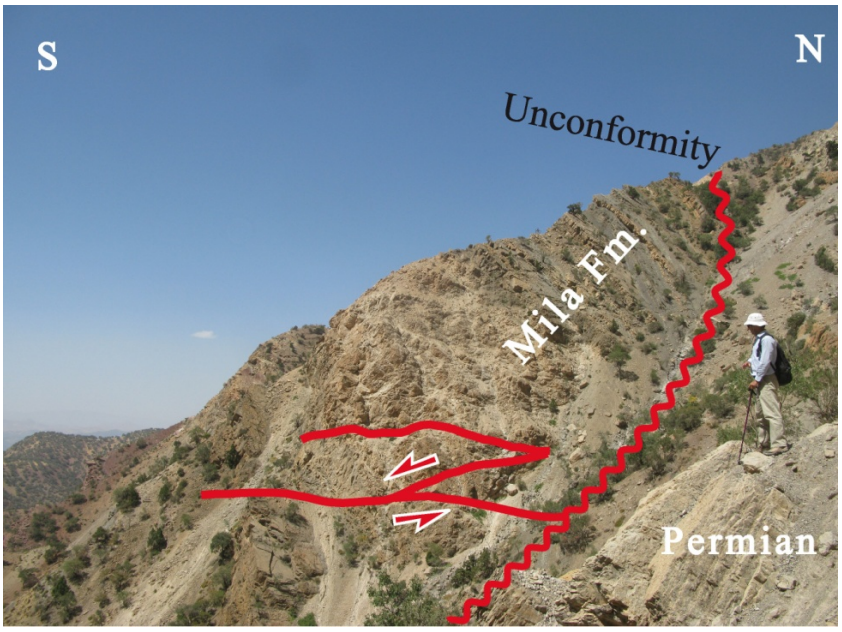

Fig.II.6. *Field picture of Dena Mountain (Putak valley) illustrating the tilted normal faults within the Cambrian carbonate of Mila Fm. Angular unconformity at the base of Faraghan Fm caps the faults.*

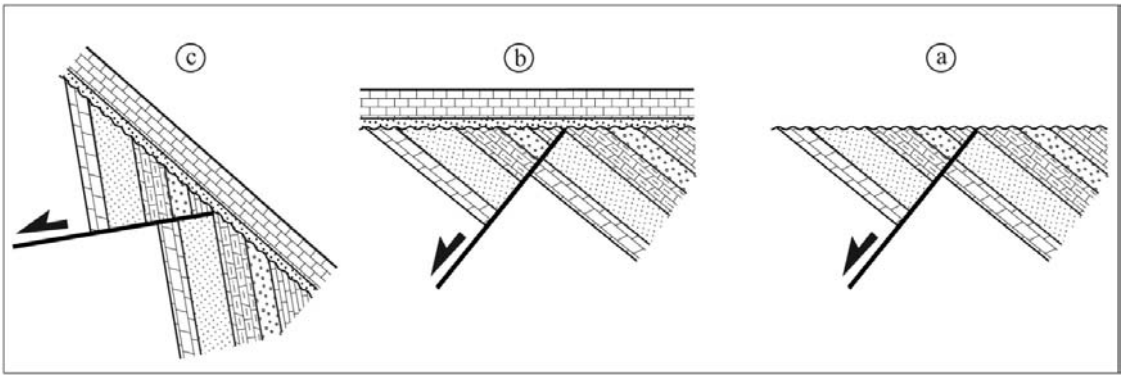

Fig. II.7. interpretative sketches of successive deformation observed in Dena Mountain. a) Tilted block and normal fault in pre-Permian uplifted sediments which is topped by erosion surface. b) Onset of deposition in carbonate platform from Permian to Cretaceous starting with basal siliciclasticts just above the unconformity. c) Rotation of preceding structures due to the late Alpine compression in Zagros.

II.3.3. Remarks from Seismic Data

II.3.3.1. Offshore Seismic studies

The northern part of Persian Gulf has been covered by the detailed "Persian Carpet" (PC) seismic project. Below, some of the structural features supporting the main proposition of the paper 2 are presented:

Pre-Permian extensional deformation, "Paleo-High" and angular unconformity

Fig.II.8 illustrates a composite seismic line owing to PC study and oriented NW-SE. Interpretation of this section reveals the existence of an Arch structure in sub-sediment horizon (basement level). The tracing of one of these deep reflectors which is most probably locating within the pre-Hormuz levels show the existence of an uplifted zone along the northward prolongation of the Qatar-Fars Arch. This structure is bounded by a couple of N-S trending normal faults, which are probably inherited from older basement faults. The N-trending paleo-highs are one of the main structural elements in the Arabian plate and exemplified by the En Nala (Ghawar) anticline and the Qatar Arch (Konert et. al, 2001). Variation of the sediment thickness in the figure II.8. from southeastern side of the bulge to the crestal area shows the rejuvenation of this structure during the deposition of pre-Faraghan sediments.

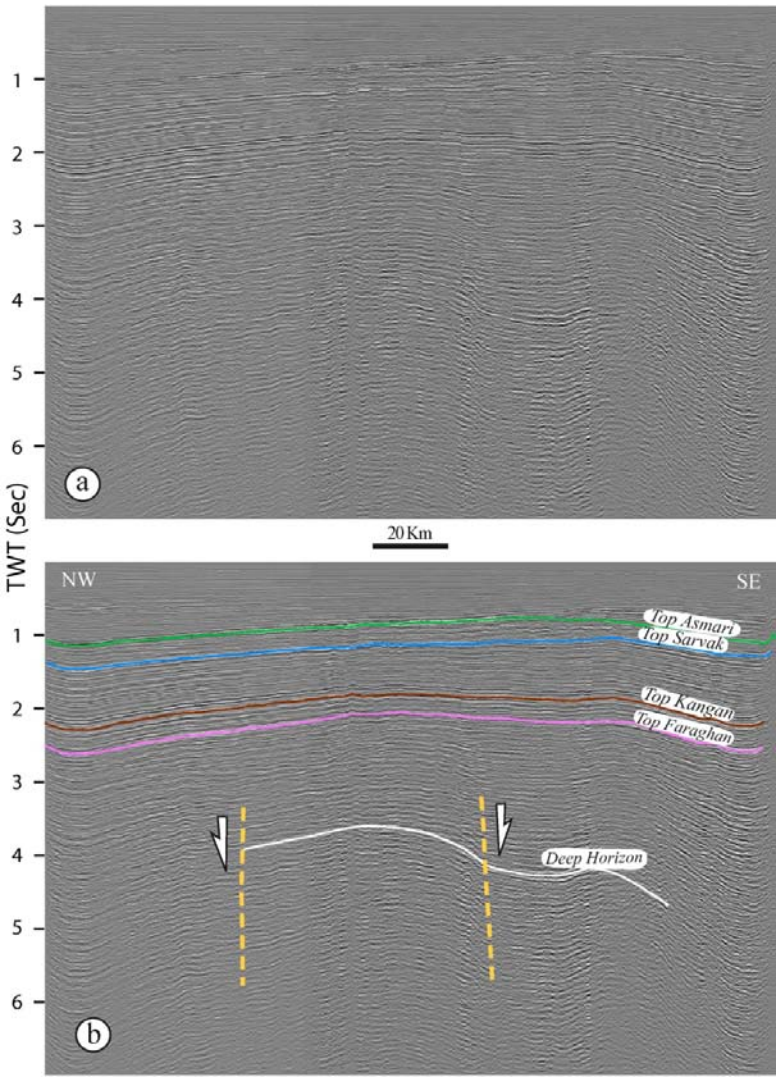

Fig. II.8. a) Non-interpreted and b) interpreted seismic strike line in the Persian Gulf Illustrates the uplifted region (Paleo-High) which is bounded to extensional faults. Note to the decreasing of pre-Faraghan thickness above this Paleo-high.

Additional example of the significant pre-Permian deformation in the Zagros Foreland basin is illustrated by another seismic line (Fig. II.9).This profile shows the variations of thickness within the sediment (Faraghan Formation) that overlies pre-Permian unconformity. This suggests the progressive onlap of the Permian deposits toward a pre-existing High. Thanks to the high resolution 2D seismic profile, we can recognize a basement vertical offset prior to the Permian deposition. The formations situated above the Permian are isopach, reflecting cessation of uplift by this age onward. The old Paleo-High in this section affected the geometry of the overlying deposits and led to develop a culmination (closure structure) just above.

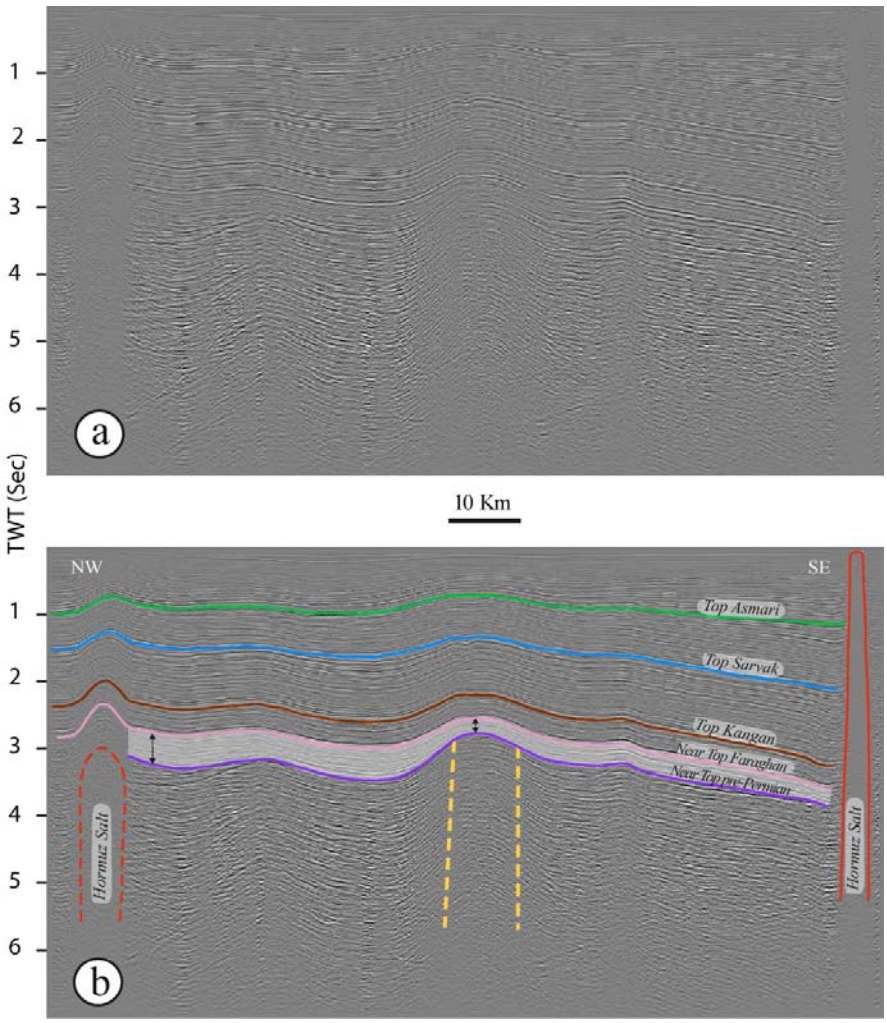

Fig.II.9. a) *Non-interpreted and* ***b)*** *interpreted seismic profile in the Persian Gulf illustrates the lateral thickness variation of Early Permian Faraghan formation.*

Halokinesis is a remarkable tectonic feature in this area. Two distinct Hormuz salt diapirs are observable in the figure II.9. They have pierced overlying beds and rose up to different levels. The one toward the southeast of the seismic profile has penetrated into the youngest strata and climbed up ultimately. It has made an emergent diapir where they reached the surface.

Fig.II.10. is another seismic section, parallel to the previous figure (Fig. II.9) and close to it. The interpreted seismic line (Fig.II.9.b) was flattened on top of the Triassic Kangan formation. Consequently, a significant reflector to the NW portion of the section was observable within the pre-Permian deposit which is pinched out below the unconformity. This horizon presents the pre-Permian angular unconformity

and underlying tilted blocks which was generated due to the rotation along normal faults.

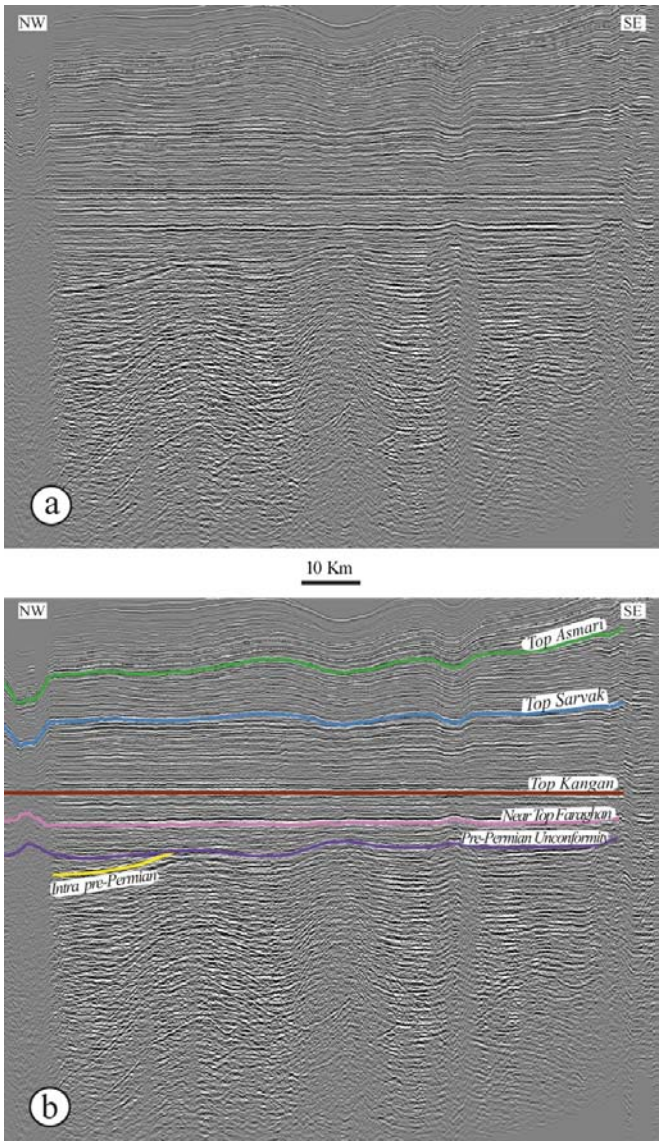

Fig.II.10. a) Non-interpreted and b) interpreted sections of the Persian Gulf seismic study (PC 2000). The flattening on top of the Kangan Fm. revealed tilted pre-Permian deposits beneath the unconformity. The rotation of pre-Permian rocks is likely attributed to the extensional deformations and uplift (See Tavakoli-Shirazi, 2012).

II.3.3.2. Onshore seismic study

Among the numerous reflection seismic database in the ZFTB, only a few lines can present the structural style at depth (Lower Paleozoic and basement). One of the seismic sections illustrating the normal faulting at these horizons is given in the figure II.11. This is a NW-SE strike line located in northern syncline of Sarbalesh structure. Western nose of this anticline adjacent to Kazerun fault, was bended to the

North due to the strike-slip movement along the same fault. Figure II.11 displays a local subsidence in the Plaeozoic basin west of the Kazerun fault. To the SE, a high angle normal fault bounded this “low” structure, which has been filled by considerable thickness of the pre-Permian deposits. The deep strong reflector (basement level) ascended rapidly toward NW suggesting presence of a “High” (Horst). This latter uplifted zone is limited by another steep normal fault to the west. The general orientation of these hidden and deep-seated faults is similar to the Kazerun fault and probably inherited as a branch of N-S Arabian lineaments.

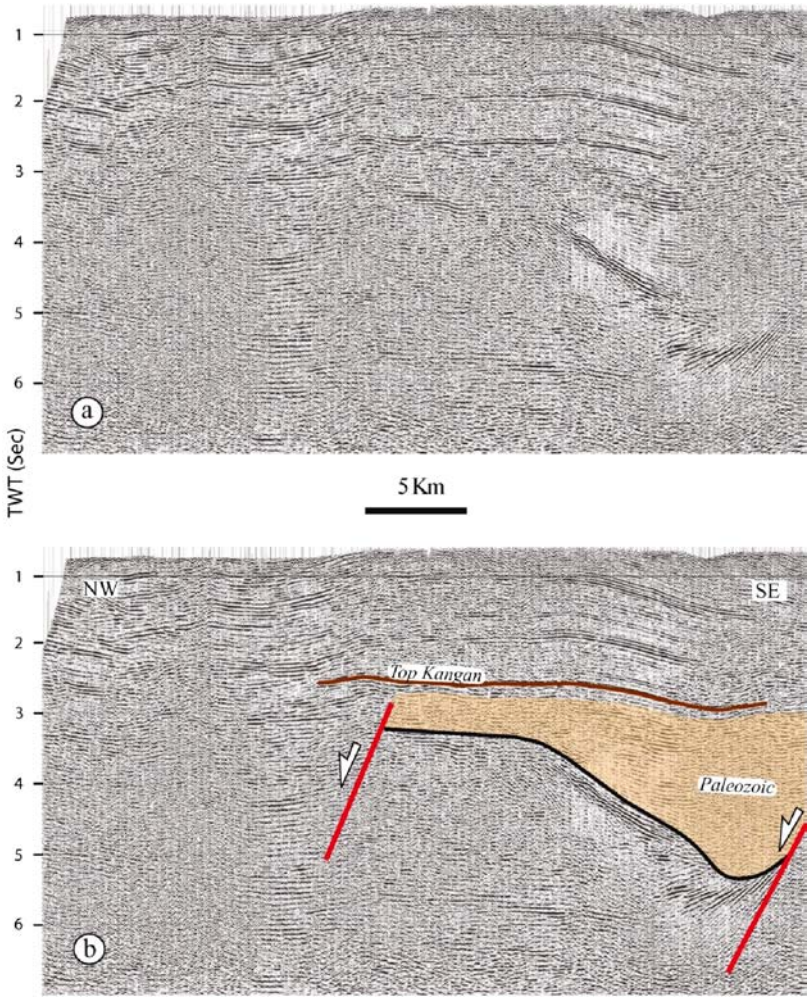

Fig. II.11. a) Non-interpreted and b) interpreted seismic profile in the west of Fars Arc.

Note1: location of all figures in the complementary notes was illustrated within the Annex 3 of this thesis.

Note2: for the legend of seismic interpretations, see figure II.a.

CHAPTER III

TOWARD UNDERSTANDING OF THE HIGH ZAGROS BELT THERMAL HISTORY

III.1) Introduction

In the Chapter II, we have shown the existence of a major sedimentary hiatus below the pre-Permian unconformity (Fig.III.1). We have also tried to demonstrate that the geodynamic process responsible for this hiatus was probably not a far-field effect of the Variscan orogeny, as generally postulated, but rather a thermal uplift associated with a diffuse extensional deformation of possible Late Devonian age. The globalization of such a thermal uplift at the scale of the whole Arabian Plate is moreover proposed in a paper of which I am the second author (see the paper by Frizon de Lamotte et al. in the annex 2).

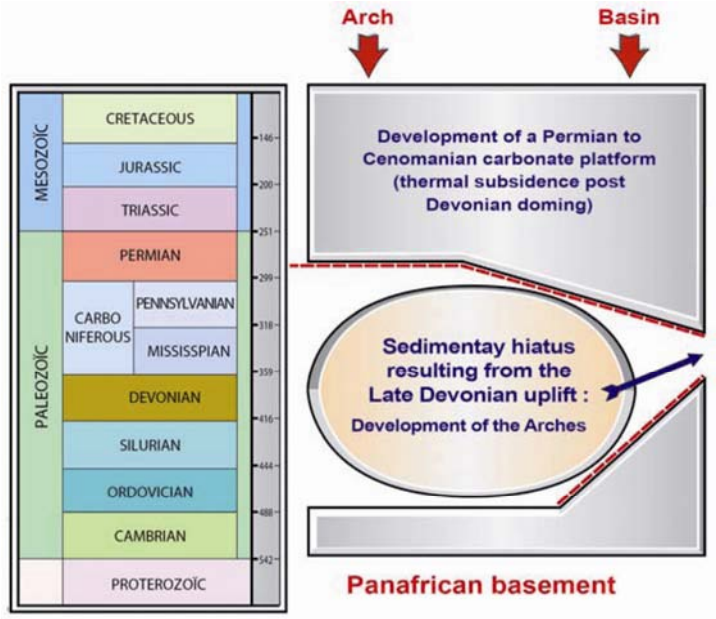

Fig. III.1. Schematic configuration of the sedimentary deposits in the Arabian Plate [from Frizon de Lamotte et al. (in press), see annex 2]

For the purpose of validating this hypothesis, it appeared important to characterize the thermal regime and, if possible, the timing of the processes controlling the uplift. For that, we have performed a systematic sampling of organic matters cropping out in the High Zagros Belt in order to measure their maturity and model their evolution through time. These organic matters are good potential source rocks for hydrocarbon generation. We have concentrated our sampling on rocks situated next to the pre-Permian unconformity. For the Mesozoic and Cenozoic, we have used samples previously collected in the Lurestan by Jean-Christophe Wrobel-

Daveau but not used in his PhD thesis (Wrobel-Daveau, 2011). In addition, we have also performed a systematic sampling of sandstones cropping out on both sides of the pre-Permian unconformity. The purpose here is to try to have an idea of timing and duration of the uplift using thermochronologic tools. We have got a set of new (U-Th)/He ages on zircon. This method was chosen due to the preliminary ages obtained by Gavillot et al. (2010) in one structure of the Central High Zagros were promising. The sample list and locations are presented in the appendix 1 of this chapter.

For the work presented in this chapter, we have collaborated with Miss Camille de La Taille, in the frame of a Master Degree (de la Taille, 2012). The samples have been prepared for measurements of the (U-Th)/He ages in the IDES lab at the Université Paris-Sud (Orsay) under the supervision of Dr. J. Barbarand. She also helped to provide the data required for the GENEX modeling which was performed in collaboration with M. N. Crépieux at TOTAL. So the results presented here are going to be considered as elements for a future scientific paper in collaboration with these persons.

III.2) An outline of High Zagros Belt Thermal History

We present here the results of preliminary Genex modeling done in TOTAL. Genex software is generally used to model the thermal history of a drill-hole. For this study we do not have maturity data of rocks from a borehole but only from outcrops. So the first step has been to construct synthetic boreholes and to replace our samples inside. The analyses are presented just below, after we report and discuss the thermal modeling results.

III.2.1. Construction of two synthetic boreholes

Given our sampling in the Western and Eastern High Zagros Belt, it was necessary to have at least two synthetic boreholes, representative of each region. To build the two logs, we have used the isopach maps of Motiei (1993) as well as data from JOGMEC-TRC (2005), Bordenave (2008, 2010), Wrobel-Daveau (2011), Molinaro *et al.* (2005b), Gavillot *et al.* (2010) and Tavakoli-Shirazi *et al.* (2012). In fact, the synthesis of Mottei (1993) represents a reference work which constitutes the base for all the other works.

For the Genex modeling it is necessary to know not only the thickness of the sedimentary pile but also the lithology of the main units forming the sedimentary pile and controlling the thermal gradient through their conductivity. We have distinguished 6 units, which are globally the same in the two regions (Figs. III.2.a and III.2.b). They are from bottom to top:

Unit 1: this unit is made up by salt and evaporite from the Hormuz Fm. For this unit we have chosen a thickness of 1000m corresponding to a mean value. As the salt is highly mobile, this thickness can vary considerably from one place to another. This is not very important because the potential source rocks are placed above. However, it is worth noting that the high thermal conductivity of salt can have some consequences on the thermal maturation of these source rocks.

Unit 2: this unit is made up by sandstone, shale and carbonate sandwiched between the Hormuz salt and the pre-Permian unconformity. The thickness is not well constrained and likely highly variable. However, this is harmless because the

samples used for the modeling are located close to the unconformity and are consequently not affected by the weight of underlying rocks.

Unit 3: this unit is made up mainly by a thick carbonate platform comprising all the formations from Dalan Fm (Permian) up to Ilam Fm (Upper Cretaceous). The thickness of this platform is remarkably constant (between 3800m in the WHZ and 3250 m in the EHZ) throughout the Zagros.

Unit 4: this unit is composed by the marls of the Gurpi and Papdeh Fms (Upper Cretaceous-Lower Eocene). The thickness is almost constant (1100 to 850m).

Unit 5: this unit comprises the carbonate platform squeezed between the marly Papdeh formation and the sandy Fars group. It is topped by the limestone of the Asmari Fm, which represents the main oil reservoir in the Zagros. The thickness of the unit 5 varies from 800m (WHZ) to 500m (EHZ).

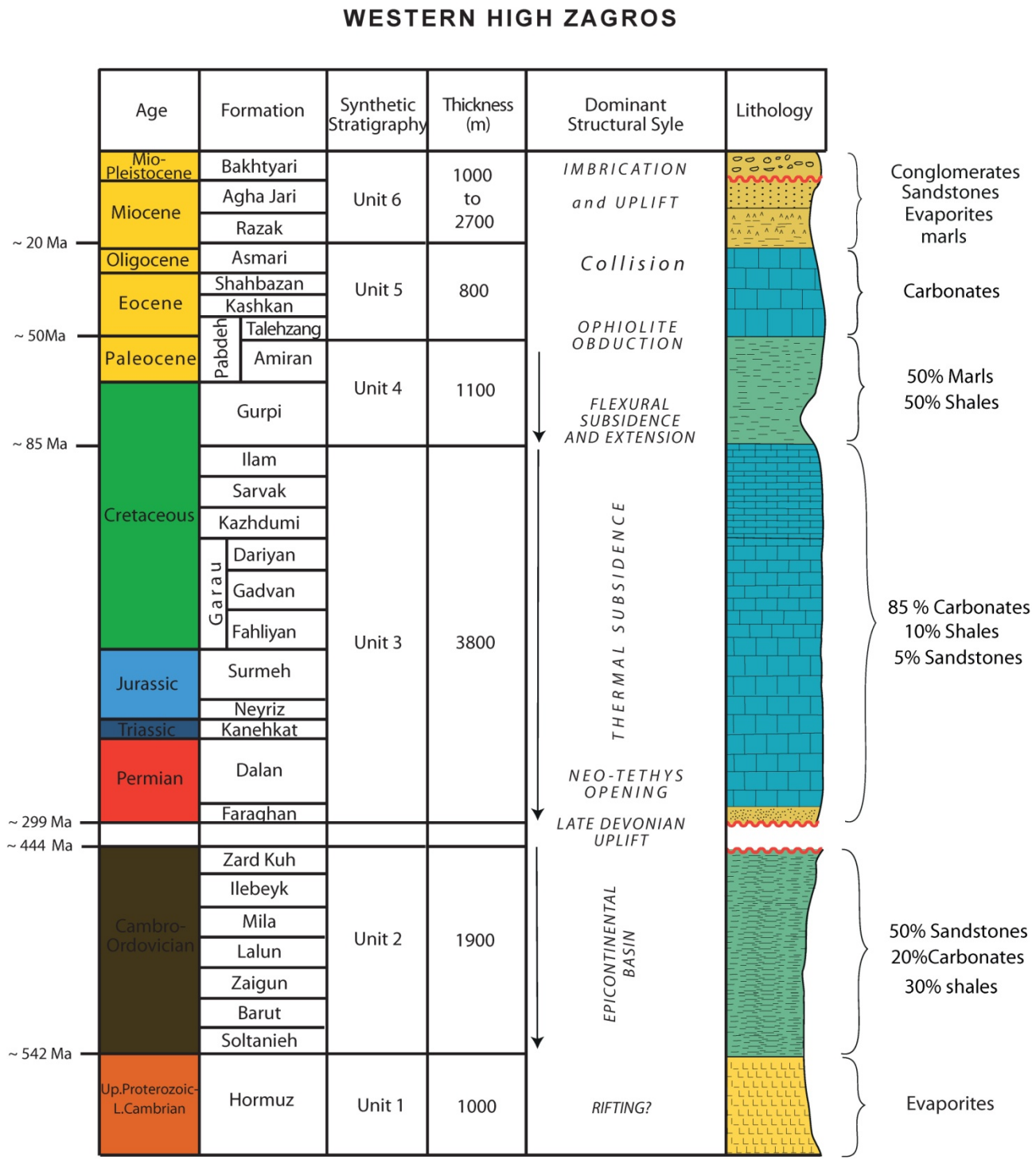

Fig. III.2.a. Synthetic borehole assumed to be typical of the Western High Zagros

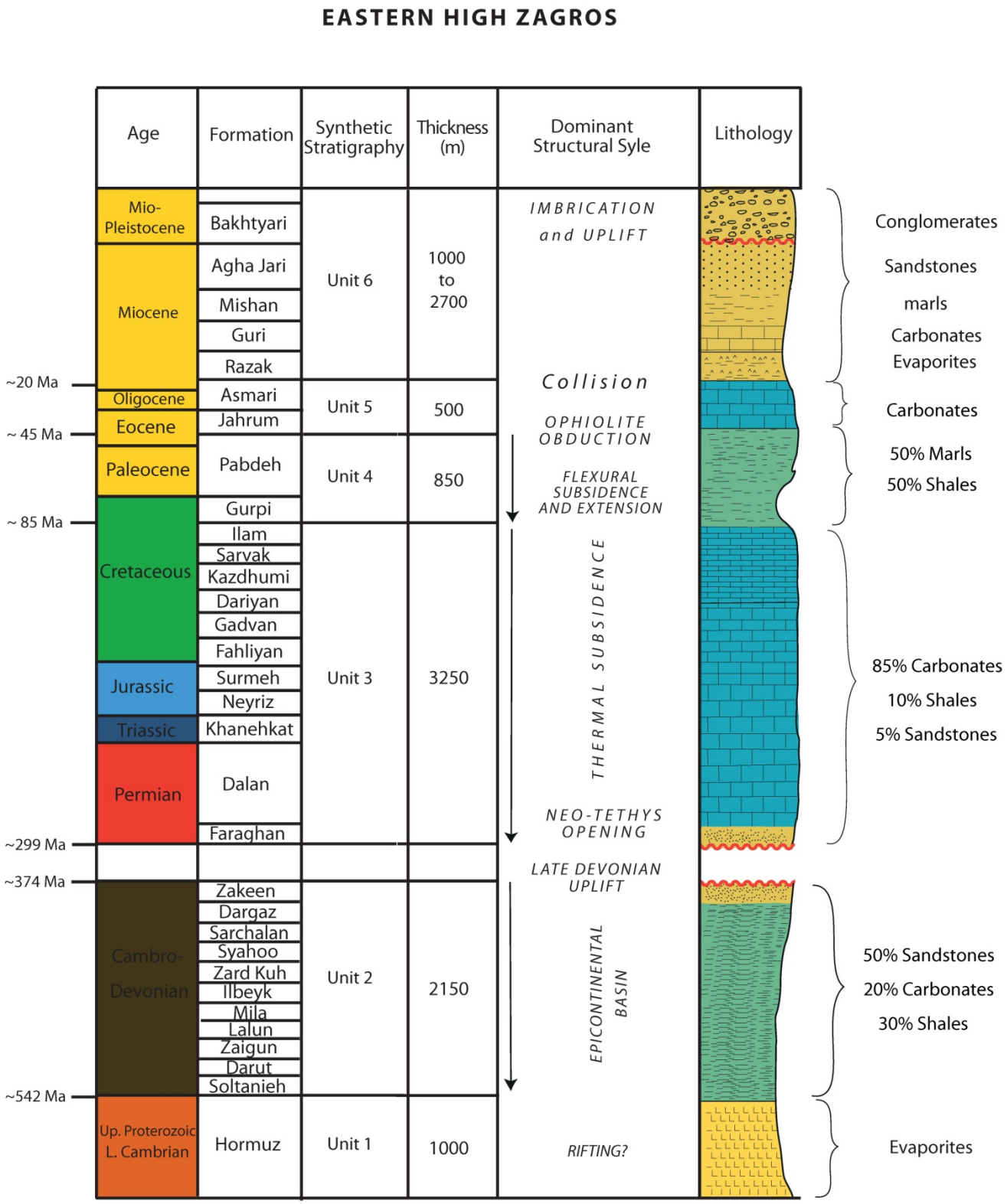

Fig. III.2.b. Synthetic borehole assumed to be typical of the Eastern High Zagros

Unit 6: this unit comprises the whole excess load superimposed to the Asmari Fm. It includes the molasses of the Miocene Fars group on the one hand and also any tectonic extra load on the other hand. We have few data to constrain the thickness and nature (molasses and/or thrust sheet) of this unit. So, we have used an indirect approach, namely the thermochronologic work did by J.C. Wrobel-Daveau (2011) in the Lurestan. Using apatite fission track and (U-Th)/He data, Wrobel-Daveau showed that in the Simply folded belt of this zone the burial of the Amiran formation (lateral equivalent of Gurpi-Papdeh) evolved from less than 2.7 km in the south to more than 2.7 km in the north. Taking into account the c.a.1km of carbonate topping Amiran (Fig. III.2), we can estimate an approximate value of 1.7km of thickness for the unit 6 probably due to the Razak Fm (Wrobel-Daveau, 2011). More to the north, in the Kermanshah Crush Zone, Wrobel-Daveau (2011) shows that the Qom Fm (equivalent of Asmari) experienced a burial at a depth between 1 and 1.9 km (with a geothermal gradient of 24°C/km). He explains this burial by a tectonic extra load due to the over-thrusting of the Sanandaj-Sirjan zone over the Kermanshah crush zone (Fig. III.3). So, it appears that in the internal part of the ZFTB in which the High Zagros is situated, the thickness of the unit 6 is likely less than 2km, a value considerably smaller than the 6km of Miocene molasses known in the more external zones of the chain.

The two reconstituted logs (Figs. III.2.a, b) are very similar confirming that the Mesozoic paleogeographic organization was quite simple. In the following, we consider the Western High Zagros section, which is more constrained.

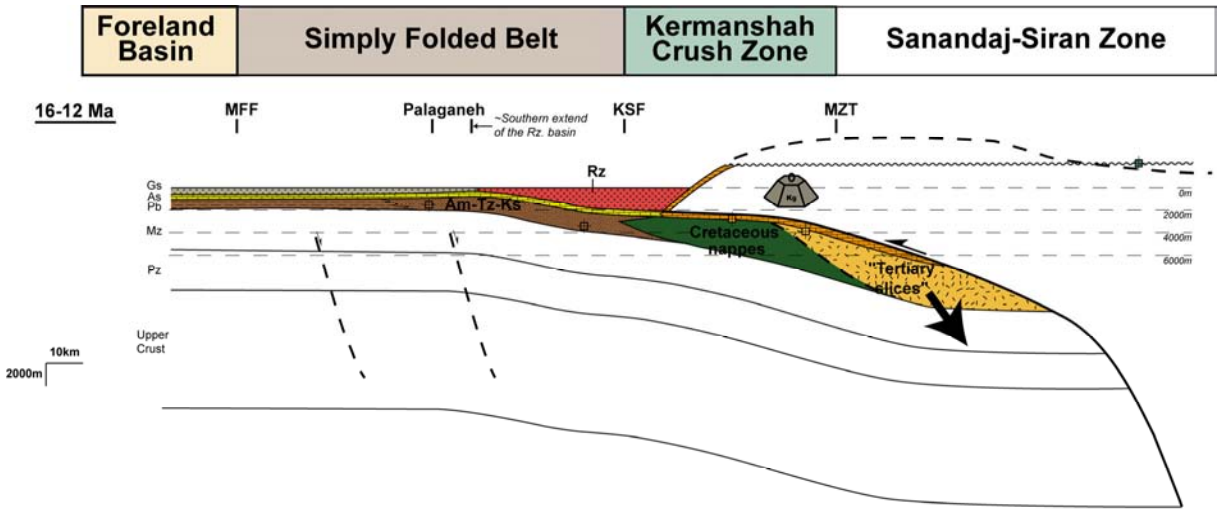

Fig. III.3. Schematic reconstruction of the Zagros before the onset of propagation of the deformation within the Arabian Plate (from Wrobel-Daveau, 2011). This drawing illustrates the origin of extra-load over the Asmari-Qom Fm. It could be either Razak Fm or a thrust-sheet issued from the Sanandaj-Sirjan Zone.

III.2.2. Thermal history Modeling

III.2.2.1. Input data

The GENEX software, developed by IFP (Institute France du Petrole), allows modeling the thermal history of a sedimentary basin. The classical input data required for thermal history modeling are the thicknesses of the sedimentary formations (subsidence history), their conductivities (depending on lithology) and the heat flow variation during the basin activity. It is the reason why we have already constructed the two synthetic boreholes (Fig.III.2).

Maturity data are used to check the validity of a given model (the list and locations of collected samples which were used to test the models and processing suffered by them are presented in the appendix 1 of this chapter). Principles of source rock maturity analysis were described briefly in appendix 2 of this chapter. For GENEX, useful data are vitrinite reflectance data (VRo). When these data were lacking, then T_{max} data have been converted into “equivalent vitrinite reflectance” (eq VRo) using a compilation of actual data. Appendix 3 presents the data obtained from the measurements on the collected potential source rocks. The table III.1 shows the

main trend of eq VRo: (1) there is a correlation between ages and VRo values (older ages correspond to higher VRo values); (2) there is a jump of VRo values when crossing the pre-Permian unconformity.

Sample ID	Formation	Age	Latitude	Longitude	Tmax	eq.VRo%
LU09_30	Amiran	Paleocene-Eocene	34,1408	46,62356	440	0,63
LU09_42	Amiran	Paleocene-Eocene	33,8085	46,66887	436	0,9/0,51
LU09_51	Gurpi	Campanien-Maestrichtien	33,41084	46,51772	438	0,43
LU09_32	Surgah	Turonian-Coniacian	33,60568	46,35837	442	0,58
LU09_64	Sarvak	Albian-Cenomanian	33,35563	46,58332	441	0,56
ZA-08-24	Gurpi	Campanian-Maestrichtian	31,63	50,46	427	0,51
Pu-STS-55	Top Faraghan	Permian	30,59045	51,22231	527	0,77
Bz-STS-37	Faraghan	Permian	32,53511	49,38017	441	0,7
La-STS-44	Faraghan	Permian	31,44726	50,52498	489	0,87
Pu-STS-51	Ilbeyk	(Ord-Sil)	30,59037	51,22186	492	1,02
Dd-STS-21	Ilbeyk	(Ord-Sil)	32,05039	50,14382	450	1,02
FA-STS-4	Sarchahan	Silurian	27, 51.771	56, 18.558		1,25
FA-STS-5	Sarchahan	Silurian	27, 44.454	56, 17.720	465	1,35
GK-STS-6	Sarchahan	Silurian	28, 05.112	55, 56.811		1,01
FA-STS-9	Syahoo	Ordovician	27, 51.605	56, 18.866	461	1,37
FA-STS-10	Syahoo	Ordovician	27, 51.369	56, 18.969	460	1,34
SU-STS-6	Syahoo	Ordvician	28, 30.659	52, 34.113		0,9
SU-STS-7	Syahoo	Ordvician	28, 30.128	52, 35.677	437	0,97
SU-STS-10	Syahoo	Ordvician	28, 30.919	52, 31.447		0,89

Table III.1. *Maturity data measured on Zagros samples*

Heat flow determination is a main concern. From the literature, it appears that the present day heat flow is poorly constrained in the Zagros: 22 mW/m² (Coster, 1947), 51 mW/m² (Sass *et al.*, 1971), 40 to 60mW/m² (Pollack *et al.*, 1993), 40mW/m² (Molinaro, 2004b), a mantle paleo-heat flow of 36mW/m² which corresponds to a surface heat flow of 64mW/m² (Bordenave, 2008), 60mW/m² (Motavalli-Anbaran *et al.*, 2011). A map from the TOTAL database synthesizing present-day heat flow is presented in figure III.4. Following this compilation, it appears that the present heat flow in the Zagros is between 40 and 60mW / m².

For the past, estimation of the paleo-heat flow is a difficult task. The only think that we can do is to consider the successive geodynamic contexts and to discuss if the postulated heat flow at a given time is compatible or not with the geodynamic

context considered at that time (Fig. III.5). In the Zagros, the tectonic history is very long (more than 550 Ma) but the tectonic context for each period is quite well established (Figs.III.2 a and b).

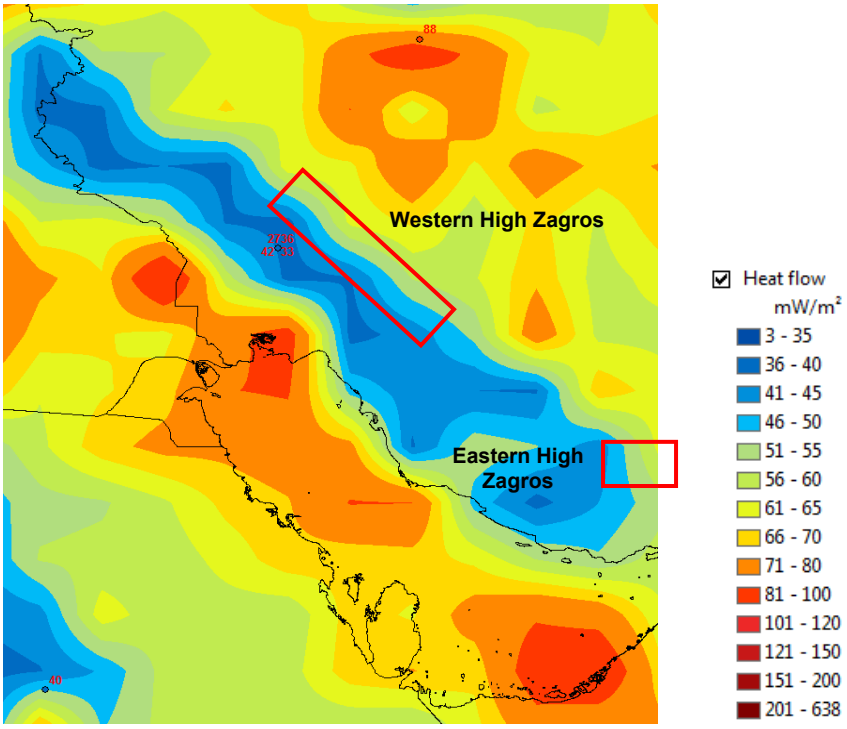

Fig. III.4. Estimated present-day heat flow in the Zagros (TOTAL database)

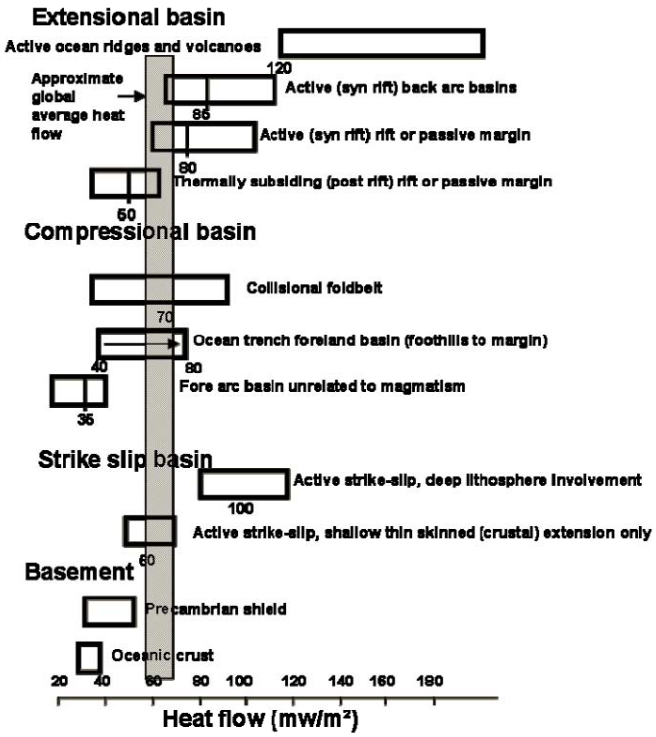

Fig. III.5. Heat-flow values for sedimentary basins in different geodynamic contexts (Allen & Allen, 1990)

III.2.2.2. Tested scenarios

To test different scenarios we used a trial-and-error method. Basic requirements to validate a model are that: (1) the surface heat flow calculated by the model for the present day must be consistent with actual data (Fig. III.4); (2) the theoretical curve plotting the Vitrinite Reflectance with depth must be consistent with the data. To test this consistency, we have calculated a mean value of the Vitrinite Reflectance (table III.1) for three groups of ages: (1) Upper Cretaceous-Paleocene; (2) Permian; (3) Lower Paleozoic. It is the reason why only 3 points are represented on the figures III.6 to III.8. It is worth noting that in the models we did not consider possible variations of thickness/lithology of sedimentary units (Figs. III.2 a and b) but only the variation of the heat flow through time.

Scenario 1: in this scenario, we test the effects of a constant and low heat flow value (16 mW/m2) since the Cambrian (N.B. in all cases the heat flow value introduced in the model is the value at the lithosphere-asthenosphere boundary with a “mean lithosphere” above). In the presented hypothesis (Fig. III.6), to fit with the VR data the model have to consider ~6 000m of erosion before the deposition of the Permian. The hypothesis of constant heat flow is clearly not realistic but gives and end-member for the modeling.

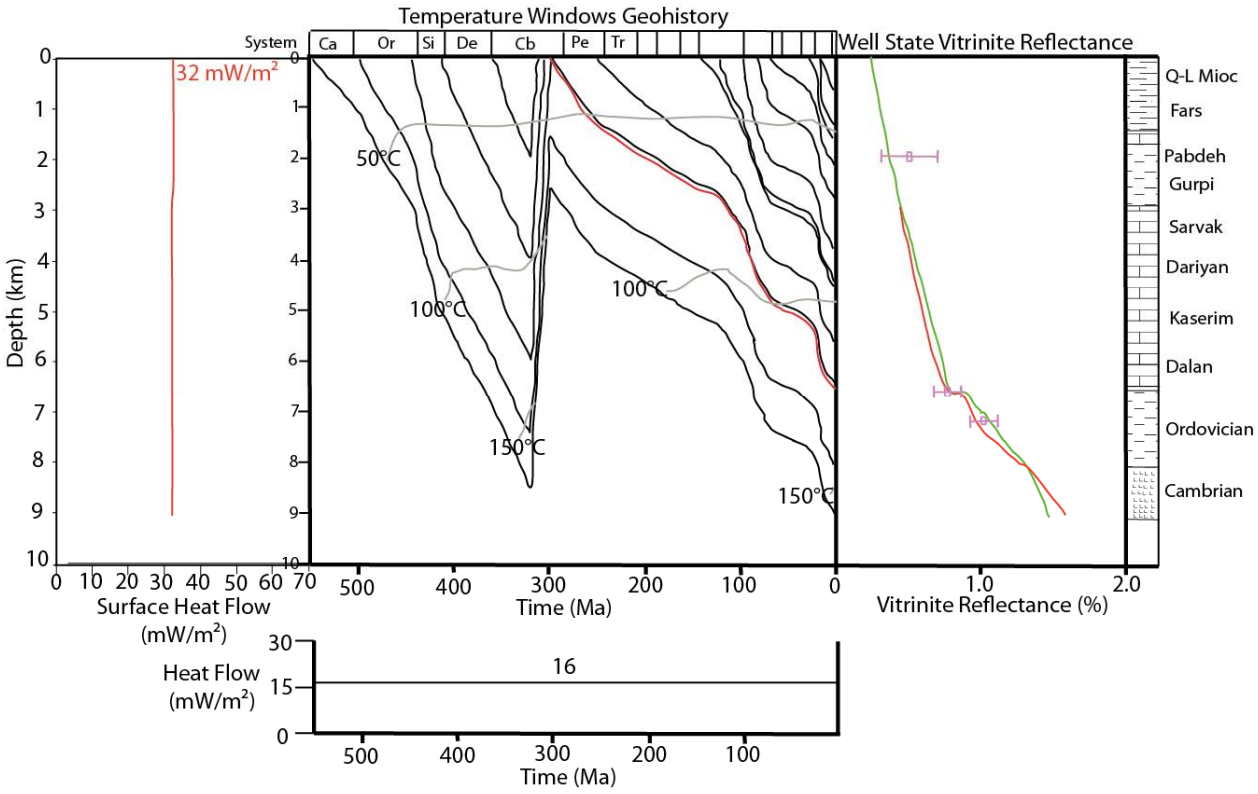

Fig. III.6. *Scenario 1: thermal 1D modeling with a constant and low heat flow value at the bottom of the crust. The central diagram gives an estimation of vertical movements through time. To the left is the computed heat flow in the sedimentary pile; to the right is the theoretical vitrinite reflectance evolution with depth (two different models, red and green respectively, are proposed).*

Scenario 2: in this scenario, we test changes in the heat flow values with a maximum (60mW/m^2) during the Devonian and then a progressive decrease by the mid-Carboniferous until now. The idea here is to test the effects of a Devonian "thermal event" as the one suggested by Kohn et al. (1992) and Veermesch et al. (2009) in the Levant Arch [see discussion in Frizon de Lamotte *et al.*, *in press*] and then a progressive thermal re-equilibration before the foreland basin final stage. With this hypothesis (Fig. III.7), to fit with the VR data the model have to consider ~3900m of erosion before the deposition of the Permian.

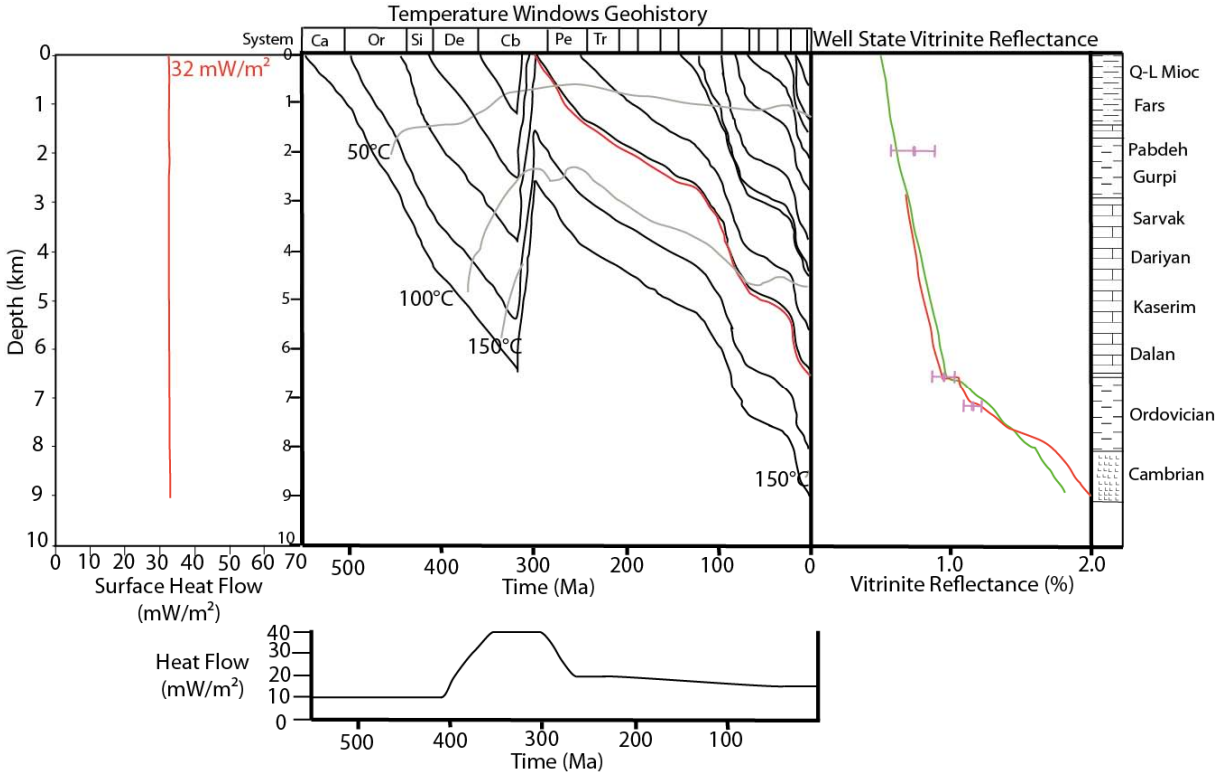

Fig. III.7. *Scenario 2: thermal 1D modeling with variable heat flow value at the bottom of the crust. Here, we have tried to model the effect of a Devonian "thermal event". The central diagram gives an estimation of vertical movements through time. To the left is the computed heat flow in the sedimentary pile; to the right is the theoretical vitrinite reflectance evolution with depth (two different models, red and green respectively, are proposed).*

Scenario 3: in this scenario, we have tried to minimize the thickness of eroded material. For that we must impose a high heat flow from Cambrian to Carboniferous and then a low value by the Permian (Fig. III.8).Regarding this hypothesis, it becomes possible to reduce the eroded thickness to less than 2000m. However, given the geodynamic context of the Arabian Plate with the development of epi-continental wide basins during the Paleozoic (Figs. III.2 a and b), it appears unrealistic maintaining a very high heat value during this very long time.

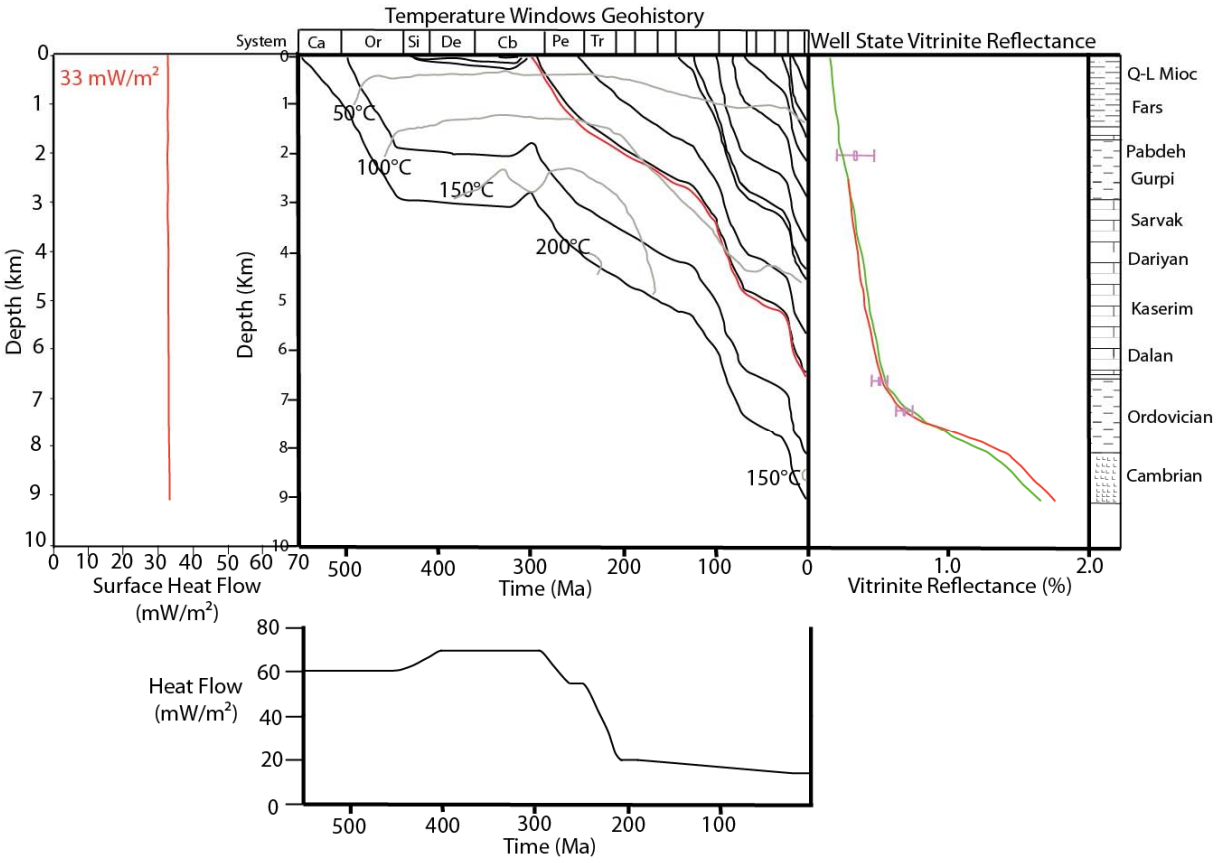

Fig. III.8. *Scenario 3: thermal 1D modeling with a quite constant and high heat flow value at the bottom of the crust during the Paleozoic. The idea is to minimize the thickness of eroded material. The central diagram gives an estimation of vertical movements through time. To the left is the computed heat flow in the sedimentary pile; to the right is the theoretical vitrinite reflectance evolution with depth (two different models, red and green respectively, are proposed).*

III.2.3. Conclusion

The models presented here must be considered as preliminary attempts to describe the thermal evolution and the vertical Paleozoic movements in the Zagros. However, at this stage, seems to be established that considerable erosion (about 4000m) occurred before the Permian and that a high heat flow existed during the Devonian and Lower Carboniferous (Fig. III.7).

This interpretation is consistent with the one proposed in the Levant Arch by Kohn et al. (1992), who suggested the existence of a “major Late Devonian or Early Carboniferous thermo-tectonic event” responsible for uplift and huge erosion. In the

same region, Vermeesch *et al*. (2009) confirmed that an abnormally steep gradient (hydrothermal event) is required.

Our results confirm that this tectono-thermal event of Devonian age is well-distributed and likely affected the whole Arabian Plate (see Frizon de Lamotte *et al.,* in press, annex 2).

III.3) (U-Th)/He thermochronology, a tool for quantifying of Paleozoic uplift

III.3.1. Analytical method

In this study, (U-Th)/He on Zircon (ZHe) method has been used to try constraining the age of exhumation during Paleozoic times in the High Zagros. Theoretically, this is a powerful tool for determination of timing and magnitude of cooling resulting from uplift and erosion. The technique is based on the decay of ^{235}U, ^{238}U, ^{232}Th by alpha (4He nucleus) emission. Helium (He) is expelled from Zircon at temperatures above ~180°C and retained below ~120°C (Tagami *et al.*, 2003; Stockli, 2005). This range of temperature is called Partial Retention Zone (PRZ). Detail of this method is given in appendix 4 of this chapter.

Samples (appendix 1 of this chapter) were collected in the western and eastern High Zagros along vertical transect of siliciclastic rocks ranging from Cambrian to early Permian. Samples called Bz-STS, Zk-STS, Dd-STS, La-STS and Pu-STS were collected from the western High Zagros. Eastern High Zagros samples were derived from Faraghan and Gahkum anticlines and indicated by Fa-STS and Gk-STS respectively. These samples were coming from layers on both sides of the pre-Faraghan unconformity.

III.3.2. Presentation of the laboratory results

The ZHe ages have been achieved through two laboratories. University of Tubingen (Germany) and University of Paris Sud (Orsay). Analysis in the University of Tubingen was made on a monograin (per aliquot). A large dispersion of ZHe ages ranging between 23 Ma to 1Ga was observed for one sample (La-STS-47, appendix

5 of this chapter). The whole ZHe protocol was performed for measurements conducted at University of Orsay because it was the first experience on Zircon for this lab. Five grains per aliquot were tested in order to avoid the risk of low concentration of Uranium (U) and Thorium (Th) within one grain. However, measured U and Th concentration showed later that single grain analysis would be possible but this procedure has not been performed.

The size, morphology, abundance of inclusions and clarity are parameters which can strongly affect the calculated ZHe ages. As a general rule, crystals with tetragonal prism widths less than 60 µm are not dated, except in rare circumstances, because uncertainties in the very large alpha-ejection corrections (and inherent assumptions about parent zonation required in conventional analyses) can lead to potentially large errors (Reiners, 2005).

Figure III.9 illustrates the radius length of the grains versus measured zircon ages. Most of the mineral radiuses are between ~35 to 60 µm. All ages that determined in Orsay laboratory are younger than ~400 Ma and mainly bounded between 40-60 µm but the Tubingen samples are more scattered in ages and particularly in radius lengths (partly smaller than 40 µm). This can suggest less reliability on the data obtained at this latter place. The radius of the Ordovician grains is very tiny and remained to be used further.

Results acquired on standard (Fish Canyon, Fig III.10) illustrate that age reproducibility and accuracy is fairly good and in agreement with published data (Tagami *et al.*, 2003). Th/U ratios are relatively higher than data already published which can be associated with an overestimation of Th and/or an underestimation of U.

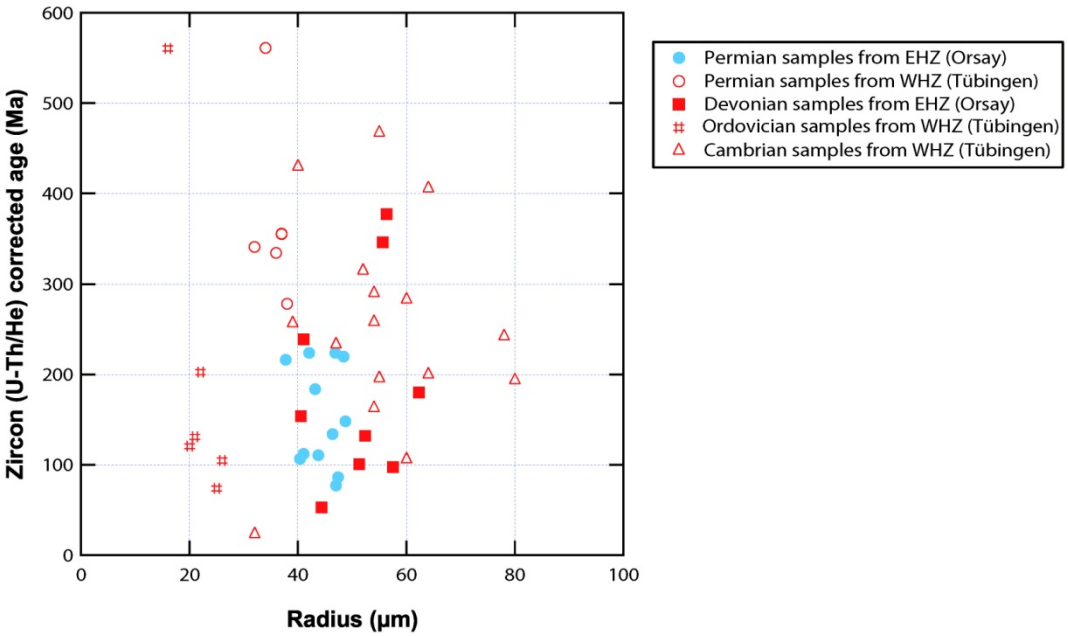

Fig. III.9. Radius length versus ZHe ages of the samples collected from the HZB

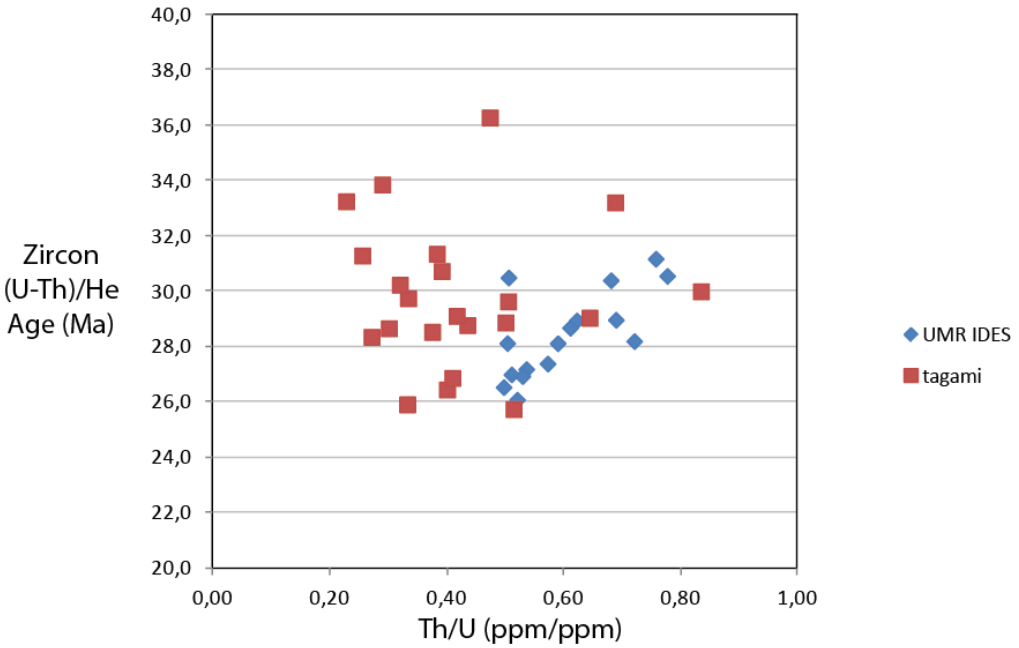

Fig. III.10. Ages of Fish Canyon Zircons from Orsay (this study) compared to Fish Canyon Zircons of Tagami et al. (2003).

The (U-Th)/He results for seven samples from Orsay, with Devonian and Permian stratigraphic ages (appendix 5 of this chapter) show a wide range of ages from 53 to 377 Ma. For example, ZHe ages for Fa-STS-3 vary between 97 and 377

Ma. The histogram in figure III.11 presents the ZHe ages which have been plotted versus number of grains. Two populations of ages are observed in this figure. A small population with old ages spanning between 350-400 Ma.

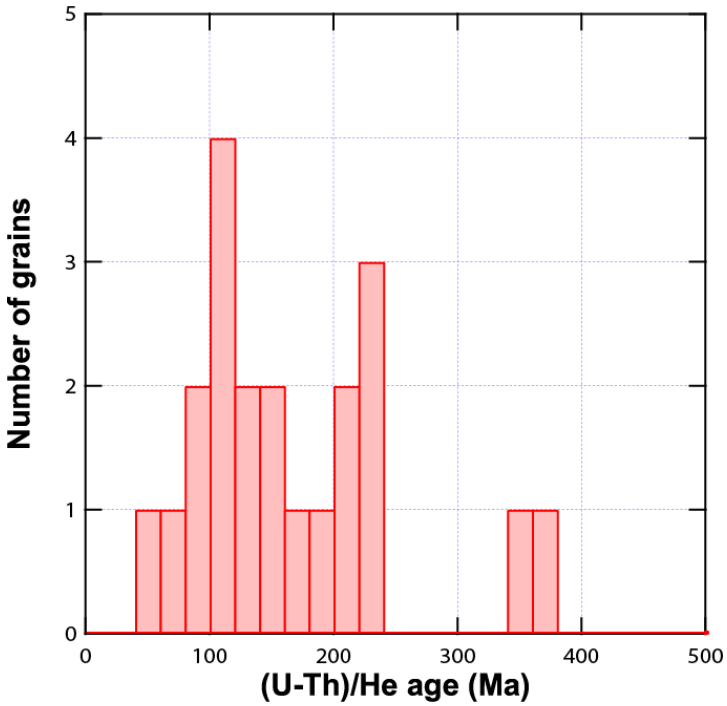

Fig. III.11. *Histogram of ZHe ages on zircons for Orsay samples*

Another population comprising younger ZHe ages in figure III.11 which displays time ranges between 50 to 250 Ma. Most of ZHe dating (19 among 21 ages) belongs to this category (also see appendix 5 of this chapter) and presents ages younger than the corresponding stratigraphic ages (Fig. III.12).

There is good evidence that He diffusion in zircon is strongly affected by relatively high degrees of radiation damage (Reiners *et al*, 2004). The emission of alpha particles from uranium, thorium and their descendants causes the movement of atoms and lead to disrupt the structure of minerals. This disorganization, called metamictization, is leading to their amorphization. The degree of metamictization increases with the amount of uranium contained in the mineral and over time. These conversions in the mineral change the closure temperature, and affect the helium

diffusion. The dose of damages is not only related to the concentration of U and Th but also to the duration of exposition. The average of uranium concentration in the samples measured in Orsay is 314ppm which was not destructive and did not result in significant He loss. Reiners *et al*, (2004) showed that a concentration of 1000ppm of uranium induces metamictization in the zircon. A similar diagram showing ZHe data versus eU values is presented in the figure III.12. It appears tentatively from this figure that, there is a higher U concentration in the Tubingen samples compare to other laboratories which may raise a question about the validity of the results from the first laboratory. The figure III.12 illustrates all available data including the ZHe ages obtained by this study and by Gavillot et al. (2010).

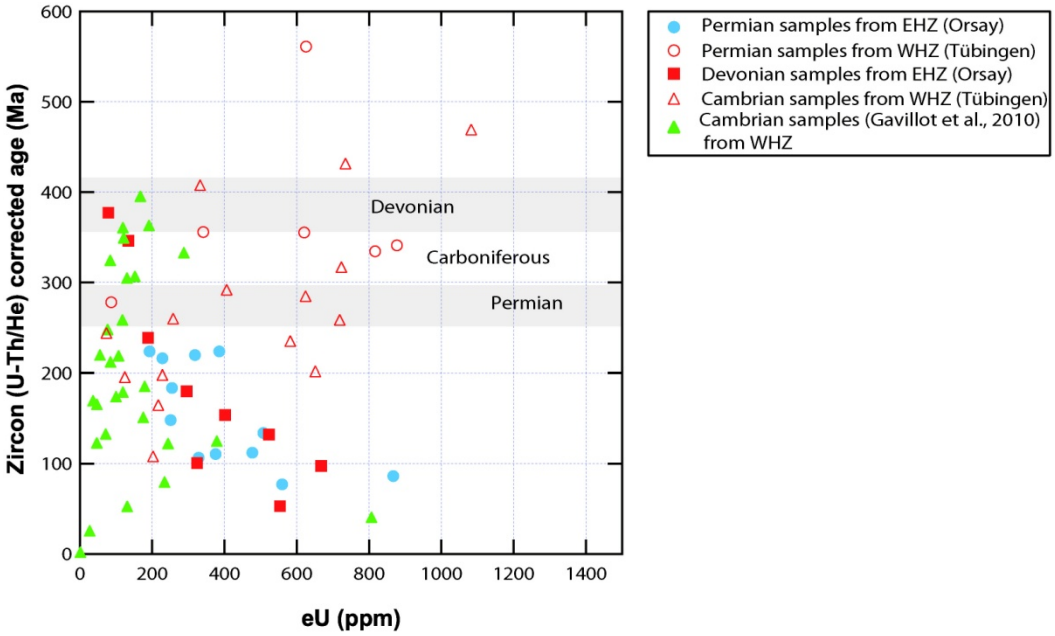

Fig. III.12. *eU (ppm) versus ZHe ages (Ma) for all data including this study and bibliography (Gavillot et al., 2010). eU is calculated after the equation eU=U+0.24xTh*

On the other hand, given alpha dose in the figure. III.13 suggests that majority of the zircon grains were not affected by radiation damage because the effects of radiation damage on He diffusivity do not become important until radiation dosages higher than about 2– $4X10^{18}$ α/g, a level at which macroscopic and crystallographic characteristics of zircon also show large changes (e.g. Nasdala *et al*. 2001, 2004). Thus, the group of ages below the mentioned value was not impacted by radiation damage and can be used confidently. Mean while, almost all ZHe ages which

correspond to the alpha doses less than the $3X10^{18}$ α/g (red vertical line) in the figure III.13 present younger ages than the stratigraphic ages. This means that only the (U-Th) / He thermochronology on zircon does cannot provide direct information about the history of Paleozoic.

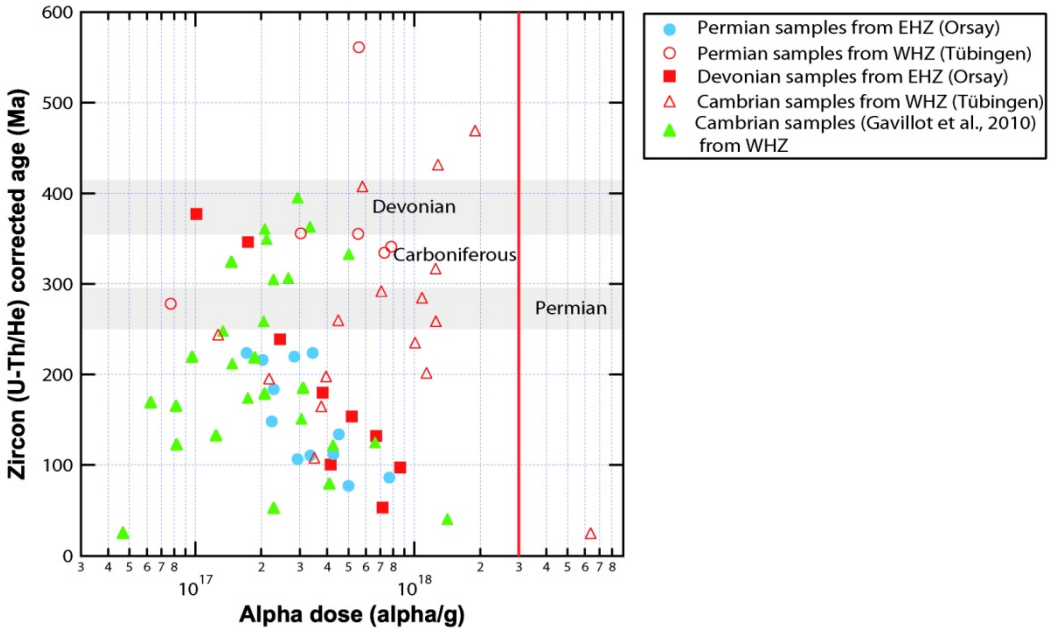

Fig. III.13. *Alpha dose versus Zircon (U-Th)/He ages (Ma) for all available data*

III.3.3. Discussion

For the purpose of the interpretation of our ZHe ages, it is useful to have an idea about the absolute ages of the detrital zircons found in the Paleozoic clastic rocks of the Zagros. A preliminary work has been done by Horton *et al.* (2008). Ion-microprobe U-Pb analyses done by these authors on detrital zircon grains from the Lajin anticline (Cambrian Lalun formation) and from the Gahkum anticline (Devonian Zakeen and Lower Permian Faraghan formations) in the High Zagros show very similar age populations (Fig. III.14), apart from the age of the bearing formation. In agreement with what has been observed in Jordan (Kolodner *et al.,* 2006) or in Israël (Avigad *et al.,* 2003), these zircons are likely originated from a Gondwanian basement comparable with the one cropping out presently in the Arabian Shield.

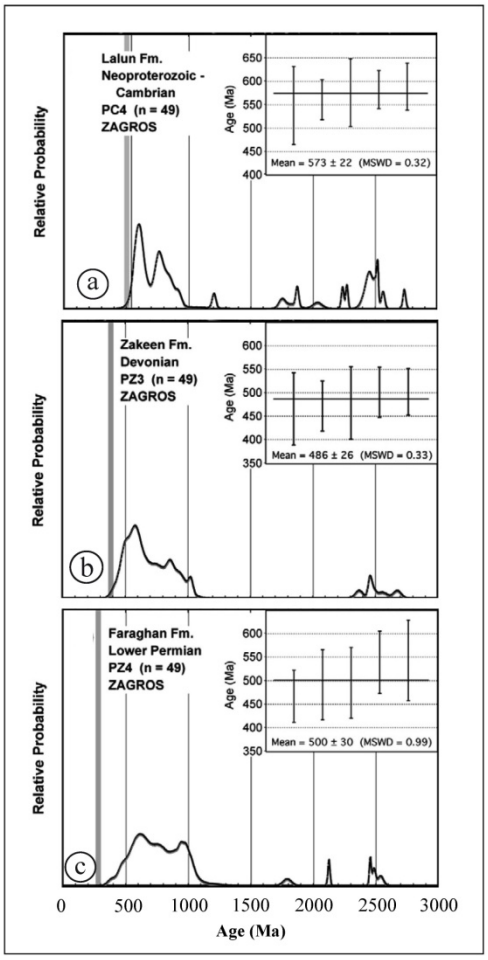

Fig. III.14. *Relative age probability diagrams displaying the U-Pb detrital zircon age distribution for Cambrian, Devonian and Permian sandstone samples from the High Zagros (after Horton et al., 2005). The samples were collected from: a) Cambrian Lalun Fm. b) Devonian Zakeen Fm c) Permian Faraghan Fm*

Contrasting with the age populations got by Horton *et al.* (2008), the ages obtained in this study by the (U-Th)/He method (e.g. figure III.12) are systematically younger than the statigraphic ages and show an extensive scattering. This result demonstrates that the samples have been heated enough to experience a partial reset (otherwise the ZHe ages should be older than the stratigraphic ages) but also that the heating remained moderate (otherwise the ages should be more clustered). It is known (Reiners, 2005) that the closure temperature for the (U-Th)/He system depends strongly on two main parameters: the size of the grain and the cooling rate (Fig. III.15). Using the review done by this author (Fig. III.15), and according to the interpretation proposed by Gavillot *et al.* (2010) on the basis of ZHe ages from

Cambrian rocks sampled along the Lajin and Dena transects (Figs. III.12 and 13, we can estimate the maximum burial temperature of exhumed strata to ≤ 180°C. On the other hand, the GENEX modeling, performed by us, (Fig.III.7), more likely indicates that a maximum burial temperature of 150°C was reached in Cambrian rocks just before the Late Paleozoic uplift. It also constrains that the temperature has not been exceeded later, prior to the Cenozoic final uplift. If correct, we can infer a relatively low cooling rate which seems consistent with the mechanism of thermal uplift that we have proposed (Tavakoli-Shirazi et al., 2012).

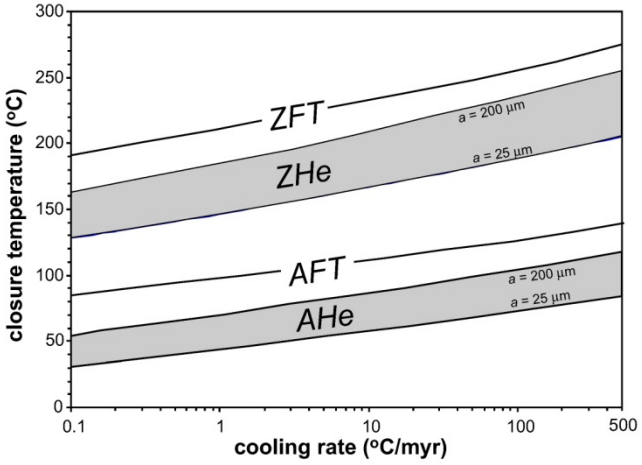

Fig. III.15. *Closure temperatures versus Cooling rate for apatite He and zircon He. (after Reiners, 2005). AFT and ZFT closure temperatures are always higher than those for the (U-Th)/He system on the same minerals.*

The only Pre-Permian ZHe ages obtained during this study and also by Gavillot *et al.* (2010) are coming from Devonian and Cambrian samples respectively and correspond to ages between 377 to 393Ma. This coincidence between the two set of results from two different laboratories, reinforced by the low values of eU (Fig. III. 12) and Alpha Dose (Fig. III.13) for these samples, inclines us to consider that these ages have a geological significance and can reflect the age of the thermal uplift discussed just above.

Further work is necessary to confirm and validate our interpretation. However, it is worth noting that these “old” ZHe ages from our study and from Gavillot *et al.* (2010), are in complete coherence with ZFT ages obtained by Kohn et al. (1992) and Veermesch *et al.* (2009) on Precambrian basement and Cambrian sedimentary rocks from the Levant Arch (Israel) and also with the mechanism of thermal uplift

postulated by these authors (see the Annex II for more discussion). These ZHe ages also relate to the age patterns deriving from a “youthful igneous source of major regional importance” described by Horton *et al.* (2008) in the Alborz.

III.4) Conclusion

This work on the origin and duration of Upper Paleozoic uplift responsible for the pre-Permian unconformity in the High Zagros (Iran) allows us to advise some robust results:

- An uplift, accompanied by an important erosion (about 4000m), took place in the High Zagros between the end of the Devonian and the Early Permian as demonstrated by the stratigraphic ages of strata located below and above the pre-Permian unconformity respectively and also by the ZHe ages obtained on some samples (appendix 5 of this chapter);

- This uplift is likely of thermal origin as indicated by the significant heat flow required to implement convenient GENEX model (Fig III. 7) and also by the partial reset of (U-Th)He system in detrital zircons from Lower Paleozoic rocks. This uplift has consequently nothing to do with the Variscan Orogeny and the term “Hercynian Unconformity” which generally used to designate the pre-Permian unconformity is confusing and inappropriate ;

- The maturity of potential Lower Paleozoic source rocks (Ordovician and Silurian) was likely acquired before the Late Paleozoic uplift and related cooling as indicated by the systematic gap between Vitrinite reflectance data from Lower Paleozoic and Permian rocks (Fig III.7). In agreement with this result, the partial reset of ZHe demonstrates that Meso-Cenozoic sedimentary and additional structural burial depths of the rocks located below the pre-Permian unconformity were insufficient to completely open zircon grains. If correct, this result has considerable importance for hydrocarbon exploration.

III.5) APPENDIXES TO CHAPTER III

APPENDIX 1: List, location maps and Photos of the samples

Sample ID	Stratigraphic Age	Formation	Latitude (Northing)°	Longitude (Easting)°	Laboratory Place	Zone
Thermochrono						
La-STS-45	Permian	Faraghan	31,74508	50,87475	Orsay	Western Zagros
Pu-STS-54	Permian	Faraghan	30,98408	51,37052	Orsay	Western Zagros
BZ-STS-32	Permian	Faraghan	32,96592	49,60802	Tubingen	Western Zagros
La-STS-47	Cambrian	Mila	31,74233	50,86547	Tubigen	Western Zagros
Pu-STS-52	Cambrian	Lalun	30,98137	51,365783	Tubingen	Western Zagros
GK-STS-2	Permian	Faraghan	28,08804	55,94848	Orsay	Eastern Zagros
GK-STS-1	Permian	Faraghan	28,08803	55,94847	Orsay	Eastern Zagros
Fa-STS-3	Devonian	Zakeen	27,8677	56,3087	Orsay	Eastern Zagros
GKSTS-4	Devonian	Zakeen	28,08635	55,9474	Orsay	Eastern Zagros
GK-STS-3	Devonian	Zakeen	28,0872	55,9479	Orsay	Eastern Zagros
BZ-STS-38	Ordovician	Ilbeyk	32,91943	49,51702	Tubingen	Eastern Zagros
Organic Matter Maturity						
ZA-08-24	Campanian-Maastrichtian	Gurpi	31,63	50,46	Total-Pau	Central Zagros
Pu-STS-55	Permian	Top Faraghan	30,98408	51,370517	Total-Pau	Central Zagros
Bz-STS-37	Permian	Faraghan	32,89185	49,633617	Total-Pau	Central Zagros
La-STS-44	Permian	Faraghan	31,74543	50,87497	Total-Pau	Central Zagros
Zk-STS-63	Ordovician	ZardKuh	32,46537	49,94123	Total-Pau	Central Zagros
La-STS-41	Ordovician	Ilbeyk	31,74797	50,87175	Total-Pau	Central Zagros
Pu-STS-51	Ordovician	Ilbeyk	30,98395	51,36977	Total-Pau	Central Zagros
Dd-STS-21	Ordovician	Ilbeyk	32,083983	50,2397	Total-Pau	Central Zagros
LU09_30	Paleocene-Eocene	Amiran	34,14	46,62	Total-Pau	Lurestan
LU09_42	Paleocene-Eocene	Amiran	33,81	46,67	Total-Pau	Lurestan
LU09_51	Campanian-Maestrichtian	Gurpi	33,41	46,52	Total-Pau	Lurestan
LU09_32	Turonian-Coniacian	Surgah	33,61	46,36	Total-Pau	Lurestan
LU09_64	Albian-Cenomanian	Sarvak	33,36	46,58	Total-Pau	Lurestan
FA-STS-4	Silurian	Sarchahan	27,86285	56,3093	Total-Pau	Eastern Zagros
FA-STS-5	Silurian	Sarchahan	27,7409	56,2953	Total-Pau	Eastern Zagros
GK-STS-6	Silurian	Sarchahan	28,0852	55,94685	Total-Pau	Eastern Zagros
FA-STS-9	Ordovician	Syahoo	27,860083	56,31443	Total-Pau	Eastern Zagros
FA-STS-10	Ordovician	Syahoo	27,85615	56,31615	Total-Pau	Eastern Zagros
SU-STS-6	Ordovician	Syahoo	28,510983	52,56855	Total-Pau	Fars Arc
SU-STS-7	Ordovician	Syahoo	28,50213	52,594617	Total-Pau	Fars Arc
SU-STS-10	Ordovician	Syahoo	28,515317	52,524117	Total-Pau	Fars Arc

Table III.2. *List of samples collected for analysis of both U-TH (He) and maturity of organic matter (OM)*

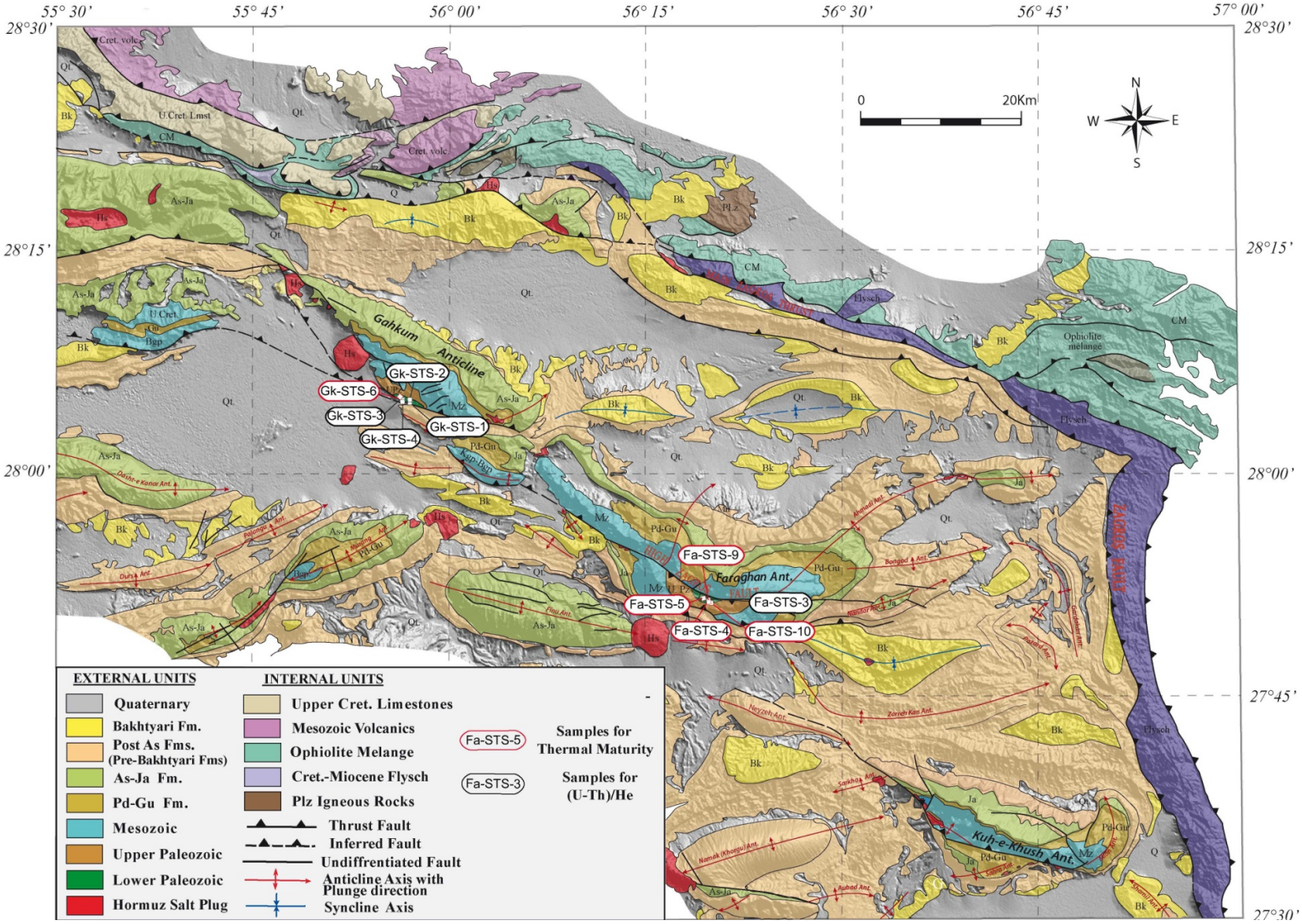

Fig. III.16. Location of Eastern High Zagros samples on the Geological map over the SRTM background

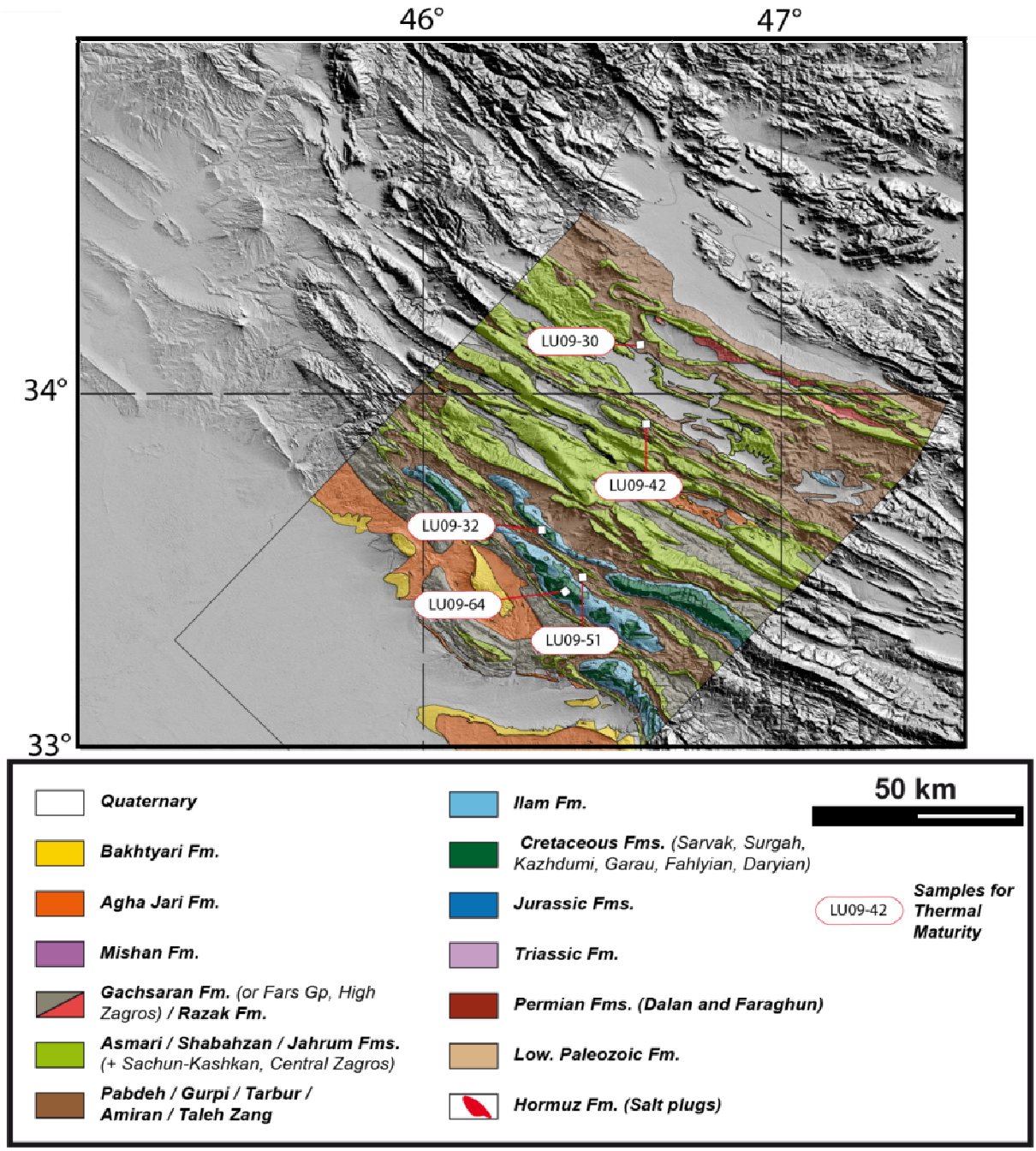

Fig. III.17. Location of Wrobel-Daveau's samples on the geological map of the Lurestan area

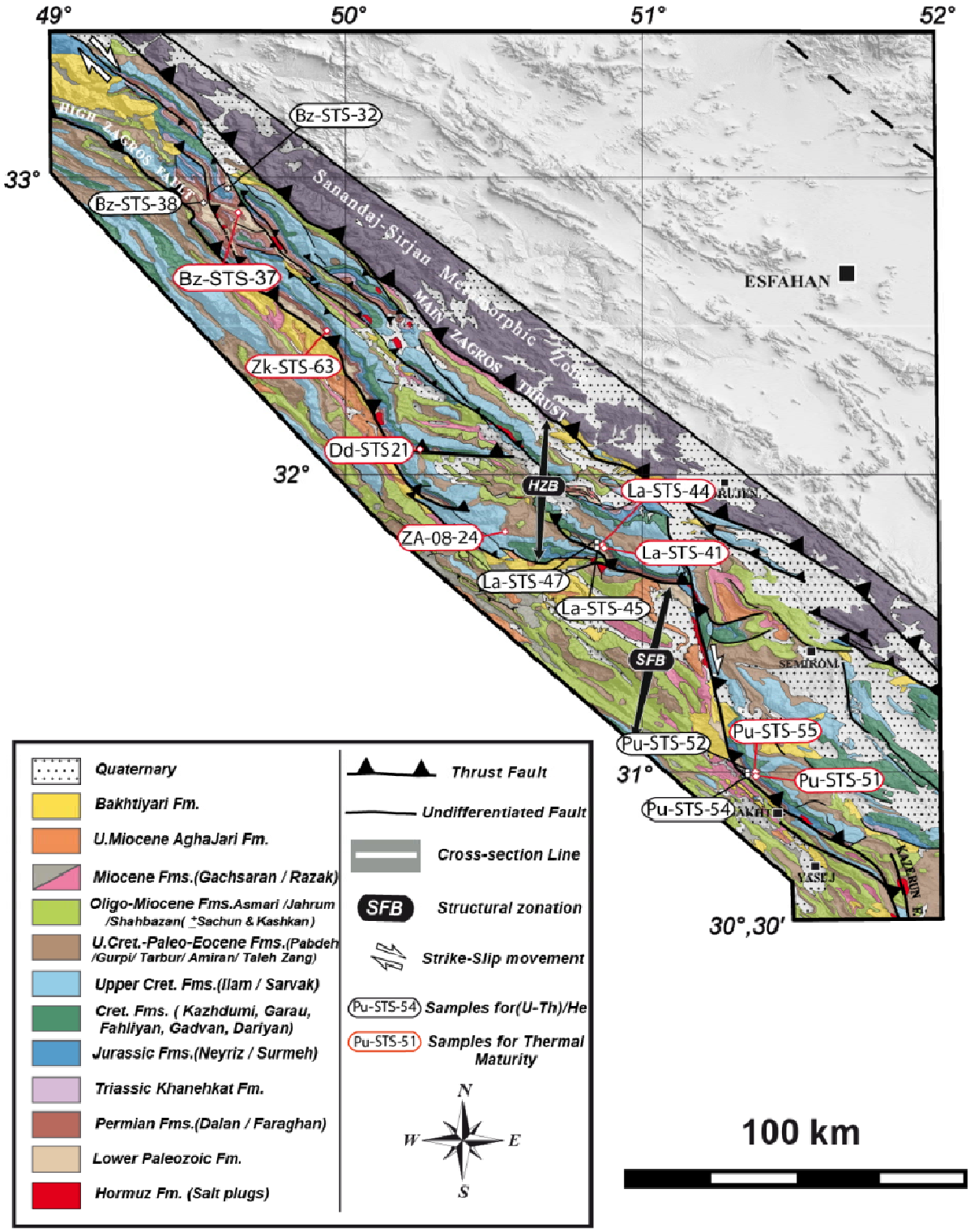

Fig. III.18. Location of Western High Zagros samples on the SRTM data overlain by Geological map

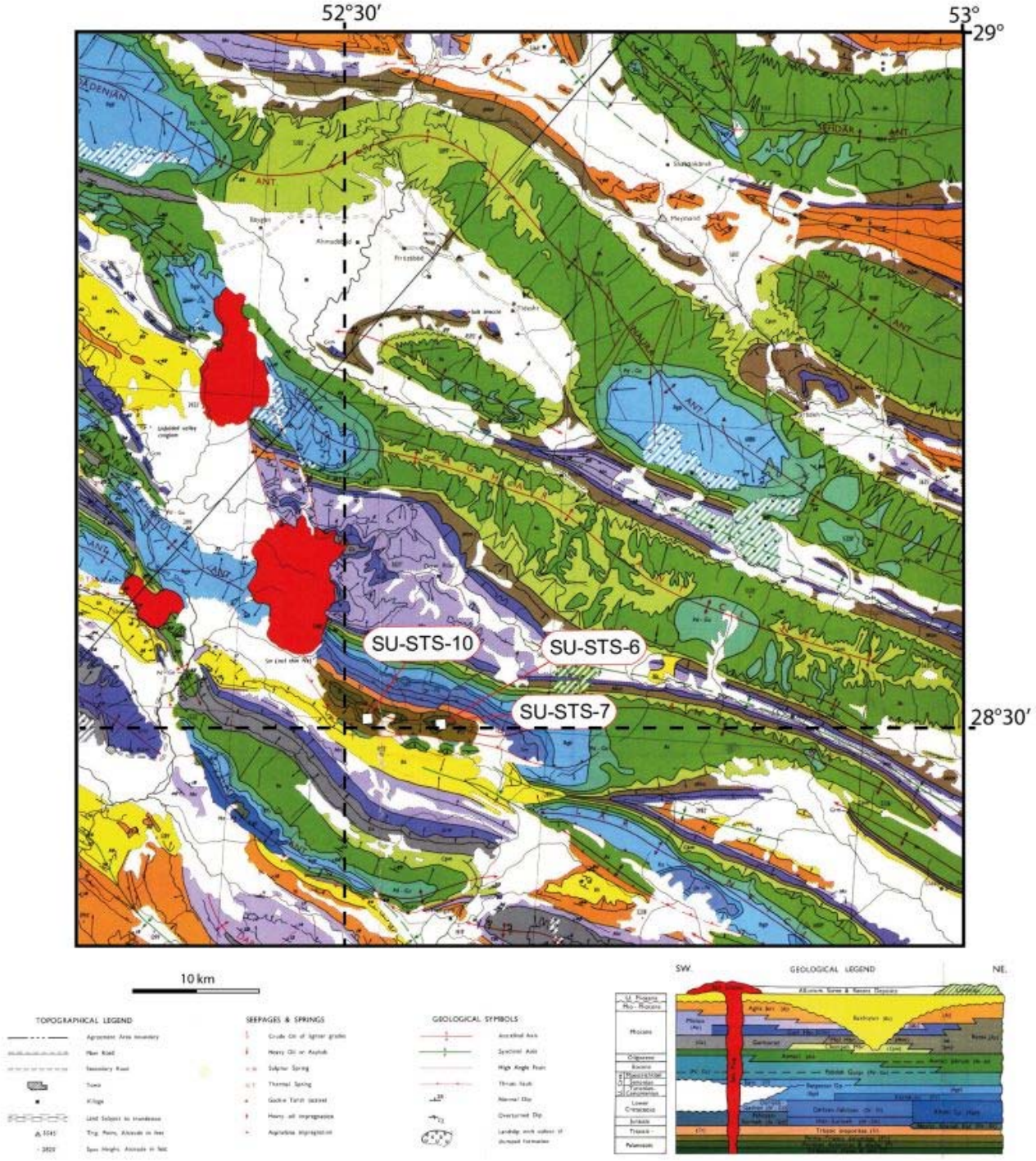

Fig. III.19. Location of the Surmeh anticline samples on the Geological map

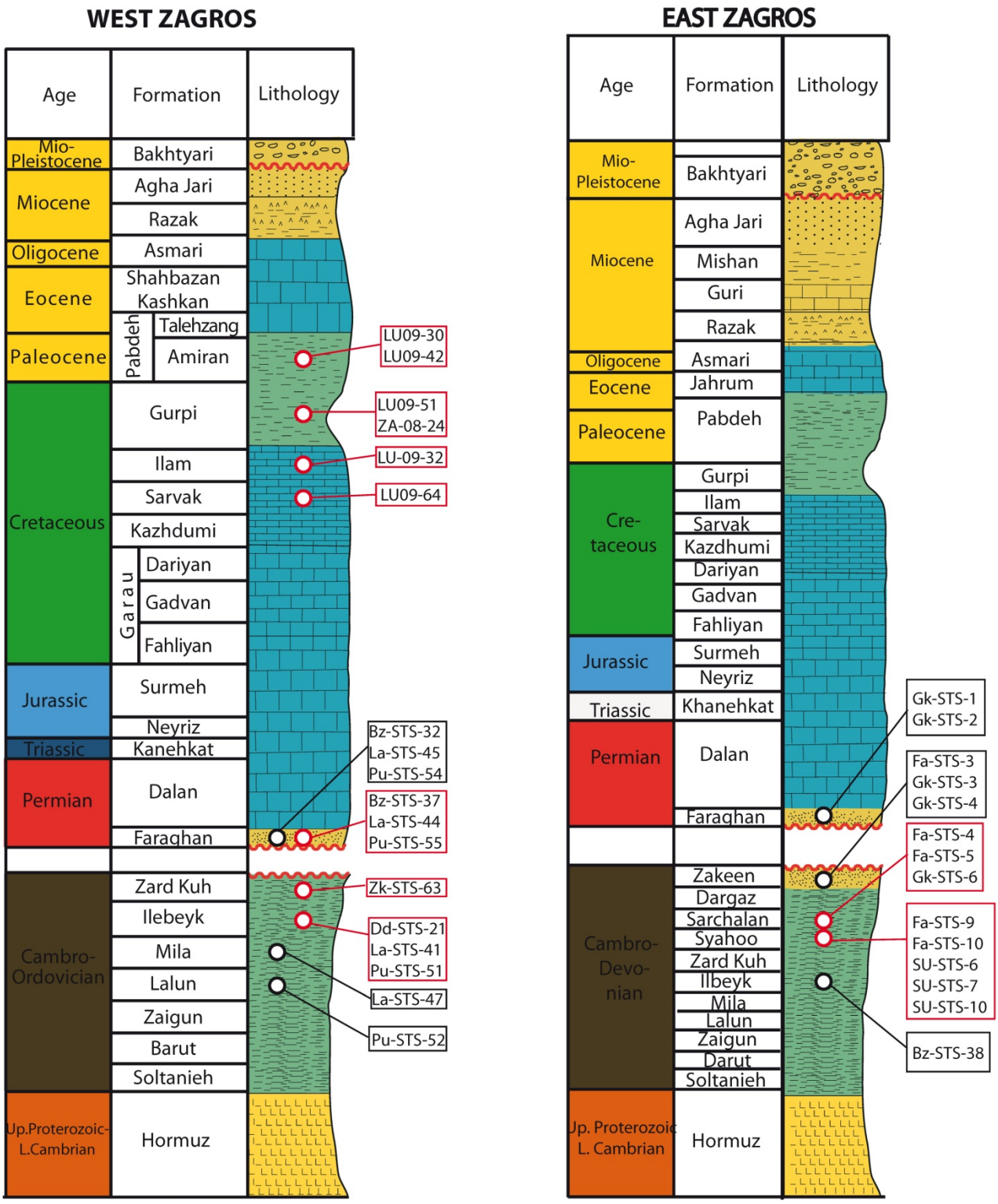

Fig.III.20. Location of samples on the synthetics boreholes.

Fig. III.21. *Samples for Organic matter tests from Western High Zagros (Locations on Fig.III.18)*

Bz-STS-37

La-STS-41

Fig. III.22. *Samples for Organic matter experiments from Surmeh and Faraghan anticlines (Locations on Figs .III.16, 19)*

Su-STS-7

Fa-STS-5

Fig. III.23. *Samples for thermochronology (U-Th)/He from Eastern High Zagros (Locations on Fig.III.16)*

Gk-STS-1

Fa-STS-3

Fig. III.24. *Samples for thermochronology (U-Th)/He from Western Zagros (Locations on Fig.III.18)*

La STS-45

Pu-STS-52

Pu-STS-54

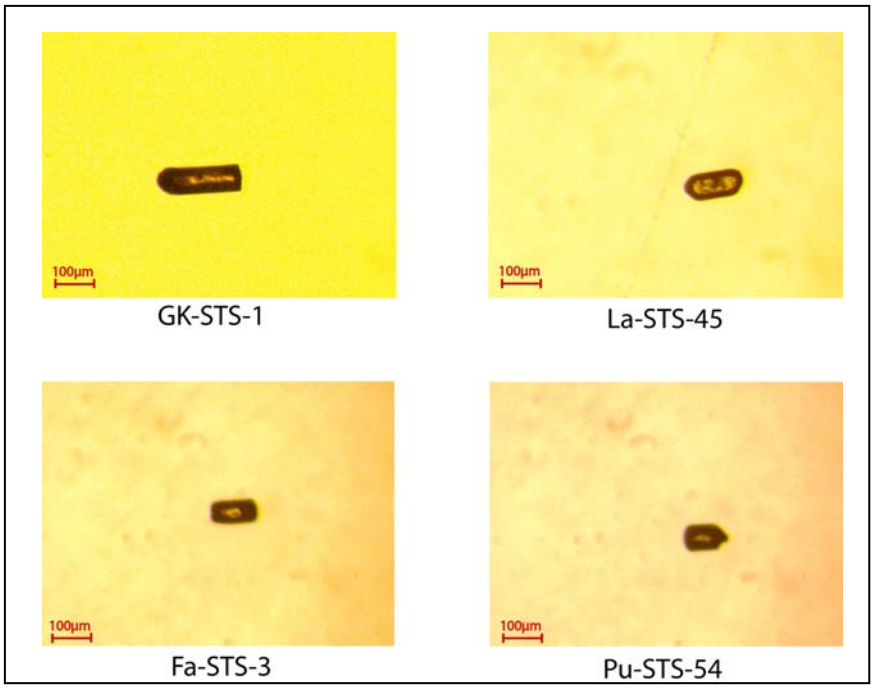

Fig.III.25. *Microscopic photos of hand-picked Zircons from High Zagros samples*

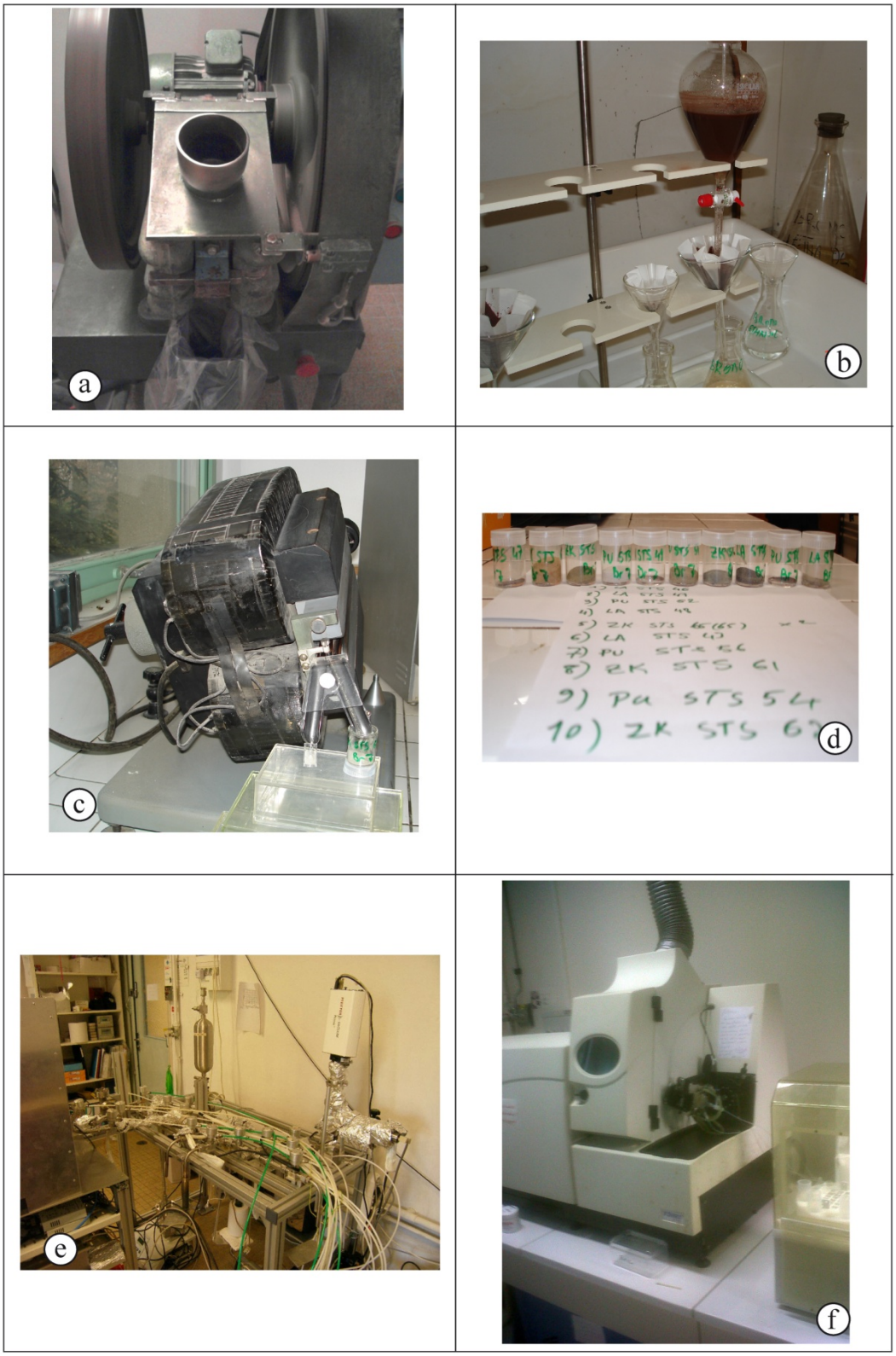

Fig. III.26.Mineral separation and (U-Th)/He measurements
a) Crushing (Jaw crusher); b) heavy liquids separation tools; c) magnetic separation (Frantz magnet); d) tubes include separated heavy minerals; e)helium line; f) mass spectrometer.

APPENDIX 2: Principles of source rock maturity analysis

The evolution with depth of organic matter can be divided into several phases in which the temperature plays an essential role (except for the initial phase of diagenesis) (Ungerer and Durand, 1987)

1) Early diagenesis, during which bacterial effects can be quite effective for generating methane gas, the so-called biogenic gas;

2) Burial diagenesis is the period during which the three types of kerogens begin to lose their oxygen in water and carbon dioxide. Note that in sedimentary basins, diagenesis starts at temperatures up to 60 ° C - 120 ° C, depending on the thermal gradient and age of the basins;

3) Catagenesis: organic matter evolves to form oil and light hydrocarbons (gas condensate). Thermal cracking is effective and the molecular weight of hydrocarbons released decreases with burial. The depth, at which this hydrocarbon genesis occurs, is called the oil window. The threshold of early catagenesis varies from 60 to 120 ° C, from 1500 to 4000 m depending on the geothermal gradients;

4) Metagenesis: formation of the dry gas (methane) and thermogenic gas, by cracking of hydrocarbons previously formed and residual kerogen. then there is formation of methane; the depth at which this process occurs is called window gas.

This evolution of the organic matter can be used to constrain the first order controlling parameter, i.e. the temperature. Two methods are routinely used: rock-eval pyrolysis and vitrinite reflectance. Measurements have been done in TOTAL technical labs in Pau (France).

Rock-eval pyrolysis

Rock-Eval pyrolysis provides different information on the organic content of rocks, such as the petroleum potential of a rock, the nature of the kerogens and their state of maturation. The method involves heating (at 25° C / min on average) of a small rock sample (approximately 100mg) in an inert atmosphere (helium). The free hydrocarbons as gas and oil contained in the rock sample are determined quantitatively and selectively; hydrocarbon and oxygen compounds (CO_2), which are expelled during the cracking of organic matter cannot be extracted from the rock (kerogen). Cycles of analyses are performed. In apparatus equipped with a carbon

module, the phases of pyrolysis and oxidation occur simultaneously, the oxidation being made on the sample pyrolyzed during the previous cycle. Referring to a rock with known standard quantities of CO_2 and hydrocarbon compounds formed during pyrolysis, and its residual organic carbon content, it is possible to calculate, for each sample analyzed, a number of parameters. The basic parameters obtained by pyrolysis of a rock sample are:

• The amount of free HC (oil and gas) that are volatilized at 300 ° C for 3 min; it corresponds to the peak of the S_1 record.

• The amount of cracking hydrocarbon compounds from, 300 to 600 ° C, the kerogen and heavy extractible compounds such as resins and asphaltenes: it corresponds to the peak of the S_2 recording.

• The temperature in degrees Celsius, when reaching the apex S_2 and this is the so-called "T max".

• The amount of CO_2 captured separately during the cracking of kerogen (S_3 peak) at lower temperatures, between 300 and 390 ° C.

• The residual organic carbon content (%weight) of the sample pyrolyzed above, obtained by combustion of the latter in air at 600 ° C. The CO_2 from combustion of this peak corresponds to S4.

From these basic parameters, index may be calculated:

• The total organic carbon content (TOC, %weight) of the sample, as the sum of residual organic carbon and pyrolyzed organic carbon. The latter is deducted from the quantities of hydrocarbons in S_1 and S_2 (Lafargue *et al.*, 1998).

$$TOC = (S_1 + S_2) \times 0.083 + \left(\frac{S_3\ CO_2 \times 12}{440}\right) + \left(\frac{S_3\ CO \times 12}{280}\right) + \left(\frac{S_4\ CO_2 \times 12}{440}\right) + \left(\frac{S_4\ CO \times 12}{280}\right) \quad (1)$$

• The hydrogen index (HI in mgHC) and the oxygen index (OI in $mgO_2/gCOT$) as the values of S_2 and S_3 respectively expressed in mg per gram of CO_2 TOC.

$$HI = \frac{S_2}{COT} \quad (2)$$

$$OI = \left(\frac{S_3\ CO_2 \times 100}{COT}\right) \times \frac{32}{44} + \left(\frac{S_3\ CO \times 100}{COT}\right) \times \frac{16}{28} \quad (3)$$

• The production index (PI) as the ratio $\frac{S_1}{(S_1+S_2)}$, that is to say the proportion of free hydrocarbons relative to the total amount of compounds hydrocarbonates obtained by pyrolysis of the analyzed sample. (Espitalié *et al.*, 1985)

Vitrinite reflectance

Vitrinite is one of the main macerals (components of coal and most sedimentary kerogens). These macerals are classified into three families, according to their origin and mode of preservation (Stach *et al.*, 1982): 1) Vitrinite, 2) Exinite and 3) Inertinite. Vitrinite results from the decomposition of higher plants consisting mainly of lignin and cellulose. Gradually, as the temperature increases, it was observed changes in the chemistry, structure and microscopic texture of vitrinite (Jiménez *et al.*, 1999). The vitrinite reflectance is the parameter most commonly used to quantitatively estimate the thermal maturity of sedimentary rocks (Houseknecht *et al.*, 1997).
The vitrinite reflectance is measured with an optical microscope and is equal to the ratio between the intensity of reflected light and the intensity of incident light. Its value is a function of (Ungerer *et al.* 1987):

- The nature of the atoms making up the substance (C, H, O);
- Their chemical structure and therefore the connexion between the atoms;
- Their microstructures, and thus the manner in which chemical structure, are arranged in space;

It was recognized early that the anisotropy of vitrinite reflectance increases with the position (thermal maturity) and the kinematic constraint. Methods were developed to obtain consistent and objective estimates of the thermal maturity

across a spectrum regardless of the orientation of the sample. These methods include measuring the reflectance of polarized light upon rotation of the microscope stage to get the maximum reflectance as a leading indicator of thermal maturity. These practices are based primarily on the assumption that the vitrinite in most coals shows reflectance properties uniaxial negative, and the maximum reflectance is observed during the rotation of the stage regardless of the orientation of the sample. However, the common method for estimating the thermal maturity of organic matter dispersed requires the measurement of the vitrinite reflectance of randomly oriented particles, without rotation. This is done using either polarized light or unpolarized, although the first is more common and is consistent with accepted standards for measuring random reflectance of coal. The measurement of random reflectance in dispersed organic matter was used primarily to evaluate the petroleum potential, and was therefore carried out on samples of relatively low thermal maturity (less than ~ 2% vitrinite reflectance) in which the anisotropy of vitrinite is low. In addition, measuring a reflectance value for each particle randomly vitrinite is faster and easier than the rotation and determination of the apparent reflectance maximum. In addition, the small size of particles dispersed vitrinite allows rotation impracticable when measuring reflectance.

The vitrinite reflectance parameter, noted $\%R_0$, evolves from 0.2 to 10%. In general, a $\%R_o$ of 0.6 characterizes the beginning of thermal diagenesis, 1.3 the end of catagenesis and during metagenesis, $\%R_o$ can increase to 10% in the later stages

Evolution of vitrinite and therefore changes in its reflectance are mainly controlled by time and temperature parameters. In theory, it is considered that the level of thermal maturity is a function of:

- temperature ;
- the length at which the organic matter is kept at this temperature;
- kinetics (first-order chemical reaction and Arrhenius equation)

Thus, in 1955, Karweil establishes a diagram from the calculation of the relationship between the level of maturation and the temperature and time at which the basin is subjected to this temperature (Xianming *et al.*, 1999). This diagram

changed in 1971 by Bostick permitted to determine paleotemperature gradients from vitrinite reflectance gradients (Xianming *et al.*, 1999). The following method disregards the effect of duration of temperature. The following equation relates the vitrinite reflectance gradient, noted ΔVRo, to reflectances of vitrinite measured for two samples (R_{H1} and R_{H2}) 1000m distant. H_1 and H_2 are the depths of samples 1 and 2.

$$\Delta VR_o = \frac{R_{H_2} - R_{H_1}}{H_2 - H_1} \quad (4)$$

The equation to convert the equivalent of vitrinite reflectance in Tmax and vice versa is as follows:

T_{max}eq%VR_o= 0.018(T_{max})-7.16 (Jarvie et al., 2001)

APPENDIX 3: Results of measurements on potential source rocks

Two sets of data in our possession. The first set is data from the Lurestan and were taken by Jean-Christophe Wrobel-Daveau (Table III.3).

For each sample, two preparations were made:

- A section of concentrated organic matter
- A section of polished rock.

Both preparations are observed in reflected light and fluorescence.

The objectives of the analysis are organic petrography, for each sample:

- To measure the reflectance
- Describe the organic matter present in the samples
- Describe the organo-mineral matrix.

An example of results, with sample LU 09-30, the concentrate of Organic Matter in reflected light gives many carbonaceous materials (Fig. III. 27) comprising:

- A majority of inertinite fragments: Semi-fusinite (1) and Sclérotinite
- From some fragments of Vitrinite (2).
- The fluorescence shows some Alginites (3) and fragments Liptodétrinites yellow orange.

In polished rock, the matrix is clayey with carbonaceous particles and has a yellow brown fluorescence

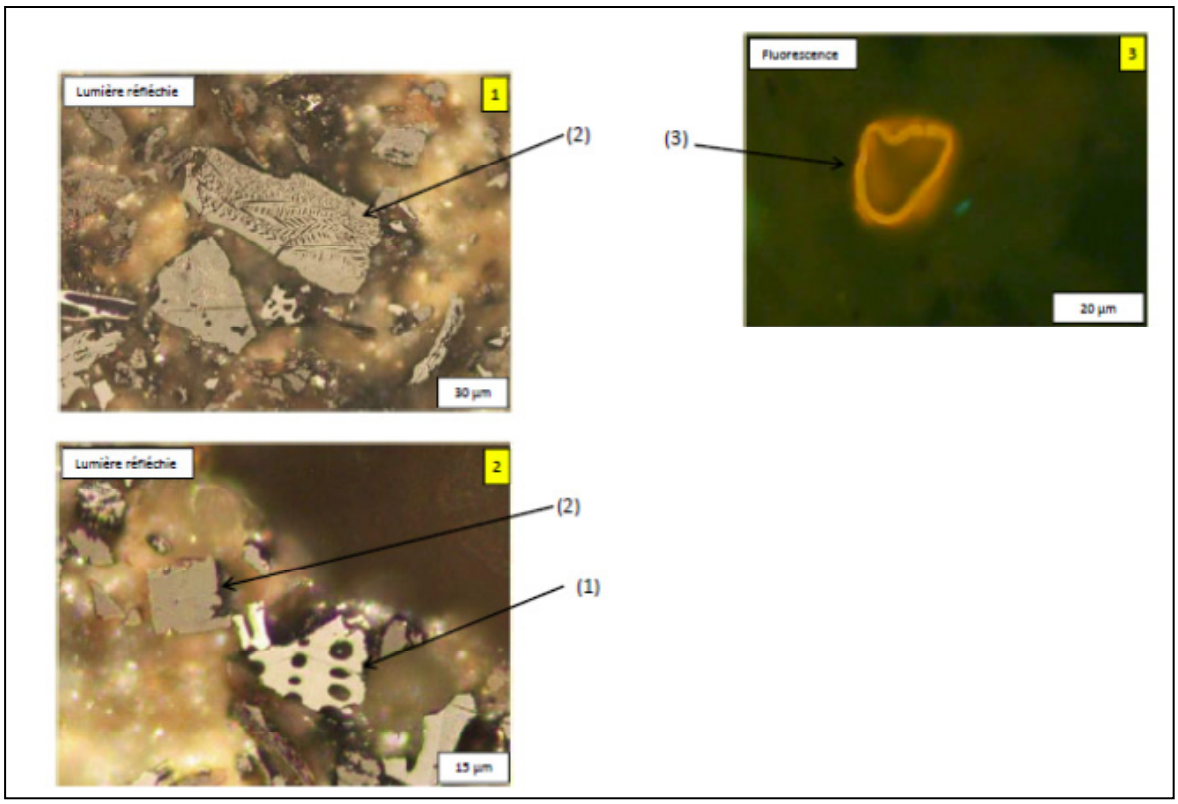

Fig. III.27. Carbonaceous materials in sample LU 09-30

Sample	Formation	Age (Ma)	Age	Latitude	Longitude	Tmax	eq. VRo%
LU09_30	Amiran	49,7	Paleo-Eocene	34,1408	46,62356	440	0,63
LU09_37	Pabdeh	49,7	Paleo-Eocene	33,62143	46,16031	435	
LU09_41	Amiran	49,7	Paleo-Eocene	33,76049	46,68252	448	
LU09_42	Amiran	49,7	Paleo-Eocene	33,8085	46,66887	436	0,9/0,51
LU09_51	Gurpi	74,5	Campanian-Maestrichtian	33,41084	46,51772	438	0,43
LU09_36	Surgah	89,65	Turonian-Coniacian	33,63128	46,1139	444	
LU09_32	Surgah	89,65	Turonian-Coniacian	33,60568	46,35837	442	0,58
LU09_64	Sarvak	102,75	Albian-Cenomanian	33,35563	46,58332	441	0,56

Table III.3. Results for Tmax and vitrinite from Lurestan

The second set is data from the Western and Eastern High Zagros Belt. Samples were collected in the frame of this thesis (Table III.4).

For each sample two types of preparation were used: concentrated organic matter polished obtained by densimetric techniques (mainly for measuring the maturity and estimated colors of fluorescence), and polished sections of grains of rock (especially for the description of the facies of organic matter). The maturity assessment was carried out with optical techniques (reflectometry and UV fluorescence) on Leica. According to the richness of organic particles, by at least 30 slides were recorded, if possible. A fragment not sooty (vitrinite) exists in the Ordovician-Silurian series due to the absence of plant material. But other types of particles are often encountered in these series; two populations often exhibit typical features (i) remains graptolites and (ii) fragments of bitumen insoluble. For maturity assessment, two correlation curves between reflectance and vitrinite reflectance (% VRO) and will be used in this study:

For graptolites: correlation of Cole - VRO% = 0,785 + 0.05% Gro.
For bitumen: the correlation of Jacob - VRO =% + 0.40% 0618 Bro.

An example of results with the sample Fa-STS-4 (Fig. III.28): In the concentrate, small organic fragments were observed. They show various aspects and the reflectance and no structure or typical form we can determine the origin of these organic remains: population with VRO 1.35 to 1.75% has an indistinct structure: possible graptolites, while the population with a reflectance the VRO of 0.7 to 1.3% is very homogeneous (bitumen, another type of zoorests?). The fluorescence is zero. The section of polished grains consists of a silty argillite with pyrite oxidised common (or microcrystalline grain framboids). The reflective organic remains are rare and small. The fluorescence is zero.

Because of the difficulty in ensuring the type of particles measured maturity is not well evaluated. The equivalent reflectance is derived from the Cole curve for the possible graptolite population (from 1.35 to 1.75%) as a maturity of around 1.25% eq.VRo. Absence of fluorescence indicates a maturity greater than 1% VRO.

Fig. III.28. Organic matter sample (Fa-STS-4) collected from Faraghan anticline

Sample ID	Formation	Age	Tmax	eq. VRo%	Domain
Pu-STS-55	Top Faraghan	Permian	527	0,77	Western Zagros
Bz-STS-35	Faraghan	Permian			
Bz-STS-37	Faraghan	Permian	441	0,7	
La-STS-44	Faraghan	Permian	489	0,87	
Zk-STS-63	ZardKuh	Ordovician	461	1,24 ?	
La-STS-41	Ilbeyk	(Ord-Sil)	488	1,53 ?	
Pu-STS-51	Ilbeyk	(Ord-Sil)	492	1,02	
Dd-STS-21	Ilbeyk	(Ord-Sil)	450	1,02	
FA-STS-4	Sarchahan	Silurian		1,25	Eastern Zagros
FA-STS-5	Sarchahan	Silurian	465	1,35	
FA-STS-9	Syahoo	Ordovician	461	1,37	
FA-STS-10	Syahoo	Ordovician	460	1,34	
GK-STS-6	Sarchahan	Silurian		1,01	
SU-STS-2	Syahoo?	Ordovician		?	
SU-STS-6	Syahoo	Ordovician		0,9	
SU-STS-7	Syahoo	Ordovician	437	0,97	
SU-STS-10	Syahoo	Ordovician		0,89	

Table III.4. Results for Tmax and vitrinite from High Zagros and Surmeh anticline

Appendix 4: Principles of (U-Th)/He thermochronology on zircon

The dating method (U-Th)/He is based on the accumulation of He (α particles) within a crystal due to the radioactive decay of ^{235}U, ^{238}U and ^{232}Th, and its subsequent diffusion through the crystal lattice at a rate that is strongly temperature dependent. In zircon, He will accumulate without significant diffusional loss (at geological timescales) below temperatures of the order of 160-180 °C (Reiners *et al.*, 2004, Reiners and Brandon, 2006) Helium production is function of U and Th content according to the equation:

$$^{4}He = 8\ ^{238}U\ (e^{\lambda_{238}t}-1) + 7\ ^{235}U\ (e^{\lambda_{235}t}-1) + 6\ ^{232}Th\ (e^{\lambda_{232}t}-1) \quad (5)$$

λ_i being different constants of radioactive decay. As the isotopic ratio $^{235}U/^{238}U$ is constant and equal to 1/137.88, the concentration of ^{235}U can be substituted into the equation resulting in:

$$^{4}He = 8\ ^{238}U\ (e^{\lambda_{238}t}-1) + 7\ (^{238}U\ /137{,}88)\ (e^{\lambda_{235}t}-1) + 6\ ^{232}Th\ (e^{\lambda_{232}t}-1) \quad (6)$$

The instantaneous production P* (t=1) will be:

$$P^{*} = 8.^{238}U\ (e^{\lambda_{238}}-1) + 7.(^{238}U/137.88)\ (e^{\lambda_{235}}-1) + 6.^{232}Th\ (e^{\lambda_{232}}-1) \quad (7)$$

Theses equations are valid only if:

1. The amount of ^{4}He atoms initially present in the mineral is negligible;
2. The production of α particle is too low to lead to the destruction of the crystal lattice by metamictization and thus helium loss is controlled only by volume diffusion.

To fulfill these two conditions, minerals should be sufficiently rich in U and Th for the initial amount of He being negligible compared to that produced over time and have a sufficiently low U and Th content to avoid metamictization. Zircon ($ZrSiO_4$) is one of the richer U and Th bearing minerals with large U and Th content (~100-500 ppm and ~10-100 ppm respectively). Metamictization may occur for the U-Th richest grains and after a long period of time.

Zircon is a common accessory mineral found in most igneous rocks and sedimentary sandstones due to its relative high hardness.

Alpha ejection

Each emitted alpha particle is characterized by a kinetic energy (4 to 9 MeV) sufficient to lead to a large stopping distance. Some particles can be ejected outside of the mineral, especially near the edges of minerals. Therefore, the amount of α particles measured in a mineral underestimates the real amount produced by the decay of U and Th. A correction has been developed to take account of He ejection from the crystal borders (Farley *et al.*, 1996). This correction takes into account the geometry of the mineral, laws of probability and distance of ejection (15,55 microns in average for the ^{238}U, 18.05 microns for the ^{235}U and 18.43 microns for the ^{232}Th (Ketcham *et al.*, 2011, Ziegler, 2008). It emphasizes the importance of selecting crystals large enough that the surface loss compared to the total volume of the crystal is small. The surface to volume ratio β of grains can be calculated for any kind of geometry (Farley, 2002; Reiners, 2005).

In case of zircon (prismatic geometry), the fraction of helium retained in the grains (F_T) is then given as a polynomial function of surface to volume ratio β:

$$F_T = 1 - \frac{3}{4}\frac{Rs}{R} + 0{,}2122\frac{(a+b+c)R^2}{abc} - 0{,}00995\frac{R^3}{abc} \quad (8)$$

With $R_S = \frac{3}{2}\frac{1}{\frac{1}{a}+\frac{1}{b}+\frac{1}{c}}$ (9)

With Rs the equivalent radius of the sphere, R the mean stopping distance, a, b and c are the sizes of the three axes (in microns) (Ketcham *et al.*, 2011). This equation is valid for homogeneous U-Th repartition in the crystal. For zoned crystals, Hourigan *et al.* (2005) have proposed some analytical solution. Additional corrections like mechanical abrasion of zircons during transport can remove the impoverished border, which requires a particular correction (Rahl *et al.*, 2003).

For homogenous or zoned crystals, and abrased effect, the F_T ejection factor can also be determined using Monte Carlo simulation using the online program from Ketcham *et al.*, 2011, Gautheron *et al.*, 2012 (http://hebergement.u-psud.fr/flojt/).

He retention and age significance

Quantitative understanding of the ZHe ages and extraction of the thermal history is mainly based on results of laboratory experiments by heating steps that determines the diffusion of He in zircon. These laboratory results of bulk diffusion kinetics for zircon in the range of activation energies (Ea) of 163 to 173 kJ/mol (30-41 kcal/mol) and diffusivities at infinite temperature (°C) of 0.09 to 1.5 cm^2 s-1 (Reiners et al, 2002, 2004, Reiners, 2005).

ZHe age will be a function of the abundance of U-Th and the He remaining in the crystal during the cooling below this closure temperature, which represents a depth of about 6km considering a regular geotherm of 30° / km. He age is given by

He age (Ma) = [He content]/ (P*) (10) with P* defined in equation (7)

Using these diffusion coefficients, closure temperature (Tc) can be determined from Dodson's (1973) formulae and represent the temperature where for a constant cooling rate, 50% of the emitted alpha particles remain in the crystal. For zircon, Tc is in the range of ~175-195 °C (average ~185 °C) (Reiners, 2005, Fig.III.15) for grains of 40-100 microns width and assuming a cooling rate of 10 ° C/Ma (Reiners *et al.*, 2002, 2004). Figure III.15 illustrates the thermal sensitivity of apatite and zircon (U-Th)/He and fission track thermochronometers, in function of the cooling rate.

(U-Th)/He analysis protocol

The following steps were followed for all samples.

1. Samples were crushed using a mechanical grinder and only the fraction below 400 µm was retained for analysis. This fraction was then washed with water to remove clays, and passed to bromoform. Bromoform was used to sort out heavy minerals.

2. Selection of grains under a binocular microscope on criteria of form, purity, and the lowest amount of inclusions. The grains must be sufficiently large to minimize the correction of form and in particular have no dimension less than 60µm.

3. The selected grains (5 grains per sample) are incorporated into a Niobium capsule and a minimum of two aliquots are prepared, after having been drawn or photographed and measured for grain size.

4. He degassing and measurement: He extraction is done in high vacuum at 1100 – 1250° C during 30 minutes. The released ^{4}He is mixed with a known amount of ^{3}He and then purified using a series of chemical traps (getters) and activated carbon cooled at liquid nitrogen temperature before being introduced into a quadrupole mass spectrometer. ^{4}He concentration is obtained by comparison with the amount of ^{3}He. During the He session, standard zircon has been analyzed for the uncertainty determination (square deviation of the standard).

5. Measurement of U and Th composition of grains for each aliquot, using acid digestion, and addition of a known amount of ^{235}U and ^{230}Th followed by ICP-MS measurement (inductively coupled plasma mass spectrometer). (Evans, *et al.*, 2005).

6. Age determination. The concentrations of ^{4}He, U and Th are calculated and used to solve the age equation. The He age is corrected for α ejection of particles by the calculated FT factor for each grain. This factor takes into account the geometry of the mineral, laws of probability and distance of transmission as explained above. Based on experience from past studies done at the Orsay He laboratory, we consider an uncertainty of 8% for the age obtained for each aliquot which represents the standard deviation of the He standard (FCT zircon, Durango and Limberg apatite, Tagami *et al.* 2003, Mc Dowell *et al.*, 2005, Kraml *et al.*, 2006, respectively).

Appendix 5: Thermochronology results (U-Th)/He ages on zircon

Sample ID	Rs	FT	U ppm	Th ppm	eU ppm	Th/U	He Age (Ma)	Formation	Stratigraphic Age	Laboratory Place
La-STS-45-A	37,7	0,718	174,2	225,3	228,2	1,29	216	Faraghan	Permian	Orsay
La-STS-45-B	40,4	0,734	260,0	285,2	328,5	1,1	107	Faraghan	Permian	Orsay
La-STS-45-C	42	0,733	157,6	145,0	192,4	0,92	224	Faraghan	Permian	Orsay
Pu-STS-54-A	46,9	0,772	316,3	289,8	385,9	0,92	224	Faraghan	Permian	Orsay
Pu-STS-54-B	48,4	0,778	243,6	310,3	318	1,27	220	Faraghan	Permian	Orsay
Pu-STS-54-C	47,4	0,769	629,6	985,5	866,1	1,57	86	Faraghan	Permian	Orsay
GK-STS-2-A	46,4	0,766	379,1	536,4	507,9	1,41	134	Faraghan	Permian	Orsay
GK-STS-2-B	43,8	0,753	340,0	144,4	374,7	0,42	111	Faraghan	Permian	Orsay
GK-STS-2-C	41	0,735	427,8	207,4	477,6	0,48	112	Faraghan	Permian	Orsay
GK-STS-1-A	48,7	0,801	231,3	79,9	250,5	0,35	148	Faraghan	Permian	Orsay
GK-STS-1-B	47	0,773	527,0	139,0	560,4	0,26	77	Faraghan	Permian	Orsay
GK-STS-1-C	43,1	0,742	231,2	98,1	254,8	0,42	184	Faraghan	Permian	Orsay
BZ-STS-32_1	34	0,692	533,7	383,1	625,6	0,72	561	Faraghan	Permian	Tübingen
BZ-STS-32_4	38	0,712	61,7	105,0	86,9	1,7	278	Faraghan	Permian	Tübingen
BZ-STS-32_5	37	0,68	282,5	243,5	341	0,86	356	Faraghan	Permian	Tübingen
BZ-STS-32_6	37	0,688	544,1	321,8	621,3	0,59	356	Faraghan	Permian	Tübingen
BZ-STS-32_7	36	0,671	363,8	367,2	451,9	1,01	698	Faraghan	Permian	Tübingen
BZ-STS-32_8	32	0,641	801,8	315,7	877,6	0,39	341	Faraghan	Permian	Tübingen
BZ-STS-32_9	36	0,673	747,6	288,2	816,7	0,39	334	Faraghan	Permian	Tübingen
Fa-STS-3-A	56,3	0,804	68,1	42,8	78,4	0,63	377	Zakeen	Devonian	Orsay
Fa-STS-3-B	62,3	0,829	266,1	121,6	295,3	0,46	180	Zakeen	Devonian	Orsay
Fa-STS-3-C	57,5	0,807	609,4	242,2	667,6	0,4	97	Zakeen	Devonian	Orsay
GK-STS-4-A	51	0,784	224,4	414,4	323,8	1,85	101	Zakeen	Devonian	Orsay
GK-STS-4-B	55,6	0,808	134,4	0,0	134,4	0	346	Zakeen	Devonian	Orsay
GK-STS-4-C	52,4	0,804	322,2	837,9	523,3	2,6	132	Zakeen	Devonian	Orsay

Sample ID	Rs	FT	U ppm	Th ppm	eU ppm	Th/U	He Age (Ma)	Formation	Stratigraphic Age	Laboratory Place
GK-STS-3-A	44,3	0,752	518,4	146,6	553,6	0,28	53	Zakeen	Devonian	Orsay
GK-STS-3-B	41	0,745	167,9	85,1	188,4	0,51	239	Zakeen	Devonian	Orsay
GK-STS-3-C	40,5	0,734	363,2	158,2	401,2	0,44	154	Zakeen	Devonian	Orsay
BZ-STS-38_1	26	0,575	1958,2	2488,6	2555,4	1,27	105	Ilbeyk	Ordovician	Tübingen
BZ-STS-38_2	20	0,48	819,6	556,9	953,3	0,68	121	Ilbeyk	Ordovician	Tübingen
BZ-STS-38_3	22	0,525	226,7	373,5	316,3	1,65	203	Ilbeyk	Ordovician	Tübingen
BZ-STS-38_4	16	0,404	1501,1	2479,9	2096,3	1,65	561	Ilbeyk	Ordovician	Tübingen
BZ-STS-38_5	25	0,556	966,9	1136,7	1239,7	1,18	74	Ilbeyk	Ordovician	Tübingen
BZ-STS-38_6	21	0,498	972,7	1132,6	1244,5	1,16	131	Ilbeyk	Ordovician	Tübingen
La-STS-47_1	54	0,772	320,4	357,4	406,2	1,12	290	Mila	Cambrian	Tübingen
La-STS-47_2	60	0,811	126,3	317,7	202,5	2,52	106	Mila	Cambrian	Tübingen
La-STS-47_3	54	0,772	150,9	275,4	217	1,83	163	Mila	Cambrian	Tübingen
La-STS-47_4	32	0,758	2968,5	2882,1	3660,2	0,97	23	Mila	Cambrian	Tübingen
La-STS-47_5	55	0,799	994,7	366,1	1082,5	0,37	467	Mila	Cambrian	Tübingen
La-STS-47_6	80	0,854	106,5	75,2	124,6	0,71	194	Mila	Cambrian	Tübingen
La-STS-47_7	55	0,797	157,3	295,7	228,3	1,88	196	Mila	Cambrian	Tübingen
La-STS-47_9	32	0,709	235,8	458,4	345,8	1,94	1151	Mila	Cambrian	Tübingen
Pu-STS 52_1	60	0,815	461,1	681,3	624,6	1,48	283	Lalun	Cambrian	Tübingen
Pu-STS 52_2	47	0,786	403,9	742,0	582	1,84	233	Lalun	Cambrian	Tübingen
Pu-STS 52_3	78	0,844	54,7	77,0	73,2	1,41	242	Lalun	Cambrian	Tübingen
Pu-STS 52_4	64	0,823	558,8	385,2	651,2	0,69	200	Lalun	Cambrian	Tübingen
Pu-STS 52_5	64	0,822	266,2	277,5	332,8	1,04	406	Lalun	Cambrian	Tübingen
Pu-STS 52_6	52	0,798	466,9	1069,3	723,5	2,29	315	Lalun	Cambrian	Tübingen
Pu-STS 52_7	40	0,746	621,2	473,6	734,8	0,76	430	Lalun	Cambrian	Tübingen
Pu-STS-52_8	54	0,799	208,2	208,2	258,1	1	258	Lalun	Cambrian	Tübingen
Pu-STS-52_9	39	0,734	592,8	525,1	718,9	0,89	257	Lalun	Cambrian	Tübingen

Table III.5. ZHe ages data for eleven samples from High Zagros Belt

GENERAL CONCLUSION

Partial conclusions of my thesis have been given at the end of each chapter; some of them have been already published or will be soon. I summarize here the main points that can be considered as acquired at the end of this work.

- We have proposed a new definition for the High Zagros Belt (HZB). Following this definition, the High Zagros is a NW-SE structural zone located south of the Main Zagros Thrust (MZT) and north of the High Zagros Fault (HZF). It includes Lower Paleozoic rocks carried out over Mesozoic and Cenozoic rocks along basement thrust faults (i.e. HZF). The HZB is exposed in two disconnected domains, east and west of the ZFTB with considerable greater area for the latter one.

- The apparent discontinuity of the High Zagros on the map view could result either from primary geometry of the Arabian Plate boundary or from partial under-thrusting below the Iranian Plate. Geodynamic evidence supports the second hypothesis (Indeed, the HZB exists everywhere along the belt but is hidden by Sanandaj- Sirjan thrust sheets).

- The High Zagros, the most imbricated zone of the Zagros Fold Thrust Belt (ZFTB), developed at the initial stages of the Cenozoic Zagros Orogeny. Ongoing contraction implied subsequently the south-westward propagation of the deformation front. Numerous reverse and thrust faults associated with strike-slip movements developed progressively as a consequence of this propagation.

- High wave length detachment folds over basal Hormuz salt initiated early within the sedimentary cover. Structural style of the anticlines was pursued by over-steepening of the frontal limbs and eventually generation of faulted detachment folds (Mitra, 2002) at more advanced stages of the deformation.

- Average shortening in the High Zagros is about 25% for the studied sections (Fig. I.7). However, contrasting with 15% calculated for the whole Zagros Simply Folded Belt (Sherkati *et al.*, 2006). This permits us to conclude that a significant part of deformation has been accommodated in the High Zagros.

On the other hand, less shortening (ca. 2%- 6%) for the basement is a paradox which may be explained either by “internal deformation” and/or by creation of “duplexes” and “horse sheets” within the under-plated domain of the basement.

- According to Molinaro *et al.* (2005) and Sherkati *et al.* (2006), we show that the High Zagros kinematic evolution comprises two main episodes. Firstly, a “thin-Skinned” phase leads to the generation of large scale detachment folds in the cover, without involvement of the pre-Cambrian basement. Intermediate décollement horizons and multiple thrust faults completed the fold architecture afterwards. Duplex structures within the Lower Paleozoic rocks of the High Zagros have been put forward for the first time as a consequence of the activation of Ordovician-Silurian shale. The second stage of kinematic scenario corresponds to the occurrence of basement thrusting. These “out-of-sequence” thrust faults cross-cut all preceding structures and are responsible for present major seismic events in the High Zagros.

- Following previous authors (e.g. Setudehnia, 1972; Motiei, 1993; Ghavidel-Syooki, 2003), we emphasize the existence of a significant Paleozoic unconformity in the High Zagros (as northern part of the Arabian platform and southern paleomargin of the Neo-Tethys). The Early Permian Faraghan Fm (Ghavidel-Syooki, 2005) overlies through an angular unconformity on Cambro-Ordovician rocks (Mila-Ilbeyk Fms) in the Western High Zagros and on the Devonian Zakeen Fm in the Eastern High Zagros. The origin of this big hiatus, resulting from uplift and erosion, is discussed in detail.

- Long distance correlations of pre-Permian formations allow us to recognize a wide Arch-and-Basin geometry in the High Zagros equivalent to the one observe in the Arabian Plate and in Northern Africa (see annex 2). More precisely, The Western High Zagros forms an Arch and the Eastern High Zagros a basin respectively. This geometry is sealed by the pre-Permian unconformity. We show that the only structures developed below the Permian are normal faults and tilted blocks developed during a diffuse extensional

tectonic event. This observation strongly modifies the previous interpretation in which the Arches were interpreted as lithospheric folds linked to the Variscan Orogeny.

- Based on a number of pre-requisite data including the results of maturity measurements on the Paleozoic fine grained organic matters (Shale, calystone and siltstone) and synthetic logs for Western and Eastern High Zagros, we developed a GENEX modeling in order to understand the thermal history of the High Zagros. In particular, we evaluate different scenarios corresponding to various hypotheses about the "heat flow" evolution through time. Following the most reasonable scenario for the heat flow and integrating geodynamic setting of the study region, the amount of the eroded sedimentary thickness is appraised about 4000 m (prior to the Permian). This result testifies for a significant pre-Permian uplift of probable thermal origin, which is in agreement with the results of Kohn *et al.* (1992) and Vermeesch *et al.* (2009) who reported a "thermo-tectonic" event of Late Devonian-Early Carboniferous in the Levant Arch.

- In the High Zagros, Paleozoic formations on both sides of the pre-Permian unconformity were systematically sampled to obtain the cooling ages of Zircon bearing rock. (U-Th)/He thermochronology results of these clastic rocks presented two populations of ages. A cluster at 350-400 Ma reinforced by Gavillot *et al.* (2010) data could correspond to the age of the "thermal uplift", which is discussed at large scale in the annex 2. The second group shows scattered age between 50 Ma-250 Ma. This dispersion is indicative of a partial reset due to sedimentary burial (at a temperature $\leq 150°C$) followed by an uplift characterized by a relatively low cooling rate, which seems consistent with the mechanism of thermal uplift that we have postulated.

ANNEX N° 1

A SHORT MEMO ON THE SURMEH STRUCTURE IN THE FARS ARC

1. Why study Surmeh anticline?

The exposures of pre-Permian rocks throughout the ZFTB are mainly limited to the High Zagros Belt where an intense tectonic activity allows the development of numerous imbricated folds and complex network of faults. Elsewhere, the only place to examine Lower Paleozoic at the surface within the external zone of the ZFTB is located in the Kuh-e-Surmeh in the Fars Arc (Fig.1). The purpose of this short memo is to improve understanding some of the geological characteristics of pre-Faraghan formations in the Surmeh anticline. It may also provide an idea about deep structural style which could have potential for future hydrocarbon exploration in the Fars area.

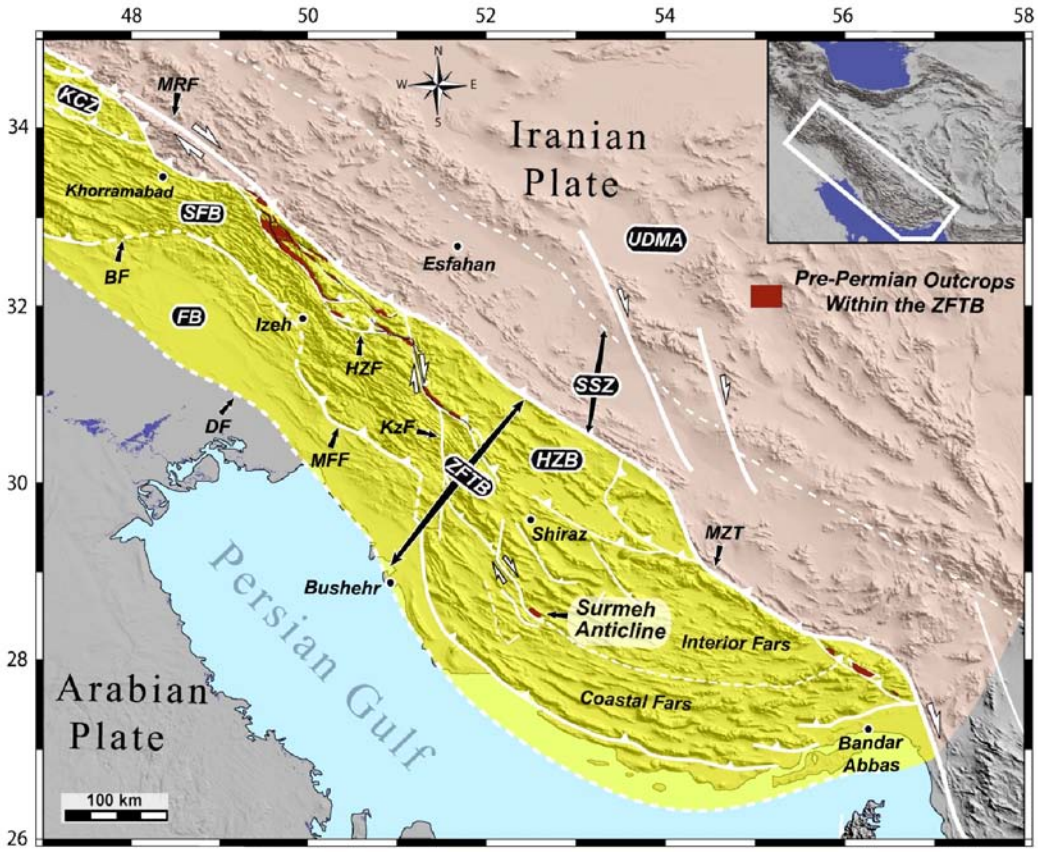

Fig.1: Location map of the Surmeh anticline in the middle of Simply Folded Belt

2. Description of the Surmeh structure

Kuh-e-Surmeh is a southward verging thrust anticline which is located at the termination of Mengharak or Karehbas (Berberian, 1995) right-lateral strike-slip fault. It is a WNW-ESE trending anticline with the length and width of about 25 and 6 km

on the Bangestan level respectively and topographic culmination of 2240 m above mean sea level. It is an asymmetric structure with average 50° flank dipping northward and high angle to vertical southern limb (mostly in the western part of the structure). The north-west plunge of Surmeh anticline is buried under the Jahani salt dome and alluvium deposits whereas the south-west continuation exhibits a wider nose and several “rabbit-ear” secondary folds at the Bangestan and Asmari levels. These secondary folds have grown over the both limbs of the major anticline and reflect the activation of underlying intermediate décollement horizons (e.g. Pabdeh-Gurpi formations). The Karehbas fault with approximately N-S trend is a basement tear fault bounded the Surmeh anticline to the west. It is actually an en-echelon fault system with several aligned Hormuz diapirs (e.g. Jahani, Namak and Gach salt plugs) along it (Fig.2). A segment of this fault system limited and turned Western nose of the Kalagh anticline. The Kareh-Bas Fault is very active and accommodates c. 5.5 mm (per year) of right-lateralstrike slip (Hatzfeld et al., 2010).

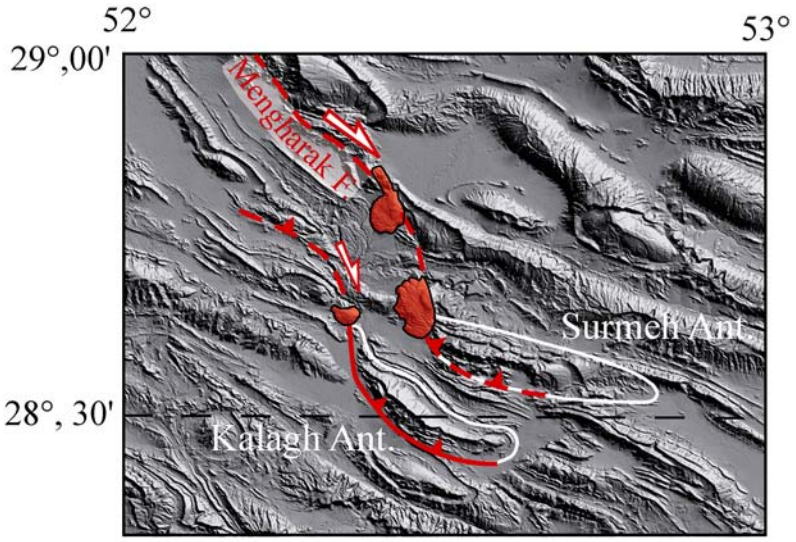

***Fig.2**. Shaded relief (SRTM data) map of the Surmeh and Kalagh Anticlinal structures. The N-S Karehbas fault system comprises of several en-echelon wrench faults. Outcropping of Hormuz salt diapirs along this fault reveals it’s deep-seated geometry*

The Surmeh and Kalagh anticlines present a typical axis bending with convexity toward the south and are structurally higher than the surrounding anticlines. Both anticlines are thrust to the south along a couple of frontal ramp located at the tip of the Karehbas right-lateral fault. This thrust fault which bounding

the Surmeh anticline to the south is hidden beneath the Bakhtyari formation (Fig.2) whereas a similar ramp has reached to surface in Kalagh southwestern flank.

The Ordovician clastic rocks are exposed in three amphitheater-like-valleys at the core of the Surmeh structure (Fig.3) and consist of about 60m of micaceous shale and fine grained silty sandstone without any macrofossil. It was dated as upper Ordovician (Caradocian-Ashgillian), *(Ghavidel-syooki M., 2005)* and was considered as lateral equivalent of Syahoo formation. The Faraghan formation seals the underlying Syahoo rocks with a gentle angular unconformity in the most eastern valley of Surmeh anticline (Fig.4). This picture illustrates the 50cm thick transgressive quartz conglomerate of Early Permian which overlies the green shale and sandstone layers of Ordovician with an angle of approximately 10 degrees. Therefore, there is a considerable hiatus with the absence of Silurian, Devonian and Carboniferous deposits in the area. The closest Lower Paleozoic outcrop is located at Kuh-e-Dena, nearly 300 km to the north-west, where pre-Permian unconformity cuts much further down the section. The Kazerun basement fault separates a regional “Arch” to the west from a large and broad “Basin” to the east of the ZFTB at the pre-Permian level (Tavakoli-Shirazi et al., 2012; Frizon de lamotte et al., Annex 2, paper in press). This geometry can explain why the latter place which is situated to the west of the Kazerun line over the Paleo-high (Arch structure), involved deeper erosion of Lower Paleozoic sequence. On the other hand, lack of Silurian to Devonian sediments in the Surmeh anticline reveals the existence of a local N-S basement uplift extending northward the Qatar-Fars Arch. This would be a minor Arch structure within East Zagros wider basin at the level of pre-Permian rocks (See Tavakoli-Shirazi et al., 2012 for further explanations).

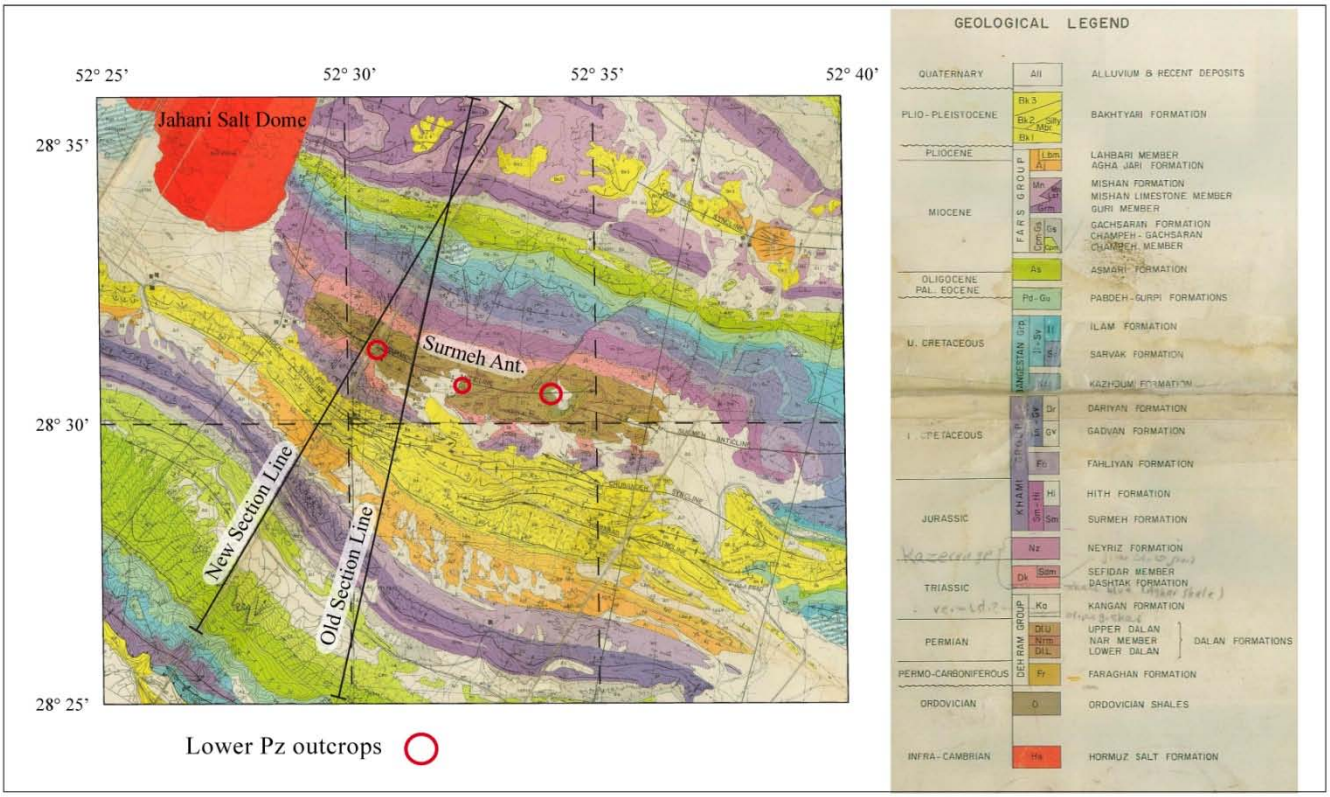

Fig3. Geological map of the Surmeh anticline and adjacent areas. Neogene to Recent deposits developed over the southern flank and mask the underlying structures (i.e. north-dipping frontal ramp to which the Surmeh rests on it's hanging-wall).

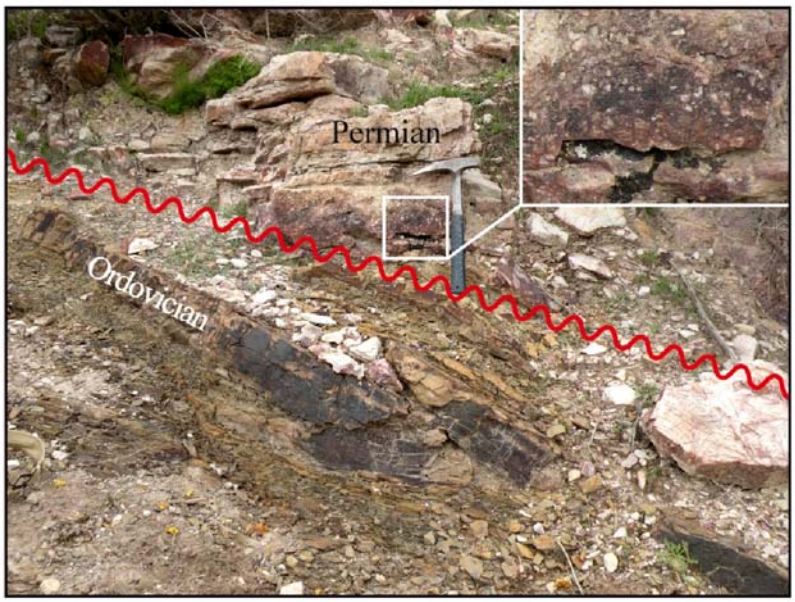

Fig.4. Low angle unconformity at the base of Early Permian Faraghan deposits in the core of Surmeh structure. The coarse Quartz grains in the framework of the conglomerate indicate post erosion fluvial sediment supply.

3. Past Structural cross-sections

Previous detailed geological study of Surmeh anticline is devoted to the NIOC internal report (Evers, H.J., et al, 1977). The authors described the geodynamic setting of the area and prepared a detailed Geology map (partly in figure 3) and several parallel structural transects in order to analyze the architecture of the Surmeh anticline (for example cross-section N° 6, figure 5). They have used their model to construct the section according to concentric folding assumption using calculation of the anticline's centre of curvature. The room problem below this point results in imbrications and faulting of underlying strata. After revisiting, I have constructed a new structural section (Fig.6) in NE-SW direction (perpendicular to the axis) over the most western domain of the anticline crossing Lower Paleozoic exposures. It is going to illustrate the structural style and kinematic evolution of it (former and new section lines were outlined over the old geology map in figure 3).

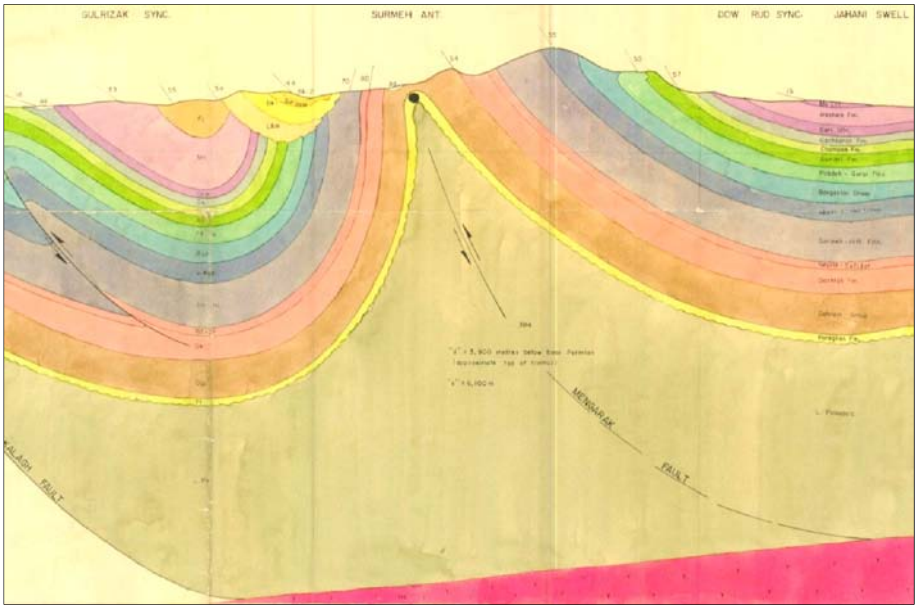

Fig.5. Structural cross-section through western part of the Surmeh anticline Evers, et al. (1977). For legend see figure 3

3.1. Geometry of the Surmeh structure

The Surmeh is a high elevated and large detachment fold. A prerequisite condition for the generation of detachment folds is the existence of a high competency contrast between the sedimentary units involved in the folding process.

(Homza and Wallace, 1997; Rowan, 1997; Mitra, 2002 and 2003). A basal incompetent layer which acts as a major detachment zone (shale or salt) and overlain by a thick competent unit (carbonates or sandstones) is consequently required. In the Surmeh anticline, Early Cambrian Hormuz salt at the base of sedimentary pile implied such circumstances and decoupled whole the succession from the crystalline rigid basement. This unit is covered by an overall competent Cambrian-Cenozoic sequence. In the Kuh-e-Surmeh, these stiff series simply wrinkled over the effective Hormuz décollement and initially formed a salt-cored buckle fold. The high angle southern limb (Fig.6) implies that the Surmeh reached to a mature stage of structural evolution which subsequently resulted in faulting within the extremely deformed part. Up-dip displacement of a basement thrust carried out the forelimb of the anticline over the footwall syncline. At present time, Surmeh illustrates a south-verging anticline locates on the hanging-wall of a deep-seated thrust fault dipping toward north.

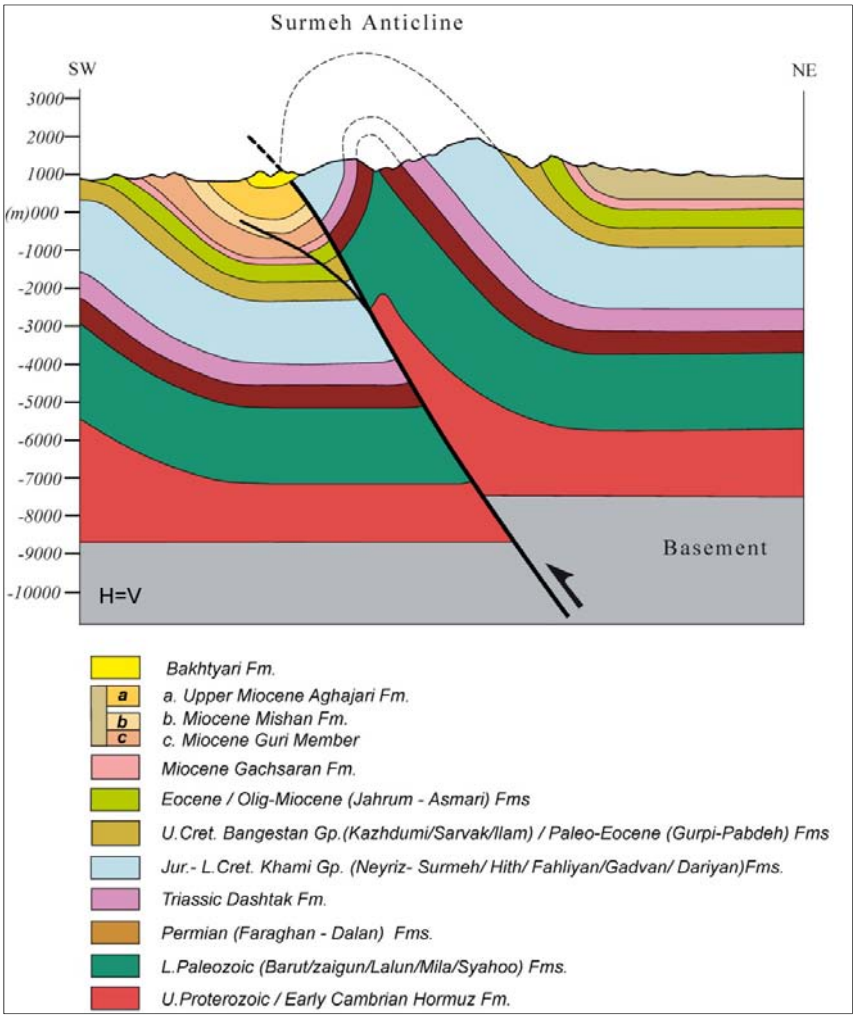

Fig.6. New structural section of the Surmeh anticline

3.2. Kinematics of the Surmeh anticline

Surmeh as a member of giant Fars anticlinal structures experienced a two-phase kinematic scenario. First, thin-skinned episode to which most likely a pre-existing Hormuz salt ridge localized the initiation of a detachment fold. Hormuz salt formation at the base of the sedimentary sequence responded in a ductile manner to the fold growth, with movement of material towards the core of the anticline from the adjacent synclines. Ongoing deformation led to accumulation of salt in core, amplification and tightening of the structure by slip above this unit. Depletion of the ductile layers at the base of the synclines might block the growth of the anticline and favored the generation of a fault through the forelimb. Further deformation and tectonic forces from NNE implied the more tilting of the limbs, steepening and probably rupture of the southern one. This latter process was a critical period in the evolution history of the structure and cover deformation was considerably decreased since this time onward. The basement had been inactive at this stage and did not involve with the cover processes.

The final episode of the Surmeh structural deformation (thick-skinned phase) begins at this stage. In previous step, the crucial state of deformation concentrated the strain and subsequently allowed failure in the over-steepened zone of the southern flank. By this time, basement which has a rigid nature compare to the cover, behaved brittle and shortening accommodated a thrust within it. This fault eventually cut whole the sedimentary pile and overlying structures as an out-of-sequence thrust. Probably, a branch of this fault transfers the deformation from depth to the upper ductile horizons.

Thick-skinned phase in the Surmeh anticline was appeared prior to the sedimentation of Bakhtyari formation, because this unit hide the surface expression of the basement thrust fault.

ANNEX N° 2

Paper in press (in Tectonics)

Evidence for Late Devonian vertical movements and extensional deformation in Northern Africa and Arabia

-Integration in the geodynamics of the Devonian world-

Dominique Frizon de Lamotte*, **, Saeid Tavakoli-Shirazi*, *, Pascale Leturmy*, Olivier Averbuch****, Nicolas Mouchot*, Camille Raulin*, François Leparmentier**, Christian Blanpied** and Jean-Claude Ringenbach*****

** Univ. Cergy-Pontoise, Dept. Géoscience & Environnement, F95 000 Cergy-Pontoise, France.*

*** TOTAL EP, Projets Nouveaux, place Jean Millier, F92 400 Paris-La Défense, France.*

**** NIOC, Exploration Directorate, Geology Dept., Seoul Ave, P.O. Box 19395-6669, Tehran, Iran.*

***** Univ. Lille I, UMR Geosystèmes, 59655 Villeneuve d'Ascq cedex, France*

****** TOTAL EP, Département d'interprétation structurale et sédimentaire, CSTJF, Av. Larribeau, F64 000 Pau, France*

Abstract:

The Upper Paleozoic geodynamic evolution is discussed at the scale of a wide part of Gondwana from North Africa to Arabia. With the aim of giving an integrated tectonic scenario for the study domain, we revisit six key areas namely the Anti-Atlas Belt (Morocco), the Bechar Basin (west Algeria), the Hassi R'Mel High (Central Algeria), the Talemezane Arch (south Tunisia), the Western Desert (Egypt) and finally the High Zagros Belt (Iran). Below the so-called "Hercynian unconformity", which is in reality a highly composite discontinuity, surface and subsurface data display a well-known Arch-and-Basin geometry, with basement highs and intervening Paleozoic basins. We show that this major feature results mainly from a Late Devonian event and can no longer be interpreted as a far effect of the Variscan Orogeny. This event is characterized by a more or less diffuse extensional deformation and accompanied either by subsidence, in the western part of the system, or by an important uplift of probable thermal origin followed by erosion and peneplanation. By the end of the Devonian, the whole region suffered a general subsidence governed by the progressive cooling of the lithosphere. Such a primary configuration is preserved in Arabia with typical sag geometry of the Carboniferous and Permian deposits but strongly disturbed elsewhere by the conjugated effects of the Variscan Orogeny during the Carboniferous and/or by subsequent uplifts linked to the Central Atlantic and Neo-Tethys rifting episodes. In conclusion, we try to integrate this new understanding in the geodynamics of the Late Devonian, which, at world scale is characterized by the onset of the Variscan orogeny on the one hand and by magmatism, rifting and basement uplift on the other hand.

Key words: *North Africa, Arabia, Late Devonian, Uplift, Subsidence, "Hercynian Unconformity".*

1. Introduction

In tectonic studies, long distance correlations allow distinguishing parochial events of local interest from regional or even global events significant at larger scale. In a given basin or mountain belt, they also permit to highlight important events hidden by the complexity of the local geology. According to such a hierarchical system, our chief purpose is to correlate tectonic events occurring in northern Gondwana during the Late Paleozoic.

The area studied here corresponds to a wide domain (8.000 x 2.000 km^2) covering the whole Sahara and Arabia and extending from Central Atlantic to the Arabian Sea (Fig. 1). The Mesozoic and Cenozoic history of this domain is currently well-known (see a review in Frizon de Lamotte et al., 2011). Two main geodynamic processes can be recognized: (1) the break-up of Pangea and the subsequent opening of both Alpine Tethys and Neo-Tethys Oceans north of Western Africa and Arabia respectively and (2) the progressive closure of these Oceans initiating by the late Cretaceous and leading to the development of different orogenic systems. North of the Western Sahara is the Atlas Belt; north of Arabia is the Zagros Mountain Belt (Fig. 1). In between the Eastern Mediterranean Sea is considered as a vestige of the Tethys margin not yet subducted below the Mediterranean ridge. By contrast, the Paleozoic history, topic of the present paper, remains poorly understood. We will focus on the Upper Paleozoic (Devonian to Permian) for which we are able to propose an unsuspected tectonic agenda.

As many intra-continental domains, the interior Paleozoic platform of the Sahara Domain (e.g. Boote et al., 1998; Craig et al., 2008; Galeazzi et al., 2010; Eschard et al., 2011) and Arabia (e.g. Konert et al., 2001; Johnson, 2008; Faqira et al., 2009) presents a common architecture with a series of broad “Basins” and intervening “Arches”, which are sometimes segmented by “Saddles” (Fig. 2). The tectonic motif involves E-W (Regibate, Talemzane, Gargaf…) and NNE-SSW (Tibesti-Sirt, Levant, Central Arabian…) Arches (Fig. 2).

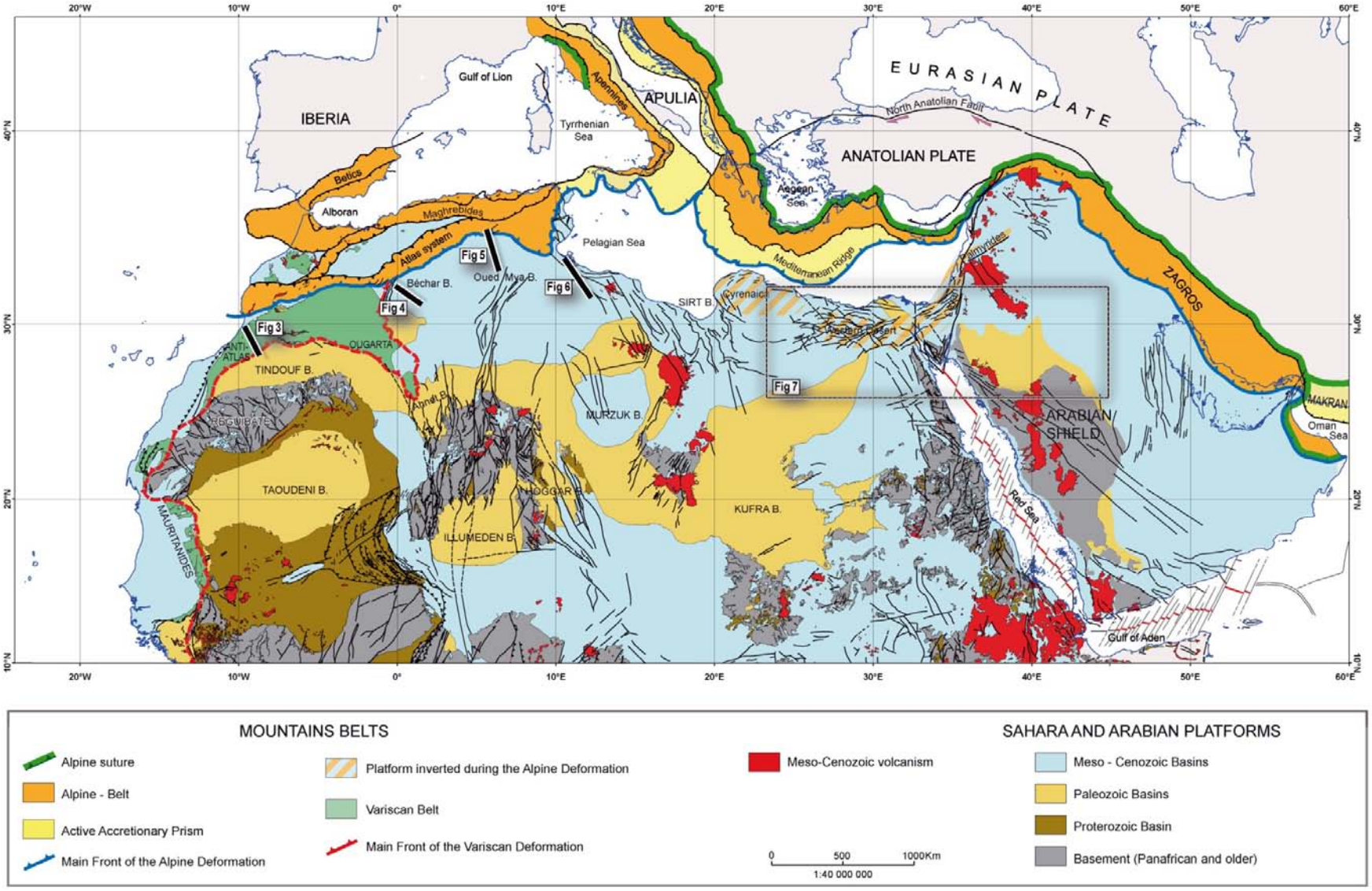

***Fig.1**: The current structural context of the South Tethys Domain with the position of the Precambian massifs and Proterozoic, Paleozoic and Meso-Cenozoic basins. The map is modified from Frizon de Lamotte and Raulin (2010) and Frizon de Lamotte et al. (2011).*

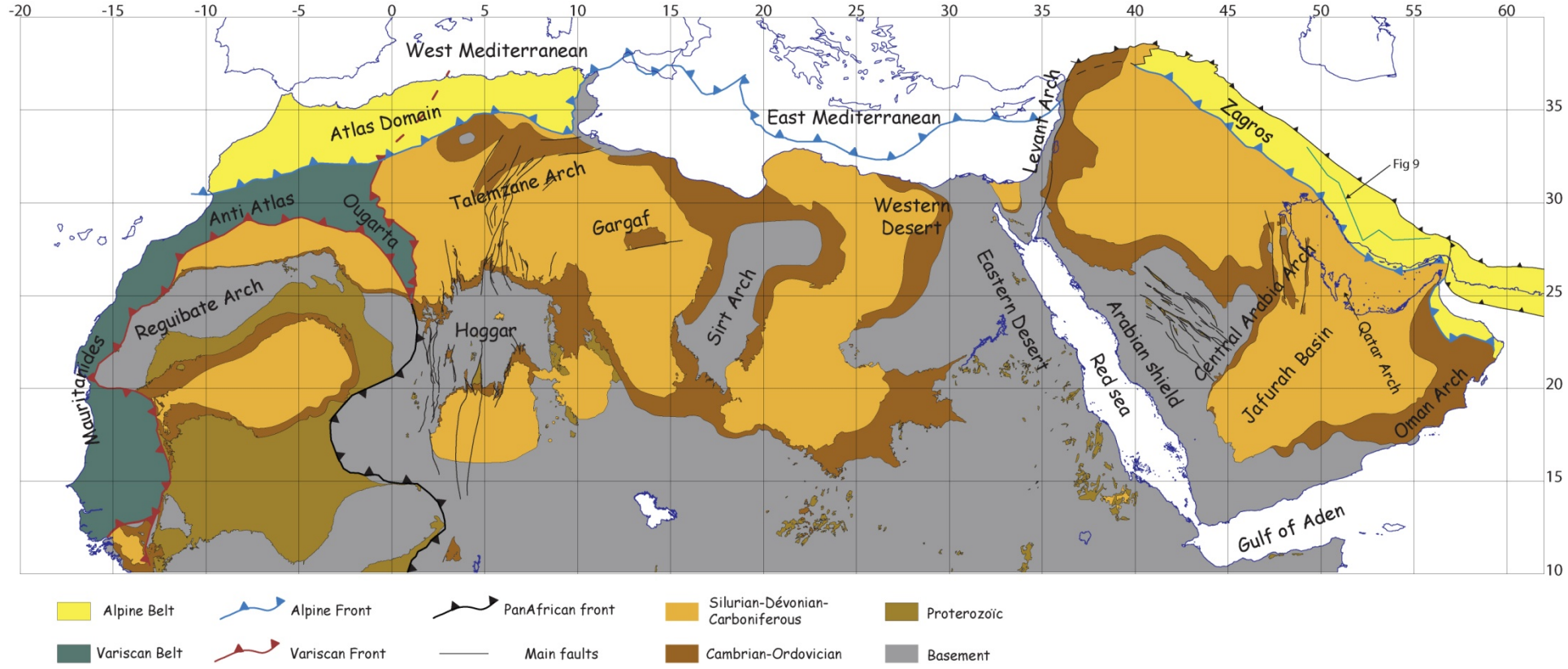

Fig. 2: *Simplified subcrop map of the Sahara and Arabia domains beneath the "Hercynian unconformity" showing the major arches and intervening Paleozoic basins as well as the Variscan and Alpine tectonic fronts. The map is based on data in Boote et al. (1998) and Frizon de Lamotte and Raulin (2010) for North Africa and from Konert et al. (2001), Faqira et al. (2009) and Total data for Arabia. Note that the « Hercynian unconformity" is a composite discontinuity having different significances (see explanations in the text).*

The origin of this “Arch and Basin” geometry remains enigmatic. It is frequently acknowledged that the arches are inherited from early Paleozoic structural events and strongly uplifted during the late Carboniferous as a more or less far-field effect of the Variscan (Hercynian) Orogeny (Boote et al., 1998; Konert et al., 2001; Craig et al., 2008; Dixon et al., 2010). However, at the scale of the studied area, the Variscan belt exists only in the northwestern part of the African continent. South of the Cenozoic Atlas system, it constitutes the Mauritanides Belt (Le Goff et al, 2001; Villeneuve et al., 2005) along the coast of the Central Atlantic Ocean. Away from the Atlantic shoreline, the Anti-Atlas Belt (Burkhard et al., 2006) in southern Morocco and the Ougarta Range in Western Algeria (Hervouet & Duée, 1996; Ghienne et al., 2007) constitute Variscan foreland fold-thrust belts (Figs. 1 and 2). North of the South Atlas Front, rock units deformed during the Variscan orogeny are cropping out in part of the High Atlas Belt, in the Moroccan Western and Eastern Mesetas and in the Algerian High Plateaus. The correlation of these Moroccan Variscides with the European Zones remains controversial (e.g. Simancas et al., 2008; Michard et al., 2010). However, the authors agree to consider that the Late Carboniferous Variscan front, which is exposed at Bechar in Western Algeria, is hidden at depth below the Sahara Atlas and the Tell Cenozoic Orogenic systems (Fig. 1).

In the Anti-Atlas, Wendt (1985), Baidder et al. (2008) and Michard et al. (2008) put forward an important extensional event during the Late Devonian. For Wendt (1985), this event corresponds to a major foundering and even “disintegration” of the northwestern Gondwana margin prior to the Variscan orogeny. Subsequently, Wendt et al. (2006) recognize a “basin and ridge system” developed during the Middle and Late Devonian in the Ahnet and Mouydir Basins, located north-west of the Hoggar Massif (Fig. 1). Eschard et al. (2011), emphasize the poly-phased evolution of several “paleohighs” (arches) situated in eastern Algeria and Libya before a complete reorganization occurring during the Late Devonian. In line with these papers, the main aim of this paper is to show that Devonian extensional deformation accompanied by important vertical movements (subsidence or uplift) exists everywhere in the study area and is at least partly responsible for its Arch-and-Basin geometry.

Another aspect is to distinguish the effects of this deformation from the subsequent ones due to the Variscan Orogeny and the rifting episodes occurring during the break-up of Pangea by the end of Paleozoic times. For the purpose of our demonstration, we will present some key areas illustrating the different geometric configurations found in Northern Africa and Arabia respectively. We will start in the western part of this wide domain, where the Variscan Belt settles and then we will follow an eastward path towards the Arabia and the Zagros Mountains (Iran), where the effects of the Variscan deformation are likely less important or even imperceptible. Afterward, we will discuss how it is possible to integrate these new data and interpretation in the worldwide events occurring in the Late Devonian.

2. Evidence for a late Devonian extensional deformation in Northern Gondwana.

We present below an analysis of the vertical movements in six particular regions located at short distance outside the front of the Alpine Belt (Fig. 1). The time span considered includes the Late Paleozoic and the Early Mesozoic.

2.1 The Anti-Atlas Belt (Morocco)

Situated south of the High Atlas, the Anti-Atlas is basically a Variscan fold-belt (Burkhard et al., 2006). However, due to a Neogene thermal uplift and related erosion (e.g. Missenard et al., 2006) it is currently elevated at a mean altitude of about 1000m (even 1500m in its central part; Guimerà et al., 2011) and presents vast exposures of Precambrian and Paleozoic rocks. Above the Pan-African Basement, which crops out in several inliers, the Paleozoic cover presents an overall thickness of 8km (western Anti-Atlas) to 4km (eastern Anti-Atlas) of shallow marine sediments (Michard et al., 2008; 2010).

The stratigraphic record of the Anti-Atlas reveals a very regular subsidence with two steps of collapse in the 540-500 Ma and 380-360 Ma time intervals (Burkhard et al., 2006) (Fig. 3). The first period corresponds to the Early Cambrian and can be correlated with a rifting episode accompanied by a magmatic suite of alkaline volcanic rocks (Soulaimani et al., 2004). The second period corresponds to the Late Devonian and is characterized by the development of platform and basin topography in a diffuse extensional context (Wendt, 1985; Baidder et al., 2008). In

view of its multidirectional extensional nature, Baidder et al. (2008) determined N-S to NW-SE direction of extension in the eastern Anti-Atlas. This deformation cannot be directly related to the Eo-Variscan (or neo-Acadian in the Appalachians) compressive events known in Europe and North America (e.g. Matte, 2001; Averbuch et al, 2005; Faure et al, 2008; Van Staal et al, 2009) and postulated in the western (Echarfaoui et al., 2002) and eastern (see review in Michard et al., 2010) Mesetas of Northern Morocco.

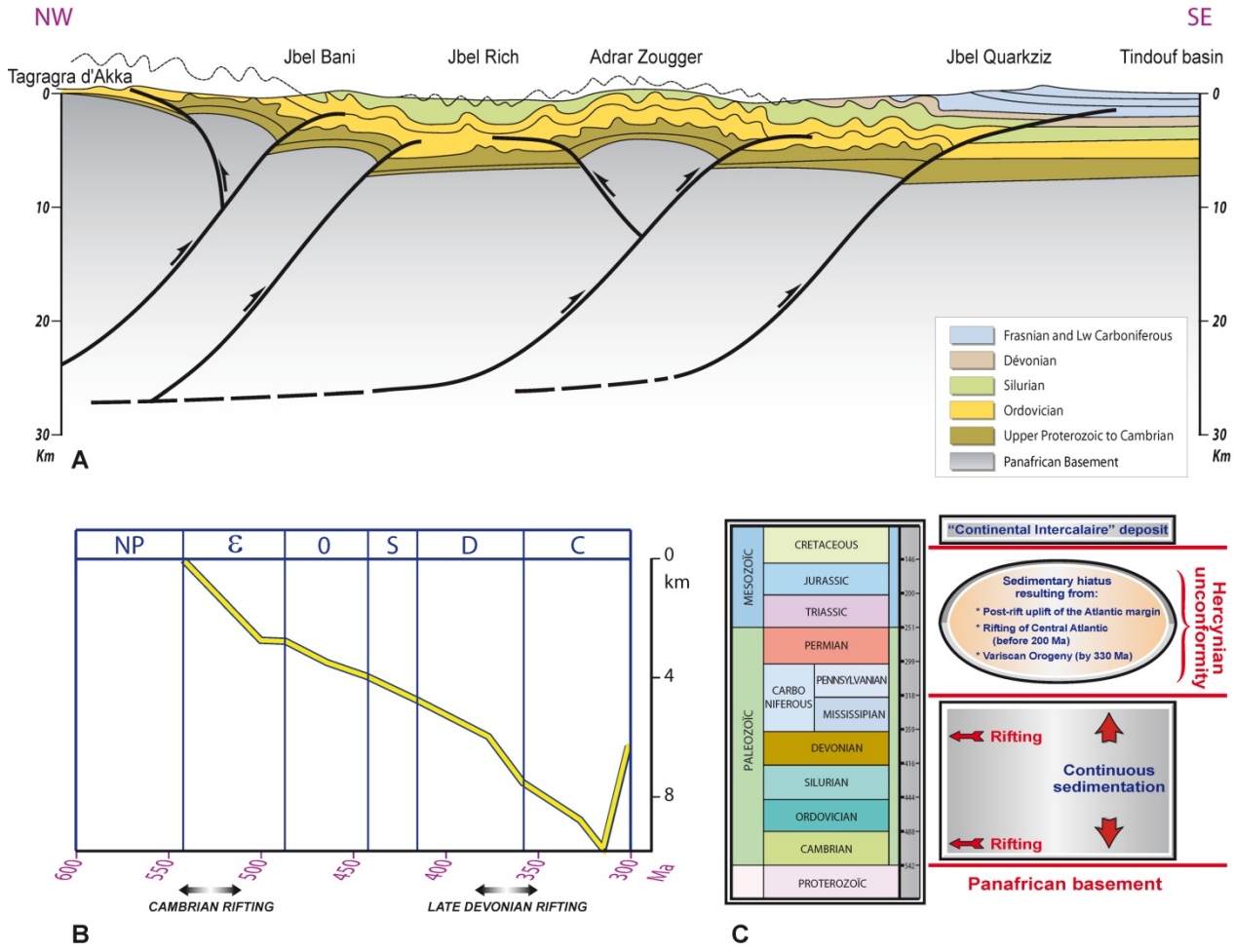

Fig. 3: *The structural context of the Anti-Atlas (Morocco). -A- Generalized cross-section illustrating the structural style of the Anti-Atlas Variscan Belt (modified from Burkhard et al., 2006), see location on figure 1. -B- Curve showing the thickness of sediment accumulation (vertical axis) through time (horizontal axis) in the western Anti-Atlas (modified from Burkhard et al., 2006). Note the two rifting episodes, Lower Cambrian and Late Devonian respectively, recorded by an increase of the sedimentation rate.*

Recent fission-track dating on zircon (Sebti et al., 2009) show that the maximum temperature of the basement, interpreted as the maximum burial, has been reached at 320 Ma (Late Mississipian). The subsequent uplift and related erosion are the direct consequence of the Late Carboniferous (early Pennsylvanian) compressive deformation responsible for the formation of the Anti-Atlas fold-belt. Such timing is consistent with the accumulation of continental molasses occurring at the same time in the adjacent Tindouf and Bechar foreland basins (Fabre, 2005).

There is no record of Permian to Jurassic sediments in the Anti-Atlas domain. On the basis of thermochronologic data (fission track and U-Th/He ages on apatite and zircon; Ruiz et al., 2011), this considerable hiatus is interpreted as the result of a protracted uplift until the Early Cretaceous. At that time clastic sediments (the so-called “continental intercalaire”) were deposited. They are topped by marine carbonate of Cenomanian to Turonian age. So during about 200 Ma (from 330 Ma to 120 Ma), the Anti-Atlas domain suffered a long-term trend of denudation following a *c.a.* 220 Ma long period of slow and continuous subsidence from 540 Ma to 320 Ma. Such a long uplift tendency (Ruiz et al., 2011; Oukassou et al., *in press*) is clearly not the result of the Variscan (Hercynian) deformation alone. Several geodynamic events, including the rifting during the Middle and Late Triassic (before 200 Ma) and then the spreading (by 175 Ma) of the Central Atlantic Ocean, occurred just west of the Anti-Atlas. Following modeling by Gouiza (2011), the evolution of the Central Atlantic passive margin alone cannot explain the Upper Jurassic-Lower Cretaceous uplift of the Anti-Atlas. An additional thermal effect is required as in the western part of the Atlas system (Frizon de Lamotte et al., 2009).

2.2 Bechar Basin (Algeria)

The Bechar Basin is located in a triangle between the eastern front of the Ougarta Range and the southern front of the Sahara Atlas (Fig. 1). By reference to the Variscan orogen, the Bechar Basin is in the situation of a foreland basin (Fabre, 2005) filled by an important thickness of Carboniferous sediments. However, a NW-SE seismic line across the basin reveals a more complex configuration (Fig. 4) with a thick “Carboniferous” basin resting unconformably on a set of tilted blocks. Both are affected by Variscan folds and are sealed by tabular Lower Jurassic strata (the “Hercynian unconformity”). The particularly important thickness of the Carboniferous

results likely from two successive effects: a post-rift thermal subsidence during the Lower Mississipian followed by a flexural subsidence up to the Pennsylvanian. Using the thicknesses given by Fabre (2005) and the timing of the Variscan deformation in the area, we can propose that about 1000m of sediments accumulated during the first step and about 2800m during the second one.

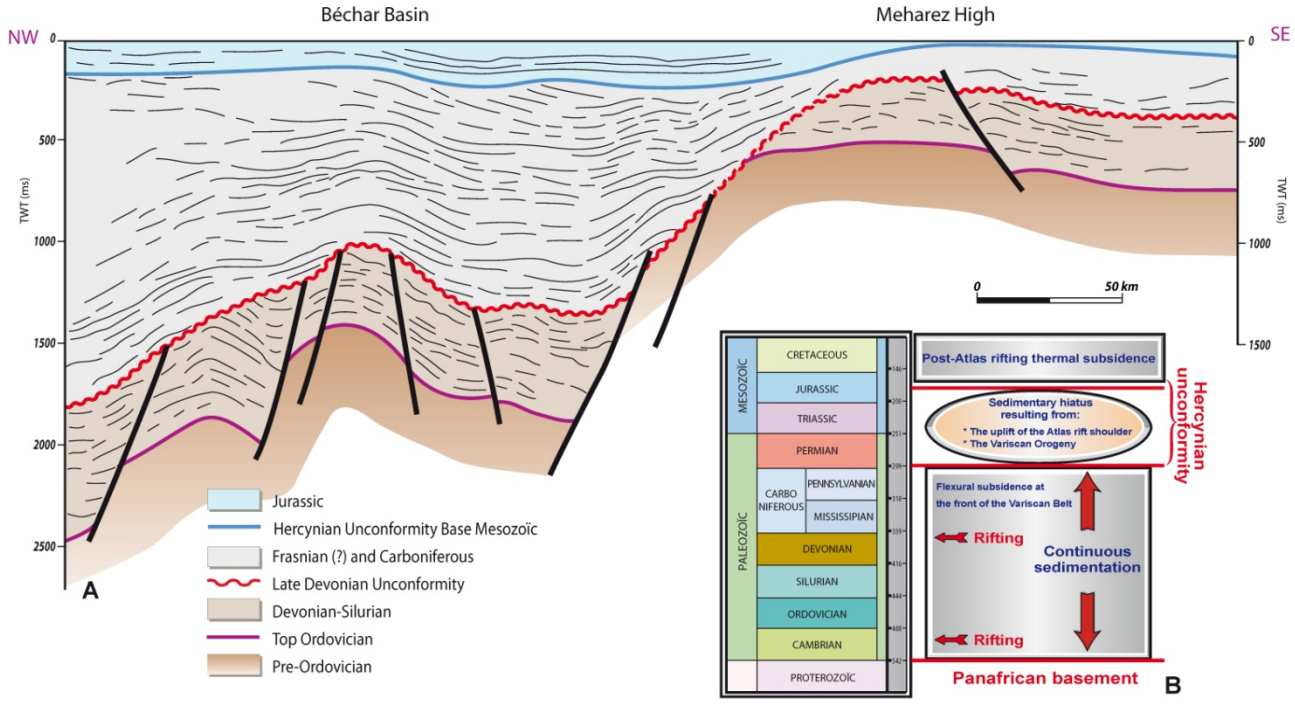

Fig. 4: *The structural context of the Bechar Basin (Algeria). -A- Line-drawing illustrating the geometry of the Bechar Basin at depth (see location on figure 1); notice that the tilted blocks at depth were folded during the Variscan Orogeny together with the Upper Devonian (?)-Carboniferous infilling of the Bechar Basin. -B- Schematic diagram synthesizing the tectonic history of the Bechar Basin during the Paleozoic and Mesozoic.*

The Bechar basin terminates abruptly to the SW along the Meharez High, which has been successively an eroded rift shoulder and a flexural fore-bulge upon which the Upper Carboniferous levels are on-lapping. There is no direct calibration (absence of bore-holes) of the age of the strata located at depth in the Bechar Basin. The Upper Devonian (top Frasnian?) age of the post-rift unconformity could be proposed by comparison with the Anti-Atlas on the one hand and from the Meharez High bore-holes on the other hand.

If correct, subsurface data allows us to revisit the classical interpretation of the Bechar Basin as a simple foreland basin and to show that it was initiated as a sag basin post-dating a Devonian rifting episode. This new interpretation questions the age of the tilted blocks observed by Robert-Charrue and Burkhard (2008) on the north-south ONAREP RS 08 seismic-line crossing the Tafilalt (easternmost part of the Anti-Atlas). The authors propose a Triassic age by reference to the rifting occurring at that time in the Atlas system. According to our observation in Bechar and in line with Baidder et al. (2008) and Saddiqi et al. (2011), we rather suggest a Late Devonian event. It is worth noting that Permian and Triassic deposits are lacking in Bechar suggesting that this region has been uplifted during this about 100 Ma-long period. This uplift could be the combined effect of two successive events: (1) the Late Carboniferous Variscan orogeny and (2) the Atlas rifting, which occurred in two successive steps during the Triassic and Early-to-Middle Jurassic respectively (see a review in Frizon de Lamotte et al., 2009). Referring to the Atlas Rift, subsequently inverted to form the Atlas Belt, the Bechar region was in the position of a rift shoulder (Fig. 1). So the unconformity located at the bottom of Jurassic beds stacks the effects of at least two different tectonic events. Its usual name, “Hercynian Unconformity”, is not completely appropriate.

2.3 Hassi R’Mel area (Algeria)

Hassi R’Mel is located at about 100km south of the southern front of the Sahara Atlas in a region characterized by a thick Mesozoic cover (up to 3000m) forming the Oued Mya Basin (Fig. 1). Regarding the Paleozoic history, Hassi R’Mel belongs to one of the major arches segmenting the Paleozoic basins of the Sahara domain: the Talemzane Arch (Fig. 2). Its geometry at depth is well known thanks to a lot of exploration data. A major unconformity, generally called “Hercynian unconformity”, is located at the bottom of the TAGI (“Trias Argilo-Gréseux Inférieur”) formation of Middle Triassic age (Fig. 5). The deposition of the TAGI was preceded by a strong erosional truncation and peneplanation.

Along the northern flank of the arch, bore-hole data reveals the existence of Upper Carboniferous (Moscovian) strata sandwiched between Triassic and Silurian beds. From these data, it appears that the pre-TAGI unconformity observed on the crest of the dome merges two distinct unconformities: pre-Middle Triassic and pre-

Moscovian respectively. The geometry of normal faults cutting out the arch shows that basically the Talemzane Arch can be interpreted as an ENE-WSW to E-W trending horst (Fig. 5). Despite evident reactivations during subsequent Mesozoic rifting episodes and Cenozoic Atlas building, it seems that the main step of the Arch building was achieved before the Moscovian and resulted from important extensional deformation.

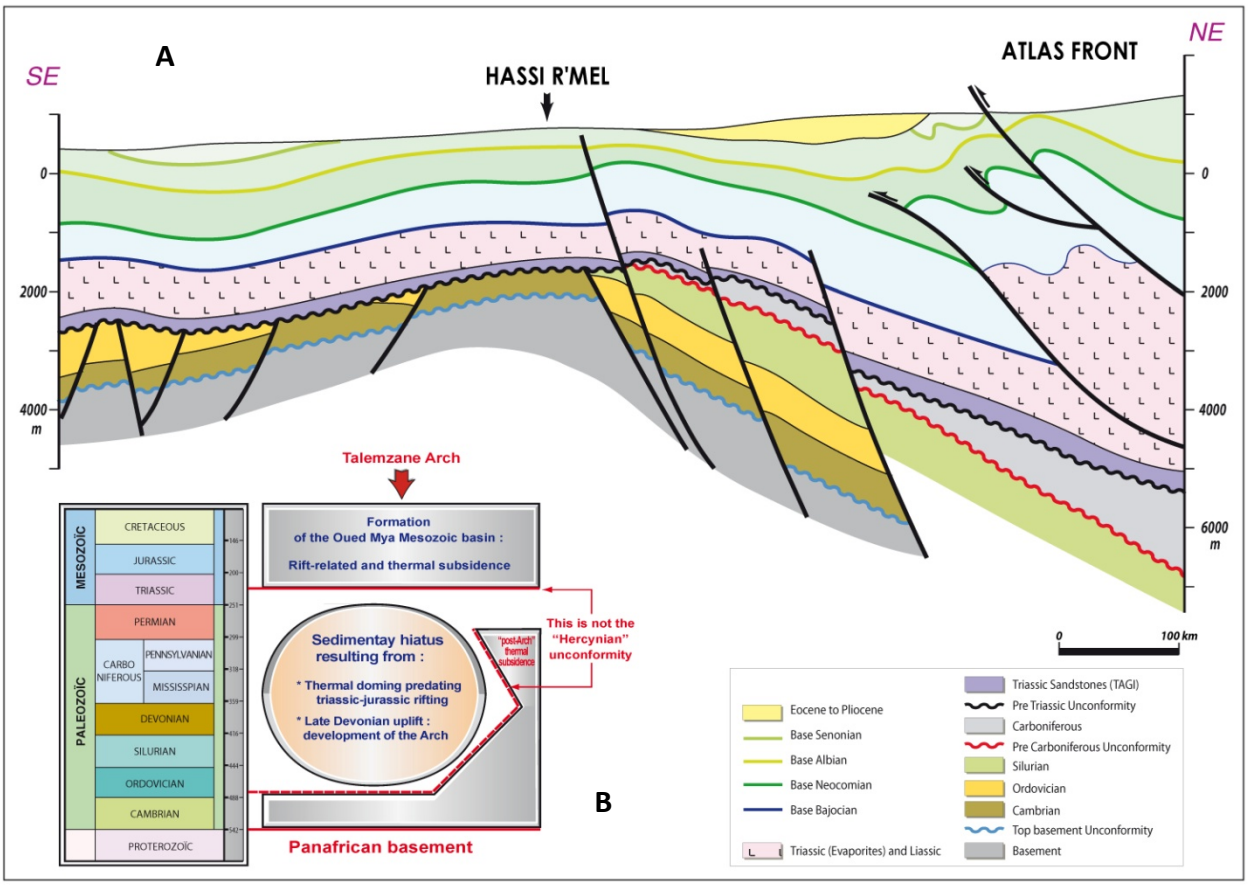

Fig. 5: *The structural context of the Hassi R'Mel area (Talemzane Arch, Algeria). -A- Composite section from Total data (see location on figure 1); the section underlines the existence of two major unconformities beneath and above the Upper Carboniferous deposits. On top of the Arch these two unconformities are stacked together. There is no clear evidence of Variscan compressive deformation in the area, so none of the unconformities really corresponds to the "Hercynian unconformity". -B- Schematic diagram synthesizing the tectonic history of the Hassi R'Mel area during the Paleozoic and Mesozoic.*

At local scale, the age of this post-Silurian and pre-Moscovian extensional deformation cannot be precisely assigned. However, given the regional geology

(Galeazzi et al., 2010), we know that the Carboniferous sequence is more complete laterally down to the so-called “Strunian unconformity” (i.e. base Carboniferous).

By reference to what has been shown in the Anti-Atlas and Bechar areas, we assume that the Talemzane Arch was already built at the end of Devonian times. If correct, the uppermost Devonian and Carboniferous could have deposited in post-rift sag basins flanking the Arch to the north and south respectively and the onlap geometry of post rift strata could explain that the Upper Carboniferous rests directly on Lower Paleozoic beds (Fig. 5).

The absence of Permian, known more to the east in the Jaffarah (see below), is a puzzling question. This hiatus could correspond either to no-deposition or to pre-Middle Triassic erosion. In the first case, the Talemzane Arch must be considered as a permanent high since the Late Devonian. In the second case, we have to consider an uplift rejuvenation before the deposition of the TAGI. Because of the absence of contractional deformation, this second episode of uplift cannot be easily interpreted as an effect of the Variscan orogeny. We rather suggest a doming pre-dating a Triassic-Jurassic new rifting episode responsible for the formation of the Oued Mya Basin (Boudjema, 1987).

In fact, the deposition of the Mesozoic sequence is clearly controlled by normal faulting, which developed up to the Middle Jurassic, and then by thermal subsidence (Fig. 5). This Triassic to Middle Jurassic rifting episode (Boudjema, 1987) can be easily correlated with the rifting observed in the Atlas System (Frizon de Lamotte et al., 2000, 2009) and, more generally, along the southern margin of the Tethys realm (Frizon de Lamotte et al., 2011). In the absence of contractional deformation, the term “Hercynian Unconformity”, used to designate the discontinuity at the bottom of the Mesozoic basin is confusing.

2.4 Talemzane Arch, Jaffarah (Tunisia, Libya)

The Jaffarah domain is located along the southern coast of the Pelagian Sea, element of the East Mediterranean margin of the Neo-Tethys realm (Fig. 1). As Hassi R’Mel, the Jaffarah domain belongs to the Talemzane Arch but in a domain located more to the east (Fig. 2). The Jaffarah is important because it exposes, at Tebaga of Medenine, the only Permian marine sediments in North Africa (Berkaloff,

1933; Mathieu, 1949; Bouaziz, 1995). This thick sequence of Permian sediments (more than 4000m thick at TB1 bore-hole) has been interpreted by Stampfli et al. (1991; 2001) as syn-rift. However, as indicated by the authors, this interpretation was done without access to relevant reflection seismic data. Thanks to the access to such data, we are able to illustrate a different configuration (Fig. 6).

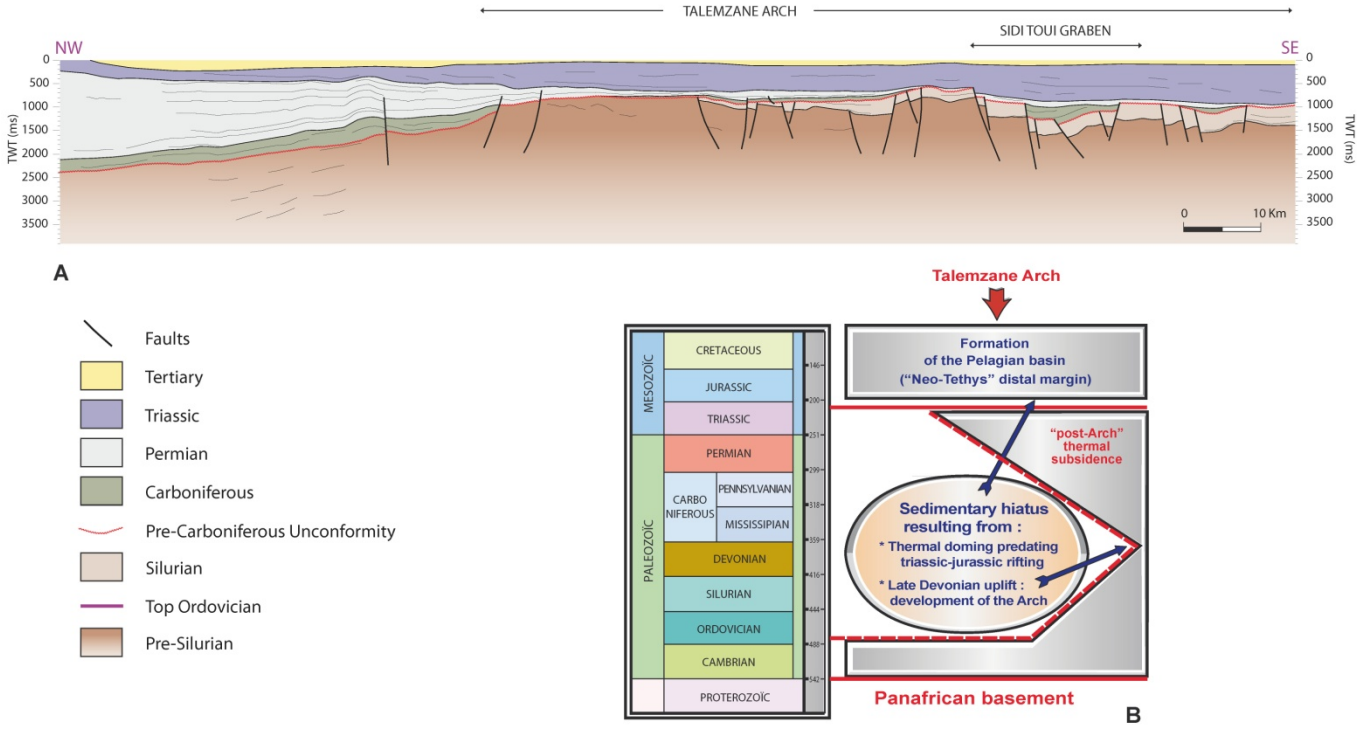

Fig. 6: *The structural context of the eastern Talemzane Arch [Jaffarah (Tunisia, Libya)]. -A- Line-drawing illustrating the geometry of the Talemzane Arch in southern Tunisia (see location on figure 1); -B- Schematic diagram synthesizing the tectonic history of the Talemzane Arch in Southern Tunisia during the Paleozoic and Mesozoic.*

The Carboniferous, Permian and Lower Triassic deposits form a huge sequence cut out by few normal faults but without important unconformities; except at the apex of the Arch where a small Carboniferous graben (Sidi Toui Graben) and a Permian fault are exposed (Fig. 6). At large scale, Carboniferous and Permian deposits display together a southward thinning and "onlap" geometry toward the top of the Talemzane Arch. At the bottom of this thick package a major unconformity seals most of the normal faults and small tilted blocks confined within the Lower Paleozoic and the underlying Pan-African basement. As at Hassi R'Mel, neither the Devonian nor the Lower Carboniferous (Tournaisian, Visean) have been reported.

Such geometry could result either from no deposition during Devonian and Lower Carboniferous or from subsequent erosion. Given the regional geology (Galeazzi et al., 2010) and given the arguments developed above, we favor the existence of important Late Devonian erosion before the deposition of the Carboniferous strata.

From these data, it appears that the interpretation of a major Permian episode of rifting proposed by Stampfli et al. (1991; 2001) and by Stampfli and Borel (2002) cannot be easily maintained. The geometry of the Carboniferous-Permian basin mimics a sag basin resting on tilted blocks of possible Devonian age. Consequently, as at Hassi R'Mel, we assume the fundamental horst status of the Talemzane Arch. After the Devonian uplift and normal faulting, the region suffered an important thermal subsidence accounting for the deposition of Lower Carboniferous to Middle Triassic deposits on-lapping the Arch.

Another regional unconformity, located at the bottom of the Upper Triassic, marks, as already suggested by Dixon et al. (2010), the true onset of the Neo-Tethys rifting. According to Soussi (2002) and Raulin et al. (2011), this rifting lasted up to the Middle Jurassic. As indicated by Raulin et al. (2011), the Jaffarah was at that time located in a very proximal part of the Neo-Tethys margin. The distal part is presently located at depth in the Pelagian Sea and separated from the Jaffarah by an important fault zone (Jongsma et al., 1985; Klett, 2001; Frizon de Lamotte et al., 2011).

2.5 Western Desert (Egypt), transition with the Levant

As the Jaffarah area, the Western Desert is situated in the proximal margin of the East Mediterranean Sea (Fig. 1). More precisely, it corresponds to E-W to ENE-WSW early Mesozoic horsts and grabens (Mahmoud and Barkooly, 1998) forming the south-western end of the Levant margin, slightly inverted in Late Cretaceous and Middle Eocene (Bosworth et al. 2008). The organization of Paleozoic units is at almost right angle to the Mesozoic one: the thicker deposits, forming the so-called Ghazalat-Tehenu Basin, are located between two N-trending Arches (Keeley and Massoud, 1998) (Figs. 2 and 7). To the west is the Sirt High, situated on the site of the present Sirt Basin. To the east is the Nubian Shield the African counterpart of the Arabian shield (Figs. 1 and 2). The whole system is deeply truncated by a post-

Permian and ante-Triassic unconformity post-dating an important phase of uplift and erosion. As elsewhere in the Sahara domain, this unconformity is called “Hercynian Unconformity”. However, it is worth noting that it is considerably younger than the Hercynian events known more to the west and that there is no evidence of contractional deformation sealed by it. On the contrary, only normal faults are observed at depth. It is the reason why, we consider that the post-Permian uplift may be related to a doming preceding the Neo-Tethys rifting, which developed in the region during the Triassic to Jurassic (Keeley, 1994; Guiraud et al., 2005; Bosworth et al., 2008).

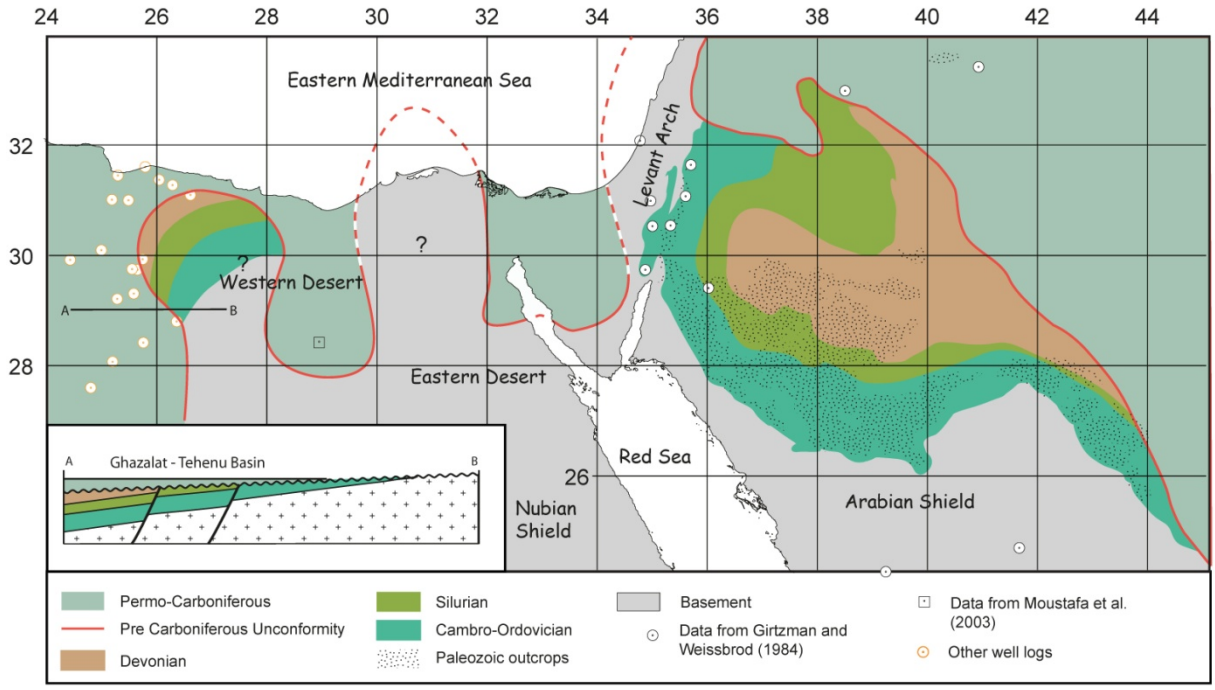

Fig. 7: *Subcrop map beneath the Meso-Cenozoic deposits illustrating the geometry of the Paleozoic basin in Western Desert and Levant regions. The map is modified from Gvirtzman and Weissbrod (1984) for the eastern part and constructed from bore-holes data in the western part. The schematic not-to-scale cross-section illustrates the postulated geometry of pre-Carboniferous deposits at depth.*

Keeley (1989) recognized an important “End Devonian” unconformity marking a change in the dynamics of the Ghazalat-Tehenu Basin. Due to the importance of the post-Permian, pre-Triassic erosion, the initial relationships of the Carboniferous-Permian deposits with their substratum have been frequentely erased. However, some boreholes located along the eastern flank of the basin show Carboniferous

strata (Visean) resting directly on the Lower Paleozoic in a manner reminding the features observed along the Talemzane Arch. From these data, we are able to produce a map showing the two main arches of the area with the onlap of Carboniferous and Permian deposits onto older rocks (Fig. 7).

This pre-Carboniferous unconformity, which is observable in the field south of the Sinai (Beyth, 1981; Weissbrod, 1980), has been also reported by Gvirtzman and Weissbrod (1984) on top of the “Hercynian Geanticline of Helez” now called “Levant Arch” (Faqira et al., 2009), which prolongs the Arabian-Nubian shield northward along the Levant margin of the Mediterranean Sea (Fig. 2). Gvirtzman and Weissbrod (1984) suggest that this structure results from a “short and strong pulse of uplift” occurring prior to the Carboniferous. The net result should be the truncation and erosion of sediments down to the Precambrian basement.

This interpretation is confirmed by Kohn et al. (1992) who indicate, in the same area, the existence of a “major Late Devonian or Early Carboniferous thermotectonic event” responsible for uplift and huge erosion. Using Zircon fission tracks (ZFT) of 17 Precambrian samples from deep boreholes and outcrops, these authors got 330-370 Ma ages. Following Kohn et al. (1992), these ages show: (1) a total resetting of zircon fission tracks clocks (temperature required: 225 +/- 50°C); (2) a Late Devonian/Early Carboniferous age for the exhumation (and related erosion); (3) a probable high thermal gradient (about 50°C/km) before the exhumation. The data obtained by Vermeesch et al. (2009) on Cambrian sandstone from southern Israel reinforce this interpretation. First of all, these authors got similar ZFT age (380 Ma) but they also notice that this age coincides with existing Rb-Sr age from authigenic clays (365-381 Ma). They conclude that the Late Devonian event, which is also at the origin of growth of authigenic apatite, is probably hydrothermal in nature. Late Devonian/Early Carboniferous ZFT ages were also found by Bojar et al. (2002) in the Nubian shield of the Eastern Desert (Egypt), which belongs to the same Arch.

Given these very important data and despite the absence of tectonic evidence allowing a discussion about the mechanisms, it seems clear that the thermal uplift evidenced in the Levant Arch can be more easily correlated with the pre-Carboniferous uplift event recognized in North Africa (see above) than as a far-field effect of the Variscan orogeny as it is generally postulated.

2.6 High Zagros Belt (Iran) in the frame of the Arabian plate

At the scale of the Arabian plate, the Paleozoic formations crop out in two specific areas: along the border of the Arabian shield and in the core of thrust-anticlines pertaining to the Iranian High Zagros Belt (Tavakoli-Shirazi et al., 2012) or to the Turkish Border folds (Ghienne et al., 2010); these two regions being close to the Alpine Suture Zone (Fig. 1). Elsewhere, except some small and scattered Paleozoic rocks exhumed with the Hormuz salt plugs in the Fars Arc (Eastern Zagros, Iran), they are only known by sub-surface data. In general, the Paleozoic is very deep and seismically rather transparent, except the bottom of Permian Carbonates of the Khuff Formation and its Iranian equivalent, the Dalan Formation (Szabo F. and Kheradpir, A. 1978; Insalaco et al., 2006).

One of the main features of the Arabian Plate is a regional unconformity occurring usually below the Unayzah Formation of Late Carboniferous age (Al-Laboun, 1988) and its lateral Iranian equivalent, the Faraghan Formation the age of which is assigned to be Early Permian (Ghavidel-Syooki, 2005). In the geological literature it is called “Hercynian Unconformity” since Gvirtzman and Weissbrod (1984), who mapped it in northwestern Arabia. This unconformity (Fig. 8) seals an “Arch-and-Basin” structure, analog to the one observed in North Africa (Konert et al., 2001) (Fig. 2). Recently, Tavakoli-Shirazi et al. (2012) show, through outcrops and bore-hole data correlations, that a similar geometry, reinterpreted as a large scale horst-and-graben structure, can be recognized in the Zagros Belt below the “Hercynian unconformity” (Fig. 9). Nevertheless, at the scale of the Arabian plate, the precise age of this unconformity is difficult to assign because of the frequent lack of Lower-Middle Carboniferous deposits, which are absent upon the arches but only preserved in lows situated in between, in particular in Syria (Brew et al., 2001). From a general point of view, this regional unconformity becomes angular only in the vicinity of the main Arches (Faqira et al., 2009).

Even if the so-called “Hercynian Unconformity” is now well illustrated in Arabia (Faqira et al., 2009), there are few data allowing a discussion about the nature of the deformation it seals. First of all we can notice that it occurred early in the Variscan chronology, somewhere between the Late Devonian and the Early Carboniferous at a time when no typical compressive deformation is known in the Gondwana

mainland (see above). Furthermore, in a recent work, Tavakoli-Shirazi et al. (2012) report evidence of post-Frasnian/pre-Permian extensional deformation in the High Zagros Belt (Iran). On this basis, the authors question about the cause of this deformation and put forward a model combining a large thermal uplift accompanied by a diffuse extensional deformation. The recent attribution of so-called "Chalki" volcanism of Iraq to the Late Devonian (Al Hadidy, 2007) is in agreement with this hypothesis.

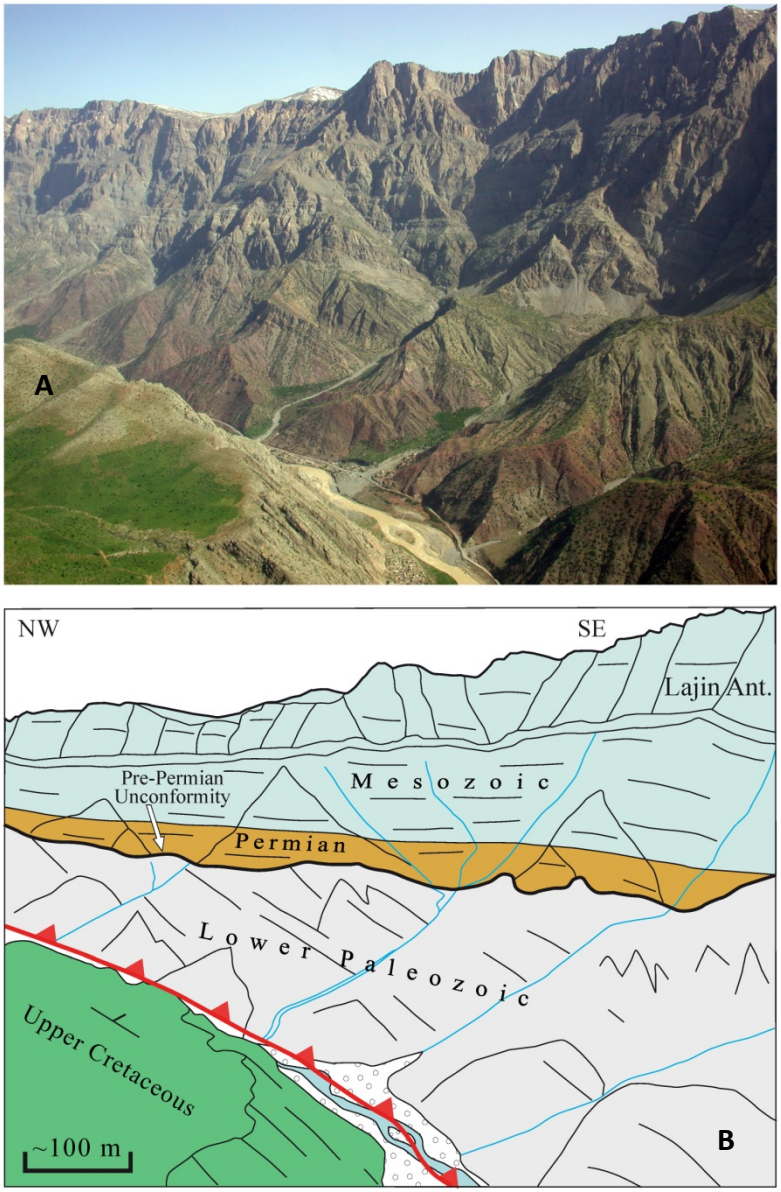

Fig. 8: *Photo from helicopter –A- and line-drawing –B- illustrating the general attitude of the "pre-Permian unconformity" in the Central High Zagros (Kue e Lajin, area; location on figure 9). The cliff is made up of a thick Permian to Cenomanian carbonate platform resting unconformably on Lower Paleozoic rocks (Cambrian and Ordovician). Both together are thrust over the Cretaceous beds exposed in the foreground.*

At the scale of the Arabian Plate, the geometry of Carboniferous-Lower Permian deposits, with thinning and pinching out towards the arches (Faqira et al., 2009), together with the Middle-Upper Permian carbonate platform of the Khuff-Dalan formation, which covers the whole system, evokes a sag basin. From this point of view, the observed geometry is identical to the one observed in North Africa, in particular in the Jaffarah where the Permian is well-developed. The main difference is that in the Arabian Plate in general and in the Zagros in particular, a thick Triassic-to-Turonian carbonate Platform developed conformably over the Permian (Fig. 8) indicating a slow but protracted subsidence without evidence of uplift linked to the Neo-Tethys rifting. By the Campanian, the flexuration of the Arabian plate in front of the proto-Zagros belt led to an acceleration of the subsidence in the NE part of the plate (Vergès et al., 2011; Saura et al., 2011), with no evidence of important uplift before the onset of Zagros collision at c.a. 35 Ma.

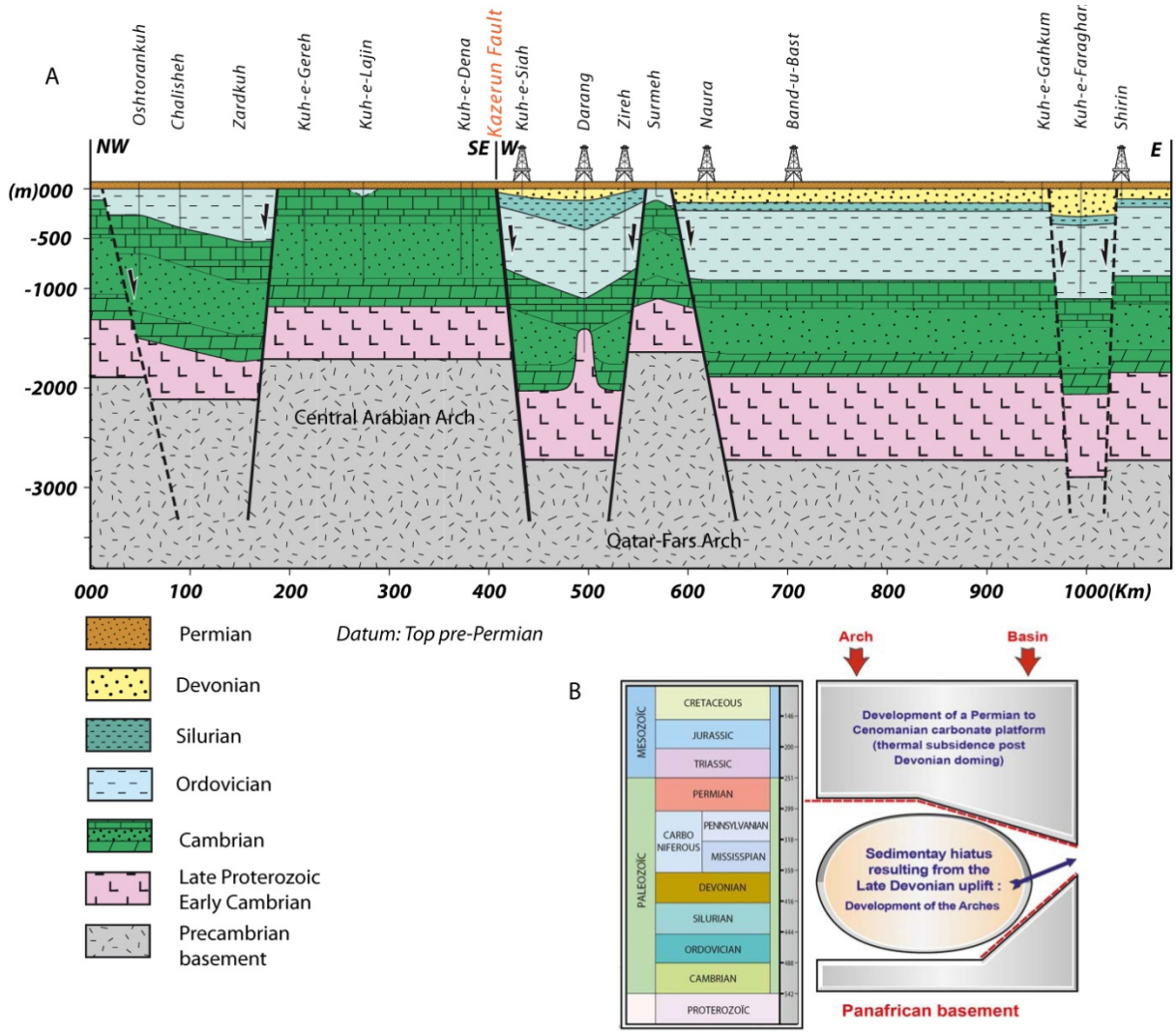

Fig. 9: *-A- profile of the pre-Permian « Arch-and-Basin » geometry in the Zagros area (modified from Tavakoli-Shirazi et al., 2012) (see the path of the correlation line on figure 2). An Arch, in the Central High Zagros, is separated from a Basin, in the Fars Arc, by the Kazerun Fault Zone. The Arch looks like an uplifted horst block located in the northward prolongation of the Central Arabian Arch (Fig. 2) whereas the Basin is located just north of the Jafurah basin (Fig. 2). A local "High", with a shorter wavelength, exists within the Basin, it could represent the northward continuation of the "Qatar Arch" (Fig. 2). Symmetrically, Ordovician outcrops on the western side of the Kazerun fault could localize a small depression (graben) in the core of the Central Zagros Arch. -B- Schematic diagram synthesizing the tectonic history of the Zagros Basin during the Paleozoic and Mesozoic.*

3. Discussion

After the presentation of key-areas, we propose to synthesize the main results at the scale of Northern Gondwana. Then, we will try to integrate the depicted evolution in a more general frame.

3.1 Extensive occurrence of Late Devonian vertical movements in the Sahara and Arabian domain, development of the "Arch-and-Basin" geometry, role of the subsequent deformation

The main result of our study is to show that a pre-Carboniferous, likely Late Devonian, unconformity exists everywhere in the northern Gondwana domain (Fig. 10). In the Anti-Atlas (Morocco) and in Bechar (Algeria), this unconformity is well calibrated and can be presented as a post-rift unconformity following a tectonic-induced subsidence controlled by normal faulting and block tilting during the Upper Devonian. Elsewhere in the study area, the unconformity follows a massive uplift associated with diffuse extensional deformation and subsequent erosion and peneplanation.

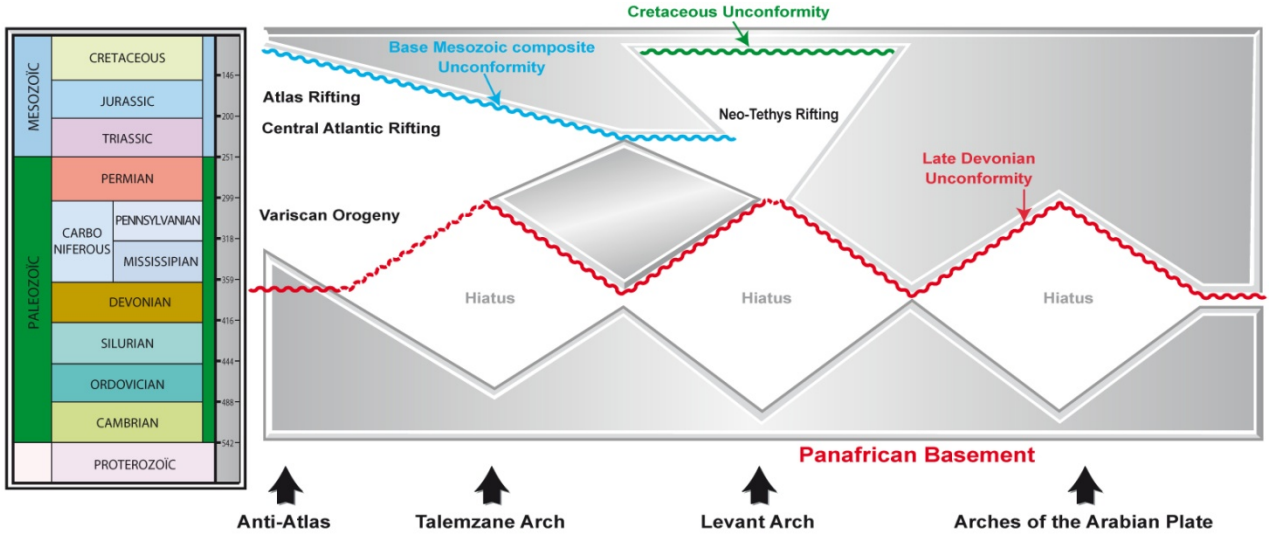

Fig. 10: *Schematic diagram synthesizing the tectonic history of the studied area during the Late Paleozoic and Mesozoic. The only unconformity that is general at the scale of the study area is the Late Devonian unconformity sealing the achievement of the Arch-and-Basin structure. This unconformity is incorrectly called "Hercynian" Unconformity in Arabia because it does not point out the same object than in Western Africa where a true "Hercynian" unconformity occurs on top of Carboniferous folds and thrust-faults (see explanation in the text). The hiatus developed subsequently (during the Mesozoic) correspond to uplifts related to the break-up of Pangea. They are particularly well expressed in the Anti-Atlas, along the Central Atlantic margin, and in the Levant, along the East Mediterranean Sea.*

We acknowledge that this period of uplift is, at least partly, responsible for the "Arch-and-Basin" geometry forming the concealed pattern of the studied area (Fig.

2). A variety of phenomena, occurring in different places of North Africa, allows us to extend the thermal uplift hypothesis already proposed for the Arabian domain (Kohn et al., 1992; Faqira et al., 2009; Tavakoli-Shirazi et al., 2012). In the Murzuk Basin, located east of the Hoggar (Fig. 1), Moreau et al. (2012), argue that massive sand injection in the form of pipes developed during the Devonian. The authors assume that the overpressures required for sand injection were triggered by a basin scale uplift associated with igneous intrusion in the Cambrian-Ordovician strata. Moreover, alkaline magmatism dated at 348 +/- 16 Ma is known in the Ordovician rocks fringing the Hoggar Massif to the south-east (Djellit et al. 2006). Following the same driving principle, the 378 +/- 17 Ma K-Ar ages obtained on clay by Bonhomme et al. (1996) in the Ougarta Range (Fig. 1) and interpreted as resulting from hydrothermal event call to mind the Late Devonian hydrothermal event proposed by Vermeesch et al. (2009) for the Levant region. So a set of convergent arguments suggest that, at the scale of the studied area, pre-Carboniferous uplifts were achieved by thermal doming associated with significant lithospheric thinning.

In Arabia, this Late Devonian event has been followed by a general subsidence allowing the deposition of clastic sediments during the Carboniferous and Early Permian then carbonate sediments during the Middle-Late Permian (at least in the eastern regions). The geometry of the Carboniferous and Permian basins strongly suggests that their formation was governed by thermal subsidence. This general cooling of the lithosphere since the Carboniferous corroborates the hypothesis of a previous heating during the Late Devonian.

In North Africa and Levant region, this initial and simple configuration has been strongly modified by subsequent uplifts linked to different tectonic events. In the western corner of Africa, the effects of the Variscan orogeny are observed in the Anti-Atlas as well as Bechar. An uplift linked to the rifting of the Central Atlantic is also present in the Anti-Atlas. Finally, Triassic pre-rift doming is proved in the Oued Mya Basin and along the border of the East Mediterranean Sea (Jaffarah, Western Desert, Levant). So the main unconformity located in these regions between Paleozoic and Mesozoic rocks, the so-called “Hercynian Unconformity”, is in reality a stack of discontinuities, which ages and significances are very different. It is worth noting that important vertical movements occurred also during the Mid-Cretaceous

(the so-called “Austrian” deformation of the Sahara Domain) and by the Late Cretaceous as a consequence of the convergence between Africa and Eurasia. Discussion about these late events is beyond the scope of the present paper (see Frizon de Lamotte et al., 2011).

In the geological literature as well as in the industrial world, it is usual to use the chart of the major orogenic events known worldwide to designate the main unconformities even when they are observed in intra-continental basins and platforms situated away from the margins and orogenic mountain belts. Following this usage, we have seen that the expression “Hercynian Unconformity” has been extensively used in the whole Sahara domain (e.g. Boote et al., 1998; Craig et al., 2008; Dixon et al., 2010) as well as in Arabia (e.g. Konert et al., 2001; Faqira et al., 2009; Johnson, 2008). If this term is employed to suggest that the deformations sealed by this unconformity are related to the Variscan (Hercynian) orogeny it is inappropriate as discussed above. If it is simply employed to indicate a time period, as suggested by Faqira et al. (2009), it is very imprecise because the time of the Hercynian orogeny lasted since 380 Ma up to 310 Ma (Matte, 2001). In any case the term “Hercynian Unconformity” is confusing because at the scale of the studied area it is not used to designate the same object. We have some doubt about the possibility to change such an old usage. However, a warning is necessary because this terminology is all but neutral.

3.2 Integration of the studied area in the Devonian world

The Late Devonian is generally considered as a period of major paleonvironmental turnover characterized by severe environmental and biotic crises (the Frasnian-Famennian and Devonian-Carboniferous boundary crises) and by the onset of a long-term cooling event (the Upper Paleozoic Icehouse stage) (e.g. Copper, 1986; Streel et al, 2000). If the origin of these changes still remains a matter of debate, recent work particularly emphasizes the role of geodynamics events as possible primary driving factors (Racki, 1998; Averbuch et al, 2005; Courtillot et al., 2010). As a matter of fact, the Late Devonian is the time for two contrasting large-scale tectonic processes: the onset of the Variscan Orogeny along the Gondwana-Laurussia margin on the one hand and the development of magmatism, rifting and domal basement uplift within these continents on the other hand.

3.2.1 The "Eo-Variscan" event in the frame of the Variscan orogeny: how it is expressed in Africa?

Late Paleozoic times are characterized by extensive deformations along the northern margin of Gondwana with the progressive accretion of Gondwana-derived continental blocks to the Laurussia continental margin, resulting at the end of the Paleozoic in a large equatorial mountain belt extending from Central America to Eastern Asia (Fig. 11). Such a wide, now strongly disrupted, orogenic belt includes from West to East, the Central-Northern American Appalachian belt (e.g. Murphy and Keppie, 1998; Van Staal et al, 2008) and its Western African counterpart, the Mauritanides (Lécorché et al., 1991; Le Goff et al, 2001; Villeneuve, 2005), the Western European-Northern African Variscan belt (e.g. Matte, 2001; Franke, 2006; Simancas et al, 2009), the Great Caucasus (e.g. Somin, 2011; Adamia et al, 2011), the Uralian (e.g. Matte et al, 1995; Mizens, 2004; Puckov, 2009) and Central Asian belts (e.g. Sengör and Natalin, 1996; Buslov et al, 2004).

Precise paleogeographic as well as kinematic reconstructions of involved terranes are, however, still largely debated and the relationships between the different segments of the belt are not completely understood. Major transverse faults, like the Teysseire-Tornquist Fault Zone (Fig. 11) at the eastern end of the European Variscan system, are likely to have played a major role in the transfer of convergence from one compressional system to another along strike but their understanding is complicated by their disruption during the break-up of Pangea by Mesozoic times and the subsequent Late Cretaceous-Tertiary Alpine collisional deformation. This is for example the case considering the connections between the European Variscides and Appalachian-Mauritanides belts that are generally considered to go through the Newfoundland-Gibraltar fracture zone and the north-western extremity of Morocco, but the geometry and kinematics of this large zone of transfer are still discussed (Simancas et al., 2009; Michard et al., 2010).

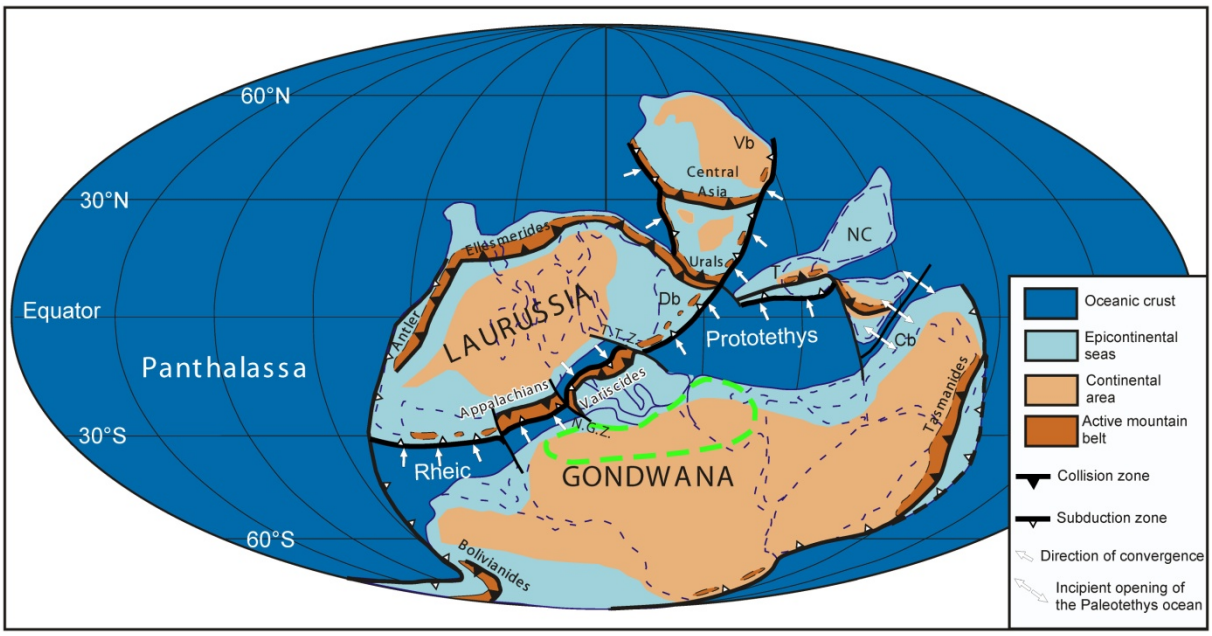

Fig. 11: A general paleo-geodynamic reconstruction of the Late Devonian world (modified from Averbuch et al, 2005, primarily based on the geometry of continents of Golonka et al, 1994) showing the incipient Eovariscan collision of Gondwana and Laurussia. Note the persistence of residual oceanic realms in the vicinity of the Eovariscan belt, whose closure by the Mid-Carboniferous will induce the final colliding process: the Rheic ocean, south of the Appalachian segment [i.e. west of the Newfoundland-Gibraltar transfer zone (N.G.Z.)] and the Lizard-Rhenohercynian Ocean, north of the European Variscan segment. Note also the continued northward subduction of the Prototethys below Eastern Europe [east of the Teysseire-Tornquist Zone (T.T.Z.)] and Western and Central Asia that will lead to the accretion of the Tarim (T) and the Northern China (NC) blocks to Asia. Note finally the incipient opening of the Paleotethys oceanic realm along the eastern side of the Northern Gondwana margin allowing the general counter-clockwise rotation of Gondwana during Carboniferous times. The zone under study in North Gondwana was submitted to thermal uplift and coeval rifting (see the text for further explanation). D.b. refers to the location of the Dniepr-Donetsk basin, V.b. to that of the Viluy basin and C.b. to that of the Canning basin.

Another matter of complexity is that the Variscan belt involves at least two major superimposed Upper Paleozoic suture zones. Along the main part of the European Variscan segment, it corresponds to a large double-verging orogenic wedge involving a Northern Upper Carboniferous Lizard-Rhenohercynian suture zone and a Southern Upper Devonian Massif Central-Moldanubian suture zone (e.g. Matte, 1986; Matte and Hirn, 1988; Autran et al, 1994; Franke, 2000). The latter exposes the most prominent orogenic tectonometamorphic markers of the belt

advocating for an early collisional event which dates from Upper Devonian times (380-360 Ma), i.e. early in the Variscan orogenic development (e.g. Matte, 2001; Averbuch et al, 2005; Murphy et al, 2009). Such an early Variscan (frequently referred to as Eo-Variscan) collisional process between the Northern Gondwana margin and the Armorica continental block is well exposed in Western Europe and Iberia, involving a large stack of S-verging metamorphic nappes (Matte, 1986; Faure et al, 2008; Ballèvre et al, 2009; Ledru et al, 1989; Simancas et al., 2009).

Does this early belt exist in NW Morocco, i.e. south of the Newfoundland-Gibraltar Fault Zone (Fig. 11)? In the westernmost part of the Western Moroccan Meseta ("Coastal Block") a nice Frasnian-Famennian unconformity is shown by subsurface data (Echarfaoui et al., 2002). It has been attributed by the authors to an Eo-Variscan contractional event, but Michard et al. (2008) suggest that the structures depicted beneath the unconformity could also result from a mega-slump formed in extensional or transtensional context. According to this interpretation, we note that the NNE-trending Sidi Bettache and Azrou-Khenifra Basins (Michard et al., 2008), situated just east of the Coastal Block developed at the same time and that such a framework is consistent with what is observed in the Anti-Atlas domain (Wendt, 1985; Baidder et al., 2008). More to the east, in the so-called Eastern Meseta, the existence of an Eo-Variscan event has been proposed on the basis of an important uplift and few K-Ar ages obtained on low- to very-low grade phyllites (Clauer et al. 1980; Huon et al., 1987). Michard et al. (2008) think that these Late Devonian ages (372 +/-8; 368 +/-8; 366 +/-6) must be taken with caution. However, we note that they are equivalent to the ages obtained by Bonhomme et al. (1996) in the Ougarta and Vermeesch et al. (2009) in the Levant Arch. So, we consider that these data are better explained by a thermal anomaly and uplift associated with an important magmatism rather than by a compressional event. From this point of view, we are in line with the interpretation given by Simancas et al. (2009) who proposed to explain the particular magmatic productivity observed in northern Morocco during the Latest Devonian and Early Carboniferous as an effect of a large-scale mantle anomaly. The Moroccan Mesetas, together with the Mauritanides and the Anti-Atlas, were subsequently involved in the Variscan Orogeny associated to the final closure of the Rheic and Lizard-Rhenohercynian Oceans by the Mid-Carboniferous.

3.2.2 Late Devonian magmatism, rifting and basement uplift outside the Variscan Belt.

North Africa and Arabia were poorly affected by Variscan compressive deformations. In the western domain where the Variscan Belt is exposed (Fig. 1), the effects of the Eo-Variscan (Devonian) events are not recorded south of the South Atlas Front and are disputable north of this Front. The Carboniferous deformation itself is poorly expressed outside the Variscan front (Fig. 1) except just north of the Hoggar Massif where wide folds developed (Haddoum et al., 2001; Craig et al., 2008). By contrast, we have shown the existence of a pre-Carboniferous unconformity sealing either massive uplift (Arabia, Hassi R'Mel, Jaffarah) or localized rifts (Bechar, Anti-Atlas, Northern Morocco). Such an evolution was not recognized previously at the scale of the study area.

Elsewhere in Gondwana, it can be correlated to different structures recognized in this mega-continent. In South America, a widespread unconformity and major change in paleogeography occurred at the end of the Devonian post-dating the development of several intra-cratonic Highs (e.g. Williams, 1995). In Austral Africa, as in Arabia (see above), a major Early and Middle Carboniferous hiatus exists beneath the basal unconformity of the Late Carboniferous-to-Jurassic Karoo Basins (e.g. Catuneanu et al., 2005; Tankard et al., 2009) suggesting the existence of a general uplift at that time. In Australia, a Late Devonian (pre-Famennian) episode of rifting has been put forward to explain the development of the Canning Basin (Chaw et al., 2004; George et al., 2009).

In Laurussia, the other mega-continent existing at that time (Fig.11), the domains located between the different branchs of the Variscan Belt were the site of basement doming associated with rifting and development of magmatism (including kimberlites). In the East European Platform, situated between the Teysseire-Tornquist Fault Zone and the Ural (Fig. 11), Wilson and Lyashkevich (1996) describe the contemporaneous development during the Late Devonian of domes and failed rifts (the so-called "Aulacogens"). Among these aulacogens, is the famous 1200 km long- 100 km wide Pripyat-Dnieper-Donets-Donbaz Basin, which is filled by more than 20 km of sediments (Stephenson et al., 2001) and probably floored by exhumed mantle (Yegorova et al., 2004). The Peri-Caspian Basin, located in

Kazakhstan at the southern termination of the Ural, developed at the same time (Brunet et al., 1999). Racki (1998), revisiting the causes of the Frasnian-Famennian crisis, underlines the existence of a Late Frasnian basement uplift occurring in the Kazakhstan-Tian Shan domain, on the eastern side of the Ural. This event was followed immediately by the formation of large troughs. In Eastern Siberia, finally, Courtillot et al. (2010) show that the Late Devonian development of the Viluy Aulacogen was accompanied by traps flooding over the adjacent basement domes.

4. Conclusion

In North Africa and Arabia, we show that the Arch-and-Basin configuration, which characterizes the Paleozoic substructure, was, for its greater part, achieved by the end of the Devonian. This could be only revealed by an investigation at large scale because in many places, notably in Africa, it is hidden by numerous subsequent events (Fig. 10). We have shown that the development of the Arch-and-Basin geometry was linked to a massive uplift accompanied by a diffuse extensional deformation. However, we don't know the amplitude of the uplift nor the mechanism responsible for the arrangement and wavelength of the Arches. In particular, the role of the heritage, i.e. the Pan-African orogeny and the subsequent Lower Paleozoic evolution (see Eschard et al., 2010), is not yet completely understood and not addressed in the present paper.

At a larger scale, one of the main points emphasized by our discussion is that, at the time of the incipient collision phase between Gondwana and Laurussia along the Variscan European-West African belt, large areas within the two mega-continents, situated outside the orogenic belt, were submitted to extensional deformations and contrasting vertical movements. Such an evolution was well known in Laurussia, where the vertical movements have been overstated with the spectacular development of deep "Aulacogens" adjacent to basement domes and large alkaline igneous provinces. By contrast, it was underestimated in Gondwana, even if the importance of a Late Devonian extensional event has been already put forward in South America and Australia.

These results question about the global causes, which are at the origin of the coeval development of mountain belts and doming or rifting in adjacent areas.

According to numerical models (Fleitout and Froideveaux, 1982), it is known that extensional deformation located in the foreland of mountain belts may be a direct consequence of the formation of deep lithosphere roots below these collision zones. On the other hand, it is well-known that continental rifting and/or doming can be related in some way to nearby subduction of oceanic lithosphere (see a review in Merle, 2011). The classical relationship between these two geodynamic processes is the formation of back-arc basins. In this case, rifts develop in the upper plate. They can, however, also develop in the lower plate as a consequence of slab pull. If we look at the global paleogeography of the world at the end of Devonian (Fig. 11), it appears that in Laurussia each part of the continent is close from an active Mountain Belt or a Subduction Zone. This is also true in Gondwana for South America and Australia but less evident for some parts of the study area like Arabia. Further work is thus clearly required to better understand this global system and give a more comprehensive insight into the geodynamical processes inducing the coeval development of collision along continental margins and nearby intraplate rifting and/or thermal doming.

Acknowledgments: This paper benefited from discussions with many colleagues in particular: J.L. Auxiètre (Total, Paris), R. Bracène (Sonatrach, Algiers), N. Chamot-Rooke (ENS, Paris), Ph. de Clarens (Total, Paris), M. Guillemin (Total, Paris), N. Haddadi (Total, Paris), J. Letouzey (UPMC, Paris), J.L. Liger (Total, Paris), A. Michard (Paris), Th. Rives (Total, Pau), F. Roure (IFPen, Rueil-Malmaison), J.L. Rubino (Total, Pau) and S. Sherkati (NIOC, Tehran). S. Tavakoli and C. Raulin acknowledge TOTAL and the Université de Cergy-Pontoise respectively for PhD Scholarships. This paper is a contribution of the "Groupe Recherche Industrie" (GRI) "Marge Sud-Tethys", a research agreement between TOTAL on the one hand and l'Ecole Normale Supérieure (ENS) , l'Université Pierre-et-Marie-Curie (UPMC) and l'Université de Cergy-Pontoise (UCP) on the other hand. We wish to thank C. Cabrit (Total) and C. Lemouchoux (UCP) for the drawings. The reviews by two anonymous reviewers and a private review by André Michard are gratefully acknowledged.

References

Adamia, S., Zakariadze, G., Chkhotua T., Sadradze N., Tsereteli, N., Chabukiani, A. and Gventsadze, A., 2011. Geology of the Caucasus: a review. *Turkish Journal of Earth Sciences*, **20**, 489-544. doi: 10.3906/yer-1005-11.

Al Hadidy, A.H., 2007. Paleozoic stratigraphic lexicon and hydrocarbon habitat of Iraq. *Geoarabia*, **12**, 63-130.

Al-Laboun, A.A., 1988. The distribution of Carboniferous-Permian siliciclastic rocks in the greater Arabian Basin. *Geol. Soc. Am. Bull.,* **100**, 362-373.

Autran, A., Lefort, J.P., Debeglia, N., Edel, J.B., Vigneresse, J.L., 1994. Gravity and magnetic expression of terranes in France and their correlation beneath overstep sequences. In: Keppie, J.D. (Ed.), Pre-Mesozoic geology in France and related areas. Springer-Verlag, Berlin, Heidelberg, pp. 49-72.

Averbuch, O., Tribovillard, N., Devleeschouwer, X., Riquier, L., Mistiaen, B., van Vliet-Lanoe, B., 2005. Mountain building-enhanced continental weathering and organic carbon burial as major causes for climatic cooling at the Frasnian-Famennian boundary (c. 376 Ma)? *Terra Nova*, **17**, 25-34.

Baidder, L., Raddi, Y., Tahiri, M., Michard, A., 2008. Devonian extension of the Pan-African crust north of the West African craton, and its bearing on the Variscan foreland deformation: evidence from eastern Anti-Atlas (Morocco). *Geological Society, London, Special Publications,* **297**, 453-465.

Ballèvre, M., Bosse, V., Ducassou, C., Pitra, P., 2009. Palaeozoic history of the Armorican massif: Models for the tectonic evolution of the suture zones. *C.R. Geoscience,* **341**, 174-201.

Berkaloff, E., 1933.Contribution à l'étude géologique de l'extrême-sud tunisien. Le territoire militaire des Matmatas. *Bulletin de la Société Géologique de France*, **3**, 83-87.

Beyth, M., 1981. Paleozoic vertical movements in Um bogma area, southwestern Sinai. *AAPG Bull.,* **65(1)**, 160-165.

Bojar, A.-V., Fritz, H., Kargl, S., Unzog, W. 2002. Phanerozoic tectonothermal history of the Arabian–Nubian shield in the Eastern Desert of Egypt: evidence from fission track and paleostress data. *Journal of African Earth Sciences*, **34**, 191-202.

Bonhomme, M.G., Fabre, J., Kaddour, M., 1996. Datations K-Ar d'événements varisques dans le Cambrien de l'Ougarta (Sahara occidental algérien). *Mém. Serv. Géol. Algérie*, **8**, 117-125.

Boote, D.R.D., Clark-Lowes, D.D., Traut, M.W., 1998. Paleozoic petroleum systems of North Africa, in Macgregor, D.S, Moody, R.T.J. & Clarke-Lowes, D.D. (eds), Petroleum Geology of North Africa. Geological Society, London, Sp. Publ. **132**, 7-68.

Bosworth, W., El-Hawat, A.S., Helgeson, D.E. and Burke, K., 2008. Cyrenaican "shock absorber" and associated inversion strain shadow in the collision zone of northeast Africa. *Geology*, **36**, 695-698.

Bouaziz, S., 1995. Etude de la tectonique cassante dans la plate-forme et l'Atlas saharien (Tunisie méridionale) : évolution des paléo-champs de contraintes et implications géodynamiques. *Thèse d'Etat de l'Université de Tunis II*, 485 p.

Boudjema, A., 1987. Evolution structural du basin pétrolier triasique du Sahara nord oriental (Algérie). Unpublished PhD Thesis, Univ Paris-Sud (Orsay), 289 p.

Brew, G., Barazangi, M., Al-Maleh, A.K., Sawaf, T., 2001. Tectonic and Geologic evolution of Syria, *GeoArabia*, **6**, 573-616.

Brunet, M.F., Volozh, Y.A., Antipov M.P.,. Lobkovsky, L.I., 1999.The geodynamic evolution of the Precaspian Basin (Kazakhstan) along a north–south section. *Tectonophysics*, **313**, 85–106.

Buslov, M.M., Watanabe, T., Fujiwara, Y., Iwata, K., Smirnova, L.V., Yu Safonova, I., Semakov, N.N., Kiryanova, A.P., 2004. Late Paleozoic faults of the Altai region, Central Asia: tectonic pattern and model of formation. *J. Asian Earth Sci.,* **23**, 655-671.

Burkhard, M., Caritg, S., Helg, U. Robert-Charrue, C., Soulaimani, A., 2006. Tectonics of the Anti-Atlas of Morocco. *C.R. Geoscience*, **338**, 11-24.

Caputo, M.V., Crowell, J.C., 1985. Migration of glacial centers across Gondwana during Paleozoic Era. *Geological Society of America Bulletin*, **96**, 1020-1036.

Catuneanu, O., Wopfner, H., Eriksson, P.G., Cairncross, B., Rubidge, B.S., Smith, R.M.H., Hancox, P.J., 2005. The Karoo basins of south-central Africa. *Journal of African Earth Sciences*, **43**, 211–253.

Clauer, N., Jeannette, D., Tisserant, D., 1980. Datation isotopique des cristallisations successives du socle cristallin et crystallophyllien de la Haute Moulouya (Maroc Hercynien). *Geol. Runsch*., **69**, 68-83.

Copper, P., 1986. Frasnian/Famennian mass extinction and cold-water oceans. *Geology*, 14, 835–839.

Courtillot, V., Kravchinsky, V.A., Quidelleur, X., Renne, P.R., Gladkochub, D.P., 2010.Preliminary dating of the Viluy traps (Eastern Siberia): Eruption at the time

of LateDevonian extinction events? Earth and Planetary *Science Letters*, **300**, 239–245

Craig, J., Rizzi, C., Said, F., Thusu, B., Luning, S., Asbali, A.I., Keeley, M.L., Bell, J.F., Durham, M.J., Eales, M.H., Beswetherick, S., Hamblett, C., 2008. Structural Styles and Prospectivities in the Precambrian and Paleozoic Hydrocarbon Systems of North Africa, Geology of East Lybia, vol. **4**, 51-122.

Dallmeyer, R.D., Martinez Catalan, J.R., Arenas, R., Gil Ibarguchi, J.I., Guttierez Alonso, G., Farias, P., Aller, J., Bastida, F., 1997. Diachronous Variscan tectonothermal activity in the NW Iberian Massif: Evidence from $^{40}Ar/^{39}Ar$ dating of regional fabrics. *Tectonophysics*, **277**, 307-337.

Dixon, D.J., Moore, J.K.S., Bourne, M., Dunn, E., Haig, D.B., Hossack, J., Roberts, N., Parsons, T., Simmons, C.J., 2010. Integrated petroleum systems and play fairway analysis in a complex Paleozoic basin : Ghadames-Illizi Basin, North Africa. *Petroleum Geology Conference series*, **7**, 735-760. Doi: 10.1144/0070735.

Djellit, H., Bellon, H., Ouabadi, A., Derder, M.E.M., Henry, B., Bayou, B., Khaldi, A., Baziz, K., Merahi, M. K., 2006. Âge 40K/40Ar, Carbonifère inférieur, du magmatisme basique filonien du synclinal paléozoïque de Tin Serririne,Sud-Est du Hoggar (Algérie). *C. R. Geoscience*, **338**, 624–631.

Echarfaoui, H., Hafid, M., Aït Salem, A., 2002. Structure sismique du socle paléozoïque du bassin des Doukkala, Môle côtier, Maroc occidental. Indication en faveur d'une phase éo-varisque. *C.R. Geoscience*, **334**, 13-20.

Eschard, R., Braik, F., Bekkouche, D., Ben Rahuma, M., Desaubliaux, G., Deschamps, R., Proust, J.N., 2011. Paleohighs : their influence on the Northern African Palaezoic petroleum systems. In Vinning, B.A. & Pickering, S.C. (eds)Petroleum Geology: From Mature Basins to New Frontiers-Proceedings of the 7th Petroleum Geology Conference (published by the Geological Society, London), 707-724.

Fabre, J., 2005. Géologie du Sahara occidental et central. Tervuren Afr. Geosci. Coll., 108, 572 pp.

Fleitout, L., Froidevaux, C., 1982. tectonics and topography for a lithosphere containing density heterogeneity. *Tectonics*, **1**, 21–56.

Faure, M., Bé Mézème E., Cocherie, A., Rossi, P., Chemenda, A., Boutelier, D., 2008. Devonian geodynamic evolution of the Variscan belt, insights from the French Massif Central and Massif Armoricain. *Tectonics*, **27**, TC2005, doi: 10.1029/2007TC002115.

Faqira, M., Rademakers, M., Afifi, A. M., 2009. New insights into the Hercynian Orogeny, and their implications for the Paleozoic Hydrocarbon System in the Arabian Plate. *Geoarabia*, **14**, 199-228.

Franke, W., 2000. The mid-European segment of the Variscides: tectonostratigraphic units, terrane boundaries and plate tectonic evolution. In: Franke, W., Haak, V., Oncken, O., Tanner, D. (Eds.), Orogenic Processes: quantification and Modelling in the Variscan Belt. *Geological Society, London, Special Publications*, **179**, pp. 35-61.

Franke, W., 2006. The Variscan orogen in Central Europe: construction and collapse. In: Gee, D.G., Stephenson, R.A. (Eds.), European Lithosphere Dynamics. *Geological Society, London, Memoirs* 32, pp. 333-343.

Frizon de Lamotte, D., Saint-Bezar, B., Bracene, R. and Mercier, E., 2000. The two main steps of the Atlas building and Geodynamics of West Mediterranean, *Tectonics*, **19**, 740-761.

Frizon de Lamotte, D., Leturmy, P., Missenard, Y., Khomsi, S., Ruiz, G., Saddiqi, O., Guillocheau, F., Michard, A., 2009. Mesozoic and Cenozoic vertical movements in the Atlas system (Algeria, Morocco, Tunisia): An overview. *Tectonophysics*, 475, 9-28.

Frizon de Lamotte, D. and Raulin, C., 2010. The sedimentary basins and margins in Tectonic Map of Africa at 1 : 10M scale, Milesi J.P., Frizon de Lamotte, D., De Kock, G. and Toteu, F., CGMW ed.

Frizon de Lamotte, D., Raulin, C., Mouchot, N., Wrobel-Daveau, J.C., Blanpied, C., Ringenbach, J.C., 2011. The southernmost margin of the Tethys realm during the Mesozoic and Cenozoic: Initial geometry and timing of the inversion processes, *Tectonics,* **30**, TC3002, doi: 10.1029/2010TC002691.

Galeazzi, S., Point, O., Haddadi, N., Mather, J., Druesne, D., 2010. Regional Geology and petroleum systems of the Illizi-Berkine area of the Algerian Saharan Platform: An overview. *Marine and Petroleum Geology*, **27**, 143-178.

Ghavidel-syooki M., 2005. Palynological study and age determination of Faraghan Formation in Kuh-e-Gahkum region at southeast of Iran. In: (eds) Contributions to the paleopalynology of Paleozoic rock units in the Zagros, Alborz and Central Iranian Basin, published book, 15–34 in Persian.

Ghienne, J.F., Boumendiel, K.B., Paris, F. Videt, B., Racheboeuf, P., Ait Salem, H., 2007. The Cambrian-Ordovician succession in the Ougarta Range (western Algeria, North Africa) and interference of the Late Ordovician glaciation on the development of the Lower Palaezoic transgression on northern Gondwana. *Bulletin of Geoscience*, **82**, 183-214.

Ghienne, J.F., Monod, O., Kozlu, H., Dean, W.T., 2010. Cambrian-Ordovician depositional sequences in the Middle East: A perspective from Turkey. *Earth Science Reviews*, **101**, 101-146.

Golonka, J., Ross, M.I., Scotese, C.R., 1994. Phanerozoic paleogeographic and paleoclimatic modelling maps. In: Embry, A.F., Beauchamp, B., Glass, D.J. (Eds.), Pangea: Global Environments and Ressources. *Can. Soc. Petrol. Geol*., **17**, 1-47.

Gouzia, M., 2011. Mesozoic Source-to-Sink Systems in NW Africa, Geology of the vertical movements during the birth and growth of the Moroccan rifted margin. PhD Thesis, Vrije Universiteit Amsterdam. 170 p.

Guimerà, J., Arboleya, M.L., Teixell, A., 2011. Structural control on present-day topography of a basement massif: the Central and Eastern Anti-Atlas (Morocco), Geoilogica Acta, **9**, 55-65.

Guiraud, R., Bosworth, W., Thierry, J. and Delplanque, A., 2005. Phanerozoic geological evolution of Northern and Central Africa: An overview. *Journal of African Earth Sciences*, **43**, 83-143.

Gvirtzman. G. and Weissbrod, T., 1984. The Hercynian Geanticline of Helez and the Late Palaeozoic history of the Levant. *Geological Society, London, Special Publications*, **17**, p. 177-186.

Haddoum, H., Guiraud, R., Moussine-Pouchkine, A., 2001. Hercynian compressional deformations of the Ahnet-Mouydir Basin, Algerian Saharan Platform : far-field stress effects of the Late Palaezoic orogeny. *Terra Nova*, **13**, 220-226.

Hervouet, Y. et Duée G., 1996. Analyse morphostructurale par imagerie satellitaire et coupes structurales modélisées des monts d'Ougarta (Sahara occidental, Algérie) : une chaîne hercynienne chevauchante à plis passifs. *Mém. Serv. Géol. Algérie*, **8**, 127-173.

Huon, S., Piqué A., Clauer N., 1987. Etude de l'orogenèse hercynienne au Maroc par la datation K/Ar de l'évolution métamorphique de schistes ardoisiers, *Sci. Géol. Bull. Strasbourg,* **40**, 273–284.

Insalaco, E., Virgone, A., Courme, B., Gaillot, J., Kamali, M., Moallemi, A., Lotfpour, M., Monibi, S., 2006. Upper Dalan Member and Kangan Formation between the Zagros Mountains and offshore Fars,Iran:depositional system, biostratigraphy and stratigraphic architecture, *GeoArabia*, **11**, 2, 75-176.

Isaacson, P.E., Diaz-Martinez, E., Grader, G.W., Kalvoda, J., Babek, O., Devuyst, F.X., 2008. Late Devonian-earliest Mississippian glaciation in Gondwanaland and its biogeographic consequences. *Palaeogeography, Palaeoclimatology, Palaeoecology*, **268**, 126-142.

Johnson, C.A., 2008, Phanerozoic Plate Reconstructions of the Middle East: Insights into the Context of Arabian Tectonics and Sedimentation. SPE 118062.

Jongsma, D., Van Hinte, J. E., Woodside, J.M., 1985. Geologic structure and neotectonics of the North African Continental Margin south of Sicily. *Marine and Petroleum Geology*, **2**, 2, 156-179.

Keeley, M.L., 1989. The Paleozoic history of the Western Desert of Egypt. *Basin Research*, **2**, 35-48.

Keeley, M.L., 1994. Phanerozoic evolutionof the basins of Northern Egypt and adjacent areas. *Geol Rundsch*, **83**, 728-742.

Keeley, M.L., Dungworth, G., Floyd, C.S., Forbes, G.A., King, C., McGarva, R.M. and Shaw, D., 1990. The Jurassic System in Northern Egypt .1. Regional Stratigraphy and Implications for Hydrocarbon Prospectivity. *Journal of Petroleum Geology*, **13**, 397-420.

Keeley, M. L. and Massoud M. S., 1998. Tectonic controls on the petroleum geology of NE Africa, in D. S. MacGregor, R. T. J. Moody and D. D. Clark-Lowes (eds.), Petroleum geology of North Africa: *Geological Society Special Publication*, **132**, 69-78.

Klett, T.R., 2001. Total Petroleum Systems of the Pelagian Province, Tunisia, Libya, Italy and Malta --The Bou Dabbous -- Tertiary and Jurassic-Cretaceous Composite. *U.S. Geological Survey Bulletin*, 2202-D.

Kohn, B. P., Eyal, M., Feinstein, S., 1992. A major Late Devonian-Early Carboniferous (Hercynian) Thermotectonic event at the NW Margin of the Arabian-Nubian Shield: Evidence from zircon fission track dating. *Tectonics*, **11**, 1018-1027.

Konert, G., A.M. Afifi, S.A. Al-Hajri, and H.J. Drost, 2001, Paleozoic Stratigraphy and Hydrocarbon Habitat of the Arabian Plate, *GeoArabia*, **6**, 407-442.

Lardeaux, J.M., Ledru, P., Daniel, I., Duchene, S., 2001. The Variscan French Massif Central- a new addition to the ultra-high pressure metamophic “club”: exhumation processes and geodynamic consequences. *Tectonophysics*, **332**, 143-167.

Lecorché, J-P., Bronner, G., Dallmeyer, R.D., Rocci, G., Roussel, J., 1991. The Mauritanide orogen and its northern extensions (western Sahara and Zemmour), West Africa. In: Dallmeyer, R.D., Lecorché J-P. (Eds.), The West African orogens and Circum-Atlantic Correlatives. Springer-Verlag, Berlin, 187-227.

Ledru, P., Lardeaux, J.-M., Santallier, D., Autran, A., Quenardel, J.-M., Floc’h, J.-P., Lerouge, G., Maillet, N., Marchand, J., Ploquin, A., 1989. Où sont les nappes

dans le Massif central français. *Bull. Société Géologique de France*, 8 (V), 605-618.

Le Goff, E., Guerrot, C., Maurin, G., Johan, V., Tegyey M., Ben Zarga, M., 2001. Découverte d'éclogites hercyniennes dans la chaîne septentrionale des Mauritanides (Afrique de l'Ouest). *C. R. Acad. Sci. Paris*, **333**, 711-718.

Mahmoud, A. and El Barkooky, A., 1998. Mesozoic valley fills incised in Paleozoic rocks potential exploration targets in the north Western Desert of Egypt, Obaiyed Area, EGPC 14th Petroleum Conference, Cairo.

Maluski, H., Patocka, F., 1997. Geochemistry and $^{40}Ar/^{39}Ar$ geochronology of the mafic metavolcanic rocks from the Richory Mountains complex (West Sudetes, Bohemian massif): paleotectonic significance. *Geol. Mag.,* **134**, 703-716.

Martinez Catalan, J.R., Arenas, R., Abati, J., Sanchez Martinez S., Diaz Garcia F., Fernandez Suarez J., Gonzalez Cuadra P., Castineiras P., Gomez Barreiro J., Diez Montes A., Gonzalez Clavijo E., Rubio Pascual, F.J., Andonaegui, P., Jeffries, T.E., Alcock, J.E., Diez Fernandez R., Lopez Carmona, A., 2009. A rootless suture and the loss of the roots of a mountain chain: The Variscan belt of NW Iberia. *C.R. Geoscience*, **341**, 114-126.

Mathieu, G., 1949. Contribution à l'étude des Monts Troglodytes dans l'Extrême Sud Tunisien. *Ann. Mines et Géol.*, Tunis, **4**, 82 p.

Matte, P., 1986. Tectonics and plate tectonics model for the Variscan belt in Western Europe. *Tectonophysics*, **126**, 329-374.

Matte, P., 1998. Continental subduction and exhumation of HP rocks in Paleozoic orogenic belts: Uralides and Variscides. *GFF 120*, 209-222.

Matte, P., 2001. The Variscan collage and orogeny (480-290 Ma) and the tectonic definition of the Armorica microplate: a review. *Terra Nova*, **13**, 122-128.

Matte, P., Hirn, A., 1988. Seismic signature and tectonic cross section of the Variscan crust in Western France. *Tectonics*, **7**, 141-155.

Merle, O., 2011. A simple continental rift classification. *Tectonophysics*, **513**, 88–95.

Michard, A. Hoepffner, C. Soulaimani, A., Baider, L., 2008. The Variscan Belt, *in* « Continental Evolution: the Geology of Morocco », Michard, A., Saddiqi, O., Chalouan, A., Frizon de Lamotte, D. eds. Springer, 65-132.

Michard, A., Soulaimani, A., Hoepffner, C., Ouanaimi, H., Baidder, L., Rjimati, E.C., Saddiqi, O., 2010. The South-Western Branch of the Variscan Belt: Evidence from Morocco, *Tectonophysics,* **492**, 1-24.

Missenard, Y., Zeyen, H., Frizon de Lamotte, D., Leturmy, P., Petit, C. and Sébrier, M., Saddiqi, O., 2006. Crustal versus Asthenospheric origin of the Relief of the Atlas Mountains of Morocco. *Journal of Geophysical Research*, **111**, B03401, doi: 10.1029/2005JB003708.

Mizens, G.A. 2004. Devonian palaeogeography of the Southern Urals. *Geol. Quarterly*, **48**, 205-216.

Moreau, J., Ghienne, J.F., Hurst, A., 2012. Kilometric-scale sand injectites in the intracratonic Murzuq Basin (south-west Libya): an igneous trigger ? *Sedimentology*, **59**, 1321-1344.

Murphy, J.B., Keppie, J.D, 1998. Late Devonian palinspastic reconstruction of the Avalon-Meguma terrane boundary: implication for terrane accretion and basin development in the Appalachian orogen. *Tectonophysics,* **284**, 221-231.

Murphy, J.B., Guttierrez-Alonso, G., Nance, R.D., Fernandez-Suarez, J., Keppie, J.D., Quesada, C., Dostal, J., Braid, J., 2009. Rheic Ocean mafic complexes : overview and synthesis. In: Murphy, J.B., Keppie, J.D.., Hynes, A.J. (Eds.), Ancient Orogens and Modern Analogues. *Geological Society, London, Special Publication* **327**, 343-369.

Oukassou, M., Saddiqi, O., Barbarand, J., Sebti, S., Baidder, L., Michard, A. *(in press).* Post-Variscan exhumation of the Central Anti-Atlas (Morocco) constrained by zircon and apatite fission-track thermochronology. *Terra Nova (in press).*

Pin, C., Fonseca, P.E., Paquette, J-L., Castro, P., Matte, P., 2008. The ca. 350 Ma Beja igneous complex: A record of transcurrent slab break-off in the Southern Iberia Variscan belt? *Tectonophysics,* **461**, 356-377. doi: 10.1016/j.tecto.2008.06.001

Piqué, A., Bossière, G., Bouillin, J-P., Chalouan, A., Hoepffner, C., 1993. Southern margin of the Variscan belt-the north-western Gondwana mobile zone (eastern Morocco and northern Algeria). *Geol. Rundsch.* **82**, 432-439.

Puchkov, V.N., 2009. The evolution of the Uralian orogeny. In: Murphy, J.B., Keppie, J.D., Hynes, A.J. (Eds.), Ancient orogens and modern analogues. Geological Society, *London, Special Publication **327***, pp. 161-195. doi:10.1144/SP327.9.

Racki, G., 1998. Frasnian-Famennian biotic crisis: undervalued tectonic control? *Palaeogeography, Palaeoclimatology, Palaeoecology*, **141**, 177-198.

Raulin, C., Frizon de Lamotte, D., Bouaziz, S., Khomsi, S., Mouchot, N., Ruiz, G., Guillocheau, F., 2011. Late Triassic-early Jurassic block tilting along E-W faults, in southern Tunisia: new interpretation of the Tebaga of Medenine. *J. Afr. Earth Sci.*, doi:10.1016/j.jafrearsci.2011.05.007.

Robert-Charrue, C., Burkhard, M., 2008. Inversion tectonics, interference pattern and extensional fault-related foding in Eastern-Anti Atlas, *Swiss J. Geosci.* **101**, 397-408.

Ruiz, G.M.H., Sebti, S., Negro, F., Saddiqi, O., Frizon de Lamotte, D., Stokli, D., Stuart, F., Barbarand, J., Shaer, J.P., 2011. From pangean rift to Neogene uplift-Anti-Atlas (SW Morocco). *Terra Nova.* **23,** 35-41

Saura, E., Verges, J., Homke, S., Blanc, E. J.-P., Serra-Kiel,J., Bernaola, G., Casciello, E., Fernandez, N., Romaire, I., Casini, G., Embry, J.-C., Sharp, I.R., Hunt, D. W. 2011. Basin architecture and growthfolding of the NW Zagros early foreland basin duringthe Late Cretaceous and early Tertiary. *Journal of the Geological Society, London* **168**, 235–50.

Saddiqi, O., Baidder, L., Michard, A., 2011. Haut Atlas et Anti-Atlas, circuit oriental. *In* Nouveaux Guides Géologiques et Miniers du Maroc, A. Michard, O. Saddiqi, A. Chalouan, E. Rjimati and A. Mouttaqi eds, Notes et Mém. Serv. Géol. Maroc, **557**, 1-111.

Sebti, S., Saddiqi, O., El Haimer F. Z., Michard, A., Ruiz, G., Bousquet, R., Baidder, L., Frizon de Lamotte, D., 2009.Vertical movements at the fringe of the West African Craton.First zircon fission track datings from the Anti-Atlas Precambrian basement, Morocco. *C. R. Geoscience*, **341**, 71–77.

Sengor, A.M., Natal'in, B., 1996. Paleotectonics of Asia: fragments of a synthesis. In: Yin A., Harrison T.M. (Eds.), The tectonic evolution of Asia. Cambridge University Press, pp. 486-640.

Simancas, F., Azor, A., Martinez-Poyatos, D., Tahiri, A., El Hadi, H., Gonzalez-Lodeiro, F., Perez-Estaun, A., Carbonell, R., 2009. Tectonic relationships of Southwest Iberia with the allochthons of Northwest Iberia and the Moroccan Variscides. *C. R. Geoscience,* **341**, 103-113. doi: 10.1016/j.crte.2008.11.003

Somin, M.L., 2011. Pre-Jurassic basement of the Greater Caucasus: Brief overview. *Turkish Journal of Earth Sciences*, **20**, 545-610. doi: 10.3906/yer-1008-6.

Soulaimani, A., Essaifi, A., Youbi, N., Hafid, A., 2004. Les marqueurs structuraux et magmatiques de l'extension crustale au Protérozoïque terminal-Cambrien basal autour du massif de Kerdous (Anti-Atlas occidental, Maroc). *C.R. Geoscience*, **336**, 1433-1441.

Stampfli, G., Marcoux, J., Baud, A., 1991. Tethyan margins in space and time. *Palaeogeography, Palaeoclimatology, Palaeoecology,* **87**, 373-409.

Stampfli, G.M., Borel, G.D., 2002. A plate tectonic model for the Paleozoic and Mesozoic constrained by dynamic plate boundaries and restored synthetic oceanic isochrones. *Earth and Planetary Sciences Letters*, **196**, 17–33.

Stampfli, G.M., Mosar, J., Faver, P., Pillevuit, A., Vannay, C.J., 2001. Permo–Mesozoic evolution of the western Tethyan realm: the Neotethys/East-Mediterranean connection. Peri-Tethys memoir 6: Peri-tethyan rift/wrench basins and passive margins. *International Geological Correlation Program*, **369**, 51–108.

Stephenson, R.A., Stova, S.M., Starostenko, V.I., 2001. Pripyat-Dniepr-Donets Basin: implications for dynamics of rifting and the tectonic history of the northern Peri-Tethyan Platforrm In Peri-Tethys Memoir 6, *Mémoire du Muséum National d'Histoire Naturelle,* **186**, 369-406.

Soussi, M., 2002. Le Jurassique de la Tunisie atlasique: stratigraphie, dynamique sédimentaire, paléogéographie et intérêt pétrolier. *Docum. Lab. Géol.*, Lyon 157, 363.

Streel, M., Caputo, M.V., Loboziak, S., Melo, J.H.G., 2000. Late Frasnian-Famennian climates based on palynomorph analyses and the question of the Late Devonian glaciation. *Earth-Science Reviews*, **52**, 121–173.

Szabo, F. and Kheradpir, A., 1978. Permian and Triassic stratigraphy, Zagros basin, south-west Iran. *Journal of Petroleum Geology*, V1, P 57-82.

Tankard, A., Welsink, H., Aukes, P., Newton, R., Stettler, E., 2009. Tectonic evolution of the Cape and Karoo basins of South Africa. *Marine and Petroleum Geology*, **26**, 1379–1412

Tavakoli-Shirazi, S., Frizon de Lamotte, D., Wrobel-Daveau, j.-C., Ringenbach, J.C., 2012. Pre-Permian uplift and diffuse extensional deformation in the High Zagros Belt (Iran): integration in the geodynamic evolution of the Arabian plate. *Arabian Journal of Geosciences*. doi: 10.1007/s12517-012-0542-5

Van Staal, C.R., Whalen, J.B., Valverde-Vaquero, P., Zagorevski, A., Rogers, N., 2009. Pre-Carboniferous, episodic accretion-related, orogenesis along the Laurentian margin of the northern Appalachians. In: Murphy, J.B., Keppie, J.D., Hynes, A.J. (Eds.), Ancient orogens and modern analogues. *Geological Society, London, Special Publications **327***, pp. 271-316. doi:10.1144/SP327.13.

Vermeesch, P., Avigad, D., McWilliams, M.O., 2009. 500 m.y. of thermal history elucidated by multi-method detrital thermochronology of North Gondwana Cambrian sandstone (Eilat area, Israel). *Geol. Soc. Am. Bull.,* **121**, 1204-1216.

Vergès, J., Saura, E., Casciello, E., Fernandez, M., Villasenor, A., Jimenez-Hunt, I., Garcia-Casellanos, D., 2011. Crustal-scale cross-section across the NW Zagros belt : implications for the Arabian margin reconstruction. *Geological Magazine*, doi: 10.1017/S00167568111000331.

Villeneuve, M., 2005. Paleozoic Basins in West Africa and the Mauritanide thrust belt. *Journal of African Earth Sciences*, **43**, 166-195.

Wender, L.E., Bryant, J.W., Dikens, M.F., Neville, A.S., Al-Moqbel, A.M., 1998. Paleozoic (Pre-Khuff) Hydrocarbon Geology of the Ghawar Area, Eastern Saudi Arabia. *Geoarabia*, 3, 2, 273-302.

Wendt, J., 1985. Desintegration of the continental margin of nortwestern Gondwana: late Devonian of the eastern Anti-Atlas (Morocco), *Geology,* **13**, 815-818.

Wendt, J., Kaufmann, B., Belka, Z., Klug. C., Lubeseder, S., 2006. Sedimentary evolution of a Palaezoic basin and ridge system: the Middle and Upper Devonian of the Ahnet and Mouydir (Algerian Sahara). *Geol. Mag.,* **143**, 269-299.

Weissbrod, T., 1980, The Paleozoic of Israel and adjacent countries [Ph.D. thesis]: Jerusalem, Hebrew University, 275 p. (in Hebrew).

Williams, K.E., 1995. Tectonic subsidence analysis and Paleozoic paleogeography of Gondwana. In “Petroleum Basins of South America”, Tankard, A.J., Suarez-Sorucco, R., Welsink, H.J., Eds., Geological Society of America Memoirs, **62**, 79-100.

Wilson, M., Lyashkevich, Z.M., 1996. Magmatism and the geodynamics of rifting of the Pripyat-Dnieper-Donets rift, East European Platform. *Tectonophysics*, **268**, 65-81.

Yegorova, T.P., Stephenson, R.A., Kostyuchenko, S.L., Baranova, E.P. Starostenko, V.I., Popolitov, K.E., 2004. Structure of the lithosphere below the southern margin of the East European Craton (Ukraine and Russia) from gravity and seismic data. *Tectonophysics*, **381**, 81–100.

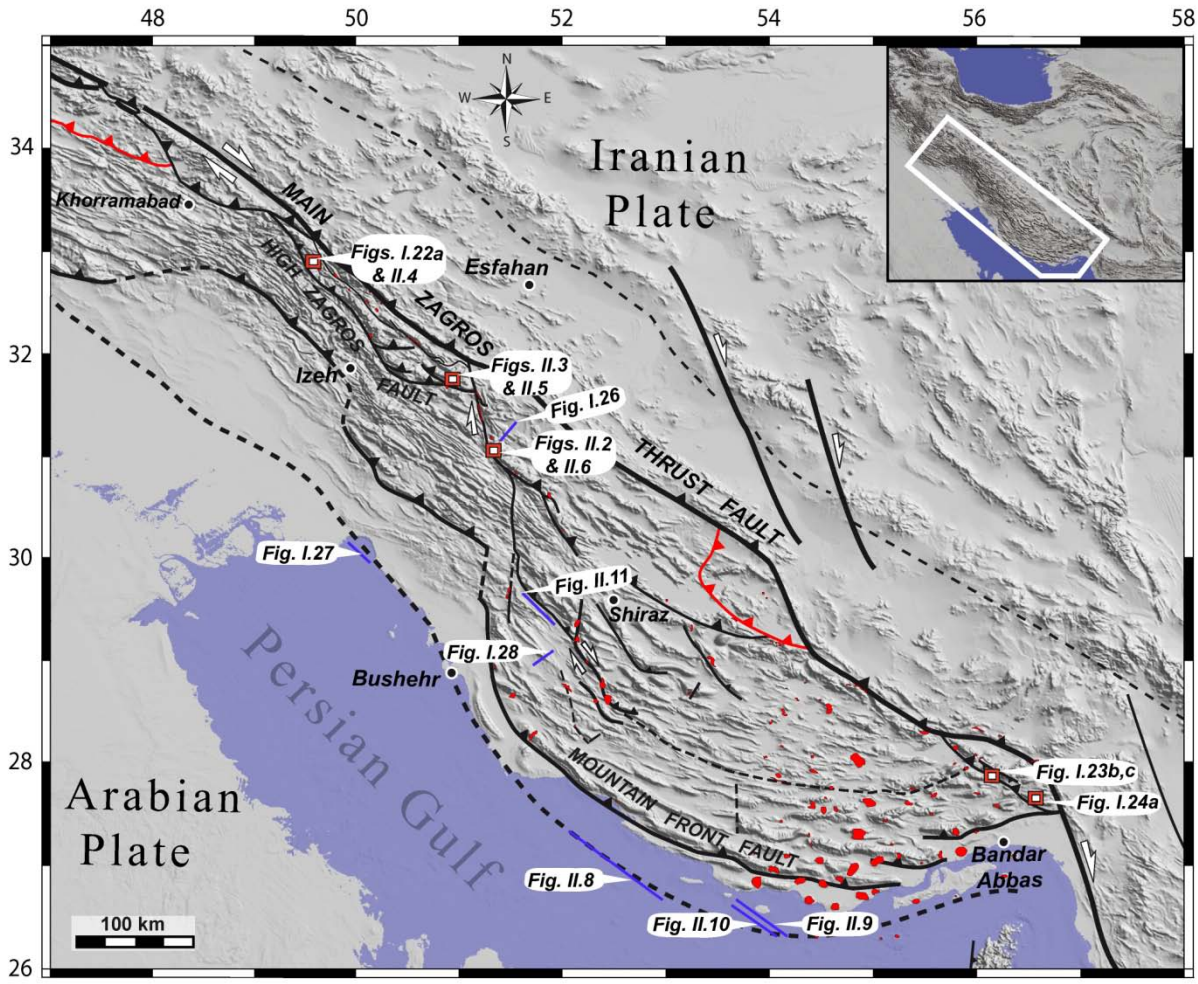

Annex 3 : Location map of the figures in complementary notes of chapter I and II over SRTM data

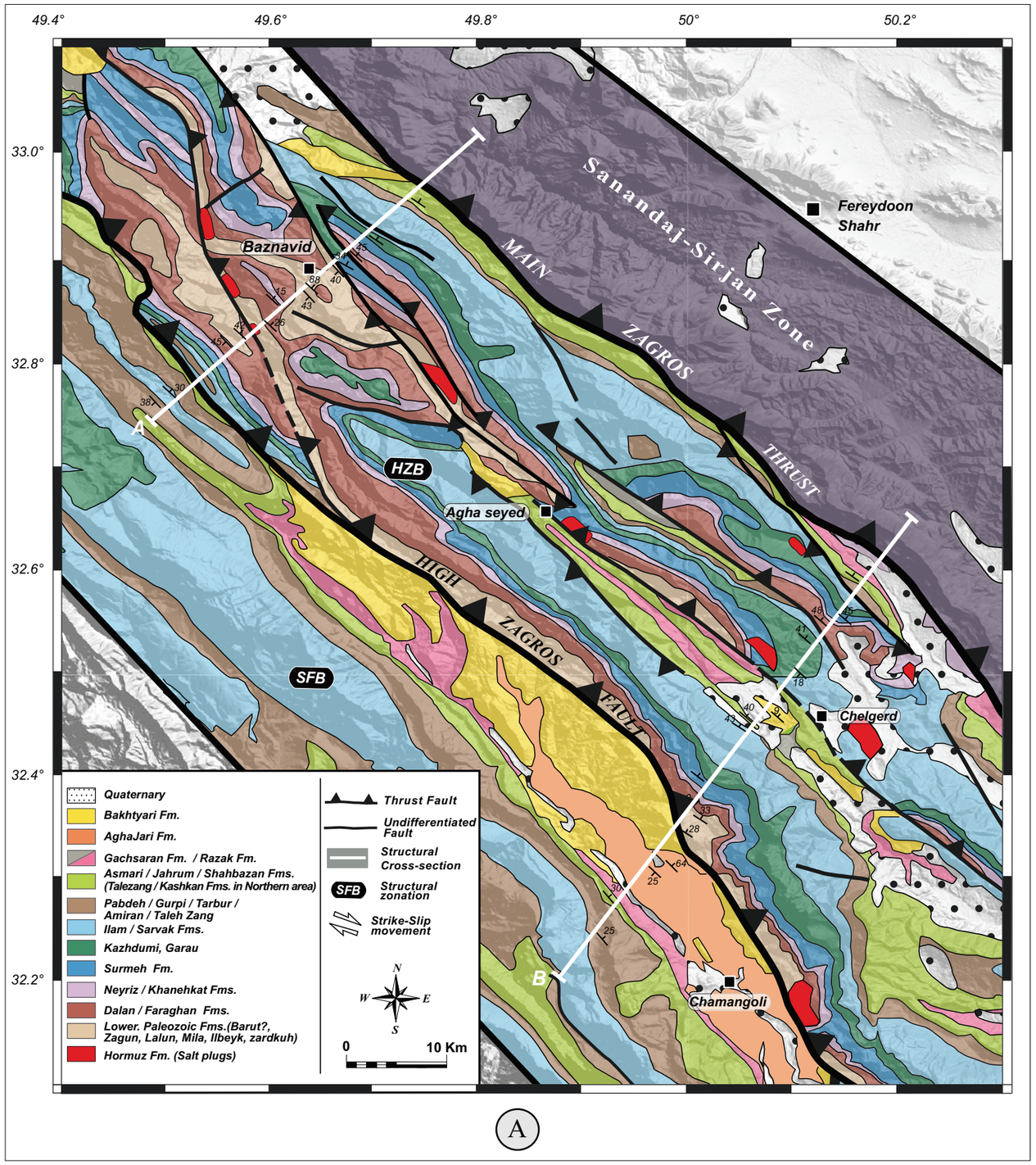

A

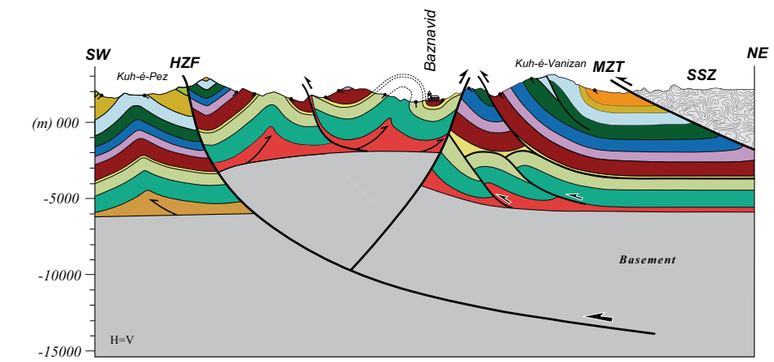

Paleogene Fms. (Amiran /Talezang / Kashkan /Shahbazan)
Eocene Carbonate (Taleh Zang)
Gurpi / Pabdeh Fms.
Bangestan Group (Kazhdumi / Sarvak / Ilam)
L.Cretaceous Fms. (Garau / Gotnia)
Jurassic Fm. (Surmeh)
Trias -- L.Jurassic Fms. (Khanehkat / Neyriz)
Permian Fms. (Faraghan / Dalan)
Ordovician Fm. (Ilbeyk-Zardkuh)
a. Mila
b.(Barut / Zaigun / Lalun)
Hormuz equivalent (Shale , evaporite,...)
Hormuz Fm.

Structural Section "A"

0 5 10(Km)

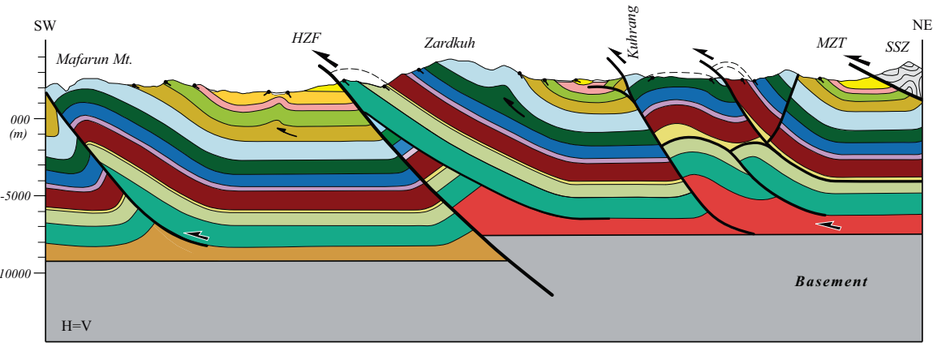

Bakhtyari Fm.
Miocene Fms. a. Mishan / Aghajari; b. Razak
Eo-Oligo - Miocene Carbonates (Jahrum /Shahbazan/Asmari)
U.Cretaceous-Paleocene Fms. (Gurpi / Pabdeh)
Bangestan Group (Kazhdumi/Sarvak/Ilam)
Garau Fm.
Surmeh Fm.
Trias.-Jur. Fms. (Khanehkat / Neyriz)
Permian Fms. (Faraghan / Dalan)
Ordovician Fms. (Ilbeyk / Zardkuh)
Cambrian Fms. a.Mila; b.(Barut / Zaigun / Lalun)
Hormuz equivalent (Shale , evaporite,...)
Hormuz Fm.

Structural Section "B"

0 5 10(Km)

B

Annex 4 : -A- Geological map of Baznavid and Zardkuh area (Western High Zagros) over SRTM data,
-B- Structural cross-sections . Sections "A" and "B" refer to Baznavid and Zardkuh respectively.

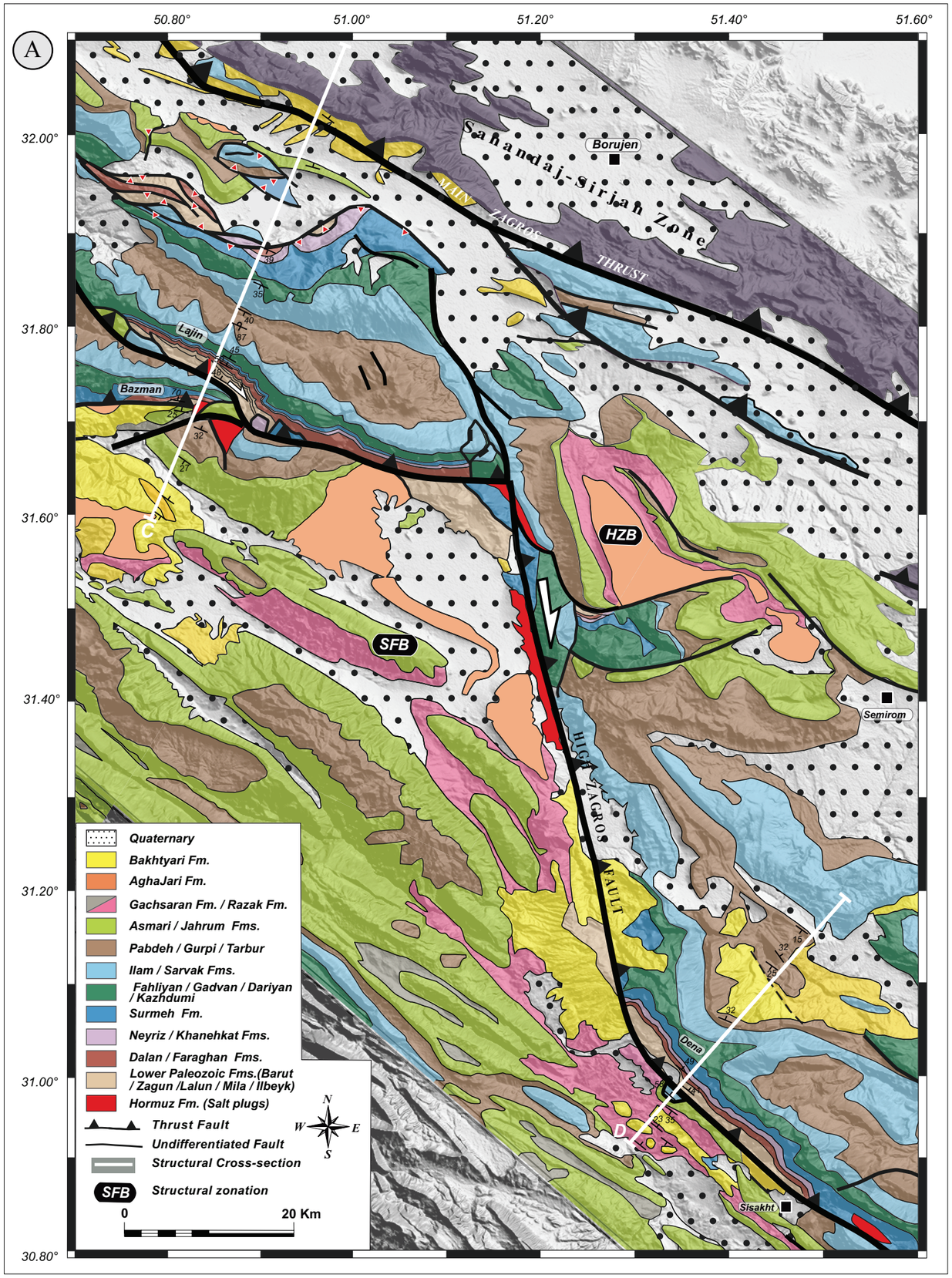

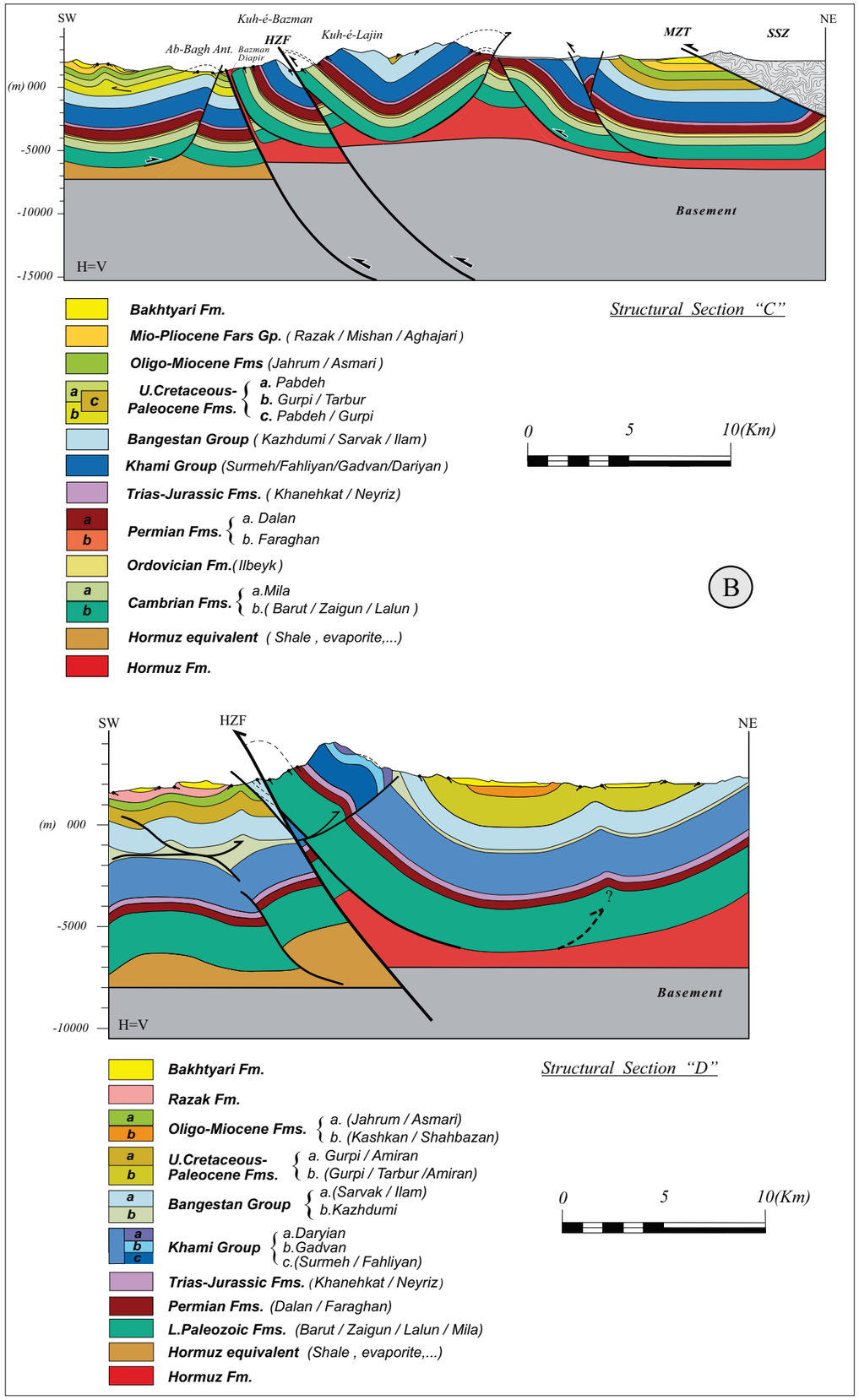

Annex 5 : -A- Geological map of Lajin and Dena area (Western High Zagros) over SRTM data, -B- Structural cross-sections . Sections "C" and "D" refer to Lajin and Dena respectively.

55° 30’ 55° 45’ 56° 00’ 56° 15’ 56° 30’ 56° 45’ 57° 00’

28°30’ 28°15’ 28°00’ 27°45’ 27°30’

0 20Km

N W E S

Annex 6-1: Geological map of Eastern area over SRTM data

Cret. volc. Qt. Bk U.Cret. Lmst CM Q Hs As-Ja PLz Flysch Ophiolite mélangé U.Cret. Gu Bgp Mz Pd-Gu Kgp-Bgp Ja Bgp. Qt. Gahkum Anticline Faraghan Ant. Kuh-e-Khush Ant. MAIN ZAGROS THRUST HIGH ZAGROS FAULT ZAGROS FAULT

Dasht-e Kanar Ant. Palangu Ant. Mirang Ant. Durs Ant. Finu Ant. Ahmadi Ant. Bongod Ant. Nandar Ant. Gardaneh Ant. Pazand Ant. Neyzeh Ant. Zarreh Kan Ant. Sarkha Ant. Namak (Khorgu) Ant. Aubad Ant. Sahra Ant. Mish Ant. Shamil Ant.

E F G

EXTERNAL UNITS

- Quaternary
- Bakhtyari Fm.
- Post As Fms. (Pre-Bakhtyari Fms)
- As-Ja Fm.
- Pd-Gu Fm.
- Mesozoic
- Upper Paleozoic
- Lower Paleozoic
- Hormuz Salt Plug

INTERNAL UNITS

- Upper Cret. Limestones
- Mesozoic Volcanics
- Ophiolite Melange
- Cret.-Miocene Flysch
- Plz Igneous Rocks
- Thrust Fault
- Inferred Fault
- Undiffrentiated Fault
- Anticline Axis with Plunge direction
- Syncline Axis

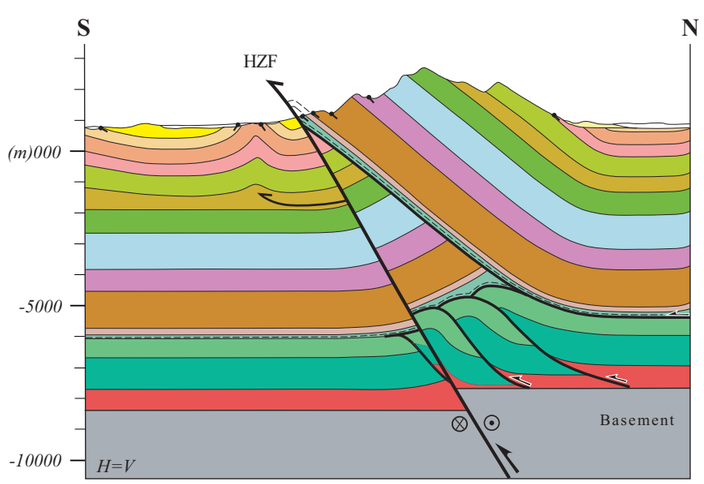

Section "E"

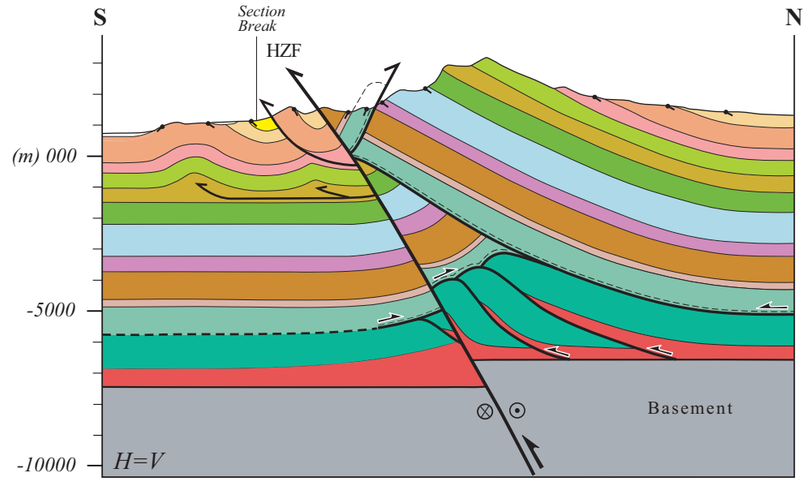

Section "F"

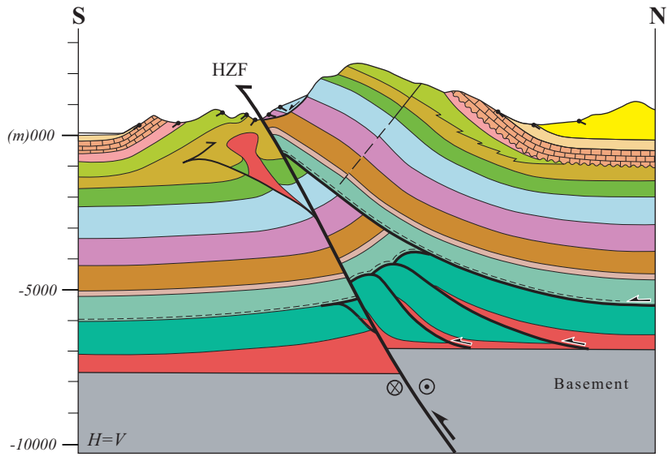

Section "G"

- Upper Miocene Aghajari Fm.
- Miocene Mishan Fm.
- Miocene Guri Member
- Miocene Razak Fm.
- Eocene / Olig-Miocene (Jahrum - Asmari) Fms.
- U.Cretaceous / Paleo-Eocene (Gurpi-Pabdeh) Fms.
- U.Cretaceous Bangestan Group (Kazhdumi/ Sarvak/ Ilam)Fms.
- U.Jur- L.Cret. Khami Group (Surmeh/ Hith/ Fahliyan/Gadvan/ Dariyan)Fms.
- Triassic - L. Jurassic (Khanekat / Neyriz) Fms.
- Permian (Faraghan - Dalan) Fms.
- Devonian Zakeen Fm.
- Hirnantian-Silurian (Dargaz/Sarchahan)Fms.
- Ordovician Syahoo Fm.
- Cambrian (Barut/zaigun/Lalun/Mila) Fms.
- U.Proterozoic / Early Cambrian Hormuz Fm.

Annex 6-2: Structural cross-sections . Sections "E", "F" and "G" refer to Gahkum, Faraghan and Kuh-e-Khush anticlines respectively

References

Abu-Ali M.A., Franz U.A., Shen J., Monnier F., Mahmoud M.D., Chambers T.M., 1991. Hydrocarbon Generation and Migration in the Paleozoic Sequence of Saudi Arabia. Society of Petroleum Engineers.

Adamia, S., Zakariadze, G., Chkhotua, T., Sadradze, N., Tsereteli, N., Chabukiani, A. and Gventsadze, A., 2011. Geology of the Caucasus: a review. *Turkish Journal of Earth Sciences*, **20**, 489-544. doi: 10.3906/yer-1005-11.

Agard, P., Omrani, J., Jolivet, L. and Mouthereau, F.,2005. Convergence history across Zagros (Iran): constraints from collisional and earlier deformation. *International Journal of Earth Sciences*, **94**, 401-419, doi 10.1007/s00531-005-0481-4

Agard, P., Omrani, J., Jolivet, L., Whitechurch, H., Vrielynck, B., Spakman W., Monié P., Meyer B. and Wortel R., 2011. Zagros orogeny:a subduction-dominated process, *Geological Magazine.* **148**, *692–725, doi: 10.1017/S001675681100046X*

Alavi, M.(compiler), 1991. Tectonic map of the Middle East: Geological Survey of Iran, scale1: 5,000,000.

Alavi, M., 1994. Tectonics of the Zagros orogenic belt of Iran: new data and interpretations. *Tectonophysics*, **229**, 211-238.

Alavi, M. 2004. Regional Stratigraphy of the Zagros fold-thrust belt of Iran and its proforeland evolution, Am. J. Sci., **304**, 1 – 20, doi:10.2475/ajs.304.1.1.

Al-Hadidy, A.H., 2007. Paleozoic stratigraphic lexicon and hydrocarbon habitat of Iraq. *Geoarabia*, **12**, 63-130.

Al-Laboun, A.A., 1988. The distribution of Carboniferous-Permian siliciclastic rocks in the greater Arabian Basin. *Geol. Soc. Am. Bull.,* **100**, 362-373.

AL Husseini, M.I., 1990. The Cambro-Ordovician Arabian and adjoining plates: a glacio-eustatic model. Journ. Petrol. Geol., **13**, 267–288.

Autran, A., Lefort, J.P., Debeglia, N., Edel, J.B., Vigneresse, J.L., 1994. Gravity and magnetic expression of terranes in France and their correlation beneath overstep sequences. In: Keppie, J.D. (Ed.), Pre-Mesozoic geology in France and related areas. Springer-Verlag, Berlin, Heidelberg, pp. 49-72.

Averbuch, O., Tribovillard, N., Devleeschouwer, X., Riquier, L., Mistiaen, B., van Vliet-Lanoe, B., 2005. Mountain building-enhanced continental weathering and organic carbon burial as major causes for climatic cooling at the Frasnian-Famennian boundary (c. 376 Ma)? *Terra Nova*, **17**, 25-34.

Avigad, D., Kolodner, K., McWilliams, M., Persing, H., Weissbrod, T., 2003. Origin of northern Gondwana Cambrian sandstone revealed by detrital zircon SHRIMP dating. *Geology*, **31**, 227–230

Baidder, L., Raddi, Y., Tahiri, M., Michard, A., 2008. Devonian extension of the Pan-African crust north of the West African craton, and its bearing on the Variscan foreland deformation: evidence from eastern Anti-Atlas (Morocco). *Geological Society, London, Special Publications,* **297**, 453-465.

Ballèvre, M., Bosse, V., Ducassou, C., Pitra, P., 2009. Palaeozoic history of the Armorican massif: Models for the tectonic evolution of the suture zones. *C.R. Geoscience,* **341**, 174-201.

Berberian, M. and King, GCP, 1981. Towards a paleogeography and tectonic evolution of Iran. Canadian Journal of Earth Sciences **18 (2)**, 210–265, doi:10.1139/e81-019

Berberian, M.,1995. Master "blind" thrust faults hidden under the Zagros folds: active basement tectonics and surface morphotectonics, *Tectonophysics,* **241**, 193-224.

Berkaloff, E., 1933.Contribution à l'étude géologique de l'extrême-sud tunisien. Le territoire militaire des Matmatas. *Bulletin de la Société Géologique de France*, **3**, 83-87.

Beyth, M., 1981. Paleozoic vertical movements in Um bogma area, southwestern Sinai. *AAPG Bull.,* **65(1)**, 160-165.

Blanc, E JP., Allen, MB. Inger, S. and Hassani, H., 2003. Structural styles in the Zagros simple folded zone, Iran, *Journal of the Geological Society, London,* **160**, 401–12.

Bojar, A.-V., Fritz, H., Kargl, S., Unzog, W. 2002. Phanerozoic tectonothermal history of the Arabian–Nubian shield in the Eastern Desert of Egypt: evidence from fission track and paleostress data. *Journal of African Earth Sciences*, **34**, 191-202.

Bonhomme, M.G., Fabre, J., Kaddour, M., 1996. Datations K-Ar d'événements varisques dans le Cambrien de l'Ougarta (Sahara occidental algérien). *Mém. Serv. Géol. Algérie*, **8**, 117-125.

Boote, D.R.D., Clark-Lowes, D.D., Traut, M.W., 1998. Paleozoic petroleum systems of North Africa, in Macgregor, D.S, Moody, R.T.J. & Clarke-Lowes, D.D. (eds), Petroleum Geology of North Africa. Geological Society, London, Sp. Publ. **132**, 7-68.

Bordenave, M. L., 2008, The origin of the permo-triassic gas accumulations in the iranian zagros foldbelt and contiguous offshore areas: a review of the palaeozoic petroleum system, *Journal of Petroleum Geology*, **31**(1), 3-42

Bordanave M.L., Hegre J.A., 2010. Current distribution of oil and gas fields in the Zagros Fold Belt of Iran and contiguous offshore as the result of the petroleum, (Geol. Soc., Lond., Spec. Publ.,2010, Tectonic and Stratigraphic Evolution of Zagros and Makran during the Mesozoic–Cenozoic edited by Leturmy, P. and Robin, B., V. **330**, pp. 353)

Bosold A, Schwarzhans W, Julapour A, Ashrafzadeh AR, Ehsani SM (2005). The structural geology of the High Central Zagros revisited (Iran), *Petroleum Geoscience*, **11**, 225–238.

Bosworth, W., El-Hawat, A.S., Helgeson, D.E. and Burke, K., 2008. Cyrenaican "shock absorber" and associated inversion strain shadow in the collision zone of northeast Africa. *Geology*, **36**, 695-698.

Bouaziz, S., 1995. Etude de la tectonique cassante dans la plate-forme et l'Atlas saharien (Tunisie méridionale) : évolution des paléo-champs de contraintes et implications géodynamiques. *Thèse d'Etat de l'Université de Tunis II*, 485 p.

Boudjema, A., 1987. Evolution structural du basin pétrolier triasique du Sahara nord oriental (Algérie). Unpublished PhD Thesis, Univ Paris-Sud (Orsay), 289 p.

Brew, G., Barazangi, M., Al-Maleh, A.K., Sawaf, T., 2001. Tectonic and Geologic evolution of Syria, *GeoArabia*, **6**, 573-616.

Brunet, M.F., Volozh, Y.A., Antipov M.P.,. Lobkovsky, L.I., 1999.The geodynamic evolution of the Precaspian Basin (Kazakhstan) along a north–south section. *Tectonophysics*, **313**, 85–106.

Burkhard, M., Caritg, S., Helg, U. Robert-Charrue, C., Soulaimani, A., 2006. Tectonics of the Anti-Atlas of Morocco. *C.R. Geoscience*, **338**, 11-24.

Buslov, M.M., Watanabe, T., Fujiwara, Y., Iwata, K., Smirnova, L.V., Yu Safonova, I., Semakov, N.N., Kiryanova, A.P., 2004. Late Paleozoic faults of the Altai region, Central Asia: tectonic pattern and model of formation. *J. Asian Earth Sci.,* **23**, 655-671.

Callot, J. P., S. Jahani, and J. Letouzey, 2007. The role of pre-existing diapirs in fold and thrust belt development, in Thrust Belt and Foreland Basin, edited by O. Lacombe et al., pp. 307 – 323, Springer, Berlin.

Caputo, M.V., Crowell, J.C., 1985. Migration of glacial centers across Gondwana during Paleozoic Era. *Geological Society of America Bulletin*, **96**, 1020-1036.

Carminati, E., 2009. Neglected basement ductile deformation in balanced-section restoration: An example from the Central Southern Alps (Northern Italy), Tectonophysics, doi:10.1016/j.tecto.2008.09.042

Catuneanu, O., Wopfner, H., Eriksson, P.G., Cairncross, B., Rubidge, B.S., Smith, R.M.H., Hancox, P.J., 2005. The Karoo basins of south-central Africa. *Journal of African Earth Sciences*, **43**, 211–253.

Clauer, N., Jeannette, D., Tisserant, D., 1980. Datation isotopique des cristallisations successives du socle cristallin et crystallophyllien de la Haute Moulouya (Maroc Hercynien). *Geol. Runsch*., **69**, 68-83.

Colman-Sadd, S. P., 1978, Fold development in Zagros simply folded belt, southwest Iran, AAPG Bull., **62**, 984 – 1003.

Copper, P., 1986. Frasnian/Famennian mass extinction and cold-water oceans. *Geology*, 14, 835–839.

Coster, H.P., 1947, Terrestrial heat flow in Persia, *Mon. Not. R. Astr. Soc. Geophys. Suppl*, **5**, 131-145.

Cotton, J. T., and H. A. Koyi , 2000. Modelling of thrust fronts above ductile and frictional detachments: Application to structures in the Salt Range and Potwar Plateau, Pakistan, Geol. Soc. Am. Bull., **112**, 351 – 363.

Courtillot, V., Kravchinsky, V.A., Quidelleur, X., Renne, P.R., Gladkochub, D.P., 201O.Preliminary dating of the Viluy traps (Eastern Siberia): Eruption at the time of LateDevonian extinction events? Earth and Planetary *Science Letters*, **300**, 239–245

Craig, J., Rizzi, C., Said, F., Thusu, B., Luning, S., Asbali, A.I., Keeley, M.L., Bell, J.F., Durham, M.J., Eales, M.H., Beswetherick, S., Hamblett, C., 2008. Structural Styles and Prospectivities in the Precambrian and Paleozoic Hydrocarbon Systems of North Africa, Geology of East Lybia, vol. **4**, 51-122.

Dahlstrom, C.D.A., 1969. Balanced cross sections, Canadian Journal of Earth Sciences., **6**, 743 – 757.

Dallmeyer, R.D., Martinez Catalan, J.R., Arenas, R., Gil Ibarguchi, J.I., Guttierez Alonso, G., Farias, P., Aller, J., Bastida, F., 1997. Diachronous Variscan tectonothermal activity in the NW Iberian Massif: Evidence from $^{40}Ar/^{39}Ar$ dating of regional fabrics. *Tectonophysics*, **277**, 307-337.

Davis, D.M., and R.J. Lillie,1994. Changing mechanical response during continental collision: Active examples from the foreland thrust belts of Pakistan, J. Struct. Geol., **16**, 21 – 34.

Davis, D.M., and T. Engelder, 1985. The role of salt in fold-and-thrust belts, Tectonophysics, **119**, 67–88.

Dixon, D.J., Moore, J.K.S., Bourne, M., Dunn, E., Haig, D.B., Hossack, J., Roberts, N., Parsons, T., Simmons, C.J., 2010. Integrated petroleum systems and play fairway analysis in a complex Paleozoic basin: Ghadames-Illizi Basin, North Africa. *Petroleum Geology Conference series*, **7**, 735-760. Doi: 10.1144/0070735.

Djellit, H., Bellon, H., Ouabadi, A., Derder, M.E.M., Henry, B., Bayou, B., Khaldi, A., Baziz, K., Merahi, M. K., 2006. Âge 40K/40Ar, Carbonifère inférieur, du magmatisme basique filonien du synclinal paléozoïque de Tin Serririne,Sud-Est du Hoggar (Algérie). *C. R. Geoscience*, **338**, 624–631.

Dodson, M., 1973, Closure Temperature in Cooling Geochronological and Petrological Systems, *Contr. Mineral. and Petrol.*, **40**, 259—274

Echarfaoui, H., Hafid, M., Aït Salem, A., 2002. Structure sismique du socle paléozoïque du bassin des Doukkala, Môle côtier, Maroc occidental. Indication en faveur d'une phase éo-varisque. *C.R. Geoscience*, **334**, 13-20.

Ehsanbakhsh-Kermani et al. (1996) *Geological map of Ardal, 1:100,000,* Gelogical Survey of Iran Ed.

Emami H., Vergés J., Nalpas T., Gillespie P., Sharp I., Karpuz R., Blanc E. P. and Goodarzi M.G.H., 2010. Structure of the Mountain Front Flexure along the Anaran anticline in the Pusht-e Kuh Arc (NW Zagros, Iran): insights from sand box models, (Geol. Soc., Lond., Spec. Publ., 2010, Tectonic and Stratigraphic Evolution of Zagros

and Makran during the Mesozoic–Cenozoic edited by Leturmy, P. and Robin, B., V. **330**, pp. 353).

Eschard, R., Braik, F., Bekkouche, D., Ben Rahuma, M., Desaubliaux, G., Deschamps, R., Proust, J.N., 2011. Paleohighs : their influence on the Northern African Palaezoic petroleum systems. In Vinning, B.A. & Pickering, S.C. (eds)Petroleum Geology: From Mature Basins to New Frontiers-Proceedings of the 7th Petroleum Geology Conference (published by the Geological Society, London), 707-724.

Espitalié, J., Deroo,G., Marquis, F., 1985, La pyrolyse Rock-eval et ses applications, première partie, *Revue de l'institut français du pétrole*, **40** (5), 563-579

Espitalié, J., Deroo,G., Marquis, F., 1985, La pyrolyse Rock-eval et ses applications, deuxième partie, *Revue de l'institut français du pétrole*, **40** (6), 755-784

Espitalié, J., Deroo,G., Marquis, F., 1985, La pyrolyse Rock-eval et ses applications, troisième partie, *Revue de l'institut français du pétrole*, **41** (1), 73-89

Evans,N.J., Byrne, J.P., Keegan, J.T., Dotter, L.E., 2005, Determination of uranium and thorium in Zircon, apatite, and fluorite: Application to laser (U-Th)/He thermochronology, *Journal of analytical chemistry*, **60** (12), 1159-1165

Evers, H.J.; Fakhari, M. and Verall, P., 1977, The Geology of the Surmeh and Surrounding Structures, Fars North area. NIOC internal Report N° 1251

Fabre, J., 2005. Géologie du Sahara occidental et central. Tervuren Afr. Geosci. Coll., 108, 572 pp.

Fakhari, M., G. J. Axen, B. K. Horton, J. Hassanzadeh, and A. Amini, 2008, Revised age of proximal deposits in the Zagros foreland basin and implications for Cenozoic evolution of the High Zagros, Tectonophysics, **451**, 170–185, doi:10.1016/j. tecto.2007.11.064.

Falcon N.L., 1974 Southern Iran: Zagros Mountains. *In:* (eds) *Mesozoic – Cenozoic orogenic belts*. Geological Society, London, Special Publications, **4**, 199–211, doi:10.1144/GSL.SP.2005.

Faqira M, Rademakers M, Afifi A.M. 2009. New insights into the Hercynian Orogeny, and their implications for the Paleozoic Hydrocarbon System in the Arabian Plate. *GeoArabia*, **14**, 3, 199-228.

Farley K., Wolf R. et Silver L., 1996, The effects of long alpha-stopping distances on (U-Th)/He ages, *Geochimica et Cosmochimica Acta*, **60**(21), 4223–4229.

Farley, K.A., 2002, (U-Th)/He Dating: Techniques, Calibrations, and Applications, *Reviews in Mineralogy and Geochemistry*, **47** (1), 819-844

Faure, M., Bé Mézème E., Cocherie, A., Rossi, P., Chemenda, A., Boutelier, D., 2008. Devonian geodynamic evolution of the Variscan belt, insights from the French Massif Central and Massif Armoricain. *Tectonics*, **27**, TC2005, doi: 10.1029/2007TC002115.

Fleitout, L., Froidevaux, C., 1982. tectonics and topography for a lithosphere containing density heterogeneity. *Tectonics*, **1**, 21–56.

Franke, W., 2000. The mid-European segment of the Variscides: tectonostratigraphic units, terrane boundaries and plate tectonic evolution. In: Franke, W., Haak, V., Oncken, O., Tanner, D. (Eds.), Orogenic Processes: quantification and Modelling in the Variscan Belt. *Geological Society, London, Special Publications*, **179**, pp. 35-61.

Franke, W., 2006. The Variscan orogen in Central Europe: construction and collapse. In: Gee, D.G., Stephenson, R.A. (Eds.), European Lithosphere Dynamics. *Geological Society, London, Memoirs* **32**, pp. 333-343.

Frizon de Lamotte, D., Leturmy, P., Missenard, Y., Khomsi, S., Ruiz, G., Saddiqi, O., Guillocheau, F., Michard, A., 2009. Mesozoic and Cenozoic vertical movements in the Atlas system (Algeria, Morocco, Tunisia): An overview. *Tectonophysics*, **475**, 9-28.

Frizon de Lamotte, D., Saint-Bezar, B., Bracene, R. and Mercier, E., 2000. The two main steps of the Atlas building and Geodynamics of West Mediterranean, *Tectonics*, **19**, 740-761.

Frizon de Lamotte, D. and Raulin, C., 2010. The sedimentary basins and margins in Tectonic Map of Africa at 1 : 10M scale, Milesi J.P., Frizon de Lamotte, D., De Kock, G. and Toteu, F., CGMW ed.

Frizon de Lamotte, D., Raulin, C., Mouchot, N., Wrobel-Daveau, J.C., Blanpied, C., Ringenbach, J.C., 2011. The southernmost margin of the Tethys realm during the Mesozoic and Cenozoic: Initial geometry and timing of the inversion processes, *Tectonics,* **30**, TC3002, doi: 10.1029/2010TC002691.

Galeazzi, S., Point, O., Haddadi, N., Mather, J., Druesne, D., 2010. Regional Geology and petroleum systems of the Illizi-Berkine area of the Algerian Saharan Platform: An overview*. Marine and Petroleum Geology*, **27**, 143-178.

Gautheron, C., Tassan-got, L., Ketcham, R.A. and Dobson, K.J., 2012, Accounting for long alpha-particle stopping distances in (U-Th-Sm)/He geochronology: 3D modeling of diffusion, zoning, implantation, and abrasion*, review at GCA.*

Gavillot Y., Axen G.J., Stockli D.F., Horton B.K, and Fakhari M., 2010. Timing of thrust activity in the High Zagros fold-thrust belt, Iran, from (U-Th)/He thermochronometry. Tectonics,**29**, TC4025. doi:10.1029/2009TC002484

Ghavidel-syooki M., 2003. Palynostratigraphy of Devonian sediments in the Zagros Basin, southern Iran. Review of Paleobotany and Palynology **127**, 241–268. doi:10.1016/S0034-6667(03)00122-2

Ghavidel-syooki M., 2005. Palynological study and age determination of Faraghan Formation in Kuh-e-Gahkum region at southeast of Iran. In: (eds) Contributions to the paleopalynology of Paleozoic rock units in the Zagros, Alborz and Central Iranian Basin, published book, 15–34 in Persian.

Ghavidel-syooki M., 2005a. Palynological study and age determination of Faraghan Formation in Kuh-e-Gahkum region at southeast of Iran, *In:* (eds) *Contributions to*

the Paleopalynology of Paleozoic Rock Units in the Zagros, Alborz and Central Iranian Basin, 15-34, in Persian

Ghavidel-syooki M. 2005b. Palynological study and age determination of Ordovician sediments and Faraghan Formation in Kuh-e-Surmeh at southern Iran. In: (eds) Contributions to the paleopalynology of paleozoic rock units in the Zagros, Alborz and Central Iranian Basin, published book, 96–104 in Persian

Ghavidel-syooki M, Álvaro JJ, Popov L, Ghobadi Pour M, Ehsani MH, Suyarkova A., 2011. Stratigraphic evidence for the Hirnantian (latest Ordovician) glaciation in the Zagros Mountains, Iran.Palaeogeography, Palaeoclimatology, Palaeoecology 307:1–16.doi:10.1016/j.palaeo.2011.04.011

Ghienne, J.F., Boumendiel, K.B., Paris, F. Videt, B., Racheboeuf, P., Ait Salem, H., 2007. The Cambrian-Ordovician succession in the Ougarta Range (western Algeria, North Africa) and interference of the Late Ordovician glaciation on the development of the Lower Palaezoic transgression on northern Gondwana. *Bulletin of Geoscience*, **82**, 183-214.

Ghienne, J.F., Monod, O., Kozlu, H., Dean, W.T., 2010. Cambrian-Ordovician depositional sequences in the Middle East: A perspective from Turkey. *Earth Science Reviews*, **101**, 101-146.

Golonka, J., Ross, M.I., Scotese, C.R., 1994. Phanerozoic paleogeographic and paleoclimatic modelling maps. In: Embry, A.F., Beauchamp, B., Glass, D.J. (Eds.), Pangea: Global Environments and Ressources*. Can. Soc. Petrol. Geol*., **17**, 1-47.

Gouzia, M., 2011. Mesozoic Source-to-Sink Systems in NW Africa, Geology of the vertical movements during the birth and growth of the Moroccan rifted margin. PhD Thesis, Vrije Universiteit Amsterdam. 170 p.

Guimerà, J., Arboleya, M.L., Teixell, A., 2011. Structural control on present-day topography of a basement massif: the Central and Eastern Anti-Atlas (Morocco), Geoilogica Acta, **9**, 55-65.

Guiraud, R., Bosworth, W., Thierry, J. and Delplanque, A., 2005. Phanerozoic geological evolution of Northern and Central Africa: An overview. *Journal of African Earth Sciences*, **43**, 83-143.

Gvirtzman. G. and Weissbrod, T., 1984. The Hercynian Geanticline of Helez and the Late Palaeozoic history of the Levant. *Geological Society, London, Special Publications*, **17**, p. 177-186.

Haddoum, H., Guiraud, R., Moussine-Pouchkine, A., 2001. Hercynian compressional deformations of the Ahnet-Mouydir Basin, Algerian Saharan Platform : far-field stress effects of the Late Palaezoic orogeny. *Terra Nova*, **13**, 220-226.

Hatzfeld, D., Authemayou, C., van der Beek, P., Bellier, O., Lavé, J., Oveisi, B., Tatar, M., Tavakoli, F.,. Walpersdorf A. and F. Yamini-Fard., 2010, The Kinematics of the Zagros Mountaines (Iran), Geol. Soc., Lond., Spec. Publ.,2010, Tectonic and Stratigraphic Evolution of Zagros and Makran during the Mesozoic–Cenozoic edited by Leturmy, P. and Robin, B., V. **330**, pp. 353

Haynes, S. J. and McQuillan, H., 1974. Evolution of the Zagros Suture Zone, Southern Iran. *Geol. Soc. Am. Bull.* **85**, 739-744.

Hervouet, Y. et Duée G., 1996. Analyse morphostructurale par imagerie satellitaire et coupes structurales modélisées des monts d'Ougarta (Sahara occidental, Algérie) : une chaîne hercynienne chevauchante à plis passifs. *Mém. Serv. Géol. Algérie*, **8**, 127-173.

Hessami, K., Koyi H. A., Talbot C. J., Tabasi H., and Shabanian E., 2001. Progressive unconformities within an evolving foreland fold-thrust belt, Zagros Mountains, J. Geol. Soc. London, **158**, 969 – 981.

Homke,S., Vergés,J., Garcés,M., Emami,H. and Karpuz,R. 2004. Magnetostratigraphy of Miocene–Pliocene Zagros foreland deposits in the front of the Pusht-e Kuh Arc (Lurestan Province, Iran). Earth and Planetary Science Letters, **225**, 397_410

Homke, S., Verges, J., Serra-Kiel, J., Bernaola, G., Sharp, I., Garces, M., Monteroverdu, I., Karpuz, R., Goodarzi ,M.H., 2009. Late Cretaceous – Paleocene formation of the proto-Zagros foreland basin, Lurestan province, SW Iran. Geol Soc Am Bull. doi:910.1130/B26035.26031

Homza, T. X. & Wallace, W. K. 1997. Detachment folds with fixed hinges and variable detachment depth, northeastern Brooks Range, Alaska. *J. Struct. Geol.* **19(3-4)**, 337-354.

Horton, B.K., Hassanzadeh, J, Stockli, D.F., Axen, G.J., Gillis, R.J., Guest, B., Amini, A., Fakhari, M.D., Zamanzadeh, S.M., Grove, M., 2008. Detrital zircon provenance of Neoproterozoic to Cenozoic deposits in Iran: Implications for chronostratigraphy and collisional tectonics, *Tectonophysics*, 451, 97–122, doi:10.1016/j.tecto.2007.11.063

Hourigan J., Reiners P., Brandon M., 2005. U-Th zonation-dependent alpha-ejection in (U-Th)/He chronometry, *Geochimica et Cosmochimica Acta*, **69**(13), 3349–3365.

Houseknecht D. W., Weesner, C.M.B., 1997, Rotational reflectance of dispersed vitrinite from the Arkoma basin**,** *Organic Geochemistry,* **26** (3/4), 191-206

Huon, S., Piqué A., Clauer N., 1987. Etude de l'orogenèse hercynienne au Maroc par la datation K/Ar de l'évolution métamorphique de schistes ardoisiers, *Sci. Géol. Bull. Strasbourg,* **40**, 273–284.

Insalaco, E, Virgone, A, Courme, B, Gaillot, J, Kamali, M, Moallemi, A, Lotfpour, M, Monibi, S. 2006. Upper Dalan Member and Kangan formations between Zagros Mountains and offshore Fars,Iran: depositional system, biostratigraphy and stratigraphic architecture, *GeoArabia*, **11**, 2, 75-176.

Isaacson, P.E., Diaz-Martinez, E., Grader, G.W., Kalvoda, J., Babek, O., Devuyst, F.X., 2008. Late Devonian-earliest Mississippian glaciation in Gondwanaland and its biogeographic consequences. *Palaeogeography, Palaeoclimatology, Palaeoecology*, **268**, 126-142.

Jahani, S, Callot, J.P., Letouzey, J. and Frizon de Lamotte, D. 2009. The eastern termination of the Zagros Fold-and-Thrust Belt, Iran: structures, evolution, and relationships between salt plugs, folding, and faulting. Tectonics **28**, TC6004. doi:10.1029/2008TC002418

James, G.A., and Wynd, J.G., 1965. Stratigraphic nomenclature of Iranian Oil Consortium Agreement area. Am. Assoc. Pet. Geol. Bull. 49, 2182–2245.JOLIVT, L., and FACCENNA C. 2000. Mediterranean extension and the Africa-Eurasia collision, Tectonics, **19**, 1095–1106, doi:10.1029/2000TC900018.

Jiménez, A., Iglesias, M.J., Laggoun-Defarge, F. and Suarez-Ruiz, I., 1999, Effect of the increase in temperature on the evolution of the physical and chemical structure of vitrinite. *Journal of Analytical and Applied Pyrolysis*, **50**, 117-148.

JOGMEC-TRC, 2005, Geochemical evaluation and basin modeling in the Zagros Basin of Iran – Source rock potential of the Paleozoic sequence, **Part 4,**

Johnson, C.A., 2008, Phanerozoic Plate Reconstructions of the Middle East: Insights into the Context of Arabian Tectonics and Sedimentation. SPE 118062.

Jongsma, D., Van Hinte, J. E., Woodside, J.M., 1985. Geologic structure and neotectonics of the North African Continental Margin south of Sicily. *Marine and Petroleum Geology*, **2**, 2, 156-179.

Kazmin, V.G. 2002. The Late Paleozoic to Cenozoic intraplate deformation in North Arabia: A response to plate boundary-forces, EGU Stephan Mueller Spec. Publ. Ser., **2**, 123–138, doi:10.5194/smsps-2-123-2002.

Karweil, J., 1955. Die Metamorphose der Kohlen vom Standpunkt der physicalischen chemie. *Zeitschrift der Deutschen Geologischen Gesellschaft,* **107**, 132–139.

Ketcham R. A., Gautheron C, Tassan-Got L., 2011, Accounting for long alpha-particle stopping distances in (U–Th–Sm)/He geochronology: Refinement of the baseline case, Geochimica et Cosmochimica Acta, **75,** 7779–7791

Keeley, M. L. and Massoud M. S., 1998. Tectonic controls on the petroleum geology of NE Africa, in D. S. MacGregor, R. T. J. Moody and D. D. Clark-Lowes (eds.), Petroleum geology of North Africa: *Geological Society Special Publication*, **132**, 69-78.

Keeley, M.L., 1989. The Paleozoic history of the Western Desert of Egypt. *Basin Research*, **2**, 35-48.

Keeley, M.L., Dungworth, G., Floyd, C.S., Forbes, G.A., King, C., McGarva, R.M. and Shaw, D., 1990. The Jurassic System in Northern Egypt .1. Regional Stratigraphy and Implications for Hydrocarbon Prospectivity. *Journal of Petroleum Geology*, **13**, 397-420.

Keeley, M.L., 1994. Phanerozoic evolution of the basins of Northern Egypt and adjacent areas. *Geol Rundsch*, **83**, 728-742.

Kent, P. E., 1979. The emergent Hormuz salt diapirs of southern Iran, J. Pet. Geol., **2**, 117 – 144, doi:10.1111/j.1747-5457.1979.tb00698.x

Kheradpir, A., Khalili M. 1972. *Brief notes on facies and age relationships of the pre-Sarvak section in Dina/Zardkuh area*, Iranian Oil Operating Companies, *Technical Memo* # **115**.

Klett, T.R., 2001. Total Petroleum Systems of the Pelagian Province, Tunisia, Libya, Italy and Malta --The Bou Dabbous -- Tertiary and Jurassic-Cretaceous Composite. *U.S. Geological Survey Bulletin*, 2202-D.

Kohn BP, Eyal M, Feinstein S.,1992. A major late Devonian-early carboniferous (Hercynian) thermotectonic event at the new margin of Arabian – Nubian shield: evidence from Zircon fission track dating. *Tectonics*, **11**, 1018-1027.

Kolodner, K., Avigad, D., McWilliams, M., Wooden, J.L., Weissbrod, T.,Feinstein, S., 2006. Provenance of north Gondwana Cambrian–Ordovician sandstone: U–Pb SHRIMP dating of detrital zircons from Israel and Jordan.*Geological Magazine*, **143**, 367–391

Konert G, Afifi A.M., Al-Hajri S.A. and Drost H.J. 2001. Paleozoic stratigraphy and hydrocarbon habitat of the Arabian plate. GeoArabia **6 (3)**, 407–442

Koop W.J. and Stoneley R., 1982. Subsidence history of the Middle East Zagros Basin, Permian to Recent. Philos Trans Royal Soc London, Ser **A 305**, 149–168. doi:10.1098/rsta.1982.0031

Kraml M., Pik R., Rahn M., Selbekk R., Carignan J. et Keller J., 2006, A new multi-mineral age reference material for $^{40}Ar/^{39}Ar$, (U-Th)/He and Fission Tarck dating methods : the Limberg t3 Tuff, *Geostandards and Geoanalytical Research*, **30**(2), 73–86.

Lardeaux, J.M., Ledru, P., Daniel, I., Duchene, S., 2001. The Variscan French Massif Central- a new addition to the ultra-high pressure metamophic “club”: exhumation processes and geodynamic consequences. *Tectonophysics*, **332**, 143-167.

Le Goff, E., Guerrot, C., Maurin, G., Johan, V., Tegyey M., Ben Zarga, M., 2001. Découverte d’éclogites hercyniennes dans la chaîne septentrionale des Mauritanides (Afrique de l’Ouest). *C. R. Acad. Sci. Paris*, **333**, 711-718.

Lecorché, J-P., Bronner, G., Dallmeyer, R.D., Rocci, G., Roussel, J., 1991. The Mauritanide orogen and its northern extensions (western Sahara and Zemmour), West Africa. In: Dallmeyer, R.D., Lecorché J-P. (Eds.), The West African orogens and Circum-Atlantic Correlatives. Springer-Verlag, Berlin, 187-227.

Ledru, P., Lardeaux, J.M., Santallier, D., Autran, A., Quenardel, J.-M., Floc’h, J.-P., Lerouge, G., Maillet, N., Marchand, J., Ploquin, A., 1989. Où sont les nappes dans le Massif central français. *Bull. Société Géologique de France*, 8 (V), 605-618.

Letouzey, J., Colletta B., Vially R., and. Chermette J. C, 1995. Evolution of salt-related structures in compressional settings, in Salt Tectonics: A Global Perspective, edited by M. P. A. Jackson, D. G. Roberts, and S. Snelson, AAPG Mem., **65**, 41 – 60.

Letouzey J, Sherkati S, 2004. Salt Movement, Tectonic Events, and Structural Style in the Central Zagros Fold and Thrust Belt (Iran), *in*: *Salt sediments interactions and*

hydrocarbon prospectivity, 24th Annual GCSSEPM Foundation, Bob F. Perkins Research Conference, Houston, Texas.

Leturmy P., Molinaro M. and Frizon de Lamotte D., 2010. Structure, timing and morphological signature of hidden reverse basement faults in the Fars Arc of the Zagros (Geol. Soc., Lond., Spec. Publ.,2010, Tectonic and Stratigraphic Evolution of Zagros and Makran during the Mesozoic–Cenozoic edited by Leturmy, P. and Robin, B., V. **330**, pp. 353

Mahmoud M.D., Vaslet D., Husseini, M.I. 1992. The Lower Silurian Qalibah Formation of Saudi Arabia. AAPG Bulletin, **76**, 1491–1506.

Mahmoud, A. and El Barkooky, A., 1998. Mesozoic valley fills incised in Paleozoic rocks potential exploration targets in the north Western Desert of Egypt, Obaiyed Area, EGPC 14th Petroleum Conference, Cairo.

Maluski, H., Patocka, F., 1997. Geochemistry and $^{40}Ar/^{39}Ar$ geochronology of the mafic metavolcanic rocks from the Richory Mountains complex (West Sudetes, Bohemian massif): paleotectonic significance. *Geol. Mag.,* **134**, 703-716.

Martinez Catalan, J.R., Arenas, R., Abati, J., Sanchez Martinez S., Diaz Garcia F., Fernandez Suarez J., Gonzalez Cuadra P., Castineiras P., Gomez Barreiro J., Diez Montes A., Gonzalez Clavijo E., Rubio Pascual, F.J., Andonaegui, P., Jeffries, T.E., Alcock, J.E., Diez Fernandez R., Lopez Carmona, A., 2009. A rootless suture and the loss of the roots of a mountain chain: The Variscan belt of NW Iberia. *C.R. Geoscience*, **341**, 114-126.

Mathieu, G., 1949. Contribution à l'étude des Monts Troglodytes dans l'Extrême Sud Tunisien. *Ann. Mines et Géol.*, Tunis, **4**, 82 p.

Matte, P., 1986. Tectonics and plate tectonics model for the Variscan belt in Western Europe. *Tectonophysics*, **126**, 329-374.

Matte, P. and Hirn, A., 1988. Seismic signature and tectonic cross section of the Variscan crust in Western France. *Tectonics*, **7**, 141-155

Matte, P., 1998. Continental subduction and exhumation of HP rocks in Paleozoic orogenic belts: Uralides and Variscides. *GFF 120*, 209-222.

Matte, P., 2001. The Variscan collage and orogeny (480-290 Ma) and the tectonic definition of the Armorica microplate: a review. *Terra Nova*, **13**, 122-128.

McClay, K.R. 2000, Structural Geology for Petroleum Exploration, pp 355-369
Merle, O., 2011. A simple continental rift classification. *Tectonophysics*, **513**, 88–95.

McDowell, F.W., McIntosh, W.C., Farley, K.A., 2005, A precise $^{40}Ar–^{39}Ar$ reference age for the Durango apatite (U–Th)/He and fission-track dating standard, *Chemical Geology*, **214** (3-4), 249-263

Michard, A. Hoepffner, C. Soulaimani, A., Baider, L., 2008. The Variscan Belt, *in* « Continental Evolution: the Geology of Morocco », Michard, A., Saddiqi, O., Chalouan, A., Frizon de Lamotte, D. eds. Springer, 65-132.

Michard A, Soulaimani A, Hoepffner C, Ouanaimi H, Baidder L, Rjimati EC, Saddiqi O 2010. The South-Western Branch of the Variscan Belt: Evidence from Morocco, *Tectonophysics,* **492**, 1-24.

Missenard, Y., Zeyen, H., Frizon de Lamotte, D., Leturmy, P., Petit, C. and Sébrier, M., Saddiqi, O., 2006. Crustal versus Asthenospheric origin of the Relief of the Atlas Mountains of Morocco. *Journal of Geophysical Research*, **111**, B03401, doi: 10.1029/2005JB003708.

Mitra, S. 2002. Structural models of faulted detachment folds, AAPG bulletin, **86(9)**, 1673-1694.

Mitra, S. 2003. A unified kinematic model for the evolution of detachment folds, Journal of Structural Geology, **25(10)**, 1659-1673.

Mizens, G.A. 2004. Devonian palaeogeography of the Southern Urals. *Geol. Quarterly*, **48**, 205-216.

Molinaro, M., Leturmy, P., Guezou, J.C., Frizon de Lamotte, D. and Eshraghi, S.A., 2005a. The structure and kinematics of the southeastern Zagros fold-thrust belt, Iran: from thin-skinned to thick-skinned tectonics. Tectonics, **24**, TC3007. doi:10.1029/ 2004TC001633

Molinaro, M., H. Zeyen, Laurencin, X., 2005b. Lithospheric structure beneath the south-eastern Zagros Mountains, Iran: Recent slab breakoff? *Terra Nova*, 17, 1–6, doi:10.1111/j.1365-3121.2004.00575.x.

Moreau, J., Ghienne, J.F., Hurst, A., 2012. Kilometric-scale sand injectites in the intracratonic Murzuq Basin (south-west Libya): an igneous trigger ? *Sedimentology*, **59**, 1321-1344.

Motamedi, H., Sepehr, M., Sherkati, S., Pourkermani, M. 2011. Multi-phase hormuz salt diapirism in the Southern Zagros, SW Iran, *Journal of Petroleum Geology*, **34**, 29-44

Motiei, H. 1993. Stratigraphy of Zagros (in Persian). Geological Survey of Iran, Tehran, 536 pp

Motavalli-Anbaran, S.H., Zeyen, H., Brunet, M.F., Ardestani, V.E., 2011, Crustal and lithospheric structure of the Alborz Mountains, Iran, and surrounding areas from integrated geophysical modeling, *Tectonics*, **30**.

Mouthereau, F., Lacombe, O., Tensi, J., Bellahsen, N., Kargar, S., Amrouch, K. 2007. Mechanical constraints on the development of The Zagros Folded Belt (Fars), *in:* Lacombe, O. et al. *Thrust Belts and Foreland Basins: From Fold Kinematics to Hydrocarbon Systems*. Springer, New York. pp. 245-264.

Mouthereau, F., Tensi, J., Bellahsen, N., Lacombe, O. Deboisgrollier, T. and Kargar, S., 2007. Tertiary sequence of deformation in a thin-skinned/thick-skinned collision belt: the Zagros Folded Belt (Fars, Iran). *Tectonics,* **26**, TC5006, doi:10.1029/2007TC002098

Mouthereau, F., 2011. Timing of uplift in the Zagros belt/Iranian plateau and accommodation of late Cenozoic Arabia/Eurasia convergence. In: Lacombe, O., Grasemann, B., Simpson, G. (Eds.), Geodynamic Evolution of the Zagros. Geological Magazine,pp. 726–738.

Mouthereau, F., Lacombe, O. and Vérges, J., 2012. Building the Zagros collisional orogen: Timing, strain distribution and the dynamics of Arabia/Eurasia plate convergence, Tectonophysics, doi:10.1016/j.tecto.2012.01.022

Murphy, J.B., Keppie, J.D, 1998. Late Devonian palinspastic reconstruction of the Avalon-Meguma terrane boundary: implication for terrane accretion and basin development in the Appalachian orogen. *Tectonophysics,* **284**, 221-231.

Murphy, J.B., Guttierrez-Alonso, G., Nance, R.D., Fernandez-Suarez, J., Keppie, J.D., Quesada, C., Dostal, J., Braid, J., 2009. Rheic Ocean mafic complexes : overview and synthesis. In: Murphy, J.B., Keppie, J.D.., Hynes, A.J. (Eds.), Ancient Orogens and Modern Analogues. *Geological Society, London, Special Publication* **327**, 343-369.

Nasdala L, Wenzel M, Vavra G, Irmer G, Wenzel T, Kober B , 2001. Metamictization of natural zircon: accumulation versus thermal annealing of radioactivity-induced damage. *Contrib Mineral Petrol* **141**, 125–144

Nasdala L, Reiners PW, Garver JI, Kennedy AK, Stern RA, Balan E, Wirth R, 2004, Incomplete retention of radiation damage in zircon from Sri Lanka*. Am Mineral* **89**,219-231

National Iranian Oil Company (NIOC), 1975. Geological cross-section south-central Iran, Scale: 1:500000, Unpublished

Nicole, GL, Kheradpir, A. 1972. *Stratigraphic Column, # 20509-95, Kuh-e Gereh*, Oil Service Company of Iran.

O'Brien, C.A.E., 1950. Tectonic problems of the oilfield belt of southwest Iran. In: 18th International Geological Congress, Proceedings, Great Britain.

O'Brien, C. A. E. 1957. Salt diapirism in south Persia,Geol. Mijnbouw, **19**, 357 – 376.

Oukassou, M., Saddiqi, O., Barbarand, J., Sebti, S., Baidder, L., Michard, A. *(in press).* Post-Variscan exhumation of the Central Anti-Atlas (Morocco) constrained by zircon and apatite fission-track thermochronology. *Terra Nova.*

Paul, A., Kaviani, A., Hatzfeld, D., Vergne, J. and Mokhtari, M., 2006. Seismological evidence for crustal-scale thrusting in the Zagros mountain belt (Iran) *Geophys. Jour. Int.*, **166**., 227-237

Pin, C., Fonseca, P.E., Paquette, J-L., Castro, P., Matte, P., 2008. The ca. 350 Ma Beja igneous complex: A record of transcurrent slab break-off in the Southern Iberia Variscan belt? *Tectonophysics,* **461**, 356-377. doi: 10.1016/j.tecto.2008.06.001

Piqué, A., Bossière, G., Bouillin, J-P., Chalouan, A., Hoepffner, C., 1993. Southern margin of the Variscan belt-the north-western Gondwana mobile zone (eastern Morocco and northern Algeria). *Geol. Rundsch.* **82**, 432-439.

Pollack, H.N., Hurter, S.J., Johnson, J.R., 1993, Heat flow from the Earth's interior : Analysis of the global data set, *Reviews of Geophysics*, **31**, 267-280.

Puchkov, V.N., 2009. The evolution of the Uralian orogeny. In: Murphy, J.B., Keppie, J.D., Hynes, A.J. (Eds.), Ancient orogens and modern analogues. Geological Society, *London, Special Publication **327***, pp. 161-195. doi:10.1144/SP327.9.

Racki, G., 1998. Frasnian-Famennian biotic crisis: undervalued tectonic control? *Palaeogeography, Palaeoclimatology, Palaeoecology*, **141**, 177-198.

*Rahl, J.M., Reiners, P.W., Campbell, I.H., Nicolescu, S., Allen, C.M., 2003, Combined single-grain (U-Th)/He and U/Pb dating of detrital zircons from the Navajo Sandstone, Utah, Geology, **31** (9), 761–764*

Rask, DH. 1972. *Permo-Triassic field survey-Oshtoran Kuh, Qal'eh kuh(Chal-i-sheh) and Zard-Kuh areas*. Oil Service Company, Technical note **# 162**.

Raulin, C., Frizon de Lamotte, D., Bouaziz, S., Khomsi, S., Mouchot, N., Ruiz, G., Guillocheau, F., 2011. Late Triassic-early Jurassic block tilting along E-W faults, in southern Tunisia: new interpretation of the Tebaga of Medenine. *J. Afr. Earth Sci*., doi:10.1016/j.jafrearsci.2011.05.007.

Ricou, L. E., 1971. Le croissant ophiolitique péri-arabe. Une ceinture de nappes mises en place au Crétacé supérieur. *Rev. Geogr. Phys. Géol. Dyn.* **13(4)**, 327-350.

Ricou, L. E., 1974, L'etude ge´ologique de la re´gion de Neyriz (Zagros iranien) et l'évolution structurale des Zagrides, Ph.D. thesis, Univ. Paris-Sud, Orsay, France.

Ricou, L., Braud, J. and Brunn, J. H., 1977.Le Zagros. *Mem. Soc. Géol. France,* **8**, 33-52.

Reiners, P.W., 2002, He diffusion and (U-Th) thermochronometry of zircon : initial results from Fish Canyon Tuff and Gold Butte, *Tectonophysics*, **349**, 297-308

Reiners P., Spell T., Nicolescu S. et Zanetti K., 2004. Zircon (U-Th)/He thermochronometry: He diffusion and comparisons with 40Ar/39Ar dating, *Geochimica et Cosmochimica Acta*, **68**, 1857–1887.

Reiners, P. W., 2005, Zircon (U-Th)/He Thermochronometry, *Reviews in Mineralogy & Geochemistry*, **58**, 151-179

Reiners, P., Brandon, M., 2006. Using thermochronology to understand orogenic erosion, *Annual Review of Earth and Planetary Sciences*, **34**, 419–466.

Robert-Charrue, C., Burkhard, M., 2008. Inversion tectonics, interference pattern and extensional fault-related foding in Eastern-Anti Atlas, *Swiss J. Geosci.* **101**, 397-408.

Robin, C., Gorican, S., Guillocheau, F., Razin, P., Dromart, G. and Mosaffa, H., 2010. Mesozoic deep-water carbonate deposits from the southern Tethyan passive margin in Iran (Pichakun nappes, Neyriz area): biostratigraphy, facies sedimentology and sequence stratigraphy, *Geological Society, London, Special Publications*; v. **330**; p. 179-210, doi:10.1144/SP330.10

Rowan, M. G. 1997. Three-dimensional geometry and evolution of a segmented detachment fold, Mississippi Fan foldbelt, Gulf of Mexico. Journal of Structural Geology **19(3-4)**, 463-480.

Ruiz, G.M.H., Sebti, S., Negro, F., Saddiqi, O., Frizon de Lamotte, D., Stokli, D., Stuart, F., Barbarand, J., Shaer, J.P., 2011. From pangean rift to Neogene uplift-Anti-Atlas (SW Morocco). *Terra Nova.* **23,** 35-41

Saddiqi, O., Baidder, L., Michard, A., 2011. Haut Atlas et Anti-Atlas, circuit oriental. *In* Nouveaux Guides Géologiques et Miniers du Maroc, A. Michard, O. Saddiqi, A. Chalouan, E. Rjimati and A. Mouttaqi eds, Notes et Mém. Serv. Géol. Maroc, **557**, 1-111.

Sass, J.H., Lachenbruch, A.H., Munroe, R.J., 1971, Thermal conductivity of rocks from measurements on fragments and its application to heat flow determinations, *J. Geophys. Res.*, **76**, 3391-3401.

Saura, E., Verges, J., Homke, S., Blanc, E. J.-P., Serra-Kiel,J., Bernaola, G., Casciello, E., Fernandez, N., Romaire, I., Casini, G., Embry, J.-C., Sharp, I.R., Hunt, D. W. 2011. Basin architecture and growthfolding of the NW Zagros early foreland basin duringthe Late Cretaceous and early Tertiary. *Journal of the Geological Society, London* **168**, 235–50.

Sebti, S., Saddiqi, O., El Haimer F. Z., Michard, A., Ruiz, G., Bousquet, R., Baidder, L., Frizon de Lamotte, D., 2009.Vertical movements at the fringe of the West African Craton.First zircon fission track datings from the Anti-Atlas Precambrian basement, Morocco. *C. R. Geoscience*, **341**, 71–77.

Sengor, A.M., Natal'in, B., 1996. Paleotectonics of Asia: fragments of a synthesis. In: Yin A., Harrison T.M. (Eds.), The tectonic evolution of Asia. Cambridge University Press, pp. 486-640.

Sepehr, M., Cosgrove, J., and MOIENI M., 2006. The impact of cover rock rheology on the style of folding in the Zagros fold-thrust belt, Tectonophysics, **427**, 265 – 281, doi:10.1016/j.tecto.2006.05.021.

Setudehnia, A., 1972. The Paleozoic sequence at Zardkuh and Keh-e- Dinar. Iranian Oil Operating Companies, Report **# 1196**

Setudehnia, A., 1978. The Mesozoic sequence in south-west Iran and adjacent areas, J. Petrol. Geol., **1**, 3 – 42.

Sherkati, S. and Letouzey, J., 2004. Variation of structural style and basin evolution in the central Zagros (Izeh zone and Dezful embayment), Iran. Mar. Pet. Geol. **21 (5)**, 535–554.

Sherkati, S., Molinaro M., Frizon de Lamotte D., Letouzey J., 2005. Detachment folding in the central and eastern Zagros fold-belt (Iran), Jour. Struct. Geol., **27**, 1680 – 1696.

Sherkati, S., Letouzey, J., Frizon de Lamotte, D., 2006. Central Zagros foldthrust belt (Iran): new insights from seismic data, field observation, and sandbox modeling. Tectonics **25**,TC4007. doi:10.1029/2004TC001766

Simancas, F., Azor, A., Martinez-Poyatos, D., Tahiri, A., El Hadi, H., Gonzalez-Lodeiro, F., Perez-Estaun, A., Carbonell, R., 2009. Tectonic relationships of Southwest Iberia with the allochthons of Northwest Iberia and the Moroccan Variscides. *C. R. Geoscience,* **341**, 103-113. doi: 10.1016/j.crte.2008.11.003

Somin, M.L., 2011. Pre-Jurassic basement of the Greater Caucasus: Brief overview. *Turkish Journal of Earth Sciences*, **20**, 545-610. doi: 10.3906/yer-1008-6.

Soulaimani, A., Essaifi, A., Youbi, N., Hafid, A., 2004. Les marqueurs structuraux et magmatiques de l'extension crustale au Protérozoïque terminal-Cambrien basal autour du massif de Kerdous (Anti-Atlas occidental, Maroc). *C.R. Geoscience*, **336**, 1433-1441.

Soussi, M., 2002. Le Jurassique de la Tunisie atlasique: stratigraphie, dynamique sédimentaire, paléogéographie et intérêt pétrolier. *Docum. Lab. Géol.*, Lyon 157, 363.

Stach, E. *et al.*, 1982. Stach's Textbook of Coal Petrology, Berlin, Stuttgart.

Stampfli, G., Marcoux, J. and Baud, A., 1991. Tethyan margins in space and time. *Palaeogeography, Palaeoclimatology, Palaeoecology,* **87**, 373-409. G

Stampfli, G.M., Mosar, J., Faver, P., Pillevuit, A., Vannay, C.J., 2001. Permo–Mesozoic evolution of the western Tethyan realm: the Neotethys/East Mediterranean connection. Peri-Tethys memoir 6: Peri-tethyan rift/wrench basins and passive margins. *International Geological Correlation Program*, **369**, 51–108.

Stampfli, G.M., Borel, G.D., 2002. A plate tectonic model for the Paleozoic and Mesozoic constrained by dynamic plate boundaries and restored synthetic oceanic isochrones. *Earth and Planetary Sciences Letters*, **196**, 17–33.

Stephenson, R.A., Stova, S.M., Starostenko, V.I., 2001. Pripyat-Dniepr-Donets Basin: implications for dynamics of rifting and the tectonic history of the northern Peri-Tethyan Platforrm In Peri-Tethys Memoir 6, *Mémoire du Muséum National d'Histoire Naturelle,* **186**, 369-406.

Stockli, D. F., 2005. Application of low temperature thermochronology to extensional tectonic settings in Low Temperature Thermochronology: Techniques, Interpretations, and Applications, *Rev. Mineral. Geochem., vol. 58, edited by P. W. Reiners and T. A. Ehlers, pp. 411‐448, Mineral. Soc. of Am.,Chantilly, Va.*

Stocklin, J., 1968. Structural history and tectonics of Iran: a review. *AAPG bull.* **52(7)**, 1229-1258.

Streel, M., Caputo, M.V., Loboziak, S., Melo, J.H.G., 2000. Late Frasnian-Famennian climates based on palynomorph analyses and the question of the Late Devonian glaciation. *Earth-Science Reviews*, **52**, 121–173.

Szabo,, F. 1977. *Permian and Triassic stratigraphy Zagros basin, SouthWest Iran*, Oil Service Company, Report **# 1261**.

Szabo, F, Kheradpir, A. 1978. Permian and Triassic stratigraphy, Zagros Basin, south-west Iran. *Journal of Petroleum Geology*, **1**, 57–82.

Tagami, T., Farley, K.A., Stockli, D.F., 2003, (U-Th)/He geochronology of single zircon grains of known Tertiary eruption age, *Earth and Planetary Science Letters*, **207**, 57-67

Tankard, A., Welsink, H., Aukes, P., Newton, R., Stettler, E., 2009. Tectonic evolution of the Cape and Karoo basins of South Africa. *Marine and Petroleum Geology*, **26**, 1379–1412

Tavakoli-Shirazi, S., Frizon de Lamotte, D., Wrobel-Daveau, J.C. and Ringenbach,J.C., 2012. Pre-Permian uplift and diffuse extensional deformation in the High Zagros Belt (Iran): integration in the geodynamic evolution of the Arabian plate, Arabian Journal of Geosciences, doi: 10.1007/s12517-012-0542-5

Ungerer, P. and Durand, B., 1987. La géochimie organique pétrolière. *Bulletin de la Société Géologique de France*, **8**, t. III(7), 1343-1356.

Van Staal, C.R., Whalen, J.B., Valverde-Vaquero, P., Zagorevski, A., Rogers, N., 2009. Pre-Carboniferous, episodic accretion-related, orogenesis along the Laurentian margin of the northern Appalachians. In: Murphy, J.B., Keppie, J.D., Hynes, A.J. (Eds.), Ancient orogens and modern analogues. *Geological Society, London, Special Publications **327***, pp. 271-316. doi:10.1144/SP327.13.

VanBuchem, F., Gaumet, F., Baghbani, D., Ashrafzadeh, R., and Keyvani, F. 2003. The relative impact of inherited tectonic features and eustatic sea level variations on the Jurassic/Cretaceous evolution of the Dezful Embayment, central Zagros, Iran, paper presented at AAPG International Conference, Barcelona, Spain.

Vergés, J., Saura, E., Casciello, E., M. Fernandez, A. Villasenor,I . Jiménez Munt and Garcia Castellanos D. 2011. Crustal-scale cross-sections across the NW Zagros belt: implications for the Arabian margin reconstruction. Geological Magazine, 1-23, doi:10.1017/S0016756811000331

Vermeesch, P., Avigad, D., McWilliams, M.O., 2009. 500 m.y. of thermal history elucidated by multi-method detrital thermochronology of North Gondwana Cambrian sandstone (Eilat area, Israel). *Geol. Soc. Am. Bull.,* **121**, 1204-1216.

Versfelt, Jr. P.L., 2001. Major Hydrocarbon Potential in Iran (abstract). *AAPG Memoirs,* **74**, 417– 427.

Villeneuve, M., 2005. Paleozoic Basins in West Africa and the Mauritanide thrust belt. *Journal of African Earth Sciences*, **43**, 166-195.

Weissbrod, T., 1980, The Paleozoic of Israel and adjacent countries [Ph.D. thesis]: Jerusalem, Hebrew University, 275 p. (in Hebrew).

Wender, L.E., Bryant, J.W., Dikens, M.F., Neville, A.S., Al-Moqbel, A.M., 1998. Paleozoic (Pre-Khuff) Hydrocarbon Geology of the Ghawar Area, Eastern Saudi Arabia. *Geoarabia*, 3, 2, 273-302.

Wendt , J., 1985. Desintegration of the continental margin of nortwestern Gondwana: late Devonian of the eastern Anti-Atlas (Morocco), *Geology,* **13**, 815-818.

Wendt, J., Kaufmann, B., Belka, Z., Klug. C., Lubeseder, S., 2006. Sedimentary evolution of a Palaezoic basin and ridge system: the Middle and Upper Devonian of the Ahnet and Mouydir (Algerian Sahara). *Geol. Mag.,* **143**, 269-299.

Williams, K.E., 1995. Tectonic subsidence analysis and Paleozoic paleogeography of Gondwana. In “Petroleum Basins of South America”, Tankard, A.J., Suarez-Sorucco, R., Welsink, H.J., Eds., Geological Society of America Memoirs, **62**, 79-100.

Wilson, M., Lyashkevich, Z.M., 1996. Magmatism and the geodynamics of rifting of the Pripyat-Dnieper-Donets rift, East European Platform. *Tectonophysics*, **268**, 65-81.

Woodward, N. B., Boyer, S. E. and Suppe, J. 1985. An outline of balanced cross sections, in Studies in Geology II, 170 pp., Dep. of Geol. Sci., Univ. of Tenn., Knoxville.

Wrobel-Daveau J.C., Ringenbach J.C., Tavakoli S, Ruiz G.M.H., Masse P. and Frizon de Lamotte D., 2010 .Evidence for mantle exhumation along the Arabian margin in the Zagros (Kermanshah area, Iran), Arabian Journal of Geosciences, doi: 10.1007/s12517-010-0209-z

Wrobel-Daveau, J.C., 2011. From the Rifting to the Current Collision, Vertical Movements and Propagation of the Deformation in the Zagros Belt, Iran, Unpublished PhD thesis.

Xianming, X., Zufa, L., Jiagui, S. and Dehan, L., 1999. A new method based on vitrinite gradient reflectance of a petroleum-bearing basin. *Chinese Science Bulletin*, **44**(17), 1593-1596.

Yegorova, T.P., Stephenson, R.A., Kostyuchenko, S.L., Baranova, E.P. Starostenko, V.I., Popolitov, K.E., 2004. Structure of the lithosphere below the southern margin of the East European Craton (Ukraine and Russia) from gravity and seismic data. *Tectonophysics*, **381**, 81–100.

Zanchi A., Zanchetta S., Berra F., Mattei M., Garzanti E., Molyneux S., Nawab A. and Sabouri J., 2009. The Eo-Cimmerian (Late? Triassic) orogeny in Northern Iran, (Geol. Soc., Lond., Spec. Publ.,2009, South Caspian to Central Iran Basins edited by Brunet,M.F.,Wilmsen, M., Granath, J.W. V. 312, pp. 343

Ziegler, J.F., 2008. SRIM-2008 The stopping range of ions in matter. *United States Naval Academy, Annapolis*.